# KINETICS OF NUCLEATION AND CRYSTALLIZATION

Thesis by

Frank Guojun Shi

In Partial Fulfillment of the Requirements

for the Degree of

Doctor of Philosophy

California Institute of Technology

Pasadena, California

1992

(Defended May 15, 1992)

# ACKNOWLEDGEMENTS

Valuable discussions with Drs. Richard C. Flagan, William L. Johnson, Paul E. Wagner and Bin Zhao, and encouragement from Drs. Dimo Kashchiev, Howard Reiss, and King-Ning Tu during different phases of the work covered in this thesis are gratefully acknowledged.

Special thanks goes to my advisor, Dr. John H. Seinfeld, for his guidance, ideas, encouragement and for trusting my abilities. I also would like to thank Dr. Kikuo Okuyama for his understanding, support and many long-hour discussions.

# ABSTRACT

A link between nucleation models and experimental kinetic measurements has been established as a result of the present studies of the general transient kinetics of nucleation in the barrier region and beyond. Based on the new results on the transient kinetics of nucleation, a theoretical basis for measuring directly the nucleation energy barrier and its temperature dependency is developed, an approach for determining the interfacial atomic transfer mechanism in the nucleation process is presented and some new experimental strategies for conducting nucleation and crystallization kinetic measurements are outlined. A new mathematical approach developed for solving the nucleation kinetic equation in the barrier region and beyond is described. The results are also presented for the nucleation kinetics in some spatially inhomogeneous systems where there are mechanisms for subcritical clusters loss from the system. In addition, a chemical-nucleation model developed for the cluster formation in a chemically reacting system is outlined.

# TABLE OF CONTENTS

# CHAPTER 1

# INTRODUCTION

# 1 HISTORICAL NOTE: NUCLEATION STUDIES SINCE FARKAS

Farkas (1927) derived for the first time the steady state rate of homogeneous nucleation by treating the detailed kinetics of the molecular addition to, and dissociation from, a nucleus of the new phase. In his paper, Farkas not only introduced a concept that is known today as the "Markovian birth and death process," but also developed the "population-over-flux" approach that has been widely used for calculating the rate of particles escaping from a metastable state. Farkas' work laid down not only the basis for modern kinetic theory of nucleation, but also for the modern rate theory of barrier-crossing in general, as recognized as late as the 1990s by physicists and chemists (Hanggi et al. 1990). It is ironic that the now more renowned work on the diffusional escape of a particle from a potential well by Kramers (1940) was in fact solved by Farkas in 1927 with greater generality in dealing with the rate of homogeneous nucleation. Curiously enough, Kramers did not cite this pioneering work of Farkas (Hanggi et al. 1990).

## 1.1 THE FARKAS MODEL OR QUASI-CHEMICAL MODEL

In his paper, Farkas attributed his ideas to L. Szilard. The Farkas-Szilard model for the kinetics of nucleation, on which practically all the modern theories of nucleation are based, describes the supersaturated vapor (liquid solution or solid solution) as an ideal mixture of monomers and clusters (in the following we will only refer to the vapor-liquid case). This model adopts the following assumptions: a mixture of clusters behaves as an ideal gas, thus neglecting the interactions among monomers and clusters and the interaction among clusters; cluster growth or shrinkage is assumed to be an

isothermal process and this implies that the relaxation of the heat bath is much faster than that of the system; clusters can grow and shrink by the addition or removal of single monomers; the nucleating system is infinite in the sense of negligible change in the monomer concentration and the system temperature during nucleation; the nucleation process only occurs in a closed system where there is no mechanism for subcritical cluster loss from the system. Under those conditions, the discrete master equation for nucleation can be written for the cluster concentration at size $g$ and time $t$, $f_g(t)$,

$$\frac{\partial f_g(t)}{\partial t} = J_g - J_{g-1}$$

$$J_g = \beta_g f_g(t) - \alpha_{g+1} f_{g+1}(t), \tag{1}$$

where $\beta_g$ is the addition rate of monomer to, $\alpha_g$ is the rate of monomer dissociation from a $g$-mer cluster and $J_g$ is the cluster flux in the size space, $g$. Now, $\alpha_g$ can be obtained by detailed balancing (Farkas 1927),

$$\alpha_g = \beta_g \frac{n_g}{n_{g+1}} \tag{2}$$

to give the rate of nucleation,

$$J_g = \beta_g n_g [\frac{f_{g+1}(t)}{n_{g+1}} - \frac{f_g(t)}{n_g}], \tag{3}$$

where $n(g)$ is the equilibrium cluster population of $g$-mers. Replacing the difference in Eq. [3] by differential and keep only the first-order differential of $f/n$, the so called Zeldovich equation is obtained (Zeldovich 1943),

$$\frac{\partial f(g,t)}{\partial t} = -\frac{\partial J(g)}{\partial g}$$

$$J(g) \approx -\beta(g) n(g) \frac{\partial}{\partial g} \frac{f(g,t)}{n(g)}. \tag{4}$$

There are some different treatments of transforming the discrete master equation, Eq. [1] to an equation such as Eq. [4] (e.g., Shizgal and Barrett 1989). The nucleation process, according to Eq. [4], is solely described by $\beta(g)$ and $n(g)$ since $\alpha(g)$ is estimated by the detailed balancing. It can be shown that the detailed balancing can be performed at the true equilibrium state to obtain $\alpha(g)$ in some special cases such as nucleation from a vapor at a constant temperature. In general, however, $\alpha(g)$ has to be estimated by using $n(g)$ even for nucleation from a vapor in the case of a constant monomer concentration. It is $n(g)$ that has attracted most of the attention in nucleation studies.

Smoluchowski in 1908 and Einstein in 1910 suggested that the probability of an isothermal fluctuation is proportional to $\exp(-\Delta F/kT)$ where $\Delta F$ is the Helmholtz free energy associated with formation of the fluctuation. Along the same line, Volmer and Weber (1926) proposed that $n(g_*)$ and thus the rate of nucleation $\propto \exp(-W_*/kT)$, where $W_*$ is the reversible work in forming a critical cluster of $g_*$-mer given by Gibbs in 1878. Gibbs found $W_* = \frac{1}{3}\sigma A_*$ based on Kelvin equation, where $\sigma$ in the bulk surface tension and $A_*$ is the surface area of the critical cluster evaluated using bulk liquid properties. The same exponential term is still present in the expression for the nucleation rate given by various nucleation theories, the form of $n(g)$ and/or $W(g)$, and thus the preexponential factor in the expression for the rate of nucleation has been the attention of studies since then.

Farkas for the first time suggested that $n(g) = C\exp(-W(g)/kT)$ and obtained an expression for the rate of nucleation, where $W(g)$ is the reversible work in forming a cluster of size $g$ which was given by using the capillary approximation and $C$ is the undetermined constant. The so-called

Zeldovich factor was in fact first correctly derived by Farkas. Subsequent developments have concentrated on estimating the value of $C$. It is Becker and Doring (1935) who proposed that $C = n_1$, the monomer concentration in the initially homogeneous system. This proposal was criticized for applying the Kelvin equation down to a monomer (Kuhrt, 1952). However, it is Frenkel (1939), Bank (1939) and Bijl (1938) who derived independently the same expression for $n(g)$ by formally adopting a quasi-chemical point of view in which the clusters of different sizes are treated as molecules of a different kind in a chemically heterogeneous mixture. Other subsequent work (Zeldovich 1943; Kaischew and Stranski 1934) also confirmed Farkas's result. From then on, such a nucleation theory based solely on thermodynamic considerations has successfully been employed in many fields to obtain qualitative results for many complex problems, including 3-D growth of epilayers (Jagannadham and Naragyan 1991), bubble formation in liquid helium at negative pressure (Maris and Xiong 1989), displacement transformation in metallic and non-metallic materials (Tanner and Wuttig 1990), formation of voids in nuclear reactor materials (Katz and Wiedersich 1971), and electron-hole liquid formation in semiconductors (Westervelt 1976), metallic glasses (Johnson 1986). More examples of the applications of basic concepts of nucleation in different fields can be found in the books by Hirth and Pound (1963), Christian (1975), Lews and Anderson (1978), Zettlemoyer (1969; 1977) and Koch (1984) and articles by Gunton et al. (1983) and Russell (1980). However, there has been no substantial progress made for the general thermodynamics and kinetics of nucleation since Frenkel (1939), Bank (1939) and Bijl (1938) as discussed below.

## 1.2 ENERGETICS

In the capillary approximation of classical theory the formation of an $g$-mer is equated to the formation of a spherical drop of a homogeneous liquid containing the same number of monomers, having the same properties as the bulk phase, and surrounded by an interface having the properties of the macroscopic surface (see also reviews by Abraham 1974; Christian 1975; Frenkel 1946; Gunton and Dorze 1983; Koch 1984; Kotake and Glass 1981; Lews and Anderson 1978, Ulbricht et al. 1988; Zettlemoyer 1977; 1969). In this case the free energy of formation of an $g$-mer is a sum of a surface and a volume term.

The debate regarding the applicability of the capillary approximation has lasted until today.

The apparent inconsistency in using bulk properties in treating small clusters has lead to consideration of the curvature dependency of surface tension (Pound and LaMer 1951; Vogelsberger et al. 1988; Huang 1990) in the classical Gibbs free energy of formation. This treatment is physically inconsistent and has not been proved to be useful for two reasons. Firstly as the size of a cluster decreases, not only surface tension but also the density of a cluster will change. Secondly the structure of a small cluster is different from that of the corresponding bulk material. The structure should be properly taken into account in using any size-dependent properties. That the classical theory works well in some cases could be a result of the cancellation of errors.

Using the density functional theory it is possible to obtain the density profiles as well as the surface tension (Phillips 1984; Lee et al. 1986). But this approach does not consider the geometrical structure of a cluster either.

The approach considers the geometrical structure based on given interaction potential is the so-called atomistic theory and its extension (see Hoare 1979 for a review). Of course the concept of surface tension is discarded here. This approach is limited by the lack of realistic potentials and the small size can be treated only for crystalline cluster.

There have been a number of attempts to calculate free energies of formation of clusters without using the surface tension concept. The most important approaches for the current discussion are harmonic models (atomistic models), Monte Carlo studies, and molecular dynamics calculations (e.g., Abraham 1974; Zettlemoyer 1977; Freeman and Doll 1988; Li and Scheraga 1990; Reiss et al. 1990; Ellerby et al. 1991).

Methods of numerical modelling which have been developed do not permit direct calculation of the Gibbs free energy of formation, since direct calculation of the corresponding statistical sum is practically impossible (Abraham 1974; Binder 1987). This aim may only be achieved in the Monte Carlo studies, for example, by the state integration method, by integrating the internal energy calculated along the isobar at many temperatures points over the inverse temperature in the conventional Monte Carlo method. Also there is no single view on what definition of a cluster is correct in the literature (which is the part of the cause for the famous debate about the so-called replacement factor in the 1960s; Reiss 1977; Reiss et al. 1990; Ellerby et al. 1991). In addition, conclusions about the validity of corresponding numerical studies are difficult to verify since many assumptions have to be made about the intermolecular or interatomic potentials.

The fundamental flaw of the statistical mechanical formulation of the nucleation energetics is that the statistical mechanics is only applicable to a

truly equilibrium system while nucleation is addressing metastable problems.

Field theory was developed by Langer in early 1970 to describe nucleation near $T_c$ (see the book by Gunton and Dorze 1983 for a review). Recently Oxtoby and Evans (1988) modified the approach by avoiding some approximations which limit the applicability of the theory to nucleation near $T_c$. The theory does not change any kinetic part of nucleation. A classical relativistic approach to the nucleation processes introduced by Nielsen and Providencia (1990) confirmed the form of the classical expression for $W(g)$.

Nucleation in the pure model system, Ising system, was first studied by Binder in 1977. Contributions to the development of nucleation in the Ising system are also by Penrose and his group (Penrose and Bukagiar, 1983). The model system studies seem to justify the classical theory (Toral and Marro 1986).

A nonequilibrium statistical treatment of nucleation by Bashkirov (1992) also gives a kinetic equation similar to classical, including a kinetic equation similar to Eq. [4]. Other non-conventional considerations, for example by Desre et al. (1990), have produced almost the same form of $W(g)$ as the classical one, even though some classical concepts have been replaced.

To sum up, the most fruitful result of those studies and other non-classical nucleation theories in treating the energetics of nucleation seems to justify and interpret the classical nucleation theory. Since acceptably realistic potentials have been proposed only for argon and water clusters so far, studies of nucleation by numerical methods and other new approaches have been confined to those substances and very often to purely model systems.

## 1.3 KINETICS

### 1.3.1 Kinetics at $g_*$

The steady-state kinetics of nucleation was essentially solved by Farkas in 1927. However, the desire to interpret the kinetic observations from condensed matter systems has pushed one to understand the transient kinetics of nucleation. The first such attempt was by Zeldovich in 1943 in studying the cavitation of liquids. In trying to estimate the time required to observe a steady-state rate of nucleation, Zeldovich obtained a time-dependent form of the rate of nucleation,

$$J(t) = J_s \exp(-\frac{t_o}{t}) \tag{5}$$

and estimated the time lag to be $t_o = \frac{(g_*-g_1)^2}{4\beta_*}$ where the size $g_1$ is that for $g > g_1$, $f(g,t) = 0$ and for $g < g_1$, $f(g,t) = n(g)$. The value of $g_1$ was undecided. Zeldovich wrote down Eq. [4] based on the known results for the particle diffusion in a potential field. Even though Eq. [5] is generally not correct for describing the time dependency of the rate of nucleation due to transient effects, the reasoning that, after the establishment of a given supersaturation, the population of some cluster sizes of smaller than $g_1$ reaches its equilibrium in a time smaller than $t_o$ is correct as shown later in this thesis. The $g_1$ is determined to be $g_* - \delta$, where $\delta$ is the half width of the nucleation barrier region. Zeldovich's concept that the time lag is mainly the time spent by clusters around the top of the nucleation barrier led the subsequent work (Kantrowitz 1951; Wakeshima 1954, 1955; Collins 1955; Andres and Boudart 1965; Kashchiev 1969; Binder and Stauffer 1976; K-Dannetschek and Stauffer 1981) on the same subject to transform Eq. [4] into a diffusion equation assuming $\beta(g)$ in Eq. [4] could be replaced by a

constant $\beta(g_*)$. Most of them gave the form of

$$t_o \approx \frac{1}{Z^2\beta_*}$$

for the time lag. Feder et al. (1966) obtained $t_o = \frac{1}{2Z^2\beta_*}$ by solely treating the nucleation process as a random walk process in the barrier region without resorting to Eq. [4]. The valuable contribution of Feder et al. is the correct identification of the width ($2\delta$) of the nucleation barrier region, $g_* - \delta \leq g \leq g_* + \delta$. Wakeshima (1954, 1955) obtained a form different from Eq. [5].

Most of the previous studies estimated the $t_o$, by transforming Eq. [4] into a diffusion equation assuming $\beta(g)$ in Eq. [4] could be replaced by a constant $\beta(g_*)$. Such an approximate diffusion equation seems to be only correct in the barrier region defined by Feder et al., however, the usual boundary conditions such as $f/n_1 \rightarrow 1$, as $g \rightarrow 1$ certainly cannot be applied in the barrier region. A possible improvement is to solve Eq. [4] in different regions then match solutions using the standard asymptotic matching techniques. Using such ideas, Shniedman (1987) obtained a different form of $J(t)$ from Eq. [5]. However, none of previous results for $J(t)$, including Eq. [5], are valid at the initial stage of nucleation.

One of the important early attempts comes from the work of Kashchiev (1969), who tried to solve Eq. [4] by using the method of eigenvalue expansion. Kaschiev's mathematical treatment was found to be flawed as analyzed by Binder and Stauffer (1976) and more recently by Shizgal and Barrett (1989). A similar approach was also used by Gitterman et al. (1984). Trinkaus and Yoo (1987) introduced the Green's functional approach to solve Eq. [4] in the nucleation barrier region. The common problem with these two methods is that the real boundary conditions have to be shifted to an unphysical domain in solving the associated eigenvalue problem.

Turnbull (1948)made the first attempt to solve Eq. [4] numerically, and confirmed the expression given by Zeldovich. Since then numerical solutions have been attempted by Courtney (1962), Abraham (1969), Kelton et al. (1983), Volterra (1985), Miloshev and Miloshev (1990), Evans and Stiffler (1991). The numerical solutions also involved serious approximations. One of them is that the cluster population below an arbitrary size is assumed to be in equilibrium, which is similar to that used by Zeldovich in 1943. Presently using numerical approach, it is not yet possible to follow the temporal evolution of clusters with size ranging from several molecules to millions.

### 1.3.2 Kinetics at Detectable Size

Most of the previous results have considered only clusters in the vicinity of the critical cluster size, which is usually much smaller than the resolution limit of various instruments which have been avaiable to make reliable kinetic measurements such as X-ray diffraction and Raman scattering (Suzuki et al. 1988). The high resolution electron microscopy is more suitable for the single cluster studies (see Andres et. al. 1989 for a good review). The relation

$$N(g_d, t) = N[g_*, t - t_d(g_*, g_d)] \tag{6}$$

and its variants have often been proposed to obtain $N(g_d, t)$, where $t_d(g_*, g_d)$ would be the time needed for a cluster at $g_*$ to grow to $g_d$ which is a detectable size. The underlying assumption in Eq. [9] that the number density of clusters measured at $g_*$, $N(g_*, t)$, is conserved over the time to grow from $g_*$ to $g_d$ and is equal to the number density measured at $g_d$, $N(g_d, t)$, is physically invalid. Since critical clusters of size $g_*$ have an equal average

probability to grow and decay (for a symmetrical barrier), not every cluster that reaches size $g_*$ will subsequently grow to $g_d$.

### 1.3.3 Basic Question

To sum up, transient solution of Eq. [4] has proved to be difficult to obtain even for the simplest initial and boundary conditions, and has challenged a number of investigators (see also reviews by Russel 1980; Kelton 1992; Kozisek 1991). The basic question of the subject still remains, that is, to understand the transient evolution of the CSD, $f(g,t)$, which underlies prediction of all the transient features of nucleation. In particular, understanding the temporal evolution of the CSD at sizes beyond the critical one is the most essential, since expressions for the transient kinetics of nucleation at instrumentally detectable sizes offer a connection between nucleation models and experimental observations.

## 2 OVERALL GOAL

As reviewed briefly above, various interesting fundamental questions about nucleation remain. Any ideas and models proposed for those questions have to be tested against experimental observations. To make such tests possible, one has to know the kinetics of nucleation for a given nucleation model, in particular the transient kinetics of nucleation, since nucleation in many materials may exhibit a considerable transient period, from several seconds to hours depending on temperature and materials (for example, Suzuki et al. 1988; Kambayash et al. 1989; Zallama et al. 1979; Koster 1978; Bisaro et al. 1989; Im and Atwater 1990). Reliable kinetic observations, if available, are usually at cluster sizes well beyond those in the barrier region. It is,

therefore, necessary to understand the transient kinetics of nucleation for $g > g_*$ to link theory and experiment.

The initial stage of nucleation is strongly time-dependent. The manipulation of the initial stage of nucleation is the basis for many emerging technologies (Inverson and Reif 1987; Ishiwara et al. 1986; Johnson 1981 and 1986). o understand the very early stage of nucleation, one must able to predict the transient kinetics at small times.

Therefore, for the verification and development of nucleation models, for the data interpretation, and for the possible application of experimental findings in the process improvement and control, one must understand the transient kinetics of nucleation, that is, the transient evolution of the CSD, $f(g,t)$, which underlies prediction of all the transient features of nucleation. In particular, understanding the temporal evolution of the CSD at sizes beyond the critical one is most essential. One of two main issues dealt in this thesis is the transient evolution of $f(g,t)$ for $t \geq 0$ and $g$ in the nucleation barrier region and, in particular, the region beyond the barrier. The second main issue of this thesis is the kinetics and thermodynamics of nucleation in some important complex systems. Understanding the nucleation process in many complex systems can be useful in the improvement and design of processes to tailor nucleation to specific requirements. The connection between these two issues is the approach for solving Eq. [4] based on the boundary-layer theory (Bender and Orszag, 1978).

The subsequent chapters are structured as following. Chapters 2 and 3 deal with the nucleation kinetics in the case of subcritical loss due to scavenging by particles of different sizes. Chapter 4 is about the kinetics of nucleation in spatially inhomogeneous systems. Chapter 5 deals with

the selective nucleation of silicon clusters in CVD systems by presenting a nucleation model that includes chemical etching of atoms as an additional loss process besides thermal dissociation that competes with the process of atom addition in forming a cluster. Chapter 6 presents the approach based on boundary-layer theory for solving transient nucleation problems. Results for the transient kinetics in the barrier region are presented. Chapter 7 presents the transient kinetics of binary nucleation and the problem of multiple pathways and saddle-point avoidance. Chapter 8 defines the size of the nucleated cluster size and obtains the transient solution at that size, also some time scales in nucleation problems are defined. In Chapter 9, we apply the new results for transient nucleation to study the time dependency of crystallized volume fraction using the Avrami model. Chapter 10 presents the approach and results for the transient kinetics of nucleation at sizes far beyond the critical one. Chapter 11 obtains the universal cluster size distribution in nucleation. Chapter 12 presents an approach for directly measuring the nucleation barrier and a method for testing models for monomer addition rate. Chapter 13 summarizes our approach based on the boundary-layer theory for nucleation problems. In Chapter 14, a summary is given and some suggestions for further studies are outlined.

# REFERENCES


Abraham, F. F., *Homogeneous Nucleation Theory* (Academic, New York, 1974)

Abraham, F. F., J. Chem. Phys., **51**, 1632(1969)

Andres, R. P., R. S. Averback, W. L. Brown, L. E. Brus, W. A. Goddard, A. Kaldor, S. G. Louie, M. Moscovits, P. S. Peercy, J. Materials Res., **4**, 704(1989)

Andres, R. P. and M. Boudart, J. Chem. Phys., **42**, 2057(1965)

Bank, W., J. Chem. Phys., **7**, 324(1939)

Bashkirov, A. G., J. Chem. Phys., **96**, 1484(1992)

Becker, R. and W. Doring, Ann. d. Phys., **24**, 719(1935)

Bender, C. M. and S. A. Orszag,*Advanced Mathematical Methods for Scientists and Engineers*, (McGraw-Hill Co., New York, 1978)

Bijl, A., Ph. D. dissertation, University of Leiden, 1938.

Binder, K., Rep. Prog. Phys., **50**, 783(1987).

Binder, K., Adv. Colloid. Inter. Sci., **7**, 279(1977)

Binder, K. and D. Stauffer, Adv. Phys., **25**, 343(1976)

Bisaro, R., J. Magarino, Y. Pastol, P. Germain and K. Zellama, Phys. Rev. B **40** 7655(1989)

Christian, J. W., *The Theory of Transformations in Metals and Alloys*, (Pergamon, Oxford, 1975)

Collins, F. C., Z. Electrochem., **59**, 404(1955)

Courtney, W. G., J. Chem. Phys., **36**, 2009(1962)

Dannetschek, I. K. and D. Stauffer, J. Aero. Sci., **12**, 105(1981)

Desre, P., A. R. Yavari and P. Hicter, Philo. Mag., **B61**, 1(1990)

Ellerby, H. M., C. Weakliem and H. Reiss, J. Chem. Phys., **95**, 9209(1991)

Evans, P. V. and S. R. Stiffler, Acta. metal. mater., **39**, 2727(1991)

Farkas, L., Z. Phys. Chem., **125**, 236(1927)

Feder, J., K. C. Russell, J. Lothe and G. M. Pound, Adv. Phys., **5**, 111(1966)

Ford, I. J. and C. F. Clement, J. Phys., **A22**, 4007(1989)

Freeman, D. L. and J. D. Doll, Adv. Chem. Phys., **49**, 139(1988).

Frenkel, J. I., *Kinetic Theory of Liquids*, (Clarendon, London, 1946)

Frenkel, J. I., J. Phys., **1**, 315(1939)

Gibbs, J. W., *The Scientific Papers of J. W. Gibbs*, vol. 1, (Longmans Green and Co., New York, 1928)

Gitterman, M., I. Edrel and Y. Rabin, in *Application of Field Theory to Statistical Mechanics*, edited by L. Garrido, Lecture Notes in Physics, Vol. 216 (Springer, Heidelberg, 1984)

Gunton, J. D., and M. Dorze, *Introduction to the Theory of Metastable and Unstable States*, Lecture notes in physics, **183**, (Springer-Verlag, Berlin, 1983)

Gunton, J. D., et al., in *Phase Transitions and Critical Phenomena*, **7**, 267(Acad. Press, NY, 1983).

Hanggi, P., P. Talker and M. Brokovec, Rev. Moden. Phys., **62**, 251(1990)

Hirth, J. P. and G. M. Pound, *Condensation and Evaporation* (Pergman Press, London 1963)

Hoare, M. R., Adv. Chem Phys., **40**, 49(1979).

Hodgson, A. W., Adv. Coll. Inter. Sci., **21**, 303(1984).

Huang, D., Ph.D. thesis, Caltech, 1990.

Im, J. S., and H. A. Atwater, Appl. Phys. Lett. **57**, 1766(1990)

Inverson, R. B., and R. Reif, J. Appl. Phys. **62**, 1675(1987)

Ishiwara, H., A. Tamba and S. Turukawa, Appl. Phys. Lett. **48**, 733(1986)

Jagannadham, K. and J. Naragyan, J. Elect. Mater. **20**, 767(1991)

Johnson, W. L., in Glassy Metals I, ed H. S. Güntherodt and H. Beck (Springer-Verlay, Berlin, 1981)

Johnson, W. L., Prog. Mater. Sci., **30**, 81(1986)

Kaischew, R. and I. N. Stranski, Z. Phys. Chem., **B26**, 317(1934)

Kambayash, S., S. Onga, I. Mizushima, K. Hignchi and H. Kuwano, Extended Abs. of the 21st Conf. on Solid State Devices and Mater., Tokoyo, 1989, p.169

Kantrowitz, A., J. Chem. Phys., **19**, 1097(1951)

Kashchiev, D., J. Surface Sci., **14**, 209(1969)

Katz, J. L. and H. Wiedersich, J. Chem. Phys. **55**, 1414(1971)

Kelton, K. F., Solid State Phys., **45**, 75(1992)

Kelton, K. F., A. L. Greer and C. V. Thomoson, J. Chem. Phys., **79**, 6261(1983)

Koch, S. W., *Dynamics of First-Order Phase Transition in Equilibrium and Non-equilibrium Systems*, Lecture Notes in Physics **207** (Springer-Verlag, Berlin, 1984).

Kochanski, E. and E. Constantin, J. Chem. Phys., **87**, 1661(1986)

Koster, U., Phys. Status Solidi **48**, 313(1978)

Kotake, S. and I. I. Glass, Prog. Aerospace Sic., **19**, 129(1981).

Kozisek, Z., In *Kinetic Phase Diagrams: Nonequilibrium Phase Transitions*, Z. Chvoj, J. Sestak and A. Triska (Eds.), (Elsevier, New York, 277-331, 1991)

Kramers, K. A. Physica, **7**, 284(1940)

Kuhrt, F., Z. Phys., **131**, 185(1952)

Lee, D. J., M. M. Telo da Gama and K. E. Gubbins, J. Chem. Phys., **85**, 490(1986)

Lee, J. K., J. A. Barker and F. F. Abraham, J. Chem. Phys., **55**, 580(1971)

Lews, B. and J. C. Anderson, *Nucleation and Growth of Thin Films* (Academic, New York 1978)

Li, Z. and H. A. Scheraga, J. Chem. Phys., **92**, 5499(1990)

Lippman, D., W. C. Schieve and C. Canestaro, J. Chem. Phys., **81**, 4946(1984)

Maris, H. J., and Q. Xiong, Phys. Rev. Lett. **63**, 1078(1989)

Miloshev, N. and G. Miloshev, Atom. Res., *25*, 417(1990)

Nielsen, M. and J da Providencia, J. Phys. G: Nucl. Pat. Phys., **16**649(1990)

Oxtoby, D. W., and R. Evans, J. Chem. Phys., **89**, 7521(1988)

Penrose, O. and A. Bukagiar, J. Sta. Phys., **30**, 217(1983)

Phillips, P., Mol. Phys., **52**, 155(1984)

Pound, G. M. and K. K. LaMer, J. Chem. Phys., **19**, 506(1951)

Reiss, H., Adv. Coll. Inter. Sci., **7**, 1(1977)

Reiss, H., A. Tabazadeh and J. Talbot, J. Chem. Phys., **92**, 1266(1990)

Russell, K. C., Adv. Coll. Interf. Sci., **13**, 205(1980)

Schelling, W. F. J., and H. Reiss, J. Chem. Phys., **74**, 3527(1981)

Shizgal, B., and J. C. Barrett, J. Chem. Phys., **91**, 6505(1989)

Shneidman, V. A., Sov. Phys. Tech. Phys., **32**, 76(1987)

Shugard, W. J., and H. Reiss, J. Chem. Phys., **65**, 2827(1976)

Smoluchowski, M. von, Ann. d. Phys. **25**, 205(1908)

Suzuki, M., M. Hiramoto, M. Oyuura, W. Kamisaka and S. Hasegawa, Jpn. J. Appl. Phys. **27**, L1380(1988)

Tanner, L. E. and M. Wuttig, Mater. Sci. and Eng. **A127**, 137(1990)

Toral, R. and J. Marro, Surf. Sci., **177**, 14(1986)

Toschev, S. and I. Gutzow, Phys. Stat. Sol., **21**, 683(1967)

Trinkaus, H. and M. H. Yoo, Phil. Mag., **A55**, 269(1987)

Turnbull, D., Trans. Am. Inst. Min. Engrs., **175**, 774(1948)

Ulbricht, H., J. Schmelzer, R. Mahnke and F. Schweitzee, *Thermodynamics of Finite Systems and the Kinetics of First-Order Phase Transitions* (Tenbner-Texte, Berlin 1988)

Vogelsberger, W., H. G. Fritsche and E. Muller, Phys. Stat. Sol., **148**, 1555(1988)

Volmer, M. and A. Weber, Z. Phys. Chem., **119**, 277(1926)

Volterra, V. and A. R. Cooper, J. Non-Crystal. Solids, **74**, 85(1985)

Wakeshima, H., J. Chem. Phys., **19**, 1614(1954)

Wakeshima, H., J. Phys. Soc. Jpn, **10**, 374(1955)

Westervelt, R. M., Phys. Stat. Sol. (b) **74**, 727(1976)

Wilemskii, G., J. Chem. Phys., **62**, 3772(1975)

Zallama, K., P Germain, S. Squeland, J. C. Bourjoin and P. A. Thomas, Appl. Phys. **50**, 6995(1979)

Zeldovich, J. B., Acta. Physicochim. URSS, **18**, 1(1943)

Zettlemoyer, A. C., (ed), *Nucleation Phenomena* (Elsevier Scientific, New York 1977)

Zettlemoyer, A. C., (ed), *Nucleation* (R. Decker, New York 1969)

Zhang, C. G., J. Coll. Interf. Sci., **124**, 262(1988)

Zurek, W. H. and W.C. Schieve, J. Chem. Phys., **68**, 840(1978)

Zurek, W. H. and W.C. Schieve, J. Chem. Phys., **84**, 1470(1980)

# PART II

# NUCLEATION KINETICS AND THERMODYNAMICS IN SPATIALLY INHOMOGENEOUS AND CHEMICALLY REACTING SYSTEMS

# CHAPTER 2

# HOMOGENEOUS NUCLEATION IN THE PRESENCE OF AN AEROSOL

# Homogeneous Nucleation in the Presence of an Aerosol

GUOJUN SHI AND JOHN H. SEINFELD[1]

*Department of Chemical Engineering, California Institute of Technology, Pasadena, California 91125*

Received March 28, 1989; accepted June 7, 1989

The explicit dependence of the homogeneous nucleation rate on the surface area concentration of preexisting free molecule particles is obtained by solving the Zeldovich–Frenkel–Becker-Döring equation modified to account for cluster scavenging. The present analytical solution is found to be in full agreement with numerical results. 

## INTRODUCTION

The effect of cluster scavenging by a preexisting aerosol on homogeneous nucleation has been considered previously (1–7). By generalizing classical nucleation theory the effect of scavenging by preexisting particles is represented in the cluster balance equations by a sink term that is proportional to the surface area concentration of particles. A closed-form expression for the rate of nucleation in the presence of preexisting particles has not heretofore been available; rather, the nucleation rate has had to be obtained by solving the governing equations numerically. [McGraw and Marlow (4) obtained a continued fraction form for the steady-state cluster distribution and nucleation rate in the presence of free-molecule regime particles which improved the efficiency of numerical calculation.]

An analytical expression for the rate of homogeneous nucleation in the presence of preexisting particles can be coupled with the balance equation for the monomer concentration to study the dynamics of aerosol formation theoretically or to interpret experimental results in systems where nucleation occurs as a result of monomer generation.

In the present report an analytical expression is derived for the rate of homogeneous nucleation in the presence of a free-molecule aerosol by using the method of singular perturbation. The relative roles of monomer depletion and cluster scavenging in reducing the homogeneous nucleation rate are also discussed.

## BASIC EQUATIONS

Most current theories of the formation of a new phase from a supersaturated vapor are based on the so-called Szillard model (8), according to which a supersaturated vapor consists of a mixture of monomeric molecules and molecular aggregates or clusters. Clusters are able to grow or evaporate by adding or losing monomers and clusters. Such a system is described by an infinite series of differential–difference equations

$$\frac{df_g}{dt} = \frac{1}{2}\sum_{k=1}^{g-1} \beta_{g-k,k} f_{g-k} f_k - f_g \sum_{k=1}^{\infty} \beta_{gk} f_k + \sum_{k=g+1}^{\infty} \alpha^k_{k-g,g} f_k - \frac{1}{2} f_g \sum_{k=1}^{g-1} \alpha^g_{g-k,k}, \quad [1]$$

where $f_g$ is the concentration of clusters containing $g$ molecules, $\beta_{ij}$ is the probability of formation of a cluster of size $g$ by the collision of $i$- and $j$-sized clusters, and $\alpha^g_{ij}$ is the probability that a cluster of size $g$ will fission into clusters of sizes $i$ and $j$.

Defining the cluster flux as arising by addition or evaporation only of individual molecules, i.e.,

[1] To whom all correspondence should be addressed.



0021-9797/90 $3.00

$$J_g = \beta_{g-1,1} f_{g-1} - \alpha_g f_g, \quad [2]$$

then Eq. [1] can be rearranged as

$$\frac{df_g}{dt} = J_g - J_{g+1} + \frac{1}{2}\sum_{k=2}^{g-2} \beta_{g-k,k} f_{g-k} f_k - f_g \sum_{k=2}^{\infty} \beta_{gk} f_k. \quad [3]$$

The last two terms in Eq. [3] describe cluster–cluster coagulation. Neglecting interaction among subcritical clusters, as in classical nucleation theory, but including cluster scavenging by supercritical clusters in the free molecule regime, we express Eq. [3] as

$$\frac{df_g}{dt} = J_g - J_{g+1} - f_g\left(\frac{kT}{2\pi m_1}\right)^{1/2} A g^{-1/2}, \quad [4]$$

where $A$ is the surface area concentration of supercritical free molecule particles and where we have expressed $\beta_{ij}$ for free molecule clusters (8).

As a standard practice in nucleation theory, detailed balancing is used to relate the $\alpha_{ij}$ to $\beta_{ij}$ and the equilibrium concentration of clusters. As a result, we have

$$J_{g+1} = -\beta_{1,g} n_g (f_{g+1}/n_{g+1} - f_g/n_g), \quad [5]$$

where $n_g$ is the equilibrium cluster size distribution corresponding to the monomer $n_1$ (not to the bulk liquid) and $\beta_{1,g}$ is the product of the surface area of a cluster containing $g$-monomers with the rate, based on the Maxwell–Boltzmann distribution of velocities, at which a unit surface area is hit by monomers. $\beta_{1,g}$ is equivalent to $\beta(g, t)$ given below.

Within the limits of classical nucleation theory of Frenkel, Becker-Döring, and Zeldovich (8), $J_g$ may be replaced by $J(g, t)$, which is the cluster flux defined in the continuous cluster size space ($g$), and its relationship with the continuous cluster size distribution $f(g, t)$ immediately follows as

$$\frac{\partial f(g, t)}{\partial t} = -\frac{\partial J(g, t)}{\partial g} - \gamma g^{-7/6} \beta(g, t) f(g, t) \quad [6]$$

and

$$J(g, t) = -\beta(g, t) n(g, t) \frac{\partial}{\partial g} \frac{f(g, t)}{n(g, t)}, \quad [7]$$

where

$$\beta(g, t) = f(1, t) s_1 g^{2/3} (kT/2\pi m_1)^{1/2} \quad [8]$$

and

$$n(g, t) = n(1, t) \exp[-W(g, t)/kT], \quad [9]$$

with $s_1$, $m_1$ the surface area and mass of the monomer, respectively, and $\gamma$ a dimensionless surface area concentration parameter defined by

$$\gamma = \frac{A}{s_1 f(1, t)}. \quad [10]$$

The critical size

$$g_* = \left(\frac{2\theta}{3 \ln S}\right)^3 \quad [11]$$

is the size of cluster corresponding to the maximum free energy of cluster formation,

$$W(g, t) = -gkT \ln S(t) + s_1 g^{2/3} \sigma, \quad [12]$$

where $\theta = s_1\sigma/kT$, the saturation $S(t) = n(1, t)/n_{eq}(1)$, and $n_{eq}$ is the saturation monomer concentration.

About $g_*$ a critical region exists in which the difference between $W(g)$ and $W(g_*)$ is smaller than $kT$ (9), i.e.,

$$[W(g) - W(g_*)] \leq kT, \quad [13]$$

the width of which is given by (9)

$$\delta = \left[-\frac{1}{2kT}\frac{\partial^2 W}{\partial g^2}\right]^{-1/2}\Bigg|_{g=g_*}, \quad [14]$$

which is related to the Zeldovich factor $Z$ by

$$\delta = \frac{1}{\sqrt{\pi} Z} = 3 g_*^{2/3} \theta^{-1/2}. \quad [15]$$

By imposing the boundary conditions

$$f(1, t) = n(1, t) \quad [16]$$

$$f(\infty, t) = 0, \quad [17]$$

solution to Eq. [6] without the last term on the r.h.s. can be obtained formally in terms of integrals in the limiting case of steady-state nucleation arising from constant supersaturation and constant temperature. The classical nucleation rate is then obtained by evaluating these integrals by using the condition that $\delta/g_* \ll 1$.

## NUCLEATION IN THE PRESENCE OF FREE MOLECULE PARTICLES—THE SINGULAR PERTURBATION APPROACH

As shown in Fig. 1, a difference between the equilibrium and steady-state distributions of clusters develops within the critical region. The normalized cluster size distribution $f(g)/n(g)$ exhibits a boundary layer (transition layer) structure close to $g = g_*$.

The boundary layer structure of the normalized cluster distribution is a feature of the classical homogeneous nucleation problem (in the absence of preexisting aerosol). Boundary layer problems are characterized by a small parameter, denoted as $\epsilon$, which appears multiplying the term containing the highest derivative in the governing equation. The small parameter in the nucleation problem is related to the width of the critical region $\delta$. A singular perturbation approach can be used to analytically solve boundary layer problems in which solutions outside and inside the boundary layer regime are obtained and appropriately matched. We will employ such an approach to obtain the steady-state homogeneous nucleation rate in the presence, and, of course, also in the absence, of a preexisting aerosol.

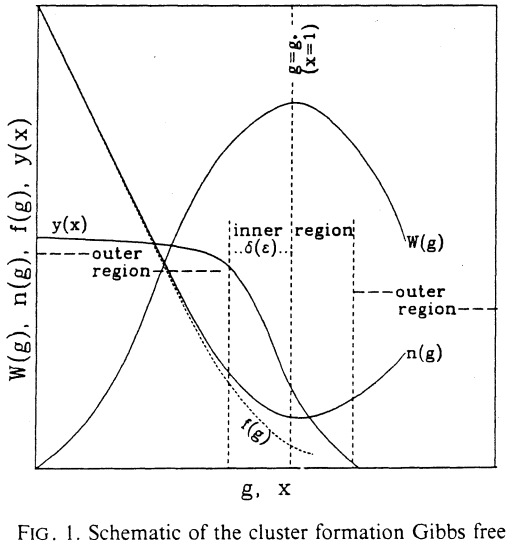


FIG. 1. Schematic of the cluster formation Gibbs free energy $W(g)$, the thermodynamic and kinetic cluster size distributions $n(g)$, $f(g)$, and the normalized cluster distribution $f(g)/n(g)$.

With this in mind, we first transform the steady-state form of Eq. [6] in terms of the new independent variables $y = f(g)/n(g)$ and $x = g/g_*$ into

$$\left(\frac{\delta}{g_*}\right)^2 \frac{d^2y}{dx^2} + \left[\frac{2}{3x}\left(\frac{\delta}{g_*}\right)^2 + 6(1 - x^{-1/3})\right]\frac{dy}{dx} - \gamma\delta^2 g_*^{-7/6} x^{-7/6} y = 0, \quad [18]$$

in which Eqs. [9], [11], [12], and [14] have been used. Letting $\delta/g_* \equiv \epsilon$, Eq. [18] becomes

$$\epsilon^2 \frac{d^2y}{dx^2} + \left[\frac{2}{3x}\epsilon^2 + 6(1 - x^{-1/3})\right]\frac{dy}{dx} - 2mx^{-7/6} y = 0, \quad [19]$$

where $m$ is given by

$$m = \frac{1}{2}\gamma\delta^2 g_*^{-7/6} = \frac{9}{2}\gamma\theta^{-1} g_*^{1/6}. \quad [20]$$

The condition $\epsilon \ll 1$ requires that $\ln S \ll \frac{2}{9}\theta^{3/2}$, which is the case in nearly all practical situations. Eq. [19] together with the boundary conditions

$$y(1/g_*) = 1, \quad y(\infty) = 0 \quad [21]$$

can now be solved by the method of singular perturbation. Since the dominant term containing $dy/dx$ changes sign at $x = 1$ in the interval $[1/g_*, \infty]$, we expect a boundary layer (transition layer) at $x = 1$ as described above. Thus there are two outer solutions: a $y^{\mathrm{l}}_{\mathrm{out}}$ that satisfies the left boundary condition at $x = 1/g_*$ and a $y^{\mathrm{r}}_{\mathrm{out}}$ that satisfies the right boundary condition at $x \to \infty$. The outer solution is expected to be valid everywhere except in a small region (inner region) around $x = 1$ (Fig. 1).

First, we seek an outer solution in the form of a perturbation series in powers of $\epsilon$:

$$y_{out} = y_0(x) + \epsilon y_1(x) + \epsilon^2 y_2(x) + \cdots, \quad \epsilon \to 0+. \qquad [22]$$

The outer solution is valid far from the critical region (Fig. 1) and must satisfy the boundary condition $y^l_{out}(1/g_*) = 1$ and $y^r_{out}(\infty) = 0$, which we write as

$$y^l_0(1/g_*) = 1, \quad y^l_n(1/g_*) = 0, \quad n \geq 1 \qquad [23]$$

and

$$y^r_n(\infty) = 0, \quad n \geq 0. \qquad [24]$$

Equation [22] is substituted into Eq. [19] and equating coefficients of like powers of $\epsilon$ yields

$$\frac{dy_0}{dx} = \frac{1}{3} m \frac{x^{-7/6}}{(1 - x^{-1/3})} y_0 \qquad [25]$$

$$\frac{dy_1}{dx} = \frac{1}{3} m \frac{x^{-7/6}}{(1 - x^{-1/3})} y_1 \qquad [26]$$

$$\frac{d^2y_{n-2}}{dx^2} + \frac{2}{3x}\frac{dy_{n-2}}{dx} + 6(1 - x^{-1/3})\frac{dy_n}{dx} = 2mx^{-7/6}y_n, \quad n \geq 2. \qquad [27]$$

The solutions to these equations that satisfy the boundary conditions are

$$y^l_0 = \left(\frac{1 - x^{1/6}}{1 + x^{1/6}}\right)^m \eta^{-m} \qquad [28]$$

$$y^l_1 = 0 \qquad [29]$$

and

$$y^l_2 = \frac{m}{9}\left(\frac{1 - x^{1/6}}{1 + x^{1/6}}\right)\left[\frac{1}{3}\ln\frac{1 - x^{1/6}}{1 + x^{1/6}} - \frac{1}{3}\ln\eta + \left(\frac{m}{2} - \frac{1}{3}\right)\left(\frac{1}{1 - x^{1/3}} - \frac{1}{1 - g_*^{-1/3}}\right)\right], \qquad [30]$$

where

$$\eta = \frac{1 - g_*^{-1/6}}{1 + g_*^{-1/6}} \qquad [31]$$

and

$$y^r_n = 0 \quad n \geq 0. \qquad [32]$$

Thus, the outer solutions to second order in $\epsilon$ are

$$y^l_{out} = \left(\frac{1 - x^{1/6}}{1 + x^{1/6}}\right)^m \eta^{-m} + \epsilon^2 \frac{m}{9}\left(\frac{1 - x^{1/6}}{1 + x^{1/6}}\right) \times \left[\frac{1}{3}\ln\frac{1 - x^{1/6}}{1 + x^{1/6}} - \frac{1}{3}\ln\eta + \left(\frac{m}{2} - \frac{1}{3}\right) \times \left(\frac{1}{1 - x^{1/3}} - \frac{1}{1 - g_*^{-1/3}}\right)\right] \qquad [33]$$

and

$$y^r_{out} = 0. \qquad [34]$$

As expected, the outer solutions are not valid near $x = 1$, so a boundary layer at $x = 1$ exists. Since the thickness of this boundary layer is $\epsilon$, we introduce the inner variables $X = (x - 1)/\epsilon^\lambda$ ($\lambda > 0$) and $Y_{in}(X) \equiv y_{in}(x)$. In terms of these variables, Eq. [19] becomes

$$\frac{\epsilon^{2-\lambda}}{3}\frac{dY_{in}}{dX} + \frac{1}{2}\epsilon^{2(1-\lambda)}(1 + \epsilon^\lambda X)\frac{d^2Y_{in}}{dX^2} + 3\epsilon^{-\lambda}(1 + \epsilon^\lambda X)[1 - (1 + \epsilon^\lambda X)^{-1/3}] \times \frac{dY_{in}}{dX} = m(1 + \epsilon^\lambda X)^{-1/6}Y_{in}. \qquad [35]$$

As $\epsilon \to 0$ with $X$ being fixed, the distinguished limit of Eq. [35] corresponds to $\lambda = 1$. Representing $Y_{in}$ as a perturbation series in powers of $\epsilon$,

$$Y_{in} = Y_0(X) + \epsilon Y_1(X) + \epsilon^2 Y_2(X) + \cdots, \quad \epsilon \to 0, \qquad [36]$$

the boundary condition $y(\infty) = 0$ translates into

$$Y_0(\infty) = 0, \quad Y_n(\infty) = 0, \quad n \geq 1. \qquad [37]$$

Putting $\lambda = 1$ in Eq. [35] and substituting Eq. [36] into Eq. [35] and equating coefficients of like powers of $\epsilon$, Eq. [35] is converted into a sequence of second-order differential equations:

$$\frac{1}{2}\frac{d^2Y_0}{dX^2} + X\frac{dY_0}{dX} = mY_0 \qquad [38]$$

$$\frac{1}{2}\frac{d^2Y_n}{dX^2} + X\frac{dY_n}{dX} = mY_n - \frac{1}{3}\frac{dY_{n-1}}{dX} - \frac{7}{6}mXY_{n-1}, \quad n \geq 1. \quad [39]$$

The solutions of Eqs. [38] and [39] that satisfy the boundary conditions are

$$Y_0 = \frac{1}{2}A_0 i^m\text{erfc}(X) + \frac{1}{2}B_0 i^m\text{erfc}(-X), \quad [40]$$

$$Y_1 = \frac{1}{2}A_1 i^m\text{erfc}(X) + \frac{1}{2}B_1 i^m\text{erfc}(-X) - \frac{m}{12}XY_0, \quad [41]$$

and

$$Y_n = \frac{1}{2}A_n i^m\text{erfc}(X) + \frac{1}{2}B_n i^m\text{erfc}(-X) + P_n, \; n \geq 2, \quad [42]$$

where $i^m\text{erfc}(X)$ is a repeated error function, $P_n$ is a particular solution to Eq. [41], and the constants $A_0$, $B_0$, $A_1$, $B_1$, $A_n$, and $B_n$ must be determined by asymptotically matching the outer and inner solutions. The match consists of requiring that at the intermediate limits [$\epsilon \to 0+$, $x \to 1-$, $X \to -\infty$; $\epsilon \to 0-$, $x \to 1+$, $X \to +\infty$] the inner and outer solutions agree. The leading-order match gives

$$A_0 = \left(\frac{\epsilon}{12}\right)^m \eta^{-m}\Gamma(m+1), \quad B_0 = 0. \quad [43]$$

Matching to the next order in $\epsilon$ requires

$$A_1 = -\frac{1}{12}mA_0\tilde{X}, \quad B_1 = 0. \quad [44]$$

The cluster size distribution that is uniformly valid over all sizes can be constructed from $y_{\text{unif}}(x) = y_{\text{out}}(x) + y_{\text{in}}(x) - y_{\text{match}}(x)$, where $y_{\text{match}}(x)$ is the expansion of either the inner or outer solutions in the matching region (10). However, to determine the nucleation rate we are most interested in the cluster size distribution near the critical size which is given by the inner solution (to first order in $\epsilon$, more properly to $\epsilon^{m+1}$)

$$y(x) = \frac{1}{2}\left(\frac{\epsilon}{12}\right)^m \eta^{-m}\Gamma(m+1)\left[1 - \frac{1}{12} \times m\epsilon\frac{x-1}{\epsilon}\right] i^m\text{erfc}\left(\frac{x-1}{\epsilon}\right). \quad [45]$$

The cluster size distribution in the critical region in the classical case is the limit of Eq. [44] as $\gamma \to 0$ (i.e., in the limit of no preexisting aerosol) (9),

$$f(g) = \frac{1}{2}n(g)\text{erfc}\left(\frac{g - g_*}{\delta}\right). \quad [46]$$

The nucleation rate in the presence of a free molecule aerosol is

$$J(g_*) = -\beta(g_*)n(g_*)\frac{\partial}{\partial g}\frac{f(g)}{n(g)}\bigg|_{g=g_*} = J_0\eta^{-m}\sqrt{\pi}\left(\frac{\epsilon}{24}\right)^m \frac{\Gamma(m+1)}{\Gamma\left(\frac{m}{2}+\frac{1}{2}\right)} \times \left[1 + \epsilon\frac{m}{24}\delta\frac{\Gamma\left(\frac{m}{2}+\frac{1}{2}\right)}{\Gamma\left(\frac{m}{2}+1\right)}\right], \quad [47]$$

where $J_0$ is the classical homogeneous nucleation rate in the absence of preexisting aerosols,

$$J_0 = Z\beta(g_*)n(g_*). \quad [48]$$

Of course, in the limit of no preexisting particles, i.e., as $\gamma \to 0$, $J(g_*) = J_0$.

## DISCUSSION

The ratio of the nucleation rate predicted from Eq. [47] to the corresponding classical value is shown as a function of the dimensionless particle surface area $\gamma$ for fixed values of $\theta$ and $S$ in Fig. 2. Also shown in Fig. 2 are numerical values of this ratio for $0 \leq \gamma \leq 1$ presented by Larson (7). It is clear from Fig. 2 that the leading-order results (to $\epsilon^m$) are quite close to the numerical solutions and including

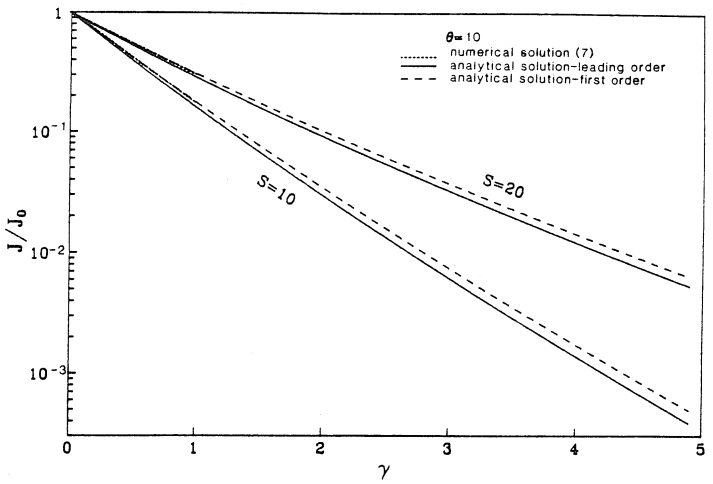


FIG. 2. Comparison between the analytic prediction for the rate of nucleation in the presence of preexisting free molecule particles and the numerical solution at $S = 10$, 20 and $\theta = 10$.

the next-order correction in $\epsilon$ brings the two solutions into full agreement. The value of $\theta$ chosen for these calculations is 10, which is typical of that for condensable organic compounds found in the atmosphere (4) ($\theta = 6.2$ for water vapor at $T = 298$ K). A decrease in the value of $\theta$ is equivalent to an increase in the value of $\gamma$ in reducing the nucleation rate (Eq. [20]). Since $\gamma = A/s_1 n_1$, the value of $\gamma$ can vary over a wide range reflecting the wide variation possible in $A$. For atmospheric applications, a typical value of $A$ is $2 \times 10^{-5}$ $cm^{-1}$ and $s_1 = 1.5 \times 10^{-14}$ $cm^2$ (4). For these two parameter values $\gamma$ can range from 0.1 for compounds with $p_{eq} = 10^{-8}$ Torr to 8.2 for $p_{eq} = 10^{-10}$ Torr at $S = 50$, $T = 298$ K.

The values of the critical supersaturation $S_{crit}$ (at $J = 1$ $cm^{-3}$ $s^{-1}$) corresponding to different compounds (with different equilibrium vapor pressures) in the presence of scavenging aerosols are shown in Fig. 3. Physical parameters chosen in the present calculations are $\sigma = 30$ dyn $cm^{-1}$, $s_1 = 1.5 \times 10^{-14}$ $cm^2$, $m_1 = 1.6 \times 10^{-22}$ g, and $T = 293$ K. The critical supersaturation for compounds with an equilibrium vapor pressure lower than $10^{-8}$ Torr is seen to be significantly increased compared with that in the absence of any scavenging aerosol, while for those compounds with $p_{eq}$ larger than $10^{-7}$ Torr no effect on $S_{crit}$ is found (since $\gamma$ is far less than 0.1) which is in general agreement with the results over the region covered in Fig. 3 obtained by solving the kinetic difference equations numerically (4). In view of the close agreement with the numerical results of Larson (Fig. 2), who obtained the nucleation rate by solving the kinetic differential equations, the quite small differences in the predicted values of $S_{crit}$ between the present result and that in Ref. (4) (not shown in the figure) is most likely the result of differences between solving the kinetic difference equations and the kinetic differential equations.

It has been shown that allowance for scavenging of clusters of all sizes by existing particles leads to an effective increase in the nucleation barrier (an increase in the value of $S_{crit}$, Fig. 3). The nucleation barrier results in this case not from the "thermodynamic force," i.e., by the competition between evaporation and attachment of monomer, but by the kinetics of cluster scavenging by existing particles. As a result, for a system with a given $S$, the homogeneous nucleation rate depends strongly on the surface area concentration of existing free-molecule particles (Figs. 2 and 3).

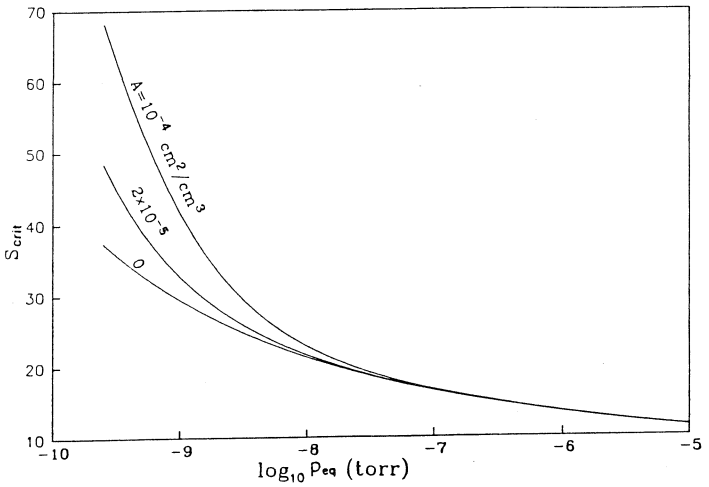


FIG. 3. Critical supersaturation versus equilibrium vapor pressure in the presence of different area concentrations of preexisting free molecule particles.

However, in systems where nucleation occurs as a result of monomer generation, the supersaturation in the system is often controlled by the monomer depletion. Condensation onto existing particles will limit the supersaturation and make the rate of homogeneous nucleation completely negligible in the absence of cluster scavenging (6).

## CONCLUSIONS

A closed form expression for the rate of homogeneous nucleation in the presence of preexisting free-molecule particles has been obtained by the method of singular perturbation.

The reduction in nucleation rate by the preexisting aerosol results from the deviation of the kinetic cluster size distribution of subcritical clusters from the thermodynamic equilibrium size distribution (by comparison with the equality between these two distributions outside of the critical region in the absence of aerosol). This deviation depends on the ratio between the surface area concentration of the scavenging particles and the monomer, and saturation ratio. Analysis indicates that monomer depletion and the cluster scavenging can be of comparable importance in reducing the rate of nucleation in the presence of free-molecule particles.

## ACKNOWLEDGMENT

This work was supported by National Science Foundation grant ATM-8503103.

## REFERENCES

1. Friedlander, S. K., *J. Colloid Interface Sci.* **82,** 465 (1978).
2. Friedlander, S. K., *Aerosol Sci. Technol.* **1,** 3 (1982).
3. Pesthy, A., Flagan, R. C., and Seinfeld, J. H., *J. Colloid Interface Sci.* **91,** 525 (1983).
4. McGraw, R., and Marlow, W. H., *J. Chem. Phys.* **78,** 2542 (1983).
5. McGraw, R., and McMurry, P. H., *J. Colloid Interface Sci.* **92,** 584 (1983).
6. Warren, D. R., and Seinfeld, J. H., *Aerosol Sci. Technol.* **3,** 135 (1984).
7. Larson, R. S., *J. Chem. Phys.* **88,** 5064 (1988).
8. Abraham, F. F., "Homogeneous Nucleation Theory." Academic Press, New York, 1974.
9. Binder, K., *Rep. Prog. Phys.* **50,** 783 (1987).
10. Bender, C. M., and Orszag, S. A., "Advanced Mathematical Methods for Scientists and Engineers." McGraw—Hill, New York, 1978.

# CHAPTER 3

# EFFECT OF CLUSTER SCAVENGING ON HOMOGENEOUS NUCLEATION

# Effect of cluster scavenging on homogeneous nucleation

G. Shi and J. H. Seinfeld
*California Institute of Technology, Pasadena, California 91125*

(Received 2 August 1989; accepted 13 September 1989)

A closed-form expression for the effect of cluster scavenging on the rate of homogeneous nucleation of a vapor in the presence of continuum regime particles is obtained by solving the kinetic equation of nucleation by the method of singular perturbation. The reduction in nucleation rate of a condensing species at a given supersaturation is shown to be dependent largely on the number concentration, the size of the sink particles, and the molecular number concentration of the background gas. The reduction in the rate of nucleation due to the cluster scavenging by transition regime particles is also discussed.

## I. INTRODUCTION

Homogeneous nucleation occurs when a vapor becomes sufficiently supersaturated that critical sized clusters form at a detectable rate. Preexisting or nucleated particles act to scavenge vapor molecules as well as clusters and therefore to depress the rate of homogeneous nucleation below that in their absence. When the scavenging particles have radii much smaller than the mean free paths of the vapor molecules and clusters, the so called free molecule regime, the depression in the overall nucleation rate is a function of saturation ratio and the ratio of the surface area concentration of scavenging particles to that of the monomer.[1] For scavenging particles with radii much larger than the mean free paths, the so called continuum regime, the diffusion of monomers and clusters to the particle leads to spatial inhomogeneities in the neighborhood of each particle. Because the effectiveness of the scavenging depends on the particle size and number concentration, the rate of homogeneous nucleation occurring in the bulk system will depend on the size and number concentration of scavenging particles in addition to the saturation ratio.

Pesthy *et al.*[2] and Stern *et al.*[3] considered the effect of monomer depletion by scavenging particles on the rate of homogeneous nucleation of a vapor but neglected cluster scavenging. McGraw and McMurry[4] used dimensional arguments to show that cluster diffusion in the neighborhood of a 1 $\mu$m diameter particle cannot usually be neglected.

The goal of this paper is to derive an expression for the influence of cluster scavenging on the rate of homogeneous nucleation of a vapor in presence of continuum regime particles. The result will be obtained in a form showing explicitly the deviation from the rate of homogeneous nucleation considering only monomer depletion.

## II. BASIC EQUATIONS

The dynamic behavior of a spectrum of growing and evaporating clusters in a spatially nonuniform system is governed by

$$\frac{df_g}{dt} - D_g \nabla^2 f_g = \frac{1}{2}\sum_{k=1}^{g-1} \beta_{g-k,k} f_{g-k} f_k - f_g \sum_{k=1}^{\infty} \beta_{g,k} f_k + \sum_{k=g-1}^{\infty} \alpha^k_{k-g,g} f_k - \frac{1}{2} f_g \sum_{k=1}^{g-1} \alpha^g_{g-k,k}, \tag{1}$$

where $f_g$ is the concentration of clusters containing $g$ monomers, $D_g$ is the diffusion coefficient of the $g$-sized cluster, $\beta_{i,j}$ is the probability of formation of a cluster of size $g$ by the collision of $i$- and $j$-sized clusters, and $\alpha^g_{i,j}$ is the probability that a cluster of size $g$ will fission into clusters of sizes $i$ and $j$. Equation (1) has also been written in a slightly different context by other authors.[5]

Defining the cluster flux arising by addition or evaporation only of individual monomers, i.e., neglecting cluster–cluster coagulation as in classical nucleation theory, we can introduce the flux

$$J_g = \beta_{g-1,1} f_{g-1} - \alpha_g f_g \tag{2}$$

and Eq. (1) can be rearranged as

$$\frac{df_g}{dt} = J_g - J_{g+1} + D_g \nabla^2 f_g. \tag{3}$$

As a standard practice in nucleation theory, detailed balancing is used to relate the $\alpha_{ij}$ to $\beta_{ij}$ and the equilibrium (with respect to the monomer) concentration of clusters. As a result, we have

$$J_g = -\beta_{1,g} n_g (f_{g+1}/n_{g+1} - f_g/n_g), \tag{4}$$

where $n_g$ is the equilibrium cluster size distribution corresponding to the monomer $n_1$ (not to the bulk liquid) and $\beta_{1,g}$ is the product of the surface area of cluster containing $g$ monomers with the rate, based on the Maxwell–Boltzmann distribution of velocities, at which a unit surface area is hit by monomers. $\beta_{1,g}$ is equivalent to $\beta(g,t)$ given below.

Within the limits of the classical nucleation theory of Frenkel, Becker-Döring, and Zeldovich,[6] $J_g$ may be replaced by $J(g,t)$ which is the cluster flux defined in the continuous cluster size space and its relationship with the continuous cluster size distribution, $f(g,t)$, immediately follows as

$$\frac{\partial f(g,\mathbf{r},t)}{\partial t} = -\frac{\partial J(g,\mathbf{r},t)}{\partial g} + D(g)\nabla^2 f(g,\mathbf{r},t), \tag{5}$$

where $\mathbf{r}$ is the spatial coordinate vector and

$$J(g,\mathbf{r},t) = -\beta(g,\mathbf{r},t) n(g,\mathbf{r},t) \frac{\partial}{\partial g} \frac{f(g,\mathbf{r},t)}{n(g,\mathbf{r},t)}. \tag{6}$$

One boundary condition on Eq. (5) expresses the fact that the equilibrium and steady-state monomer concentrations are equal,

 0021-9606/90/010687-07$03.00  

$$f(1,\mathbf{r},t) = n(1,\mathbf{r},t). \tag{7}$$

The second boundary condition on $g$ is that there are no particles of infinite size

$$f(\infty,\mathbf{r},t) = 0. \tag{8}$$

Two more boundary conditions on the spatial coordinate are needed in addition to the above two boundary conditions on $g$. Also in Eq. (6),

$$\beta(g,\mathbf{r},t) = f(1,t)s_1 g^{2/3}(kT/2\pi m_1)^{1/2} \tag{9}$$

with $s_1, m_1$ the surface area and mass of the monomer and the diffusivity of a $g$-mer with its size much smaller than the mean free path of the background gas, is given by

$$D(g) = \frac{1.105g^{-2/3}}{s_1 n_a}\left(\frac{\pi kT}{2m_1}\right)^{1/2}, \tag{10}$$

where $n_a$ is the molecular number concentration of the background gas. The classical equilibrium cluster distribution is

$$n(g) = n(1)\exp(g\ln S - \theta g^{2/3}), \tag{11}$$

where $\theta$ is a dimensionless surface tension

$$\theta = s_1\sigma/kT \tag{12}$$

and where the saturation ratio $S = n(1)/n_{eq}(1)$, $\sigma$ is the surface tension of the planar liquid, and $n_{eq}(1)$ the equilibrium number concentration of the monomer.

Equation (5) is solved in the steady-state spatially homogeneous case to obtain the classical nucleation rate.[6] In the present case the inhomogeneities of monomer and clusters in the neighborhood of each scavenging particle make the rate of homogeneous nucleation a function of spatial position. The procedure used in Ref. 1 can only be followed after obtaining an effective kinetic equation for the cluster balances in which the effect of scavenging is represented as a volumetric sink term. The first necessary step lies in the construction of a realistic procedure of averaging to obtain the effective governing equation. The influence of cluster scavenging will be presented as a ratio of the rate of homogeneous nucleation considering monomer depletion and cluster scavenging and that considering only monomer depletion.

## III. EFFECTIVE EQUATION AND GROWTH RATE

### A. Effective equation

To account for the potential many-body effect, a method of averaging over the configurational ensemble of the particle sinks in the system must be established. In a system without a phase transition such as in diffusion-controlled reactions, the effective equations are obtained through truncation of the chain of equations for the many-particle distribution functions with the aid of the cluster expansion method, scaling expansion approach, and other standard approaches of statistical mechanics,[7-14] which rely on expansions in the smallness of the spatial gradients or sink concentration or in the slowness of temporal change. A more tractable averaging makes use of effective medium theories. Averaging Eq. (5) over the spherical volume elements containing many particles but of the same order as the diffusion length scale $l$, we have

$$\frac{\partial\langle f(g,\mathbf{r},t)\rangle}{\partial t} = -\left\langle\frac{\partial J(g,\mathbf{r},t)}{\partial g}\right\rangle + \langle D(g)\nabla^2 f(g,\mathbf{r},t)\rangle, \tag{13}$$

where $\langle f(g,\mathbf{r},t)\rangle$ is the cluster concentration averaged in the indicated manner, i.e.,

$$\langle f(g,\mathbf{r},t)\rangle \equiv \frac{1}{V}\int\int\int_V f(g,\mathbf{r},t)\,dv. \tag{14}$$

Equation (13) describes the time variation of the average cluster concentration $\langle f(g,\mathbf{r},t)\rangle$ as the result of nucleation as well as capture and evaporation by the sink particles. The first two terms in the above equation are obtained naturally from Eq. (5). The decomposition of the last term on the right-hand side of Eq. (13) requires more attention. In the case of a macroscopically spatially homogeneous system, the spatial coordinate is excluded from any averaged quantity. In addition, we can assume div $[-D(g)\nabla\langle f\rangle] = 0$, i.e., inhomogeneties over the scale of $l$ are negligible. With allowance for the boundary condition Eq. (8), we have

$$\langle D(g)\nabla^2 f(g,t)\rangle = \frac{4\pi D(g)}{V}\sum_{i=1}^{N} R_i^2\nabla f|_{\mathbf{r}=\mathbf{r}_i+\mathbf{R}_i} = 4\pi D(g)\rho\int_{R^*}^{\infty} R^2\nabla f|_{\mathbf{r}=\mathbf{r}_i+\mathbf{R}_i} P(R)\,dR, \tag{15}$$

where $P(R)$ is the probability size distribution of the existing particles which is assumed to be independent of position, $R^*$ is a lower limit for particle radii in the diffusion regime, $N$ is the total number of particles in the volume $V$, and $\rho$ is the number density of the particles. In deriving the above expression, Gauss's theorem is used to reduce the volume integral to an integral over all particle surfaces and over the outer boundary of the volume $V$ which, subject to the condition of spatial inhomogeneity, results in the summation of all fluxes over all the sinks in the volume $V$ and diffusion over the length scale $l$ which is neglected in the present case.

To find $\nabla f$, in principle, it is necessary to solve Eq. (5) in the vicinity of each particle with appropriate boundary conditions. However some reasonable assumptions based on considering the time scale of each physical process [each term of Eq. (5)] enable us to determine $\nabla f$. We are assuming that the characteristic time to establish the steady-state cluster distribution is short compared to changes in the saturation ratio $S$, the term $\partial f/\partial t$ can be omitted from Eq. (5). Secondly, the characteristic relaxation time for establishment of the steady-state spatial distribution is $\tau_d \sim d^2/D(g)$, where $d$ is the characteristic length. The steady-state cluster distribution over $g$ is established in a time $\tau_n \sim g/\beta(g)$. For the condition $\tau_n/\tau_d \gg 1$ to hold requires that $p_{eq} \ll 4.441g^{-1/3}S^{-1}$ at $T = 298$ K and 1 atm of the pressure of the background gas and $d = 10^{-4}$ cm. $p_{eq}$ is in Torr. For $S = 10$ to 1000 and $g = 50$, the critical range for $p_{eq}$ is 0.12–$10^{-4}$ Torr. Therefore for values of $p_{eq}$ in the range we are most interested in (organic vapors and other particle-forming species), $\tau_d \ll \tau_n$ holds and the nucleation term in Eq. (5) can be omitted for the present purpose of estimating $\nabla f$ in Eq. (15). By also neglecting the Stefan flow and the effect of latent heat associated with condensation, determining $\nabla f$ in Eq. (15) reduces to solving the diffusion equation

$$\nabla^2 f(g,\mathbf{r}) = 0 \tag{16}$$

with appropriate boundary conditions.

It should be noted that the similar arguments were also made in the work of Pesthy *et al.*[2]

### B. Growth rate by *g*-mer scavenging

The cluster concentration field around a particle with its center at the origin takes the following form from solving Eq. (16) in the case where the growth rate is diffusion limited

$$f(g,r) = f(g,\infty) + \frac{R}{r}[f(g,R) - f(g,\infty)], \tag{17}$$

where $f(g,\infty)$ is the cluster size distribution at a position far from the particle. By substituting Eq. (17) into Eq. (13) and using Eq. (15), we obtain

$$\frac{\partial \langle f(g,t)\rangle}{\partial t} = -\left\langle \frac{\partial J(g,t)}{\partial g}\right\rangle - 4\pi \int_{R^*}^{\infty} \rho R^2 \frac{dR}{dt} P(R)\,dR, \tag{18}$$

where

$$\frac{dR}{dt} = D(g)\nabla f|_{r=R} = \frac{D(g)}{R}[f(g,\infty) - f(g,R)] \tag{19}$$

is the partial growth rate, i.e., the contribution to the growth rate of a particle of radius $R$ as a result of $g$-sized cluster scavenging.

At a nonzero concentration of sink particles, Eq. (17) has to be significantly modified. The reason that the modification is qualitatively significant even for dilute systems is that the steady-state concentration field surrounding a particle is of long range. One of the boundary conditions used in obtaining Eq. (17) is $f(g,r) \to f(g,\infty)$ as $r \to \infty$, which is only applicable in the limit of zero sink concentration. At finite concentration of sink particles, the full many-body problem can reduce to the consideration of an isolated particle in an effective medium if a mean-field approximation is invoked. In the mean-field picture, a single particle grows as a result of the diffusion-limited flux of monomers and clusters from the effective medium. We can specify a boundary condition at $l$ for Eq. (16), i.e.,

$$f|_{r=l} = f(g,l). \tag{20}$$

Accordingly, the effect of sink particles of different sizes within a volume of characteristic length $l$ is represented by the profile around a particle of average size which is given by

$$f(g,r) = f(g,l) + \frac{\bar{R}}{r}\frac{l-r}{l-\bar{R}}[f(g,\bar{R}) - f(g,l)]. \tag{21}$$

Since the characteristic length scale of a diffusion process is $\sqrt{D(g)t_c}$, we can take $l \propto \sqrt{D(g)t_c}$. The characteristic time scale $t_c$ for removal of clusters from this characteristic volume is given by

$$t_c = \frac{1}{4\pi D_g \bar{R}\rho}, \tag{22}$$

where $\bar{R}$ is the average particle radius. Thus the length scale $l$ is given by

$$l = \text{const}\frac{1}{\sqrt{4\pi\bar{R}\rho}}, \tag{23}$$

which is seen to be inversely proportional to the product of the number concentration of particles and their average radius. In the following $P(R)$ is taken to equal 1 for convenience, i.e., $R = \bar{R}$.

Consistent with our approximations above, we can relate $f(g,l)$ to $\langle f(g,r)\rangle$ by averaging Eq. (21)

$$\langle f(g)\rangle \equiv \langle f(g,r)\rangle = \frac{1}{V}\int\int\int_V f(g,r)\,dv = f(g,l) + \alpha[f(g,R) - f(g,l)], \tag{24}$$

which turns out to be independent of the spatial coordinate as desired and where

$$\alpha = \left\{\frac{R}{l}\left[\frac{1}{2}\left(1+\frac{R}{l}\right) - \left(\frac{R}{l}\right)^2\right]\right\} \times \left\{\left(1-\frac{R}{l}\right)\left[1+\frac{R}{l}+\left(\frac{R}{l}\right)^2\right]\right\}^{-1}. \tag{25}$$

Thus

$$f(g,l) = \frac{\langle f(g)\rangle}{1-\alpha} - \frac{\alpha}{1-\alpha} f(g,R). \tag{26}$$

In this case, we have

$$\frac{dR}{dt} = \frac{D(g)}{R}[\langle f(g,r)\rangle - f(g,R)]\frac{1}{1-\alpha}\frac{l}{l-R}, \tag{27}$$

which reduces to Eq. (19) in the limit of $R/l \to 0$. By neglecting second- and higher-order powers in $R/l$, i.e., in the limit of small but finite sink volume fraction, Eq. (27) becomes

$$\frac{dR}{dt} = \frac{D(g)}{R}[\langle f(g)\rangle - f(g,R)][1 + R\sqrt{4\pi\rho\bar{R}}], \tag{28}$$

which is in the same form as obtained by the method of multiple scattering[13] (the constant appearing in $l$ is taken as 3/2). Also, the rate of diffusion-controlled reaction in the presence of random traps can be obtained from the above result which is in agreement with the commonly accepted expression for the first-order concentration dependence of the reaction rate.[7-14] In particular, the result is numerically in agreement with that obtained by Mattern and Felderhof[11] up to a volume fraction $\phi(=4/3\pi\rho R^3)$ about 0.15.

In the following, we will obtain the nucleation rate in a field of nonzero volume fraction of sink particles using the growth rate given by Eq. (28).

## IV. STEADY-STATE SIZE DISTRIBUTION AND NUCLEATION RATE

Assuming the sink particle size distribution is sufficiently narrow as to be characterized by a single average radius $R$, with the growth law obtained in the last section, Eq. (28), the governing equation for the cluster size distribution, Eq. (13) takes the form

$$\frac{\partial \langle f(g,t)\rangle}{\partial t} = -\left\langle \frac{\partial J(g,t)}{\partial g}\right\rangle - 4\pi D(g)\rho[\langle f(g,t)\rangle - f_R(g,t)] \times R(1 + R\sqrt{4\pi R\rho})$$
$$\langle f(1,t)\rangle = \langle n(1,t)\rangle, \quad \langle f(\infty,t)\rangle = 0 \tag{29}$$

where $f_R(g,t)$ is $f(g,t)$ at a particle surface.

Our goal is to obtain the effect of cluster ($g \geqslant 2$) scavenging by continuum regime particles on the nucleation rate. Previous work has addressed the effect of monomer scavenging only.[2,3] Because of the strong dependence of the nucleation rate on $S$, nucleation will be suppressed in the immediate vicinity of a particle where the monomer is being removed. Moreover, the strong nonlinear dependence of the nucleation rate on $S$ invalidates the equality between $J(\langle S \rangle)$ and $\langle J(S) \rangle$. Representing the effect of cluster scavenging as a mean volumetric sink term in the kinetic equation of nucleation [Eq. (29)] and thereby obtaining the overall nucleation rate based on the spatial average saturation ratio $\langle S \rangle$ is our main approximation. A similar approximation was used in previous work[15] and was assessed later by comparison with the cell model.[16] It was found that if the volume fraction $\phi$ of preexisting aerosol is less than about $10^{-6}$, $J\langle S \rangle$ will be indistinguishable from $\langle J(S) \rangle$. Thus our results obtained below are limited to $\phi < 10^{-6}$.

Introducing the new independent variables $y = \langle f(g) \rangle / \langle n(g) \rangle$, $x = g/g_*$, where

$$g_* = \left(\frac{2\theta}{3 \ln\langle S \rangle}\right)^3, \tag{30}$$

Eq. (29) under steady-state condition becomes

$$\epsilon^2 \frac{d^2y}{dx^2} + \left(\frac{2}{3x}\epsilon^2 + 6(1 - x^{-1/3})\right)\frac{dy}{dx} - 2\eta x^{-4/3} y = 0, \tag{31}$$

where $\epsilon = \delta/g_*$, the width of the critical region $\delta = 3g_*^{2/3}\theta^{-1/2}$. We can specify $f_R(g) = 0$ and $\eta$ in Eq. (31) is given by

$$\eta = \frac{4\pi\rho R D(g_*)(1 + R\sqrt{4\pi R})\delta^2}{\beta(g_*)} = \frac{19.884\pi^2\rho R(1 - \sqrt{3\phi})}{\theta s_1^2 n_1 n_a}. \tag{32}$$

The dimensionless parameter $\eta$ represents the ratio of the flux of clusters to preexisting particles to the flux in the cluster size space over the Gibbs energy barrier at $g = g_*$. In the absence of preexisting particles $\eta = 0$. An increasing level of preexisting particles is reflected in an increasing value of $\eta$. Equation (31) together with the boundary conditions

$$y(1/g_*) = 1, \quad y(\infty) = 0 \tag{33}$$

can now be solved by the method of singular perturbation. Since the dominant term of $dy/dx$ changes sign at $x = 1$ in the interval $[1/g_*, \infty]$, we expect a transition layer at $x = 1$. Thus there are two outer solutions: a $y^l_{\text{out}}$ that satisfies the left boundary condition at $x = 1/g_*$ and a $y^r_{\text{out}}$ that satisfies the right boundary condition at $x \to \infty$. The outer solution is expected to be valid everywhere except in a small region (inner region) around $x = 1$.

The outer solutions are valid far from the critical region and must satisfy the boundary conditions

$$y^l_0(1/g_*) = 1, \quad y^l_n(1/g_*) = 0, \quad n \geqslant 1 \tag{34}$$

and

$$y^r_n(\infty) = 0, \quad n \geqslant 0. \tag{35}$$

The outer solutions are

$$y^l_{\text{out}} = \left(\frac{x^{-1/3} - 1}{g_*^{1/3} - 1}\right)^\eta \tag{36}$$

and

$$y^r_{\text{out}} = 0. \tag{37}$$

As expected, the outer solution is not valid near $x = 1$, so a boundary layer at $x = 1$ exists. Since the thickness of this boundary layer is $\epsilon$, we introduce the inner variables $X = (x - 1)/\epsilon$ and $Y_{\text{in}}(X) \equiv y_{\text{in}}(x)$. In terms of these variables, Eq. (31) becomes

$$\frac{\epsilon}{3}\frac{dY_{\text{in}}}{dX} + \frac{1}{2}(1 + \epsilon X)\frac{d^2Y_{\text{in}}}{dX^2} + 3\frac{(1 + \epsilon X)}{\epsilon}[1 - (1 + \epsilon X)^{-1/3}]\frac{dY_{\text{in}}}{dX} = \eta(1 + \epsilon X)^{-1/3} Y_{\text{in}}, \quad Y_{\text{in}}(\infty) = 0. \tag{38}$$

Representing $Y_{\text{in}}$ as a perturbation series in powers of $\epsilon$, Eq. (38) can be converted into a sequence of second-order differential equations. We solve the leading equation

$$\frac{1}{2}\frac{d^2Y_0}{dX^2} + X\frac{dY_0}{dX} = \eta Y_0 \tag{39}$$

to obtain the leading-order inner solution as

$$Y_0 = \tfrac{1}{2}A i^\eta \operatorname{erfc}(X) + \tfrac{1}{2}B i^\eta \operatorname{erfc}(-X), \tag{40}$$

where $i^\eta \operatorname{erfc}(X)$ is a repeated error function and the constant $A$ has to be determined by asymptotically matching the outer and inner solutions. The match consists of requiring that the intermediate limits [$\epsilon \to 0+$, $x \to 1-$, $X \to -\infty$] of the inner and outer solutions agree. The leading-order match gives

$$A = \left(\frac{\epsilon}{3}\right)^\eta \Gamma(\eta + 1)(g_*^{1/3} - 1)^{-\eta}, \quad B = 0. \tag{41}$$

However, to determine the nucleation rate, we are most interested in the cluster size distribution near the critical size which is given by the inner solution (leading order in $\epsilon$)

$$y(g) = \frac{1}{2}\left(\frac{\epsilon}{3}\right)^\eta \Gamma(\eta + 1)(g_*^{1/3} - 1) - \eta i^\eta \operatorname{erfc}\left(\frac{g - g_*}{\delta}\right). \tag{42}$$

In the limit of no existing sinks, i.e., $\eta \to 0$, the cluster size distribution in the critical region is[17]

$$f(g) = \frac{1}{2} n(g) \operatorname{erfc}\left(\frac{g - g_*}{\delta}\right). \tag{43}$$

The rate of nucleation in the presence of preexisting continuum regime particles is

$$\langle J(g_*) \rangle = -\beta(g_*) n(g_*) \frac{\partial}{\partial g}\frac{f(g)}{n(g)}\bigg|_{g = g_*} = \langle J_0 \rangle \left(\frac{\epsilon}{6(g_*^{1/3} - 1)}\right)^\eta \sqrt{\pi}\frac{\Gamma(\eta + 1)}{\Gamma(\eta/2 + \frac{1}{2})}, \tag{44}$$

where $\langle J_0 \rangle$ is the rate of homogeneous nucleation of a vapor taking into account the effect of monomer depletion but neglecting cluster scavenging. In the absence of any preexisting particles, $\langle J(g_*) \rangle = \langle J_0(g_*) \rangle$.

From Eq. (27), the spatial average saturation ratio for $\phi \ll 1$ can be approximated as

$$\langle S \rangle \approx (1-\alpha)S + \alpha \approx (1 - \tfrac{3}{4}\sqrt{3\phi})S + \tfrac{3}{4}\sqrt{3\phi} \qquad (45)$$

by assuming that $f(1,l)$ equals the monomer number concentration in the absence of existing particles and neglecting the Kelvin effect.

## V. DISCUSSION

The major significance of scavenging is its effect on the steady-state nonequilibrium cluster size distribution and consequently on the rate of nucleation. Such distributions are presented in Fig. 1(a) in the presence of cluster scavenging [Eqs. (36) and (42)] and in its absence [Eq. (43)] for $\eta = 1$. Not surprisingly, in comparison to the classical distribution, scavenging by particles greatly depletes the nonequilibrium number concentration of clusters. Since the nucleation rate is determined by the rate of collision of the monomer with critical sized clusters, a decrease in the number concentration of critical sized clusters results in a decrease in the rate of nucleation. Also shown in Fig. 1(a) is the thermodynamic equilibrium cluster size distribution $n(g)$. It can be seen that the deviation of the steady-state distribution from the equilibrium is greater in the presence of cluster scavenging. In Fig. 1(b), the normalized cluster size distributions are shown. In the absence of scavenging particles, the normalized nonequilibrium cluster size distribution obeys a complementary error function. In the case with cluster scavenging, $f(g)/n(g)$ changes with $g/g_*$ almost exponentially. The value of $-\partial(f/n)/\partial g$ at $x = 1$ is related to the rate of nucleation and a smaller slope at this point in the presence of scavenging leads to a lower rate of nucleation.

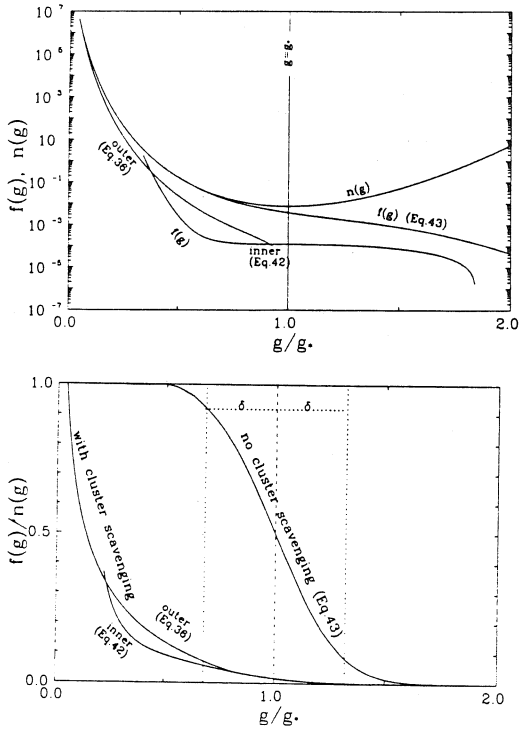


FIG. 1. The steady-state nonequilibrium cluster size distributions in (a) the case of cluster scavenging [Eqs. (36) and (42)—left outer and inner solutions] and (b) in its absence [Eq. (43)].

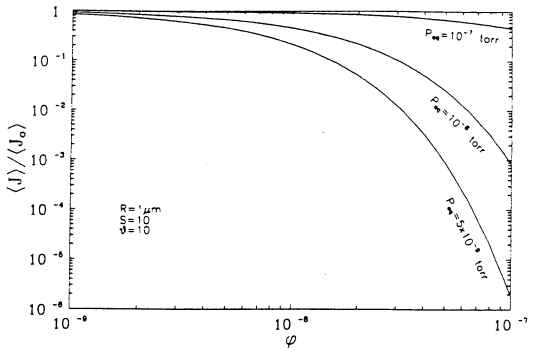


FIG. 2. The effect of cluster scavenging as a function of volume fraction $\phi$.

The reduction in the rate of nucleation due to the cluster scavenging depends on several factors which appears explicitly in Eq. (44). The ratio $\langle J(g_*) \rangle / \langle J_0 \rangle$ is a function of the dimensionless parameters $\epsilon$, $g_*$, and $\eta$. While $g_*$ and $\epsilon$ are determined by the dimensionless variables $S$ and $\theta$, $\eta$ is determined not only by the physical properties of the condensable species, characterized by $\theta$, $s_1$, and $n_1$, and the number concentration of sink particles ($\rho$) and their sizes ($R$), but also by the molecular number concentration of the background gas ($n_a$).

The ratio of the nucleation rate predicted from Eq. (44) to the corresponding nucleation rate considering only monomer scavenging is shown as a function of the volume fraction $\phi$ for fixed values of $\theta$, $S$, and $R$ for different condensing species characterized by $p_{eq}$ in Fig. 2. The value of $\theta$ chosen for these calculations is 10 which is typical of that for condensable compounds found in the atmosphere ($\theta = 6.2$ for water vapor at $T = 298$ K). For atmospheric applications, a typical value of $\phi$ is of the order of $10^{-8}$ taking the number

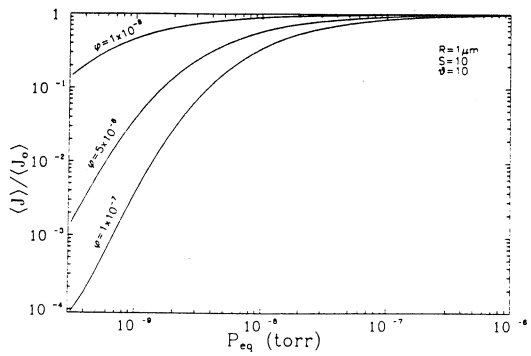


FIG. 3. The effect of cluster scavenging as a function of equilibrium vapor pressure $p_{eq}$.

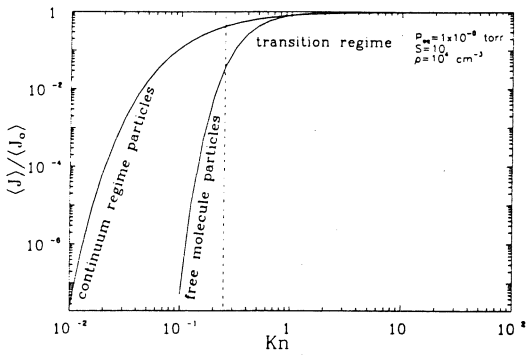


FIG. 4. The effect of cluster scavenging as a function of Knudsen number Kn.

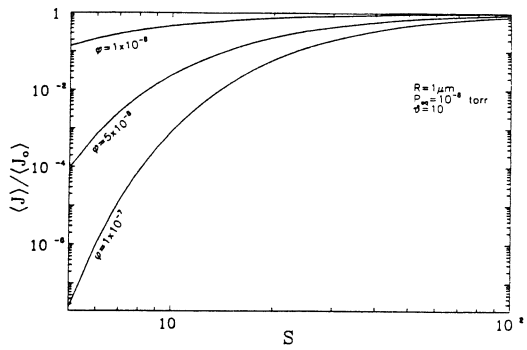


FIG. 6. The effect of cluster scavenging as a function of supersaturation ratio $S$.

concentration of primary particles as $\rho = 10^4$ cm$^{-3}$ of 1 $\mu$m in radius. We note that the ratio $\langle J\rangle/\langle J_0\rangle$ decreases as the volume fraction of preexisting particles increases. As in the case of cluster scavenging in the presence of a free molecule aerosol,[1] cluster scavenging has the most pronounced effect for species with lower vapor pressure. Since $\eta$ increases with decreasing $p_{eq}$, a larger value of $\eta$ results in a greater depletion of the nonequilibrium number concentration of critical sized clusters, thus a larger reduction in the ratio $\langle J\rangle/\langle J_0\rangle$. This feature is also clearly shown in Fig. 3. From both Figs. 2 and 3, it can be seen that for typical values of $\phi$ in the atmosphere, the scavenging of prenucleation embryos by any preexisting continuum regime particles of condensible species with vapor pressures higher than about $10^{-7}$ Torr can be generally ignored. Many species, however, that are suggested to be responsible for the formation of new aerosol[18] are those with vapor pressures lower than this value.

The ratio $\langle J\rangle/\langle J_0\rangle$ is shown as a function of the size of the preexisting particles in Fig. 4 based on the above result and that obtained in Ref. 1 for free molecule particles. Here the Knudsen number is defined as the ratio of the mean free path of the background gas to the radius of the sink particle. For the results shown, the mean free path is calculated by assuming the pressure of the background gas is 1 atm at $T = 298$ K. If the transition regime is characterized by the value of Kn in the interval of 0.25 to 10, the reduction in the nucleation rate due to cluster scavenging by transition regime particles can be estimated by the formula obtained above for continuum regime particles.

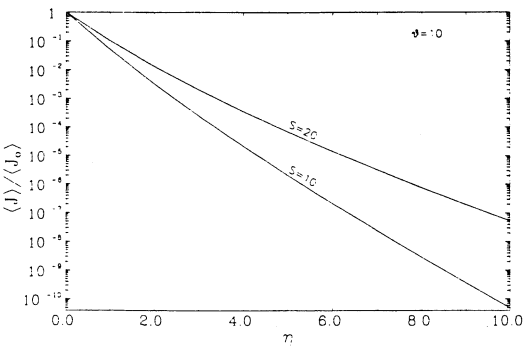


FIG. 5. The effect of cluster scavenging as a function of $\eta$.

In Fig. 5, we plot the ratio $\langle J\rangle/\langle J_0\rangle$ as a function of the dimensionless parameter $\eta$. As discussed above, a larger value of $\eta$ results in a greater depletion of the nonequilibrium number concentration of critical sized clusters, thus a larger reduction in the nucleation rate. The value of $\eta$, as given by Eq. (32) can vary substantially. If there are no preexisting particles, $\eta = 0$. For $S = 10$, $\theta = 10$, $p_{eq} = 10^{-8}$ atm, $\rho = 10^4$ cm$^{-3}$, $R = 10^{-4}$ cm at $T = 298$ K and 1 atm, $\eta \approx 10$. Since $\eta$ is inversely proportional to $n_a$, the molecular number concentration of the background gas, a reduction in pressure at a constant concentration of preexisting particles leads to a larger value of $\eta$ and greater effect of cluster scavenging. Indeed, certain experimental nucleation systems involve operation at reduced pressure, such as ones utilizing jet expansion.[19]

An increase in supersaturation lowers the energy barrier and promotes nucleation. In the competition for clusters between the process of nucleation and scavenging by sink particles, it is expected that as $S$ increases, the ratio $\langle J\rangle/\langle J_0\rangle$ becomes larger, as shown in Fig. 6. As $S$ approaches 100, the ratio approaches unity for $\phi$ in the range of $10^{-8}$ to $10^{-7}$.

The results presented here are applicable to steady-state nucleation in which the characteristic time for change in the saturation ratio is so long compared with the characteristic time to establish a steady-state cluster distribution. For a rapid change in saturation ratio that might occur in certain experimental systems, a general nonstationary solution is still not available. Finally, the system we have considered is taken to be spatial uniform. The effect of spatial inhomogeneities of preexisting particles on the rate of nucleation has yet to be considered.

In summary, a closed-form expression for the influence of cluster scavenging on the rate of homogeneous nucleation of a vapor in the presence of continuum regime particles is obtained by solving the spatially averaged kinetic equation for cluster balance by the method of singular perturbation. The reduction in nucleation rate due to cluster scavenging is shown to be dependent largely on the number concentration,

size of the sink particles, and the molecular number concentration of the background gas.

## ACKNOWLEDGMENT

This work was supported by National Science Foundation Grant No. ATM-8503103.

[1] G. Shi and J. H. Seinfeld, J. Colloid Interface Sci. (to be published).
[2] A. Pesthy, R. C. Flagan, and J. H. Seinfeld, J. Colloid Interface Sci. **91**, 525 (1983).
[3] J. E. Stern, J-J. Wu, R. C. Flagan, and J. H. Seinfeld, J. Colloid Interface Sci. **110**, 533 (1986).
[4] R. McGraw and P. H. McMurry, J. Colloid Interface Sci. **92**, 584 (1983).
[5] K. Binder, Phys. Rev. B **15**, 4424 (1977).
[6] K. Binder, Phys. Rev. B **15**, 4424 (1977).
[6] F. F. Abraham, *Homogeneous Nucleation Theory* (Academic, New York, 1974).
[7] M. Muthukumar, J. Chem. Phys. **76**, 2667 (1982).
[8] J. A. Marques and J. Ross, J. Chem. Phys. **81**, 536 (1984).
[9] M. Fixman, J. Chem. Phys. **81**, 3666 (1984).
[10] N. G. van Kampen, Int. J. Quantum Chem. Symp. **16**, 101 (1982).
[11] K. Mattern and B. U. Felderhof, Phys. Status Solidi A **143**, 1 (1987).
[12] M. Tokuyama and R. I. Cukier, J. Chem. Phys. **76**, 6202 (1982).
[13] J. Rubinstein and S. Torquato, J. Chem. Phys. **88**, 6372 (1988).
[14] C. W. J. Beenakker and J. Ross, J. Chem. Phys. **84**, 3857 (1986).
[15] D. R. Warren and J. H. Seinfeld, J. Colloid Interface Sci. **105**, 136 (1985).
[16] D. R. Warren, K. Okuyama, Y. Kousaka, J. H. Seinfeld, and R. C. Flagan, J. Colloid Interface Sci. **116**, 562 (1987).
[17] K. Binder, Rep. Prog. Phys. **50**, 783 (1987).
[18] J. H. Seinfeld, Science **243**, 745 (1989).
[19] D. Kotake and I. I. Glass, Prog. Aerospace Sci. **19**, 129 (1981).

# CHAPTER 4

# NUCLEATION IN SPATIALLY INHOMOGENEOUS SYSTEMS

# Homogeneous nucleation in spatially inhomogeneous systems

G. Shi and J. H. Seinfeld
*Department of Chemical Engineering, California Institute of Technology, Pasadena, California 91125*
K. Okuyama
*Department of Chemical Engineering, University of Osaka Perfecture, Sakai, Osaka 591 Japan*

(Received 5 March 1990; accepted for publication 9 July 1990)

Homogeneous nucleation of a vapor in the presence of the loss of clusters by diffusion and thermophoretic drift is investigated. Analytical results are obtained for the cluster size distribution and the rate of nucleation by solving the modified kinetic equation for nucleation. The implications of cluster loss by diffusion and phoretic drift on the onset of the homogeneous nucleation of silicon vapor in the horizontal epitaxial chemical vapor deposition reactor is discussed. The range of conditions under which the loss of subcritical clusters by diffusion and drift becomes important for the interpretation of diffusion cloud chamber experimental data of the onset conditions of the homogeneous nucleation of vapors is also delineated.

## I. INTRODUCTION

Many systems in which nucleation occurs are spatially nonuniform, and nucleation occurs only in those regions in which the supersaturation exceeds the critical value. Subcritical clusters formed within this region may leave it by diffusion or by drift under the influence of an external potential. Such diffusional and drift loss processes compete with the growth of clusters to the critical size and may reduce the rate of nucleation below that predicted by conventional nucleation theories in which the subcritical cluster loss is not included. The goal of the present work is to extend classical homogeneous nucleation theory to include subcritical cluster loss by diffusion and phoretic drift. The implications of subcritical cluster loss by diffusion and phoretic drift to the possible control of the onset of nucleation of silicon particles in a horizontal epitaxial chemical vapor deposition (CVD) reactor is discussed in light of the present theoretical results. We will also investigate the implications of subcritical cluster loss by diffusion and thermophoretic drift to the interpretation of experimental data from the diffusion cloud chamber which is often employed to study the onset conditions of homogeneous nucleation.

## II. FORMULATION OF THE PROBLEM

Consider a cluster containing $g$ monomers, within a one-dimensional region of thickness $d_0$. Such a cluster may grow or evaporate or diffuse or drift out of the region. We consider the cluster size $g$ as a continuous variable. Then the cluster distribution function $f(g,z,t)$ at position $z$ obeys the continuity equation:

$$\frac{\partial f(g,z,t)}{\partial t}+\frac{\partial j(g,z,t)}{\partial g}+\frac{\partial h(g,z,t)}{\partial z}=0, \tag{1}$$

where we have introduced the fluxes of clusters in the cluster size space, $j(g,z,t)$, and in the physical space, $h(g,z,t)$. The flux $h(g,z,t)$ is assumed to include contributions from Brownian diffusion and thermophoretic drift,

$$h(g,z,t)=-D(g)\frac{\partial f}{\partial z}-V_T f, \tag{2}$$

where $D(g)$, the Brownian diffusion coefficient for a $g$-sized cluster, is given by[1]

$$D(g)=\frac{12\pi(kT)^{2/3}g^{-2/3}}{8p_t\sqrt{2\pi m_c}s_1} \tag{3}$$

with $m_c$ the mass of a carrier gas molecule which is assumed smaller than that of a monomer; and $V_T$ is the thermophoretic drift velocity for a cluster of free molecule size,[1]

$$V_T=-\frac{3\nu}{4}\frac{d\ln T}{dz}. \tag{4}$$

Here $\nu$ is the kinematic viscosity of the carrier gas.

An expression for the flux of the clusters in the cluster size space $j(g,z,t)$ can be written by allowing for the fact that the number concentration of clusters is substantially smaller than the number concentration of monomers, so that the motion along $g$ occurs mainly through the interaction of clusters with monomers. Then the expression for the flux $j(g,z,t)$ is[2]

$$j=-\beta n\frac{\partial}{\partial g}\frac{f}{n}, \tag{5}$$

where $n(g,z)$ is the equilibrium cluster distribution and

$$\beta=n(1)s_1g^{2/3}(kT/2\pi m_1)^{1/2} \tag{6}$$

with $s_1$ and $m_1$ the surface area and mass of the monomer, respectively. According to the capillary approximation, $n(g,z)$ can be written as[2]

$$n(g,z)=n(1,z)\exp(g\ln S-\theta g^{2/3}), \tag{7}$$

where $\theta$ is a dimensionless surface tension,

$$\theta=s_1\sigma/kT \tag{8}$$

and where the saturation ratio $S=n(1,z)/n_{eq}$, $\sigma$ is the surface tension of the particle, and $n_{eq}(1)$ is the equilibrium number concentration of the monomer. The capillary approximation will be employed because we are only interested in the conditions for the onset of homogeneous nucleation of vapors. At low rates of nucleation, it is assumed that the capillary approximation may be invoked even for the nucleation of silicon vapor at high temperatures. Boundary condi-

 0021-8979/90/214550-06$03.00  

tions are specified at two physical boundaries on $z$ besides the usual boundary conditions on $g$: $f/n = 1$, as $g \to 1$ and $f/n = 0$, as $g \to \infty$. Profiles that might be achieved in a diffusion cloud chamber and a CVD reactor are schematically shown in Figs. 1(a) and 1(b), respectively as examples of systems in which nucleation is confined to a thin spatial region.

The governing equations can be simplified if the saturation ratio is sufficiently large in the narrow region of thickness $d_0$ where nucleation occurs. The saturation ratio decreases rapidly on either side of this region, and since the concentration of clusters depends strongly on the supersaturation, virtually no clusters can be assumed exist on either side of the region. If the cluster concentrations at the two physical boundaries at distances $d_1$ and $d_2$ from the thin region $d_0$ are assumed to be zero, the gradients for diffusion toward the two boundaries can be estimated by $f/d_1$ and $f/d_2$.[2] Then the diffusion loss of $g$-sized clusters per unit time from a unit area will be

$$D(g)\left(\frac{1}{d_1}+\frac{1}{d_2}\right)f.$$

Since the region of nucleation has thickness $d_0$, the loss per unit time per unit volume will be $D(g)(d_0 d)^{-1}f$, where

$$\frac{1}{d}=\frac{1}{d_1}+\frac{1}{d_2}.$$

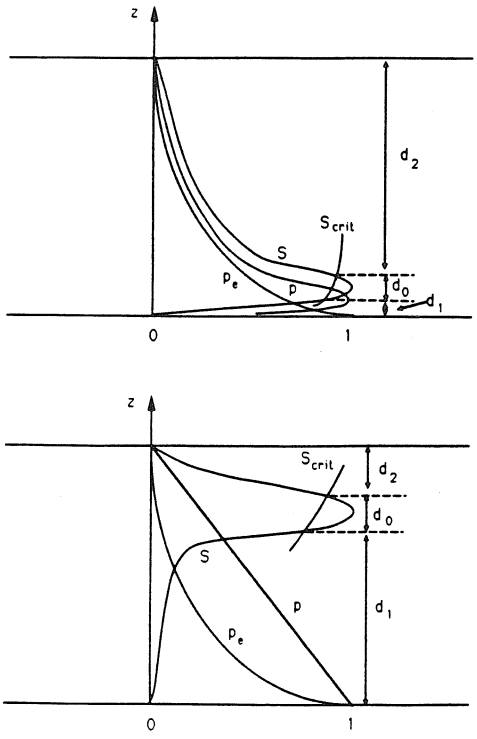


FIG. 1. Schematic profiles in a nonuniform nucleation system: (a) diffusion cloud chamber; (b) CVD reactor.

The term $V_T \partial f/\partial z$ describing the subcritical cluster loss by thermophoretic drift per unit time per unit volume will be approximated as $V_T f/d_2$ since clusters driven by the thermopheretic force will move to the upper surface when the temperature gradient is assumed to be along the $z$ direction. The gradient set up in this manner will underestimate the actual value since a subcritical cluster (which is larger than the critical size in the region $d_0$) will decompose back to monomer immediately outside the region $d_0$. With these simplifications and assuming a stationary state, Eq. (1) with Eq. (2), becomes within the region of nucleation

$$0 = -\frac{\partial j(g)}{\partial g} - D(g)\frac{1}{d}\left(\frac{3}{2}\omega+\frac{1}{d_0}\right)f - \omega\frac{3\nu}{4}\left(\frac{1}{d_2}+\omega\right)f, \tag{9}$$

where $\omega = d \ln T/dz$.

To obtain the critical conditions for the onset of homogeneous nucleation and its rate, it is necessary to determine the cluster size distribution by solving the above equation. The procedure based on matched asymptotic expansions developed by Shi and Seinfeld[3] will be followed in solving Eq. (9).

## III. CLUSTER DISTRIBUTION FUNCTION AND NUCLEATION RATE

### A. Cluster distribution function

Introducing $y = f/n$, and $x = g/g_*$, Eq. (9) becomes

$$\epsilon^2\frac{\partial^2 y}{\partial x^2}+\left(\frac{2}{3x}\epsilon^2+6(1-x^{-1/3})\right)\frac{\partial y}{\partial x} = 2(ax^{-4/3}+bx^{-2/3})y, \tag{10}$$

where $\epsilon \equiv \delta/g_*$ with $\delta$ and $g_*$ given by

$$\delta = 3g_*^{2/3}\theta^{-1/2}, \quad g_* = \left(\frac{2\theta}{3\ln S}\right)^3. \tag{11}$$

Here $g_*$ is the critical cluster size above which a cluster grows spontaneously. $\delta$ defines the width of the critical region about $g_*$ such that the difference between the Gibbs formation energy of clusters at size $g$ and those at $g_*$ is smaller than $kT$. Also, in Eq. (10),

$$a = \frac{\delta^2}{2\beta(g_*)}\left(\frac{1}{d_0}+\frac{3\omega}{2}\right)\frac{D(g_*)}{d},$$
$$b = \frac{\delta^2}{2\beta(g_*)}\left(\frac{1}{d_2}+\omega\right)\frac{3\omega\nu}{4} \tag{12}$$

are two dimensionless time scales. $a$ is the ratio between the characteristic nucleation relaxation time[4] which is given by $\delta^2/2\beta(g_*)$ and that of Brownian diffusion of clusters. Thus, a large value of $a$ implies that the response time of the nucleation process to changes in the saturation ratio is longer than the time it takes for clusters to diffuse out of the region of thickness $d_0$. On the contrary, if $a$ is small, the response time of the nucleation process to changes in the saturation ratio is shorter than the time it takes for clusters to diffuse out of the regions of thickness $d_0$. $b$ is the ratio of the characteristic nucleation relaxation time to that for the thermophoretic drift of clusters. Thus a large value of $b$ implies that the nucleation process responds slowly to changes in the satura-

tion ratio relative to the time it takes for clusters to thermally drift out of the region of thickness $d_0$, and vice versa.

To a leading-order approximation in $\epsilon$ the nonequilibrium cluster distribution function obtained by the method of matched asymptotic expansions is

$$y(x) = \left(\frac{x^{-1/3}-1}{g_*^{-1/3}-1}\right)^a \left(\frac{1-x^{1/3}}{1-g_*^{1/3}}\right)^b \exp[b(x^{1/3}-g_*^{1/3})] + \frac{1}{2}Ai^{a+b}\,\mathrm{erfc}\left(\frac{x-1}{\epsilon}\right) - A\Gamma^{-1}(a+b+1)\left(\frac{1-x}{\epsilon}\right)^{a+b}, \quad (13)$$

where

$$A = \left(\frac{\delta}{3g_*}\right)^{a+b}\Gamma(a+b+1)(g_*^{1/3}-1)^{-a}(1-g_*^{1/3})^{-b} \times \exp[b(1-g_*^{-1/3})] \quad (14)$$

and $i^n\,\mathrm{erfc}(x)$ is an integrated error function, and $\Gamma^{-1}(x)$ is the inverse of the Gamma function, $\Gamma(x)$.

In the limit of $a = b = 0$, Eq. (12) reduces to the correct limiting result for the cluster size distribution in a spatially uniform system,[5]

$$f(g) = \frac{1}{2}n(g)\,\mathrm{erfc}\left(\frac{g-g_*}{\delta}\right). \quad (15)$$

$y(x)$ is shown in Fig. 2 for $a = 0, b = 0$, the spatially uniform case, and $a = 1, 3, 5, b = 0$. It can be seen from Fig. 2 that both the concentration of the critical sized cluster and the slope of $f/n$ at $g_*$, which is related to the rate of crossing at $g_*$ [see Eq. (16) below] significantly reduced in the presence of subcritical cluster diffusion ($a \neq 0$) compared with that in its absence. These two factors directly contribute to the reduction in the rate of nucleation.

### B. Nucleation rate

The nucleation rate in the presence of subcritical cluster loss by diffusion and thermophoretic drift is given by the flux of clusters in the size space past the critical size $g_*$,

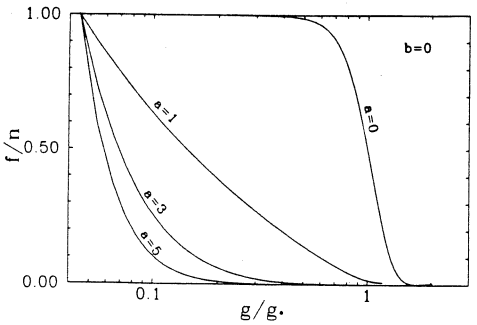


FIG. 2. Steady-state nonequilibrium cluster size distributions in the case of subcritical cluster loss by diffusion.

$$j(g_*) = -\beta(g)n(g)\frac{\partial}{\partial g}\frac{f(g)}{n(g)}\bigg|_{g=g_*} = j_u A\sqrt{\pi}2^{-(a+b)}\Gamma^{-1}\left(\frac{a+b+1}{2}\right), \quad (16)$$

where

$$j_u = \beta(g_*)n(g_*)(1/\sqrt{\pi}\delta)$$

is the rate of homogeneous nucleation in the absence of subcritical cluster loss but with other conditions being the same as in the inhomogeneous system (i.e., the same $T$ and $S$). As expected, $j(g_*)$ reduces to $j_u$ when $a = b = 0$, and the ratio $j(g_*)/j_u$ decreases with increasing values of $a$ and $b$. It is expected that $j(g_*)/j_u$ tends to zero as $a$ and/or $b \to \infty$. Eq. (16), however, does not produce this required limit. In fact the leading-order perturbation requires that $a < 3/\epsilon$ and $b < 3/\epsilon$. Thus, Eq. (16) underestimates the effect of subcritical cluster diffusion on the rate of nucleation for $a > 3/\epsilon$ and/or $b > 3/\epsilon$. (In figures presented below, we will indicate the calculations beyond these ranges by dashed lines.) A higher-order approximation in $\epsilon$ will give a solution that is valid over a wider range of $a$ and $b$. For the present purpose of studying the onset of homogeneous nucleation, it is sufficient to have this leading-order solution.

## IV. NUCLEATION IN SPATIALLY INHOMOGENEOUS SYSTEMS

### A. Particle formation in the horizontal epitaxial CVD reactor

The pyrolysis of silane ($SiH_4$) is widely used in epitaxial growth of silicon film.[6-16] Figure 1(a) indicates profiles that might be achieved in a CVD reactor in which a silicon compound is deposited from the gas phase onto a hot substrate. The reaction zone in which silicon atoms are formed from silane decomposition will be localized in a thin region near the hot surface.[6,9,10,13] Most of the silicon atoms will then diffuse to the substrate and undergo condensation to form a film. The higher deposition rates correspond to higher diffusion rates which can be achieved by steepening the concentration gradient at the interface, by increasing the silane partial pressure and by reducing the diffusion path length (reducing the total gas pressure).[6-8] An increase in silane concentration, however, does not always give a proportional increase in the deposition rate. There is a competing process which can cause nucleation of silicon vapor to form silicon particles in the gas phase resulting in a loss of silane and thus a reduction of silicon deposition rate, when the concentration of silicon atoms exceed the critical saturation ratio. Particle formed in CVD generally have a deleterious effect on film quality. At low gas temperatures the onset of gas-phase nucleation can probably be prevented, but to get a good crystalline quality of the epi-layer, a high substrate temperature (1050 °C or above) is usually required.[6,7]

Most of the work related to the onset of homogeneous nucleation of silicon vapor in epitaxial reactors has been experimental. Conventional nucleation theory has been used to investigate the temperature dependence of the nucleation rate of silicon vapor.[16] However, the main complexity in the

use of nucleation theory for such calculations is the great nonuniformity of the process when the subcritical cluster escapes as discussed in the introduction. With the necessary theoretical formulation developed above, we will investigate the implications of subcritical cluster loss by diffusion and drift on prevent from the onset of homogeneous nucleation of silicon vapor in epitaxial reactors.

First let us consider a case with the gas temperature of 1027 °C at the nucleation zone in a reactor charged with $H_2$ as a carrier gas of atmosphere pressure. Following classical nucleation theory,[16] and use the available data for the equilibrium vapor-solid pressure, the critical saturation ratio is 26.4 in the absence of subcritical cluster loss. At this otherwise critical saturation ratio $S = 26.4$, $a$ is about $12.84\phi$ and $b$ is $0.15\psi$ and the dependence of the ratio $j(g_*)/j_u$ on $a$ and $b$ is shown in Figs. 3(a) and 3(b). Here

$$\phi = \frac{1}{d}\left(\frac{1}{d_0} + \frac{3\omega}{2}\right),$$

$$\psi = 3\omega(1/d_2 + \omega),$$

$$a = \frac{4\pi}{9p_t}\sqrt{\frac{m_1}{m_c}}\left(\frac{kT}{s_1}\right)^3 \frac{\phi}{p_c S\sigma}, \tag{17}$$

and

$$b = \frac{2\sigma}{p_c p_t S \ln^2 S}\sqrt{2\pi \frac{m_1}{kT}}\frac{\nu R_g T\psi}{M_c}, \tag{18}$$

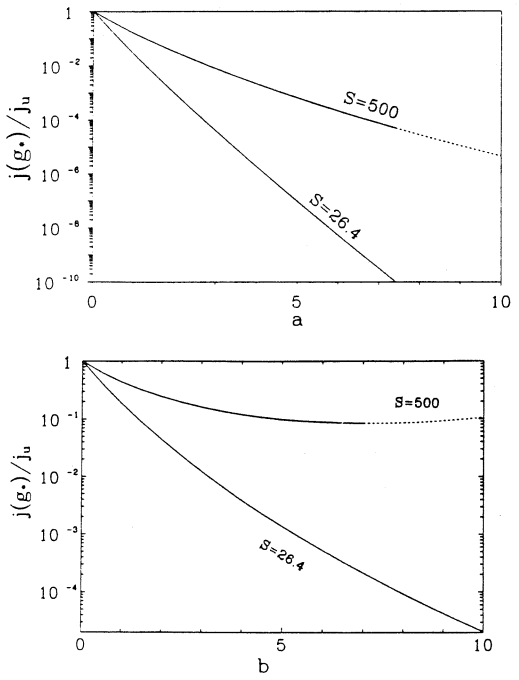


FIG. 3. Ratio between the rate of nucleation in presence of subcritical cluster loss in a horizontal epitaxial CVD reactor and that in its absence (a) by diffusion [$j(g_*)/j_u$ vs $a$ for $b = 0$] and (b) by thermophoretic drift [$j(g_*)/j_u$ vs $b$ for $a = 0$].

where the total pressure in the reactor is assumed mainly due to the carrier gas and $M_c$ is the molecular weight of the carrier gas and $R_g$ is the universal gas constant.

For an atmospheric CVD reactor with $H_2$ as the carrier gas, we can estimate $d_1 = 0.45$ cm, $d_0 = 0.3$ cm, $d_2 = 4.25$ cm based on available data.[13] If we also take $dT/dz = 1000$ °C/cm, we can obtain $\phi$ and $\psi$, thus $a$ and $b$. In this case, $a$ is about 142 and $b$ is 0.04. From Eq. (15) the ratio $j(g_*)/j_u$ is virtually zero for $S = 26.4$ Thus the onset of homogeneous nucleation of silicon vapor at this temperature is totally suppressed by the subcritical cluster loss due to the subcritical cluster loss by diffusion. Even at $S = 500$, $a$ is about 7.5 and the ratio $j(g_*)/j_u$ is about $10^{-10}$ while $j_u = 10^9$ cm$^{-3}$ s$^{-1}$. Thus the critical saturation ratio in the presence of subcritical cluster loss is about 20 times larger than that in its absence. The thermophoretic drift loss in both cases is negligible which is in contrast to previous suggestion.[6,7] Thermophoretic drift becomes relatively important for larger particles and becomes at least equally important as subcritical cluster diffusion at temperature exceeding $T = 1412$ °C.

In the above calculations, it is clear the thermal structure in the CVD reactor which determines the values of $d_0$, $d_1$, and $d_2$ is central in determining the relative importance of subcritical cluster loss to the onset of nucleation. As observed by Breiland *et al.*,[13] the maximum Si is very close to the substrate within 2 mm in a cell of 5 cm height when the substrate temperatures is in the range of 710–1000 °C. As the substrate temperature increases, the thermal boundary layer extends farther above the surface. The temperature at which silane rapidly decomposes thus occurs at larger distances ($d_1$) from the surface. Also the spatial range ($d_0$) over which particles are produced increases with increasing temperature as shown by the broadening of the profiles of Si.[13] Thus at a higher temperature, we expect a smaller $\phi$ and a smaller $\psi$ and thus a smaller effect of subcritical cluster diffusion on the nucleation rate. For example at $T = 1412$ °C, we take $d_1 = 1$ cm, $d_0 = 0.5$ cm, $d_2 = 3.5$ cm based on observed trends.[13] In this case $j(g_*)/j_u$ is $10^{-2}$ at the otherwise critical supersaturation ratio $S = 16$. This calculation shows that the kinetic nucleation barrier due to subcritical cluster loss by diffusion is also higher at lower temperature. Since at relatively low operating temperatures, the subcritical clusters take more time to accumulate in the gas phase, it should be relatively easy to suppress the occurrence of possible nucleation by optimizing operating total pressure and temperatures and using a light gas as the carrier.

The effect of carrier gas on the onset of homogeneous nucleation of silicon vapor in the CVD reactor can be in part explained by the present theory. It is observed that all other conditions being equal $H_2$ as a carrier gas suppresses particle formation compared to He, which cannot be simply accounted for by the chemical kinetic effect of $H_2$ on the gas-phase decomposition of silane.[9] The carrier gas effect is in part explained by the fact $a$ is 1.414 times larger and $b$ is 1.114 times larger in He than in $H_2$. It is noted that the effect of the possible changes in $d_0$, $d_1$, and $d_2$ due to different thermal structures in the He or $H_2$ carrier gas is not able to be evaluated.

According to Eqs. (17) and (18), $a$ and $b$ are inversely proportional to the total system pressure $p_t$ as the diffusion path lengths are inversely proportional to $p_t$. Thus a direct effect of reducing total pressure is to suppress the onset of homogeneous nucleation in the reactor. However, the position of the maximum in Si density in the reactor shifts up at a reduced pressure. It is observed that the position of this maximum shifts from 1 mm at atmosphere pressure to about 1 cm above the surface at a total pressure of about 20 Torr when the substrate temperature is 847 °C.[13] The same experiment also showed that the profiles at the reduced pressure become much broader than at an atmosphere pressure. Thus particle formation could occur in a much wider region at the reduced total pressure. Although $a$ and $b$ increase by a factor of 35 when from the reducing the total pressure from 760 to 20 Torr the change in $d_0$, $d_1$, and $d_2$, could outweigh this reduction.

Purely lowering the total pressure may not prevent the onset of homogeneous nucleation if a sufficiently thick thermal boundary layer is attained to reduce the efficiency of subcritical cluster loss by diffusion. This may have been why particle formation in the gas phase was still observed at lower pressure CVD (LPCVD).[9-10]

It is clear that the thermal structure in the CVD reactor is very important in determining the efficiency of subcritical cluster diffusion towards the substrate. If the relationship between the values of $d_0$ and $d_1$ and the total gas pressure and the substrate temperature is known experimentally[13] or by modelling,[13] one can use Eqs. (16)–(18) to select the optimal CVD conditions in order to minimize the possibility of occurrence of silicon particle formation in the gas phase while obtaining a high deposition rate for a given silane concentration.

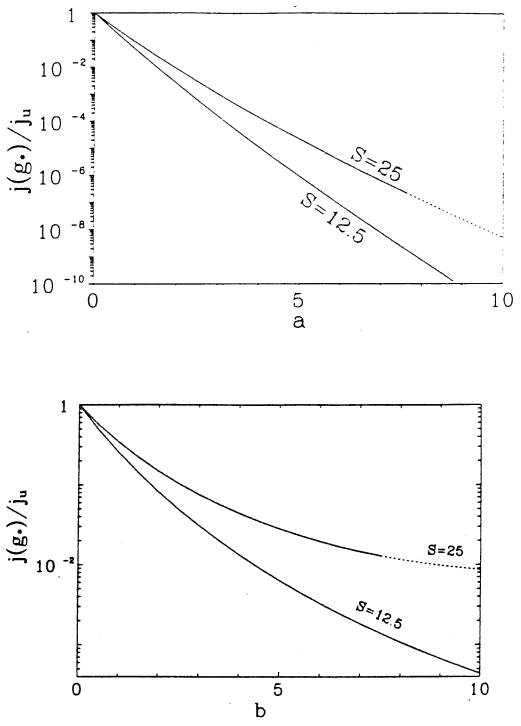


FIG. 4. Ratio between the rate of nucleation in presence of subcritical cluster loss in a diffusion cloud chamber and that in its absence (a) by diffusion [$j(g_*)/j_u$ vs $a$ for $b=0$)] and (b) by thermophoretic drift [$j(g_*)/j_u$ vs $b$ for $a=0$].

### B. Nucleation in diffusion cloud chambers

The diffusion cloud chamber is one of the principal methods for studying conditions for the onset of homogeneous nucleation. Supersaturation varies with elevation in a diffusion cloud chamber [Fig. 1(b)] and nucleation is observed in a thin region within the chamber. The possible effects of nonuniformities in the cloud chamber on the nucleation rate or the critical supersaturation ratio were suggested not to cause serious deviations from behavior in the absence of subcritical cluster loss for substances with equilibrium vapor pressures larger than $10^{-8}$ Torr.[2] It will be shown, however, that substantial deviations can be occurred for substances even with much higher equilibrium vapor pressures if the cloud chamber is operated at the reduced pressures.[17]

Consider a system with $\sigma=30$ dyne cm$^{-1}$, $s_1=1.5417\times10^{-14}$ cm$^2$, $m_1=1.6\times10^{-22}$ g, $T=20$ °C and $p_t=1$ atm with He as the carrier gas,[13] $a=4.6\times10^{-8}\phi/(p_c S)$, where $p_c$ is in Torr. As calculated earlier,[2] the critical supersaturation in the absence of subcritical cluster loss is about 12.5 for $p_c=10^{-5}$ Torr, and the value of $a$ is thus about $10^{-4}\phi$. The change of the ratio $j(g_*)/j_u$ with $a$ and $b$ for these conditions is shown in Figs. 4(a) and 4(b). Thus, there is no effect of subcritical cluster diffusion on the nucleation rate in this case if we take $\phi=5$ as adopted by Becker and Reiss.[2] The effect is found to be observable for equilibrium vapor pressures smaller than $10^{-8}$ Torr. At $p_c=10^{-8}$ Torr, $a=1.8$ and $b=6.6$ for $S=12.5$. Thus, the onset of nucleation in this case would be affected by diffusion as well as by thermophoretic. Their magnitudes are roughly equivalent, as seen from Fig. 4. Our calculations therefore confirm qualitatively the previous results[2] in which only the subcritical cluster loss only by diffusion was considered. It is also noted that the total pressure in the chamber is assumed at 1 atm.

The diffusion cloud chamber is usually operated at a reduced pressure. The total pressure in a chamber is required to satisfy the condition[17]

$$p_c\left(1-\frac{M_1}{M_c}\right)\left(1-\frac{T_0}{T_1}\right)^{-1}>p_t>2.5p_c, \tag{19}$$

where $M_1$ is molecular weight of the vapor, and $T_1$, $T_0$ are temperatures at the condensing and evaporating surfaces. The upper bound for $p_t$ is that at which the temperature gradient is balanced by a composition gradient in the vapor-gas mixture thus the thermal convection is prevented. The lower limit is estimated empirically, for which results are supposed to be independent of the amount of carrier gas used.

To maintain the difference between $j_u$ and $j(g_*)$ within a factor of $10^2$ requires $a < 1$, i.e., $p_v > 4 \times 10^{-4}$ Torr for the organic species considered above. In a similar way we require $b < 1$, i.e., $p_v > 1.1 \times 10^{-3}$ Torr. Here we have used $d_1 = 0.71h$, $d_2 = 0.19h$ and $h$ is the height of cell 4.23 cm as reported in Ref. 18. $d_0$ has been taken $0.1h$ as experimentally estimated by Daniel *et al.*[19] The resulting $\phi$ is about 4.32 and $\psi$ is about 0.25. Also we have used the upper bound for $p_i$ given by Eq. (19). We conclude that the onset of homogeneous nucleation will begin to be affected by subcritical cluster diffusion and thermophoretic drift when $p_v < 10^{-3}$ Torr. Under this condition, the subcritical cluster loss by thermophoretic drift becomes more important than that by diffusion.

It should be noted that the effect of diffusion and phoretic drift on nucleation does not limit to subcritical clusters loss. Nucleated particles, for example, can reach the upper surface before growing to a free fall size by action of phoretic forces at low pressures. Thus higher supersaturations are observed to maintain a same rate of nucleation.[20]

## V. CONCLUSION

We have investigated homogeneous nucleation process of a vapor in a spatially inhomogeneous system by extending classical nucleation theory to include subcritical cluster loss by diffusion and thermophoretic drift. Approximate analytic expressions have been obtained for cluster size distribution and rate of homogeneous nucleation. The primary results of this paper are those of Eqs. (16)–(18) which can be used to estimate the effect of subcritical cluster loss by diffusion and drift in a temperature field on the onset of homogeneous nucleation.


[1] N. A. Fuchs, *The Mechanics of Aerosols* (Dover, New York, 1989).
[2] C. Becker and H. Reiss, J. Chem. Phys. **65**, 2066 (1976).
[3] G. Shi and J. H. Seinfeld, J. Colloid Interface Sci. **135**, 252 (1990).
[4] G. Shi, J. H. Seinfeld, and K. Okuyama, Phys. Rev. A **41**, 2101 (1990).
[5] K. Binder, Rep. Prog. Phys. **50**, 783 (1987).
[6] F. C. Everstein, Philip Res. Repts. **26**, 134 (1971).
[7] J. Bloem, J. Cryst. Growth **18**, 70 (1973).
[8] J. U. M. S. Murthy, N. Miyamoto, M. Shimbo, and J. Nishizava, J. Cryst. Growth **33**, 1 (1976).
[9] Z. M. Qian, H. Michiel, A. Van Ammel, J. Nijs, and R. Mertens J. Electrochem. Soc. **135**, 2378 (1988).
[10] B. A. Scott, R. D. Estes, and J. M. Jasinski, J. Chem. Phys. **89**, 2544 (1988).
[11] G. Turban, Y. Catherine, and B. Grolleau, Thin Solid Films **60**, 147, (1979).
[12] C. W. Pearce, in *VLSI Technology*, edited by S. M. Sze (McGraw-Hill, New York, 1983).
[13] W. G. Breiland, P. Ho, and M. E. Coltrin, J. Appl. Phys. **60**, 1505 (1986) and references given therein.
[14] G. Hsu, R. Hogle, N. Rohatgi, and A. Morrison, J. Electrochem Soc. **1331**, 660 (1984).
[15] T. Furusawa, T. Kojima, and H. Hiroha, Chem. Eng. Sci. **43**, 2037 (1988).
[16] C. S. Herrick and D. W. Woodruff, J. Electrochem Soc. **131**, 2417 (1984).
[17] J. L. Katz, J. Chem. Phys. **52**, 4733 (1970).
[18] C-H. Hung, M. J. Kranopoler, and J. L. Katz, J. Chem. Phys. **90**, 1856 (1989); **92**, 7722 (E) (1990).
[19] C. F. Daniel, P. Ehrhard, and P. Mirabel, J. Chem. Phys. **75**, 4615 (1989).
[20] J. Smolik and J. Vitovec, J. Aerosol Sci. **13**, 587 (1982).

# CHAPTER 5

# SELECTIVE NUCLEATION OF SILICON CLUSTERS IN CVD

(Shi and Seinfeld, to appear in J. Mater. Res., July 1992)

# Selective Nucleation of Silicon Clusters in CVD

Frank G. Shi and John H. Seinfeld
Department of Chemical Engineering, 210-41
California Institute of Technology
Pasadena, California 91125

**Abstract**

A nucleation model is developed that includes chemical etching of atoms as an additional loss process besides thermal dissociation that competes with the process of atom addition in forming a cluster. The model has the proper qualitative features to describe observations of the evolution of cluster formation on amorphous silicon substrates in the low pressure CVD of a mixture of $SiH_2Cl_2/HCl/H_2$.

# 1 Introduction

Nucleation is generally treated as a thermal fluctuation-induced barrier-crossing process, in which the energy barrier results from the competition between atom or molecule addition and thermal dissociation in forming a cluster. Such a nucleation theory based solely on thermodynamic considerations has successfully been employed to obtain qualitative results for many complex problems including 3-D growth of epilayers,[1] bubble formation in liquid helium at negative pressure,[2] displacement transformation in metallic and non-metallic materials,[3] formation of voids in nuclear reactor materials,[4] and gas-phase nucleation.[5]

The same thermodynamics-based approach has also been used to examine gas phase and surface nucleation and growth problems in chemically reacting systems such as in CVD reactors. In a chemical reacting system, however, chemical processes may participate in the nucleus formation process directly besides providing the source for monomer. For example, Katz and Donohue[6] investigated the rate of nucleation when the arrival rate of condensing molecules and rate of surface chemical reaction are of similar magnitude. It is the goal of the present study to develop a nucleation model in chemically reacting systems where chemical etching of atoms from a cluster acts in addition to the loss due to thermal dissociation of atoms from the nucleus. By studying a particular system, a general framework for investigating complex nucleation problems in chemical reacting systems will be suggested. Such a framework enables one to gain a qualitative understanding of the nucleation process in many complex problems in chemical reacting

systems and can be useful in the improvement and design of processes to tailor nucleation to specific requirements.

The motivation for this study arises from the inability to interpret recent observations of the dynamic evolution of cluster formation on amorphous silicon surfaces in low pressure CVD systems in terms of any thermodynamics-based nucleation theory.[7,8] By measuring the cluster density and size distribution as a function of time, it is found that in the CVD of a mixture of $SiH_2Cl_2/HCl/H_2$ on $SiO_x, x < 2$, all the fine clusters of Si that are formed in the early stage of deposition do not survive in spite of the fact that they are much larger than the critical size for nucleation. It is observed, instead, that large crystalline clusters emerge when the fine ones suddenly disappear from the surface.[7,8] Using artificial nucleation sites of $Si_3N_4$ ($4\ \mu m \times 4\mu m$) on $SiO_2$, the same dynamic process can be observed, i.e., a large number of clusters formed initially on the nucleation sites disappear at the time when large crystalline clusters form.[7,8] Measurement of the time dependence of the surface coverage excludes the possibility that the observed abrupt reduction in the number of fine clusters by three orders of magnitude could be due to obscuration by large clusters. Since most of the observed large clusters have completely facetted shapes and a single crystalline structure except for twin boundaries, the possibility of coalescence of submicron clusters is also excluded. The total volume deposited is seen to have a hundred times increase when the fine clusters are reduced in number and large clusters emerge. Such a sharp increase in volume suggests that the large clusters could not be formed due to growth and contact with their neighbors, surface

migration of mobile clusters, or Ostwald ripening in an islanding process.[7,8] The possibility that fine clusters are dissociated into single atoms has been suggested with HCl (an etching agent of Si) playing a crucial role. The fine clusters would be etched by HCl accompanied by the emergence of large clusters with high growth rate.[7,8]

## 2 Competition Between Thermal Dissociation, Chemical Etching and Atom Addition: Generalized Gibbs Free Energy of Formation, $\Delta G$

Besides the competition between adatom addition and thermal dissociation, chemical processes may participate in forming clusters. Taking low pressure CVD of $SiH_2Cl_2/HCl/H_2$ as an example,[7–9] silicon adatoms will be produced dominantly by heterogeneous reactions on the substrate. HCl in the gas flow and/or Cl adsorbed on the substrate may etch silicon atoms away from the clusters as well as Si adatoms from the substrate. The consequence of the participation of atom etching on the formation process of clusters can be investigated by studying the generalized Gibbs free energy of cluster formation.

Three processes are involved in forming a cluster, adatom addition, thermal dissociation and etching. The rate of adatom addition to a cluster of size $g$ is $\beta_s g^{1/3}$. Here $\beta_s$ is proportional to the number concentration of adatoms, the diffusion rate of adatoms on the substrate. The process of adatom addition is assumed to be diffusion-limited[10,11] since silicon adatoms will be produced dominantly by heterogeneous reactions on the substrate for the system considered. Therefore the rate of adatom addition is taken pro-

portional to the radius of the cluster ($\propto g^{1/3}$). The thermal dissociation coefficient for a single atom from a $(g+1)$-sized cluster, $\alpha_{g+1}$, can be expressed in terms of the rate of adatom addition to a cluster of size $g$ by detailed balancing.[10,11] It is noted that the exact expressions for $\beta_s$ and $\alpha$ are not necessary to be known to continue our analysis.

The etching process of Si atoms from the cluster is assumed mainly due to HCl. This assumption is reasonable. Since the adsorption of atomic chlorine on silicon is very weak,[12] the etching of Si atoms from the cluster due to the adsorbed Cl is small. Considering the uncertainties associated with the previous measurements,[12] even if the adsorbed Cl is relative high, the adsorbed Cl may immediately react with Si adatoms with a very small number of the adsorbed Cl left to attack the Si clusters. Accordingly, the etching process of Si atoms from the cluster is taken to be mainly due to the HCl either produced from the source gas reaction or supplemented from an external source.[7,8] The etching rate on a silicon $g+1$-sized cluster is therefore proportional to the surface area of the cluster, $(g+1)^{2/3}/t_e$ for the case of surface site-limited reaction, where $1/t_e$ is the specific etching rate. If all the atoms constituting the cluster can be taken as reaction sites, the etching rate is proportional to the number of atoms in the cluster, $(g+1)/t_e$.

The net rate at which clusters grow from size $g$ to size $g+1$, $j_g$, can be written as

$$j_g = f_g \beta_s g^{1/3} - f_{g+1}[\alpha_{g+1} g^{1/3} + \frac{(g+1)^{2/3}}{t_e}], \qquad (1)$$

where $f_g$ is the cluster size distribution at time $t$. In the absence of chemical etching, we have the following relation for the metastable equilibrium cluster

size distribution $n_g$,

$$n_g\beta_s = n_{g+1}\alpha_{g+1}, \tag{2}$$

By analogy, in the presence of chemical etching the equilibrium distribution, $c_g$, is

$$c_g\beta_s g^{1/3} = c_{g+1}[\alpha_{g+1}g^{1/3} + \frac{1}{t_e}(g+1)^{2/3}], \tag{3}$$

Thus

$$\frac{c_{g+1}}{c_g} = \frac{n_{g+1}/n_g}{1 + \frac{(g+1)^{2/3}}{g^{1/3}t_e\alpha_{g+1}}}. \tag{4}$$

By using Eqs. [2] and [3], and the fact that $n_1 = c_1$, Eq. [4] can be written as

$$c_g = n_g \exp[-\sum_{i=1}^{g-1} \ln[1 + \frac{(i+2+\frac{1}{i})^{2/3}}{t_e\alpha_{i+1}}]]. \tag{5}$$

The above expression is obtained in a similar way to that obtained for the electron-hole drop formation within Ge and Si.[13]

For an etching rate proportional to $g$,

$$c_g = n_g \exp[-\sum_{i=1}^{g-1} \ln(1 + \frac{(i^{2/3} + i^{-1/3})}{t_e\alpha_{i+1}})]. \tag{6}$$

From Eq. [5], the generalized nucleation free energy barrier for the cluster formation process as described above is given by,

$$\Delta G_g = \Delta G_g^0 + kT\sum_{i=1}^{g-1} \ln[1 + \frac{(i+2+\frac{1}{i})^{1/3}}{t_e\alpha_{i+1}}], \tag{7}$$

where $\Delta G_g^0$ can be taken as the classical Gibbs free energy of formation,[10,11] or the Gibbs free energy given by the atomistic theory.[10,11]

# 3 Nucleation of Silicon Clusters in the Presence of Etching

It is seen from Eq. [7] that the free energy barrier for nucleation is modified in the presence of chemical etching compared with that in its absence. Fig. 1 shows $\Delta G_g$ as a function of the cluster size $g$ for different values of the ratio between the rate of adatom addition and the etching rate,

$$\chi_s \equiv \frac{1}{\beta_s t_e} = \frac{\text{etching rate}}{\text{addition rate}}. \tag{8}$$

For simplicity, the model from classical nucleation theory is used for $\Delta G_g^0$.[10,11] The parameters used in $\Delta G_g^0$ include supersaturation ratio, $S$, which is defined by the ratio of the concentration of the adatom and its equilibrium value and $u(\omega)\theta$, where for an assumed spherical cap nucleus $u(\omega) = \frac{1}{4}(2 + \cos\omega)(1 - \cos\omega)^2$ is a geometrical factor[11] and $\theta = s_1\sigma/kT$ with $s_1 = 4\pi^{1/3}3{v_1}^{2/3}$, $v_1$ is the atomic volume in the cluster, and $\sigma$ is the specific surface free energy of the cluster. For $\sigma = 1000$ ergs/cm$^2$ as cited in Ref. 14, then $\theta$ is about 21 at the temperature of deposition $T = 1223$K.[7,8] If the specific surface energies are taken equal to the surface tensions estimated by the method suggested in Ref. 17, $\sigma$ is about 820 ergs/cm$^2$. Thus $\theta$ can be considered to vary in the range of 10 to 20. SEM (Scanning Electron Microscopy) micrographies[7,8,15] show that nuclei are indeed of hemispherical shape with a contact angle $\omega > 90^o$. For $\omega > 90^o$, $u(\omega) \approx 1$. Thus typical values of $\theta u$ are taken to vary from 10 to 20 in the following discussion. However, it should be noted that the results presented in this paper are not affected qualitatively by the values assigned to the parameters.

The curves in Fig. 1 are labeled with the values of $\chi_s$ which is proportional to the ratio of the adatom addition rate $\beta_s$, and the chemical etching rate, $1/t_e$. The etching rate is $k_e p_{HCl}^2(1-\cos\omega)/2$ for the following mechanism, $(\mathrm{Si})_g + 2\mathrm{HCl} \rightarrow \mathrm{SiCl_2} \uparrow + \mathrm{H_2} + (\mathrm{Si})_{g-1}$ where $(\mathrm{Si})_g$ represents a $g-$sized silicon cluster, where $k_e$ is the forward rate constant for above etching reaction.

## 3.1 Conditions for Suppressing Surface Nucleation

For a given $S$ and $u(\omega)\theta$, the evolution of the free energy curve with the increase of the ratio between the etching rate and the collision rate can be described as follows.

First, if the ratio of the etching rate and the collision rate, $\chi_s$, is sufficiently small, for example $\chi_s < 0.1$ for $S = 100, \theta u = 15$ as shown in Fig.1, the $\Delta G$ curve is virtually the same as that in the absence of HCl or/and Cl etching of Si clusters, i.e., there is a maximum of $\Delta G$ at the critical cluster size $g_{c*}$. As $\chi_s$ increases, the $\Delta G$ curves have not only a maximum corresponding to the critical cluster size but also exhibit a minimum corresponding to the stable cluster size $g_{cs}$ which results from the balance between the atom addition and the HCl etching of the Si clusters. Fig. 1 shows that the stable cluster size decreases with an increase in $\chi_s$. As $\chi_s$ approaches a limit, about 0.24 for $S = 100, \theta u = 15$, the critical cluster size and the stable size merge and $\Delta G$ increases linearly with $g$. Beyond this limit, the critical cluster size is infinity and nucleation is completely suppressed by the HCl or/and Cl etching of the subcritical silicon clusters.

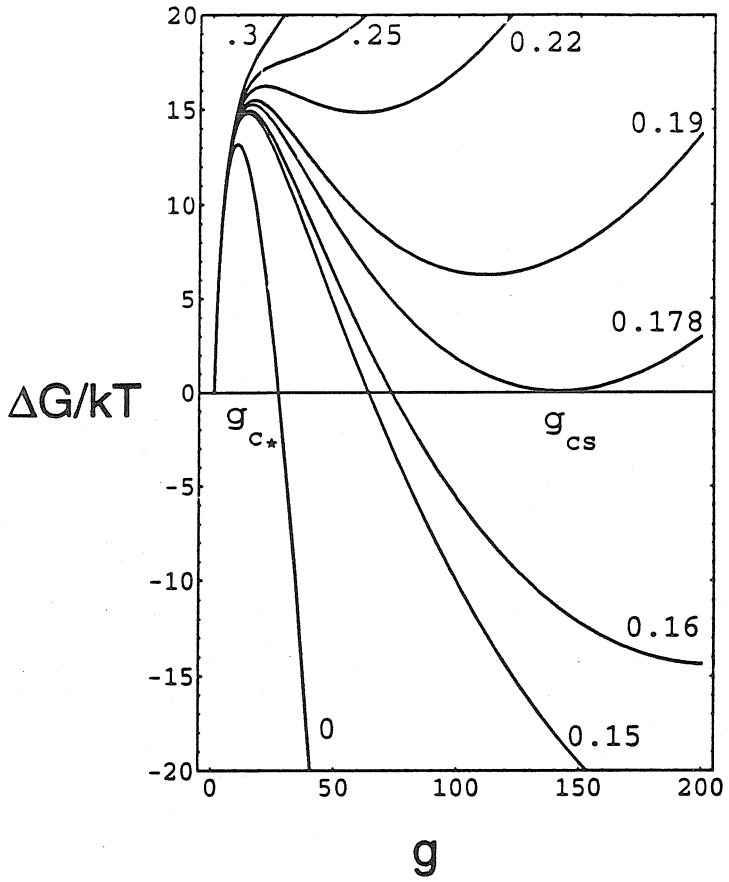


Figure 1. Generalized Gibbs free energy of nucleation $\Delta G(g)$, for diffusional adatom addition, for different values of the ratio $\chi_s$ at S=100 and $\theta$ u($\omega$)=15. At the first critical value of the ratio $\chi_s$, 0.178, all of the nucleated clusters will be dissociated by chemical etching of clusters. At the second critical value of the ratio $\chi_s$, about 0.24, the critical cluster size becomes infinity and the stable cluster size disappears.

By examining the relation

$$\frac{\partial \Delta G(g)}{\partial g} = 0 \tag{9}$$

the limiting values of $\chi_s$ beyond which nucleation is totally suppressed can be found as a function of $S$ and $\theta u$. If $g$ is treated as a continuous variable in the context of classical nucleation theory,[11] Eq. [7] can be rewritten as,

$$\Delta G(g) = \Delta G^0(g) + kT \int_1^g \ln[1 + \frac{(x + 2 + \frac{1}{x})^{1/3}}{t_e \alpha (x+1)}]dx, \tag{10}$$

where $\Delta G(g)$, $\Delta G^0(g)$ and $\alpha(g+1)$ are the continuous versions of $\Delta G_g$, $\Delta G_g^0$ and $\alpha_{g+1}$. Then Eq. [9] leads to the following relation,

$$\exp[\frac{2\theta u(\omega)}{3g_c^{1/3}}] = S[1 - \frac{1}{t_e \beta_s} \frac{(g_c+1)^{2/3}}{g_c^{1/3}}], \tag{11}$$

where $g_c$ is the critical value corresponding to $\frac{\partial \Delta G(g)}{\partial g} = 0$.

The relation between $g_c/g_*$ and $\chi_s$ given by Eq. [11] is shown in Fig. 2 for a given value of $u(\omega)\theta$ (=15) and a range of values of $S$, 10, 100 and 1000; and in Fig. 3 for a given $S$(=100) for typical values of $u(\omega)\theta$, 10, 15, 20. As shown in Figs. 3 and 4, $g_c$ equals $g_*$, the critical cluster size in the absence of chemical etching of clusters when $\chi_s = 0$. For $\chi_s < 0.1$ for $S = 100$, $g_c \approx g_*$, that is no significant effect is expected when the etching rate is smaller than about one tenth of the collision rate between the cluster and the adatoms. This should be the case at the initial stage of CVD. $g_c$ becomes a dual-valued function of $\chi_s$ as the ratio exceeds a certain value (about 0.1 for $S = 100$). The dual values of $g_c$ for a given $\chi_s$ are that of the critical cluster size and stable size. As shown in Figs. 2 and 3, the critical size ($g_{cs}$) for nucleation is almost the same as that in the absence of chemical

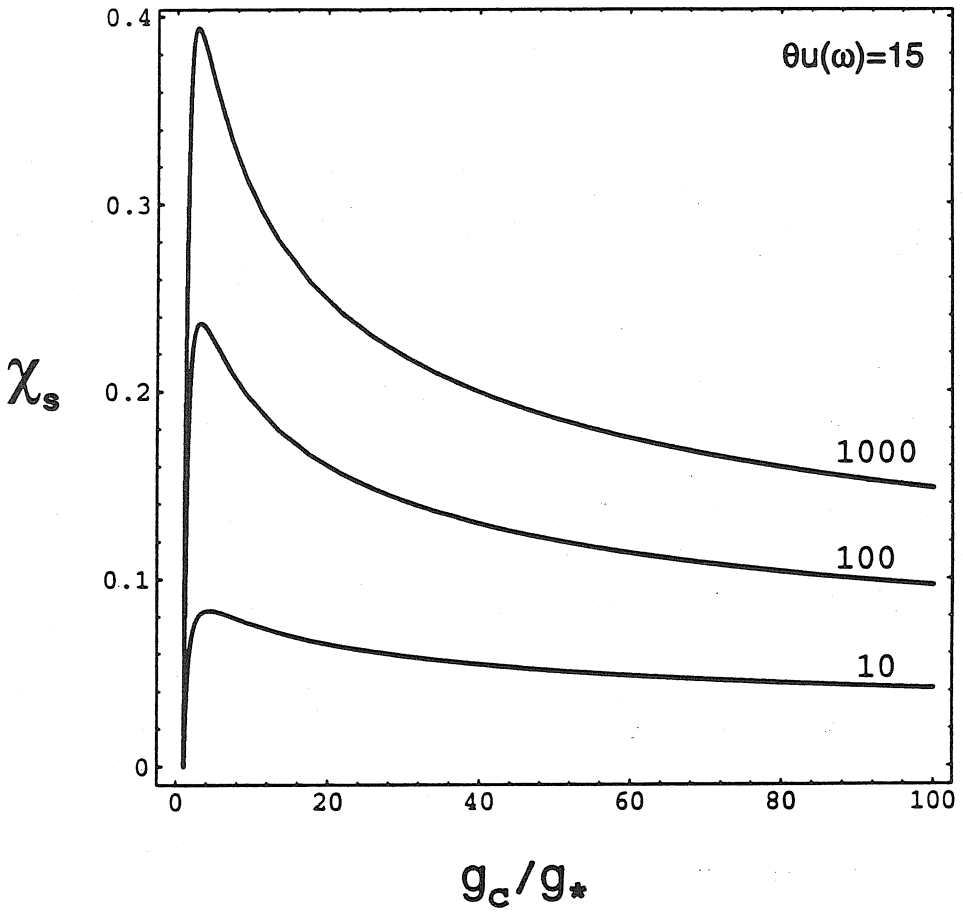


Figure 2. The ratio $g_c/g_*$ of the "critical" cluster size in the presence of chemical etching, of clusters, $g_c$, and the critical cluster cluster size for nucleation in the absence of chemical etching $g_*$, as a function of $\chi_s$ for the chemical etching rate of the silicon clusters and the adatom addition rate, for S=10, 100 and 1000 at $\theta\, u(\omega)=15$. Dual values of $g_c$ for certain ranges of $\chi_s$ correspond to the critical cluster size , $g_c$, and the stable cluster size, $g_{cs}$.

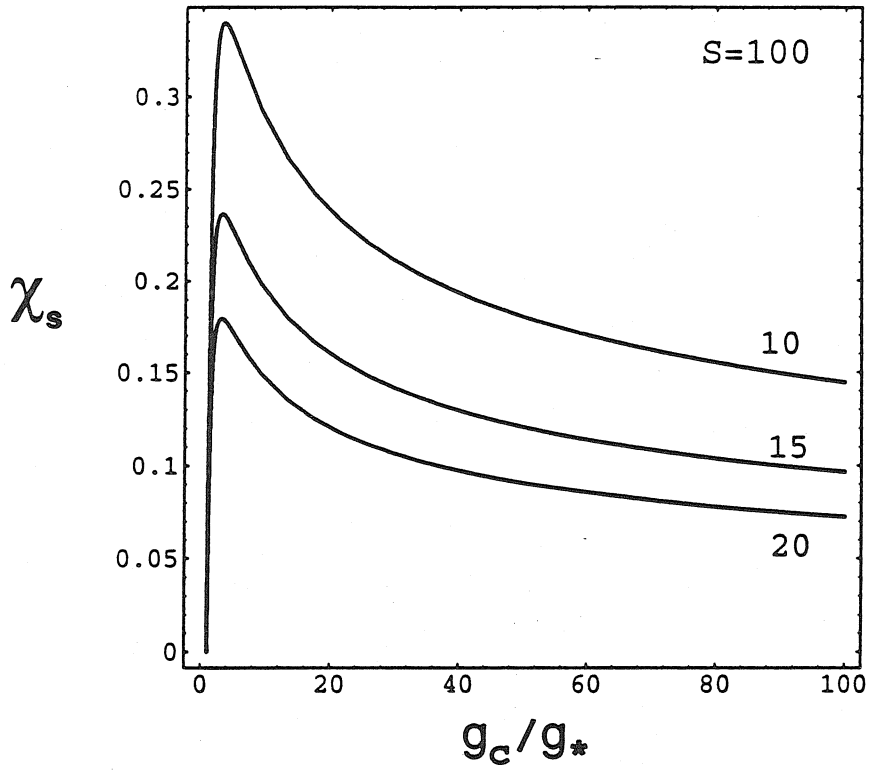


Figure 3. $g_c/g_*$ as a function of $\chi_s$ for $\theta$ u($\omega$)=10, 15 and 20 at S=100. Dual values of $g_c$ for certain ranges of $\chi_s$ correspond to the critical cluster size for nucleation, $g_{c*}$ , and the stable cluster size, $g_{cs}$ .

etching of the subcritical clusters, $g_*$, for $\chi_s$ belows its second critical value (about 0.24 for $S = 100$). While the stable size decreases significantly with increasing $\chi_s$ until the second critical value of $\chi_s$, the critical size and the stable size become identical, or, more precisely, the two sizes disappear. Beyond that limit, nucleation is suppressed completely because of chemical etching. In other words, there is a second critical value, different for different $S$ and $\theta u$ for $\chi_s$, where a small increase in the etching rate or a decrease in the collision rate can lead the critical cluster size to change from $g_{c*} \approx g_*$ to infinity.

For an etching rate proportional to $g^{2/3}$ and $g_{cs} >> g_{c*}$,

$$g_{c*} \approx g_* \approx [\frac{2\theta}{3\ln S} u(\omega)]^3. \tag{12}$$

For an etching rate proportional to $g$, we have the same $g_{c*}$.

## 3.2 Abrupt Change of Cluster Number

Also shown in Fig. 1, there is another critical value (0.178) for $\chi_s$. At $\chi_s = 0.178$, the free energy barrier for forming the clusters is equal to that for dissociating the nucleated clusters of size $g_{cs}$ by HCl or/and Cl etching. In other words, at and above the critical value of $\chi_s = 0.178$ at $S = 100$ and $\theta u(\omega) = 15$, all of the clusters nucleated will eventually dissociate back into single atoms by chemical etching (backward nucleation); no single cluster nucleated by the forward nucleation can survive.

As will be discussed in detail in Section 4, this is relevant to the experimentally observed abrupt change in the total number concentration of clusters on the surface,[7,8]

## 3.3 Conditions for Forming Equal-Sized Clusters

As shown in Fig. 1, only for $\chi_s$ smaller than its critical value, 0.178, some of the nucleated clusters will stay at the same size, $g_{cs}$. The formation of equal-sized stable clusters is basically the result of the balance between the etching process and the atom addition process. The formation rate of the surviving stable clusters will be proportional to the difference between the forward and backward nucleation rates. The time scale for the forward nucleation is the same order of magnitude as the collision rate between the critical cluster and the adatoms. The time scale for backward nucleation is of the same order of magnitude as that of the etching process. Since the etching rate of silicon clusters is the same order of magnitude as the collision rate,[16] the two time scales are expected to be the same order of magnitude.

The stable cluster size can be obtained from Eq. [11]. For an etching rate proportional to $g^{2/3}$ and $g_{cs} >> g_{c*}$,

$$g_{cs} \approx [t_e \beta_s (1 - \frac{1}{S})]^3. \tag{13}$$

For an etching rate proportional to $g$, we have the same $g_{c*}$ but

$$g_{cs} \approx [t_e \beta_s (1 - \frac{1}{S})]^{3/2}. \tag{14}$$

## 3.4 Continuing Growth of Surviving Stable Clusters: Role of Direct Impingement

Since the adatom concentration decreases with the deposition time due to the decrease of the available adsorption sites on the substrate, the dominant mode of adsorbing adatoms will change to that of direct impingement from

the vapor phase. The mode change can have an important consequence; the surviving clusters limited to the stable size $g_{cs}$ can continue to grow.

In the case of direct impingement from the vapor phase, the rate of addition of atoms to a cluster of size $g$ is given by

$$\beta_v g^{2/3} = 4\pi r_1^2 g^{2/3} \eta n_{1v} (\frac{kT}{2\pi M_{iv}})^{1/2}, \tag{15}$$

where $n_{1v}$ is the number concentration of the compound containing Si in the gas phase and $M_{1v}$ is the molecular weight of the compound and $\eta$ is the transformation efficiency from the Si-containing compound, absorbed on the cluster surface into Si atoms. Then

$$j_g = f_g \beta_v g^{2/3} - f_{g+1}[\alpha_{g+1}^v g^{2/3} + \frac{(g+1)^{2/3}}{t_e}], \tag{16}$$

where

$$\alpha_{g+1}^v = \beta_v \exp(\frac{\Delta G_{g+1} - \Delta G_g}{kT})$$

.

By repeating the steps in Section 3.1, we can obtain the generalized energy barrier as a result of competition between the atom addition from the direct impingement from the vapor phase and the atom loss due to thermal dissociation and chemical etching, as

$$\Delta G_g = \Delta G_g^0 + kT \sum_{i=1}^{g-1} \ln[1 + \frac{(1+1/i)^{2/3}}{t_e \alpha_{i+1}^v}] \tag{17}$$

with the corresponding critical cluster size given by the following relation,

$$\exp[\frac{2\theta u(\omega)}{3g_c^{1/3}}] = S[1 - \frac{1}{t_e \beta_s} \frac{(g_c+1)^{2/3}}{g_c^{2/3}}]. \tag{18}$$

The above relation is shown in Fig. 4 for different values of $S$, 10, 100, 1000 and $\theta u(\omega) = 15$. It can be seen that, differing from the case of nucleation by the mechanism of adatom diffusion, the $g_c$ is a single-valued function of $\chi_v \equiv \frac{1}{t_e \beta_v}$. In the present case, $g_c$ is the critical cluster size for nucleation, $g_{n*}$. Fig. 4 shows that $g_{n*}$ increases with increasing $\chi_v$. As $\chi_v$ approaches some limiting values which are much larger than the second critical value for $\chi_v$, nucleation becomes totally suppressed by chemical etching of Si clusters since $g_{c*}$ approaches infinity. Before reaching the critical value for the ratio of $\chi_v$, the surviving trapped clusters nucleated by adatom diffusion can grow without thermodynamic and chemical limits, if their sizes exceed $g_{n*}$. This also can be seen from Fig. 5 which shows the nucleation energy barrier given by Eq. [17].

# 4 Evolution of Cluster Number Concentration with Deposition Time

The foregoing analysis aids in interpreting the newly observed dynamical phenomena of cluster formation on $a$-Si substrates in the CVD system of $SiH_2Cl_2/HCl/H_2$ which are not explainable by using the conventional nucleation and growth theory.[7,8] The main interest lies in the abrupt drop in the total cluster number concentration on the substrate and the abrupt disappearance of small clusters on the substrate accompanied by the appearance of the large clusters.

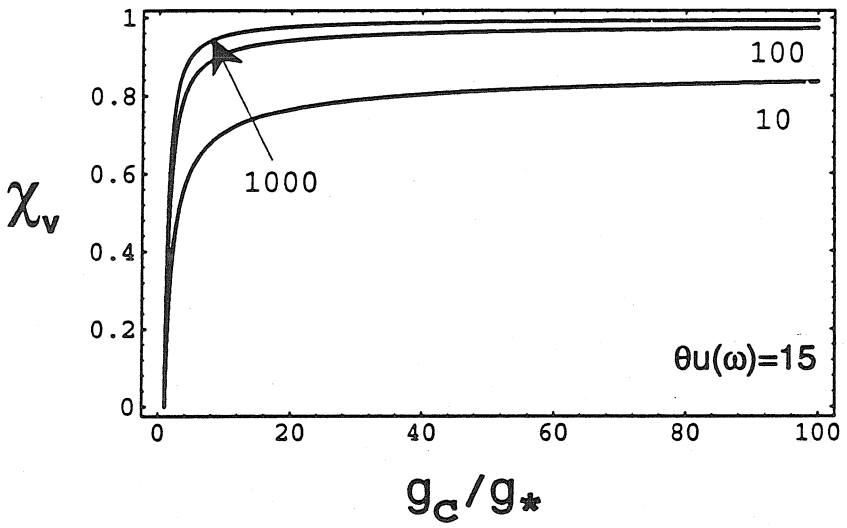


Figure 4. $g_c/g_*$ as a function of $\chi_s$ for S=10, 100 and 1000 at θ u(ω)=15. Differing from the case of the diffusion-limited atom addition, $g_c$ is a single-valued function of $\chi_v = 1/\tau_e\beta_v$. As $\chi_v$ approaches some limiting values, $g_{c*}$ approaches infinity.

## 4.1 Ratio $\chi_s$ in the CVD system of $SiH_2Cl_2/HCl/H_2$

The key parameter is the ratio between the etching rate and the collision rate of a cluster with the adatoms, $\chi_s$. The two rates are estimated to be of the same order of magnitude, i.e, about $1\mu$m per second for the particular experiments.[16] Since the experiments were done for constant deposition conditions, the input concentration of HCl is constant but the concentration of HCl in the CVD reactor increases with the deposition time since the reactions in the system of $SiH_2Cl_2/HCl/H_2$ can also generate HCl. Also $\beta_s \propto n_1$ where $n_1$ is the number concentration of adatoms. Since $n_1$ is limited by the available adsorption sites which decrease with time. Thus $\chi_s$ and the critical cluster size increase with the deposition time. As $\chi_s$ approaches the first critical value (for example, 0.178 for $S$=100 and $\theta u = 15$ in Fig. 1) the net nucleation will be zero, that is the formation nucleation rate equals the backward nucleation rate (by chemical etching). As $\chi_s$ approaches the second critical value (e.g.,$\approx 0.24$ for $S$=100 and $\theta u = 15$ in Fig. 1 or Fig. 2), forward nucleation by the adatom diffusion mechanism is totally suppressed.

## 4.2 Evolution of Cluster Number Concentration with Deposition Time

At the initial stage of the CVD deposition of silicon, and the ratio $\chi_s$ is small, the surface nucleation of silicon by adatom diffusion can proceed relatively easy since the critical cluster size is virtually the same as that in the absence of chemical etching (Figs. 1 and 2). The number concentration of clusters formed on the surface is limited by the available adsorption sites which decreases with time, and the ratio $\chi_s$ therefore increases with the

deposition time. Since the critical cluster size for nucleation, $g_{c*}$, is not affected by the ratio $\chi_s$ when the ratio is below its second critical value, the forward nucleation can proceed without a significant effect of chemical etching. However, as the ratio $\chi_s$ increases, the backward nucleation rate increases. As the ratio $\chi_s$ reaches the first critical value when the free energy barrier for the forward and backward nucleations become equal, all clusters formed by the forward nucleation will eventually disappear from the substrate.

As the ratio of $\chi_s$ approaches the second critical value at which the critical cluster size and the stable cluster size merge, a small increase in the ratio can cause the critical cluster size to change abruptly from $g_{c*} \approx g_*$ to infinity. No further forward nucleation can occur.

The total cluster number concentration on the substrate reaches a maximum value[7,8] (see Fig. 1 in Ref. 7) when the forward nucleation rate equals the backward nucleation rate. The total number concentration of clusters on the substrate should remain constant until the ratio $\chi_s$ reaches the second critical value. Since the critical cluster size changes abruptly to infinity around the second critical value, the nucleated clusters will experience an abrupt increase in the etching rate, resulting in a sudden drop in the total number concentration of clusters on the substrate as observed experimentally[7,8] (see Fig. 2 in ref. 7). This is also the reason for the abrupt disappearance of small clusters from the substrate. Thus it is concluded that *the maximum cluster concentration is reached when the ratio of* $\chi_s$ *reaches the first critical value; the sudden drop in the total cluster concentration*

*and the sudden disappearance of the small clusters occur when the ratio $\chi_s$ reaches the second critical value.*

## 4.3 Growth of Stable Clusters

At the early stage of CVD deposition, the cluster size distribution is found to have a single peak[7,8] (see Fig. 3 in ref. 7) which should correspond to the stable cluster size of the surviving clusters as predicted by the present model. But if the surface adatom diffusion is the only atom addition mechanism, the largest cluster size will be limited to be that of the stable cluster, $g_{cs}$ as shown in Fig. 1. The dominant mechanism for atom addition will change from adatom diffusion to direct impingement from the vapor phase when the rate of the latter mechanism is larger than that of the former. Direct impingement from the vapor can bring the stable clusters, limited to the size of $g_{cs}$, out of the trap. The liberated clusters can continue to grow without thermodynamic limit (see Fig. 5), except when the ratio $\chi_v$ reaches its critical value (see Fig. 4 ). Thus the trapped stable cluster predicted by considering adatom diffusion only, with their size larger than $g_{n*}$, can be liberated from the trap and continue to grow by direct impingement from the vapor phase.

If the mode change of atom addition happens at or just after the time when $\chi_s$ reaches its second critical value, it is expected to observe the formation of large clusters accompanied by a sudden drop in the total number of clusters.

Although the mechanisms of direct impingement from the vapor and adatom diffusion act simultaneously, only when the rate of atom addition

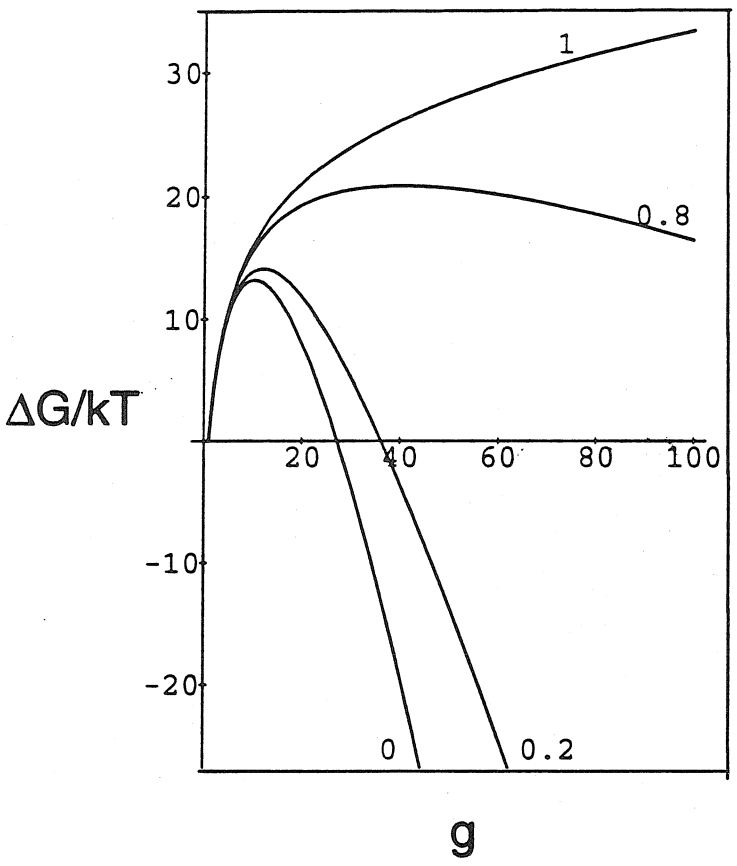


Figure 5. Generalized Gibbs free energy of nucleation for the direct impingement from the vapor phase, $\Delta G(g)$ as a function of g for a range of values of $\chi_v$ at S=100 and $\theta u(\omega)=15$.

by the former mechanism is larger than that of the latter, will the clusters trapped at the stable size will continue to grow. The stable sizes depend on the ratio $\chi_s$ (see Fig. 1) which changes with the deposition time. Not all of the trapped clusters can be reactivated by direct impingement from the vapor phase since not all of them exceed $g_{n*}$. This explains why the number concentration of the large clusters is much smaller than that at stable size.

Before $\chi_s$ reaches the critical value, the collision rate by adatom diffusion ($\beta_s g^{1/3}$) can be smaller than the rate due to direct impingement from the vapor phase ($\beta_v g^{2/3}$). For $\beta_s g^{1/3} < \beta_v g^{2/3}$, $\beta_v$ can still be far smaller than $\beta_s$. A smaller $\beta_v$ can correspond to a larger cluster size than that by adatom diffusion. As shown in Fig. 4 as the ratio of $\chi_v$ reaches its own critical value, a small increase in the ratio also can lead to the critical cluster size have a sudden change to infinity. In that case, all survived clusters formed by the adatom diffusion mechanism will eventually be etched from the substrate. This seems not to be the case for the experiments concerned.[7,8]

# 5 Conclusion

We have reported the development of a nucleation model in which direct chemical etching of atoms from a nucleus is treated as an additional process to atom addition and atom dissociation to and from a nucleus.

The important consequence is that the ratio between the rate of atom addition and the rate of chemical etching plays a crucial role in cluster formation dynamics. It is found that by adjusting operational conditions to change the ratio between atom addition and chemical etching, it is possible

to suppress nucleation completely or to form equal-sized clusters.

The analysis aids in understanding the physical and chemical origins of the newly observed dynamical phenomena of cluster formation on $a$-Si substrates in the CVD system of $SiH_2Cl_2/HCl/H_2$ which are not explainable by conventional nucleation and growth theory.[7,8]

## 6 Acknowledgment

The authors are grateful for useful discussions with Dr. T. Yonehara, Dr. R. C. Flagan and Dr. K. Okuyama.

## References

[1]K. Jagannadham and J. Naragyan, J. Elect. Mater. **20**, 767(1991)

[2]H. J. Maris and Q. Xiong, Phys. Rev. Lett. **63**, 1078(1989)

[3]L. E. Tanner and M. Wuttig, Mater. Sci. and Eng. **A127**, 137(1990)

[4]A. M. Yacout and J. F. Stubbins, Rad. Eff. Defc. in Solids, **117**, 363(1991); J. L. Katz and H. Wiedersich, J. Chem. Phys. **55**, 1414(1971)

[5]R. E. Heist and H. Reiss, J. Chem. Phys. **59**, 1025(1973)

[6]J. L. Katz and M. D. Donohue, J. Coll. and Interf. Sci. **85**, 267(1982)

[7]H. Kumomi, T. Yonehara, Y. Nishigaki and N. Sato, Appl. Surf. Sci. **41/42**, 638(1989)

[8]H. Kumomi, T. Yonehara, Appl. Phys. Lett. **54**, 2648 (1989)

[9]M. R. Goulding, J. de Phys.**C2**,745(1991); J. W. Osenbach, D. G. Schimmel, A. Feygenson, J. J. Bastek, J. C. C. Tsai, H. C. Praefcke and E. W. Bonato, J. Mater. Res. **6**, 2381(1991); J-O Carlsson, Crit. Rev. Solid State and Mater. Sci. **16**, 161(1990) and references therein

[10]J. A. Venables, Philos. Mag., **27**, 697(1973)

[11]B. Lewis and J. C. Anderson *Nucleation and Growth of Thin Films*, (Academic Press, New York, 1978)

[12]W. A. P. Claassen and J. Bloem, J. Electrochem. Soc.**128**, 1353(1981); M. Miyamara, Y. Sakisaka, M. Nishijma and M. Onchi, Surf. Sci. **72**, 243(1978)

[13]R. M. Westervelt, Phys. Stat. Sol. (b) **74**, 727(1976)

[14]W. A. P. Claassen and J. Bloem, J. Electrochem. Soc.**127**, 194(1980)

[15]T. R. Yew and R. Reif, J. Appl. Phys. **65**, 25001989)

[16]Personal Communication With Dr. T. Yonehara

[17]C. L. Yaws, L. L. Dickens, R. Lutwack and G. Hsu, Solid-State Technol. **24**, 87(1981)

# PART II

# TRANSIENT KINETICS OF NUCLEATION AND CRYSTALLIZATION

# CHAPTER 6

# TRANSIENT KINETICS OF UNIARY NUCLEATION

PHYSICAL REVIEW A VOLUME 41, NUMBER 4 15 FEBRUARY 1990

# Transient kinetics of nucleation

G. Shi and J. H. Seinfeld
*Department of Chemical Engineering, California Institute of Technology, Pasadena, California 91125*

K. Okuyama
*Department of Chemical Engineering, University of Osaka Prefecture, Sakai, Osaka 591, Japan*
(Received 7 September 1989)

Analytical solutions for the time-dependent cluster concentrations and nucleation rate in homogeneous nucleation are obtained by the singular perturbation approach. The effect of cluster scavenging by free molecule particles on the kinetics of nucleation is also investigated through analogous analytical solutions in this case. Apparent conflicting suggestions in the literature concerning the time lag of nucleation are resolved.

## I. INTRODUCTION

When the saturation ratio of a vapor is suddenly increased to a value at which homogeneous nucleation occurs, a transient period exists during which the cluster concentrations increase to their eventual steady-state values, and the nucleation rate, defined as the flux of clusters past the critical size, also increases to its steady-state value corresponding to the new vapor saturation ratio. In an effort to understand the general character of nucleation phenomena and the observations in nucleation experiments that utilize sudden changes in saturation ratio, such as expansion cloud chambers, expansion nozzles, and free-molecular expansion methods,[1] the duration of the transient period in nucleation is of interest.

Under actual nucleation conditions preexisting particles are frequently present that act as scavengers for the vapor molecules and clusters, thereby depressing the rate of new particle formation by nucleation below that in their absence. One needs also to understand the effect of preexisting particles on the transient nucleation kinetics; that is, for example, is the characteristic time required to establish a steady-state nucleation rate increased or decreased in the presence of preexisting particles over that in their absence? Such open systems occur in many different situations, such as nucleation in the presence of cluster scavenging by a preexisting aerosol,[2,3] of cluster diffusion loss to the walls in a cloud chamber,[4] and of a strong diffusion (or drift) loss of nuclei on the boundaries of a crystal in the case of an electron-hole liquid formation by nucleation.[5]

Previous studies of transient nucleation kinetics have been reviewed by several authors.[6-8] Those studies are either restricted to special numerical solutions[6,9,10] or are based on inappropriate approximations.[11,12] Kashchiev's solution of the classic kinetic equation of nucleation had generally been considered to be the most accurate and had been widely used,[7,8] although his choice of the eigenfunction cutoff was shown to lead to incorrect results.[6] Recent work by Trinkaus and Yoo,[12] which employed a Green's-function approach, confirmed the analysis of Kashchiev's work by Binder and Stauffer.[6] The earlier studies tend to predict a characteristic lag time to attain a steady state of order $10^{-5}$–$10^{-6}$ s for liquid systems, although Gitterman and co-workers[13-18] have suggested that the time lag can reach dozens of seconds. They have attributed the overlooking of this time-lag effect in the previous studies to the approximations used in those studies, including the quadratic approximation for the energy barrier and the method of the steepest descent used in evaluating the integrals involved.

In using those "diffusion" approximations the time lag obtained does not include the time needed for the subcritical clusters to reach steady state. Instead, the time lag obtained is only the time required for a cluster to diffuse across the energy barrier.

The present work is an attempt to solve the time-lag problem in nucleation. With the aid of singular pertubation theory,[2,19] an analytical time-dependent solution is presented for the cluster size distribution for realistic boundary and initial conditions. We obtain the characteristic time scales for establishing the steady-state cluster size distribution, the nucleation rate, and the total particle formation without incorrect approximation other than associated with the matched asymptotic expansion. Our solutions are free of the problem of the incorrect boundary conditions associated with several previous studies.

We also solve the time-dependent kinetic equation of nucleation in the presence of cluster scavenging by free molecule particles. Thus we provide a quantitative answer to the time-lag question in an open system in which the characteristic lifetimes of clusters also play a critical role in the kinetics of nucleation.

## II. BASIC EQUATIONS

The equation governing the continuous cluster size distribution $f(g,t)$ in a supersaturated vapor is[6,20]

$$\frac{\partial f(g,t)}{\partial t} = -\frac{\partial J(g,t)}{\partial g} , \tag{1}$$

where $J(g,t)$ is the cluster flux defined in the continuous cluster size ($g$) space

 

$$J(g,t)=-\beta(g,t)n(g,t)\frac{\partial}{\partial g}\frac{f(g,t)}{n(g,t)}\ , \tag{2}$$

and $\beta(g,t)$ is the rate of collision between monomers at concentration $f(1,t)$ and a $g$-mer

$$\beta(g,t)=f(1,t)s_1 g^{2/3}(kT/2\pi m_1)^{1/2}\ . \tag{3}$$

The equilibrium cluster size distribution corresponding to a monomer concentration $n(1,t)$ is

$$n(g,t)=n(1,t)\exp[-W(g,t)/kT]\ , \tag{4}$$

with $s_1$ and $m_1$ the surface area and mass of the monomer, respectively. The critical size

$$g_*=\left[\frac{2\theta}{3\ln S}\right]^3 \tag{5}$$

is the size of cluster corresponding to the maximum free energy of cluster formation

$$W(g,t)=-gkT\ln S+s_1 g^{2/3}\sigma\ , \tag{6}$$

where $\theta=s_1\sigma/kT$, the saturation ratio $S(t)=n(1,t)/n_{eq}(1)$, and $n_{eq}(1)$ is the saturation monomer concentration.

About $g_*$ a critical region exists in which the difference between $W(g)$ and $W(g_*)$ is smaller than $kT$, i.e.,

$$|W(g)-W(g_*)|\le kT\ , \tag{7}$$

the width of which is given by[20]

$$\delta=\left[-\frac{1}{2kT}\frac{\partial^2 W}{\partial g^2}\right]^{-1/2}\Bigg|_{g=g_*}\ , \tag{8}$$

which is related to the Zeldovich factor $Z$ by

$$\delta=\frac{1}{\sqrt{\pi}Z}=3g_*^{2/3}\theta^{-1/2}\ . \tag{9}$$

Solutions of Eq. (1) for the dynamic cluster size distribution must be subject to appropriate boundary and initial conditions. The boundary conditions can be specified at both ends of the cluster size distribution. At $g=1$, the monomer number concentration can be assumed to be the same as the value used to define the equilibrium distribution

$$\frac{f(g,t)}{n(g)}=1,\quad g\to 1\ . \tag{10}$$

While for large $g$, the boundary condition can be established by noting that above the critical region the function $n(g)$ defined by Eq. (4) increases without limit, whereas the true cluster size distribution $f(g,t)$ remains finite. Thus

$$\frac{f(g,t)}{n(g)}=0,\quad g\to\infty\ . \tag{11}$$

We wish to study the transient nucleation kinetics that occur when the saturation ratio $S$ is raised at $t=0$ to a specified value. Since the equilibrium cluster concentrations for $g\ge 2$ are much smaller than that of the monomer, it is reasonable to take the initial condition as

$$f(g,0)=n(1)\delta(g-1)\ , \tag{12}$$

where $\delta(g-1)$ is the Dirac delta function.

## III. TRANSIENT KINETICS OF NUCLEATION — THE SINGULAR PERTURBATION APPROACH

As in the steady-state case, the normalized cluster size distribution $f(g,t)/n(g)$ exhibits a boundary layer structure about the critical-sized cluster $g_*$.[2] The small parameter, denoted as $\epsilon$, which multiplies the term containing the highest derivative in the equation governing the cluster distribution, is related to the width of the critical region $\delta$. A singular perturbation approach[2,19] can be used to obtain the transient cluster size distribution, transient nucleation rate, and transient total number of particles nucleated.

We define the independent variable $y(x,t)=f(g,t)/n(g)$ and the normalized cluster size $x=g/g_*$, and transform Eq. (1) into

$$\frac{x^{-2/3}\delta^2}{\beta(g_*)}\frac{\partial y(x,t)}{\partial t}=\left[\frac{\delta}{g_*}\right]^2\frac{\partial^2 y(x,t)}{\partial x^2}+\left[\frac{2}{3x}\left[\frac{\delta}{g_*}\right]^2+6(1-x^{-1/3})\right]\times\frac{\partial y(x,t)}{\partial x}\ , \tag{13}$$

in which Eqs. (2), (4), (6), and (9) have been used and $\beta(g_*)$ is $\beta(g,t)$ evaluated by Eq. (3) at $g=g_*$ and $f(1,t)=n(1)$. Letting $\delta/g_*\equiv\epsilon$, Eq. (13) becomes

$$\epsilon^2\frac{\partial^2 y(x,t)}{\partial x^2}+\left[\frac{2}{3x}\epsilon^2+6(1-x^{-1/3})\right]\frac{\partial y(x,t)}{\partial x}-\frac{x^{-2/3}\delta^2}{\beta(g_*)}\frac{\partial y(x,t)}{\partial t}=0 \tag{14}$$

The condition $\epsilon\ll 1$ holds as long as $\ln S\ll\frac{2}{9}\theta^{3/2}$, which is the case in nearly all practical situations.

After a Laplace transformation, Eq. (14) becomes

$$\epsilon^2\frac{\partial^2 y(x,s)}{\partial x^2}+\left[\frac{2}{3x}\epsilon^2+6(1-x^{-1/3})\right]\frac{\partial y(x,s)}{\partial x}=\frac{x^{-2/3}\delta^2}{\beta(g_*)}[y(x,s)s-y(x,0)]\ , \tag{15}$$

where

$$y(x,s)=\int_0^\infty y(x,t)e^{-st}dt\ . \tag{16}$$

Equation (15) together with the boundary conditions

$$y(1/g_*,s)=\frac{1}{s},\quad y(\infty,s)=0\ , \tag{17}$$

can now be solved by the method of singular perturbation. Since the dominant term of $\partial y(x,s)/\partial x$ changes sign at $x=1$ in the interval $[1/g_*,\infty]$, we expect a boundary layer (transition layer) at $x=1$ as noted above. Thus there are two outer solutions: a $y^I_{out}(x,s)$ that

satisfies the left boundary condition at $x=1/g_*$ and a $y^r_{\rm out}(r,s)$ that satisfies the right boundary condition at $x\to\infty$. The outer solution is expected to be valid far from the critical region (inner region) around $x=1$.

The outer solution must satisfy the boundary condition $y^l_{\rm out}(1/g_*,s)=1$ and $y^r_{\rm out}(\infty,s)=0$. To the leading order in $\epsilon$ (the first-order correction vanishes), the outer solutions to Eq. (15) that satisfy the boundary conditions are

$$y^l_{\rm out}(x,s)=\frac{1}{s}\left[\frac{1-x^{1/3}}{1-g_*^{-1/3}}\right]^{s\tau}\exp[s\tau(x^{1/3}-g_*^{-1/3})] \quad (18)$$

and

$$y^r_{\rm out}(x,s)=0\ , \quad (19)$$

where $\tau=\delta^2/2\beta(g_*)$. Since the growth of the clusters near $g_*$ can be viewed as a diffusion process, the time necessary to pass through the critical region is the order of $\tau$, with $\beta(g_*)$ playing the role of an equivalent diffusion coefficient. $\tau$ is of the order of $10^{-6}$ s for liquid systems.

As expected, the outer solutions are not valid near $x=1$, so a transition layer about $x=1$ exists. Since the thickness of this boundary layer is $\epsilon$, we introduce the inner variables $X=(x-1)/\epsilon^{\lambda}(\lambda>0)$ and $Y_{\rm in}(X,s)\equiv y_{\rm in}(x,s)$. In terms of these variables, Eq. (15) becomes

$$\frac{\epsilon^{2-\lambda}}{3}\frac{\partial Y_{\rm in}(X,s)}{\partial X}+\frac{1}{2}\epsilon^{2(1-\lambda)}(1+\epsilon^{\lambda}X)\frac{\partial^2 Y_{\rm in}(X,s)}{\partial X^2}$$
$$+3\epsilon^{-\lambda}(1+\epsilon^{\lambda}X)[1-(1+\epsilon^{\lambda}X)^{-1/3}]\frac{\partial Y_{\rm in}(X,s)}{\partial X}$$
$$=\frac{\delta^2}{2\beta(g_*)}(1+\epsilon^{\lambda}X)^{-1/3}sY_{\rm in}(X,s)\ . \quad (20)$$

As $\epsilon\to 0$ with $X$ being fixed, the distinguished limit of Eq. (20) corresponds to $\lambda=1$. The boundary condition $y(\infty,s)=0$ translates into

$$Y_0(\infty,s)=0,\quad Y_n(\infty,s)=0,\quad n\geq 1\ . \quad (21)$$

The leading-order inner solution of Eq. (20) that satisfies the boundary conditions is

$$Y_{\rm in}(X,s)=\tfrac{1}{2}A(s)i^{s\tau}\mathrm{erfc}(X)+\tfrac{1}{2}B(s)i^{s\tau}\mathrm{erfc}(-X)\ , \quad (22)$$

where $i^{s\tau}\mathrm{erfc}(X)$ is a repeated error function. The constants $A(s)$ and $B(s)$ have to be determined by asymptotically matching the outer and inner solutions. The match consists of requiring that at the intermediate limits $[x\to 1-,X\to-\infty;x\to 1+,X\to+\infty]$ the inner and outer solutions agree. The leading-order match gives

$$A(s)=\frac{1}{s}(1-g_*^{-1/3})^{-s\tau}\left[\frac{\epsilon}{3}\right]^{s\tau}$$
$$\times e^{(1-g_*^{-1/3})s\tau}\Gamma(s\tau+1),\quad B(s)=0\ . \quad (23)$$

### A. Transient cluster size distribution

To determine the nucleation rate we are most interested in the cluster size distribution near the critical size which is given by the inner solution

$$y_{\rm in}(x,s)=\frac{1}{2s}(1-g_*^{-1/3})^{-s\tau}\left[\frac{\epsilon}{3}\right]^{s\tau}e^{(1-g_*^{-1/3})s\tau}$$
$$\times\Gamma(s\tau+1)i^{s\tau}\mathrm{erfc}\left[\frac{x-1}{\epsilon}\right]\ . \quad (24)$$

After an inverse Laplace transformation, we have

$$y_{\rm in}(g,t)=\frac{1}{2}\mathrm{erfc}\left[\frac{g-g_*}{\delta}+\exp\left[-\frac{t-\lambda\tau}{\tau}\right]\right]\ , \quad (25)$$

where $\lambda=g_*^{-1/3}-1+\ln[3(1-g_*^{-1/3})/\epsilon]$.

The transient cluster size distribution far from the critical region is given by the outer solutions which are the inverse Laplace transformations of Eqs. (18) and (19),

$$y^l_{\rm out}(g,t)=\Theta(t-\mu(g)\tau) \quad (26)$$

and

$$y^r_{\rm out}(g,t)=0\ , \quad (27)$$

where $\mu(g)=(g_*^{-1/3}-x^{1/3}-\ln[(1-x^{1/3})/(1-g_*^{-1/3})]$ and $\Theta$ is the unit step function: $\Theta(z)=1$ for $z>0$, $\Theta=\frac{1}{2}$ for $z=0$, and $\Theta=0$ for $z<0$.

According to Eq. (26), the subcritical clusters approach a steady state one by one with a time lag $\mu(g)\tau$. As shown in Fig. 1, the coefficient $\mu(g)$ of the characteristic time $\mu(g)\tau$ for subcritical clusters to attain steady state is not overly sensitive to the value of the critical cluster size $g_*$. On the other hand, $\mu(g)$ increases as $g$ increases, in-

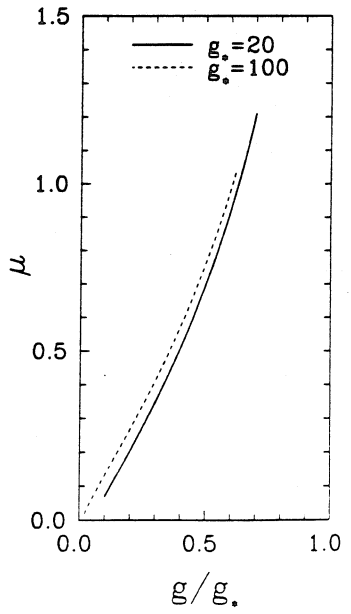


FIG. 1. Coefficient $\mu(g)$ in the effective time lag $\mu(g)\tau$ associated with the subcritical cluster size distribution as a function of the normalized cluster size $g/g_*$.

dicating that the subcritical clusters attain steady state, also equilibrium, one by one from the smaller clusters to the larger ones, such that the rapid establishment of steady state for the smaller clusters from the monomer is followed by a lengthening period for each $g$-mer as the size increases. In overcoming the larger Gibbs energy barrier to form a larger cluster the time needed in establishing a steady-state cluster distribution at larger size is longer than that for the smaller clusters.

The cluster size distribution beyond the critical region $y'_{\text{out}}$ vanishes as indicated by Eq. (27). This is also true in the stationary case as required by the boundary condition Eq. (16).[2]

The characteristic parameter in the transient behavior of the clusters in the critical region $\lambda$ is a function of $g_*$ and $\theta$. For $\theta=10$, the value of $\lambda$ is about 0.34 for $g_*=30$ and 0.45 for $g_*=100$. For $\theta=5$, its value is about 0.3 for $g_*=30$ and 0.40 for $g_*=100$. According to Eq. (25), the cluster size distribution in the critical region becomes essentially steady state (about 95% of its steady-state value) for $t>(1.5+\lambda)\tau$ (about $3\tau$), i.e.,

$$f(g)=\tfrac{1}{2}n(g)\operatorname{erfc}\left[\frac{g-g_*}{\delta}\right], \tag{28}$$

which agrees with the classical steady-state case.[18]

We can estimate the ratio between the characteristic time needed for the establishment of a steady-time subcritical cluster distribution $\mu(1-\epsilon)\tau$ and that required to form a steady-state cluster flux in the critical region $(\lambda+1.5)\tau$. For $g_*=30$ and $\theta=10$, this ratio is about 0.45. Thus about one-third of the time needed to establish full steady-state cluster distribution is spent in forming a steady-state subcritical cluster size distribution. For $g_*=100$ and $\theta=10$ this ratio of characteristic times increases to about 0.53. As $g_*$ increases, more time is spent on establishing a steady-state cluster size distribution outside the critical region. This ratio decreases with decrease in $\theta$; for $\theta=5$, this ratio is about 0.37 for $g_*=30$ and 0.47 for $g_*=100$. It is clear that in calculating the time needed to reach a steady-state cluster size distribution the time needed to reach steady state below the critical region cannot be neglected. This aspect thus has been neglected implicitly or explicitly in most previous analyatic studies.[6,11]

### B. Transient nucleation rate

The transient cluster flux at any size $g$ is given by

$$\begin{aligned}J(g,t)&=-\beta(g)n(g)\frac{\partial}{\partial g}\left[\frac{f(g,t)}{n(g)}\right]\\&=Z(g_*)\beta(g)n(g)\exp\\&\quad\times\left\{-\left[\frac{g-g_*}{\delta}+\exp\left[-\frac{t-\lambda\tau}{\tau}\right]\right]^2\right\},\end{aligned} \tag{29}$$

and the transient nucleation rate at $g=g_*$ is

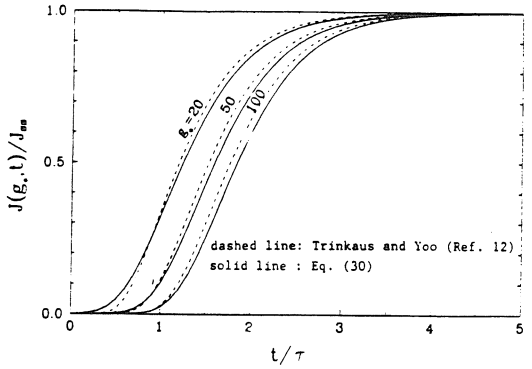


FIG. 2. Normalized transient nucleation rate $J(g_*,t)/J_{ss}$ as a function of the normalized time $t/\tau$.

$$\begin{aligned}J(g_*,t)&=-\beta(g_*)n(g_*)\frac{\partial}{\partial g}\left[\frac{f(g,t)}{n(g)}\right]\Bigg|_{g=g_*}\\&=J_{ss}\exp\left\{-\left[\exp\left[-2\frac{t-\lambda\tau}{\tau}\right]\right]\right\},\end{aligned} \tag{30}$$

where $J_{ss}$ is the steady-state homogeneous nucleation rate

$$J_{ss}=Z(g_*)\beta(g_*)n(g_*), \tag{31}$$

and $Z(g_*)$ is Zeldovich factor. In the limit as $t\to\infty$, we have from Eq. (30) that $J(g_*,t)=J_{ss}$.

It is noted that the new derived formula for the transient nucleation rate, Eq. (30), is functionally different from the previous ones which have usually been expressed[7] in the form of $J=J_{ss}[1-\exp(-t/t_c)]$, where $t_c$ is the characteristic time of relaxation of the nucleation process to a steady state. Different authors have obtained different expressions for $t_c$, but of the order of $\tau$.

In Fig. 2, we show the nucleation rate as a function of $t/\tau$ for different values of $g_*$ based on Eq. (30) and that obtained by Trinkaus and Yoo.[12] The two results are numerically consistent with each other. As shown in Fig. 2, the time lag associated with the nucleation rate is about $4\tau$.

### C. Time-dependent number density of critical clusters nucleated

The number density of critical clusters formed in the system following the increase in saturation ratio at $t=0$ is the integrated flux $N(g_*,t)=\int_0^t J(g_*,t')dt'$. The dimensionless total number is

$$\frac{N(g_*,t)}{J_{ss}\tau}=\frac{1}{2}\int_{ae^{-bt}}^{a}\frac{dx}{xe^x}=\tfrac{1}{2}[E_1(ae^{-bt})-E_1(a)], \tag{32}$$

where $a=e^{2\lambda}=[3(1-g_*^{-1/3})/\epsilon]^2e^{2(g_*^{-1/3}-1)}$ and $b=2/\tau$, and $E_1$ is the exponential integral.

As $t/\tau\to\infty$, we have $ae^{-bt}\to 0$, and $E_1(ae^{-bt})=-\gamma-\ln a+bt+O(ae^{-bt})$, thus

$$\frac{N(g_*,t)}{J_{ss}\tau}=-\frac{1}{2}[E_1(a)+\gamma_e+\ln a]+\frac{t}{\tau}, \tag{33}$$

where $\gamma_e = 0.5772$ is Euler's constant.

Equation (33) thus indicates that at large times, $N(g_*,t)$ increase linearly with time $t$ as expected. The beginning of the steady-state regime can be determined experimentally by the time at which the increase of $N(g_*,t)$ becomes linear with time. The time lag ($\tau_e$) defined in such a way is given by

$$\tau_e = \tfrac{1}{2}[E_1(a)+\gamma_e+\ln a]\tau \ . \tag{34}$$

The time dependence of $N(g_*,t)$ is shown in Fig. 3 for $g_* = 30$ and $g_* = 100$. The effective time lag associated with the approach of $N(g_*,t)$ to steady state is about $3\tau$ which, as expected, is the same order of the time lag associated with the nucleation rate. This result is in contrast with that obtained by Gitterman and his associates.[13–18] They have suggested the time lag associated with $N(g_*,t)$ can reach dozens of seconds even for liquid systems for "fast" quench cases. For a fast quench the initial condition is given by Eq. (12). It is this fast quench case that is the one considered in the present work. They have attributed the overlooking of this effective long-time lag in the previous studies to the approximations used in those studies, including the neglect of the time required to reach the steady-state cluster distribution below the critical region, the quadratic approximation for the energy barrier, and the method of steepest descent used in evaluating the integrals involved. Since the present approach is free of those approximations, and we do not find any anomalous increase in the time lag associated with $N(g_*,t)$, we conclude that the increase in the time lag found by Gitterman and co-workers must arise from one of two sources. Either it is a phenomenon related to nucleation near the critical point of phase transition, since they used critical dynamics to determine the physical parameters in the kinetic equation of nucleation, or the error was introduced by the approximation of shifting the real boundary conditions to an unphysical domain in solving the associated eigenvalue problem. However, there is no experimental evidence as reviewed in Ref. 20 to support the first possibility.

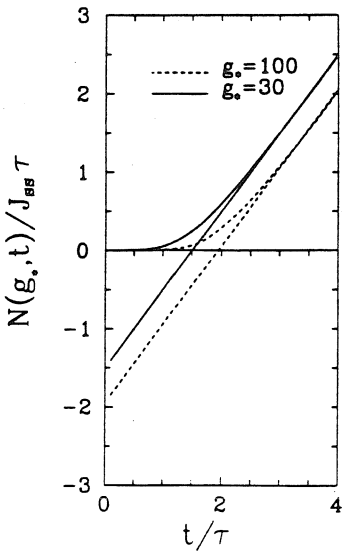


FIG. 3. Normalized number density of critical clusters formed $N(g_*,t)/J_{ss}\tau$ as a function of the normalized time $t/\tau$.

In solving for the time-dependent cluster size distribution, the problem was condensed by Gitterman and coworkers into solving the appropriate Schrödinger equation by approximating the potential as a harmonic oscillator and shifting the boundary from the lowest end of the size distribution to $-\infty$. The potential with this equation could be approximated by the harmonic oscillator only near the critical cluster size, which is equivalent to the quadratic approximation for the Gibbs energy barrier. The second assumption in shifting the boundary condition from $g=1$ to the region $g<0$ is similar to that of Trinkaus and Yoo[12] in using a Green's-function approach. A consequence of this approximation is that the solution does not satisfy the physical boundary condition. This approximation, however, may not cause serious error since the transient nucleation rate obtained by Trinkaus and Yoo[12] shows a similar behavior with ours as shown in Fig. 2.

## IV. TRANSIENT KINETICS OF NUCLEATION IN THE PRESENCE OF CLUSTER SCAVENGING

Let us consider a supersaturated vapor system with preexisting free-molecule particles of sizes larger than that of the critical cluster corresponding to the existing supersaturation in the system. The equation governing the continuous cluster size distribution is given by[2]

$$\frac{\partial f(g,t)}{\partial t} = -\frac{\partial J(g,t)}{\partial g} - \gamma g^{-7/6}\beta(g,t)f(g,t) \ , \tag{35}$$

where $\gamma$ is a dimensionless surface area concentration parameter defined by

$$\gamma = \frac{A}{s_1 f(1,t)} \ , \tag{36}$$

with $s_1$ the surface area of the monomer and $A$ the surface area density of preexisting particles.

The boundary and initial conditions to Eq. (36) are given by Eqs. (10)–(12). As in the absence of cluster scavenging, we can solve for the time dependent $f(g,t)$ by the singular perturbation approach.

To the leading order in $\epsilon$ (the first-order correction vanishes), the outer solutions to these equations that satisfy the boundary conditions are

$$y^l_{\text{out}}(x,s) = \frac{1}{s}\left[\frac{1-x^{1/3}}{1-g_*^{-1/3}}\right]^{s\tau} \exp[s\tau(x^{1/3}-g_*^{-1/3})] \times \left[\frac{1-x^{1/6}}{1+x^{1/6}}\right]^m \eta^{-m} \tag{37}$$

and

$$y^r_{\text{out}}(x,s) = 0 \ , \tag{38}$$

where $m$ is given by

$$m = \tfrac{1}{2}\gamma\delta^2 g_*^{-7/6} = \tfrac{9}{2}\gamma\theta^{-1}g_*^{1/6} \ ,$$

and $\eta=(1-g_*^{-1/6})/(1+g_*^{-1/6})$. As expected, the outer solutions are not valid near $x=1$, so a transition layer at $x=1$ exists. Since the thickness of this boundary layer is $\epsilon$, we introduce the inner variables $X=(x-1)/\epsilon$ and $Y_{in}(X,s)\equiv y_{in}(x,s)$. Using a similar method to obtaining the outer solutions we obtain the following leading-order inner solution:

$$Y_{in}(X,s)=\frac{1}{2s}\exp(-\lambda s\tau)\alpha^m\Gamma(m+s\tau+1)\times i^{s\tau+m}\mathrm{erfc}(X)\ , \tag{39}$$

where $\alpha=\epsilon/12\eta$. In the limit of $m=0$, Eqs. (37) and (39) reduce to Eqs. (18) and (24).

### A. Transient cluster size distribution

The cluster size distribution near the critical size is given by the inner solution

$$y_{in}(x,s)=\frac{1}{2s}\exp(-\lambda s\tau)\alpha^m\Gamma(m+s\tau+1)\times i^{s\tau+m}\mathrm{erfc}\left[\frac{x-1}{\epsilon}\right]\ . \tag{40}$$

After an inverse Laplace transformation, we have

$$y_{in}(g,t)=\frac{1}{2}\alpha^m\Gamma(m+1)i^m\mathrm{erfc}\left[\frac{g-g_*}{\delta}\right]-\frac{1}{\sqrt{\pi}}\int_X^{X+\exp(-t/\tau+\lambda)}\alpha^m(w-X)^m e^{-w^2}dw\ . \tag{41}$$

In the limit of $m\to 0$, Eq. (41) reduces to

$$y_{in}(g,t)=\frac{1}{2}\mathrm{erfc}\left[\frac{g-g_*}{\delta}\right]-\frac{1}{\sqrt{\pi}}\int_X^{X+\exp(-t/\tau+\lambda)}e^{-w^2}dw=\frac{1}{2}\mathrm{erfc}\left[\frac{g-g_*}{\delta}+\exp\left[-\frac{t-\lambda\tau}{\tau}\right]\right], \tag{42}$$

which is the transient cluster size distribution in the absence of cluster scavenging, Eq. (25).

The subcritical transient cluster size distribution far from the critical region is given by the outer solutions which are the inverse Laplace transformations of Eqs. (37) and (38), respectively,

$$y_{out}^{l}(g,t)=\Theta(t-\mu(g)\tau)\left[\frac{1-x^{1/6}}{1+x^{1/6}}\right]^m\eta^{-m}\ , \tag{43}$$

which reduces to Eq. (26) for $m=0$ and

$$y_{out}^{r}(g,t)=0\ . \tag{44}$$

In the subcritical region, by comparison with Eq. (26), we note that the presence of cluster scavenging does not change the time $\mu\tau$ needed to reach the steady state. The steady-state number density of subcritical clusters is the same as the equilibrium one corresponding to the Gibbs energy potential in the absence of cluster scavenging,[2] while in the presence of cluster scavenging the steady-state number density of subcritical clusters is smaller than the equilibrium one. The presence of cluster scavenging does not change the time needed for the subcritical clusters to reach steady state indicating the time for the establishment of a dynamic balance between the cluster scavenging process and the cluster flux across the $g$ space is always the same regardless of the values of $m$. A consequence of this is the cluster flux becomes $g$ dependent.

### B. Transient nucleation rate

The transient cluster flux as defined by Eq. (2) in the critical region can be obtained from Eq. (41),

$$J(g,t)=\beta(g)n(g)Z(g)\times\left[\frac{1}{2}\alpha^m\sqrt{\pi}\Gamma(m+1)i^{m-1}\mathrm{erfc}\left[\frac{g-g_*}{\delta}\right]-\int_X^{X+\exp(-t/\tau+\lambda)}2\alpha^m(w-X)^{m+1}\times e^{-w^2}dw\right], \tag{45}$$

and the cluster flux in the subcritical region is obtained from Eq. (42),

$$J(g,t)=\beta(g)n(g)\Theta(t-\beta\tau)\left[\frac{1-x^{1/6}}{1+x^{1/6}}\right]^{m-1}\times\frac{m\eta^{-m}x^{-5/6}}{3g_*(1+x^{1/6})^2}\ . \tag{46}$$

The nucleation rate defined as the cluster flux at $g_*$ is given by

$$J(g_*,t)=J_{ss}\left[\sqrt{\pi}\left[\frac{\alpha}{2}\right]^m\frac{\Gamma(m+1)}{\Gamma(m/2+1/2)}-\int_0^{\exp(-t/\tau+\lambda)}2\alpha^m w^{m+1}e^{-w^2}dw\right]\ . \tag{47}$$

In the absence of preexisting particles, that is, as $m\to 0$, we have from Eq. (25), or Eq. (46), $J(g_*,t)=J_{ss}\exp(-\{\exp[-2(t-\lambda\tau)/\tau]\})$, which is the same result as that obtained in the case without cluster scavenging, Eq. (30).

In the limit of large times, we recover the steady-state nucleation rate in the presence of cluster scavenging,[2]

$$J_{sm}=J_{ss}\eta^{-m}\sqrt{\pi}\left[\frac{\epsilon}{24}\right]^m\frac{\Gamma(m+1)}{\Gamma(m/2+1/2)}\ . \tag{48}$$

It is known previously[2] and from Eq. (46) that the nucleation rate in the presence of cluster scavenging can be reduced significantly from that in its absence depending on the surface area density present in the system.

The normalized nucleation rate $J(g_*,t)/J_{sm}$ as a function of $t/\tau$ based on Eq. (46) is shown in Fig. 4 for different values of $m$. We note that the presence of cluster scavenging shortens the time lag needed for the nucleation rate to approach the steady state. For $m=0$ we

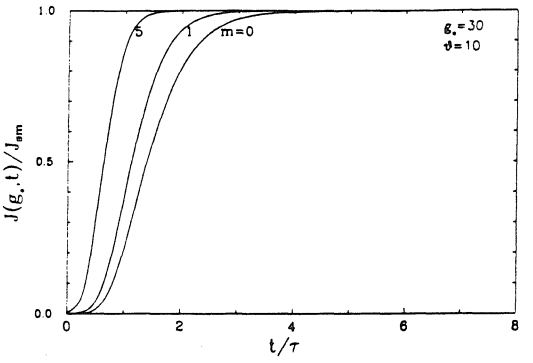


FIG. 4. Normalized nucleation rate $J(g_*,t)/J_{sm}$ as a function of normalized time $t/\tau$ for different values of $m$.

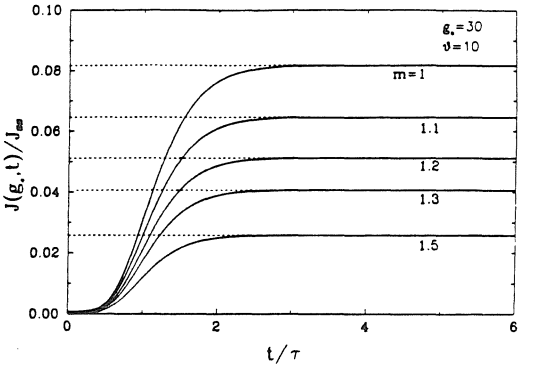


FIG. 5. Normalized nucleation rate $J(g_*,t)/J_{ss}$ as a function of normalized time $t/\tau$ for different values of $m$.

have the case of transient nucleation in the absence of cluster scavenging. Thus the suggestion that the time lag should be very long for an open system[5] is shown to be not correct. At a higher surface area density of cluster scavengers (larger $m$) present the nucleation rate reaches the steady state faster than at the lower surface area density.

This behavior can be understood by analogy to two chemical reaction systems: $A \rightleftharpoons B$ and $A \rightleftharpoons B \rightarrow C$. In the first system the concentration of $B$ reaches a steady state in a time scale $\tau_1 = 1/k_{-1}$, and $\tau_2 = 1/(k_{-1}+k_2)$ is required for $B$ to reach steady state in the second system. Here $k_{-1}$ and $k_2$ are the rate constants of the reactions of $B$ and $A$ and of $B$ and $C$, respectively. $\tau_1 > \tau_2$ as a result of the additional removal path for $B$ in the second system. By analogy, the nucleation time lag in the presence of cluster scavenging is shorter than that in its absence. As $k_2$ increases $\tau_2$ decreases, and the time lag in the case of higher surface area concentration of preexisting particles is shorter than that at lower concentrations.

Figure 5 shows $J(g_*,t)/J_{ss}$. For a suppressed nucleation rate, the time for the appearance of nuclei in a unit volume becomes very long. For example, for $J(g_*,t)/J_{ss}=0.04$ in the case presented in Fig. 5 for $m=1.3$, the time for a given concentration of critical sized clusters to appear in a unit volume in the case of cluster scavenging is about 25 times longer than in absence.

### C. Time-dependent number concentration

The time-dependent number density of critical cluster nucleation in the system with cluster scavenging is given by

$$N(g_*,t) = J_{sm}t - J_{ss}\int_0^t \int_0^{\exp(-t'/\tau+\lambda)} 2\alpha^m w^{m+1} \times e^{-w^2} dw\, dt' . \quad (49)$$

Thus the effective time lag that can be verified experimentally is

$$\tau_{em} = \int_0^t \int_0^{\exp(-t'/\tau+\lambda)} 2\alpha^m w^{m+1} e^{-w^2} dw\, dt' , \quad (50)$$

which becomes equal to $\tau_e$ given by Eq. (34) in the limit of $m=0$.

## V. CONCLUSIONS

In this work we have investigated the transient nature of nucleation by examining the time dependence of the cluster size distribution, the nucleation rate, and the time-dependent number density of critical sized clusters formed. The approach used is based on a singular perturbation method in which approximations made previously, such as, the quadratic approximation for the nucleation barrier, and the steepest descent method to evaluate the integrals involved are avoided.

We have also investigated the transient kinetics of nucleation in the presence of cluster scavenging by free-molecule particles by solving the kinetic equation of nucleation. It is shown that the presence of cluster scavenging shortens the total time lag, which decreases with increasing surface area density of cluster scavengers.

## ACKNOWLEDGMENTS

This work was supported by National Science Foundation Grant No. ATM-8503103.

[1] D. Kotake and I. I. Glass, Prog. Aerosp. Sci. **19**, 129 (1981).
[2] G. Shi and J. H. Seinfeld, J. Colloid Interface Sci. (to be published).
[3] G. Shi and J. H. Seinfeld, J. Chem. Phys. (to be published).
[4] C. Becker and H. Reiss, J. Chem. Phys. **65**, 2066 (1976).
[5] V. M. Asnin, A. A. Rogachev, N. I. Sablina, V. I. Stepanov, and A. B. Churilov, Fiz. Tverd. Tela (Leningrad) **29**, 1675 (1986) [Sov. Phys.—Solid State **29**, 964 (1987)].
[6] K. Binder and D. Stauffer, Adv. Phys. **25**, 343 (1976).
[7] K. F. Kelton, A. L. Greer, and C. V. Thomoson, J. Chem. Phys. **79**, 6261 (1983).
[8] A. I. Danilov and Yu. M. Polukarov, Russ. Chem. Rev. **56**, 619

(1987).
[9]I. K-Dannetschek and D. Stauffer, J. Aerosol Sci. **12**, 105 (1981).
[10]D. Kashchiev, J. Surface Sci. **14**, 209 (1969).
[11]V. Volterra and A. R. Cooper, J. Non-Crystal. Solids **74**, 85 (1985).
[12]H. Trinkaus and M. H. Yoo, Philos. Mag. A **55**, 269 (1987).
[13]M. Gitterman, I. Edrel, and Y. Rabin, in *Application of Field Theory to Statistical Mechanics*, Vol. 216 of *Lecture Notes in Physics*, edited by L. Garrido (Springer, Heidelberg, 1984).
[14]M. Gitterman and Y. Rabin, J. Chem. Phys. **80**, 2234 (1984).
[15]Y. Rabin and M. Gitterman, Phys. Rev. A **29**, 1496 (1984).
[16]I. Edrel and M. Gitterman, J. Chem. Phys. **85**, 190 (1986).
[17]I. Edrel and M. Gitterman, J. Phys. A **19**, 3279 (1986).
[18]I. Edrel and M. Gitterman, Phys. Rev. A **33**, 2821 (1986).
[19]C. M. Bender and S. A. Orszag, *Advanced Mathematical Methods for Scientists and Engineers* (McGraw-Hill, New York, 1978).
[20]K. Binder, Rep. Prog. Phys. **50**, 783 (1987).

# CHAPTER 7

# TRANSIENT KINETICS OF BINARY NUCLEATION: MULTIPLE PATHWAYS AND APPROACH TO STATIONARITY

# Kinetics of binary nucleation: Multiple pathways and the approach to stationarity

G. Shi and J. H. Seinfeld
*Department of Chemical Engineering, California Institute of Technology, Pasadena, California 91125*

(Received 7 June 1990; accepted 13 September 1990)

Explicit analytical expressions are obtained for the rate of nucleation over different paths in a binary system. It is shown that anisotropy in reaction rates and anisotropy in the free energy surface can cause nucleation to occur bypassing the saddle point. Homomolecular nucleation is demonstrated to be the natural limit of binary nucleation as the concentration of one component goes to zero. Explicit expressions are also obtained for the time lag of binary nucleation by using the singular perturbation approach. It is shown that the time lag associated with different paths of nucleation is essential in determining the relative importance of different nucleation pathways.

## I. INTRODUCTION

The identification of a preferred nucleation pathway is essential both for definition of the mechanism of nucleation and calculation of the nucleation rate in a binary system. The nucleation pathway in the classical theory of binary nucleation[1] is found to go across a saddle point in the free energy surface ($G$) for the formation of a mixed particle. The steepest descent path corresponding to the minimum energy direction on the surface is defined solely in terms of the geometrical properties of the formation free energy surface without consideration of the monomer concentrations in the system.[2,3] Consequently, the classical theory of binary nucleation based on the steepest descent path is not kinetically consistent in that it does not reduce correctly to one component homogeneous nucleation theory when one component vanishes.[2-4] Large discrepancy is also found between the predictions of the classical theory and experimental observations when the concentration of one component is significantly different from that of the other component.[5]

Based on a general multicluster coordinate nucleation theory,[6] Stauffer[2] has obtained the correct direction of the nucleation path by considering the properties of both the formation free energy surface and of the nucleating components. His result confirmed an earlier suggestion by Stauffer and Kiang.[3] However a correct expression for the rate of binary nucleation in a system with significantly different concentrations of the two components has not been obtained,[7] nor has an expression for the rates of nucleation taking different paths and their relative contributions to the total rate of nucleation. Recent attempts along these lines have been made by Trinkaus,[7] however a consistent theory of nucleation in a binary system, which reduces correctly to the homomolecular nucleation of one component when the other component is made to vanish, has yet to be developed.

To develop such a theory is one goal of the present paper. An additional goal is to study the role of nonstationarity at the initial stage of nucleation in determining the relative importance of different paths.

The present paper is structured as follows. We will first show that the physical picture of binary saddle point nucleation is similar to that of homomolecular nucleation and the singular pertubation approach used in uniary nucleation can be followed to treat the present binary nucleation problem. Using that approach, we will derive the steady state binary nucleation rate in the case of the cluster flux line going over the saddle point and compare the result with those existing. Then an analysis of multiple nucleation pathways will be given. The relative magnitude of the steady state rate of nucleation over different paths in a binary system will be shown to be controlled not only by the anisotropy in the reaction rates but also by the anisotropy in the shape of the free energy surface. In particular, a continuous transition between heteromolecular nucleation and homomolecular nuclation in a binary system will be predicted. Next, using the singular perturbation approach, we will derive an explicit expression for the effective time lag for binary nucleation. It will be shown that the time lag associated with establishing different nucleation paths is essential in determining the relative importance of different stationary nucleation pathways in contributing the *total* rate of nucleation.

## II. SINGLE NUCLEATION PATHWAY: CLUSTER FLUX LINES GO OVER THE SADDLE POINT

### A. Basic equations

The basic equation governing the time-dependent cluster number concentration $f(g_a,g_b,t)$ may be written as[1,2,7]

$$\frac{\partial f(g_a,g_b,t)}{\partial t} = -\frac{\partial j_a}{\partial g_a} - \frac{\partial j_b}{\partial g_b}, \tag{1}$$

where $g_i$ is the monomer number in a cluster ($i = a,b$), and the cluster flux in composition space is given by

$$j_a = -R_a f_0 \frac{\partial (f/f_0)}{\partial g_a}, \quad j_b = -R_b f_0 \frac{\partial (f/f_0)}{\partial g_b}, \tag{2}$$

where the equilibrium cluster size distribution $f_0 = n_0 \exp[-\beta G(g_a,g_b)]$ with $n_0$ the total monomer number concentration in the system and $G(g_a,g_b)$ is the formation free energy of the clusters.[2] No explicit form of $G$ is needed in treating the kinetics of nucleation in the present work. $\beta = 1/kT$ where $k$ is Boltzmann's constant and $T$ is

the absolute temperature. The reaction rate $R_i(g_a, g_b)$ is defined as the collision rate between monomer $i$ and a cluster of composition $(g_a, g_b)$. For example, in the case of gas-phase nucleation, the reaction rate $R_i$ is proportional to the cluster surface area and the $i$-component monomer number concentration.[1,2] In diffusion-limited nucleation in a condensed system, $R_i$ is proportional to the radius of a cluster and to the $i$-component monomer concentration.[7] Both cases will be considered although no explicit form of $R_i$ need be specified.

### B. Saddle-point binary nucleation

Consider the case of the saddle point nucleation in a binary system in which no single species is supersaturated with respect to its pure state, i.e., the trajectory of cluster flux lines passes only over the saddle point (conditions for saddle point nucleation will be clarified below). A supersaturation with respect to the mixed-component cluster may develop and clusters may grow spontaneously to be larger stable particles after passing over the saddle point. The cluster size at the saddle point is the so-called the critical size. Thus the physical picture of binary saddle point nucleation is similar to that of homomolecular nucleation and the approach for deriving the rate of uniary nucleation has often been followed to derive the expression for binary nucleation.[1] For uniary gas-phase nucleation it has been shown[8] that the classical steady state rate is exact to the leading order in $\epsilon$, a parameter inversely proportional to $(\beta G^*)^{1/2}$. Here $G^*$ is the formation free energy barrier at the critical point.

The approach of singular pertubation has proved to be useful in addressing a number of problems in homogeneous nucleation theory.[8-10] It will prove to be similarly useful in attacking binary nucleation problems. To provide a basis for the analytical approach of this paper, we will first derive the rate of binary saddle point nucleation by using that approach and compare the result with the existing ones.[1,2,7]

Following the procedure presented previously,[8] we will first derive the equations governing cluster number concentration valid in both the outer and inner regions. The inner region is defined as that in the vicinity of the saddle point. It also can be called the critical region in which an unstable cluster becomes a stable cluster by passing over the saddle point. It is expected that the cluster size distribution within this region is far from equilibrium. In contrast, the cluster size distribution in the outer region is close to the equilibrium distribution corresponding to the individual monomer concentrations.

#### 1. Outer solutions

Normalizing Eq. (1) by introducing $z = f/f_0$, $m = g_a/g_a^*$ and $n = g_b/g_b^*$, and by neglecting terms proportional to $\epsilon_a^2$ and $\epsilon_b^2$, where $\epsilon_a = \sqrt{R_a^*}/g_a^*$ and $\epsilon_b = \sqrt{R_b^*}/g_b^*$ which are proportional to $(g_a^*)^{-1/3}$ and $(g_b^*)^{-1/3}$, respectively, for gas-phase nucleation and $(g_a^*)^{-2/3}$ and $(g_b^*)^{-2/3}$, respectively, for nucleation in a condensed system, we obtain

$$\frac{\partial z}{\partial t} = -2\frac{R_a}{g_a^*}\beta\left[G_{aa} + \frac{G_{bb}}{g_b^*}(n-1)\right]\frac{\partial z}{\partial m} - 2\frac{R_b}{g_b^*}\beta\left[G_{bb} + \frac{G_{aa}}{g_a^*}(m-1)\right]\frac{\partial z}{\partial n}. \quad (3)$$

We have used "*" to indicate the value at the saddle point. Also we have used the quadratic expansion for $G$[1,2,6-8]

$$G = G^* + G_{aa}(g_a - g_a^*)^2 + G_{bb}(g_b - g_b^*)^2 + 2G_{ab}(g_a - g_a^*)(g_b - g_b^*), \quad (4)$$

where $G_{aa} = \frac{1}{2}\partial^2 G/\partial g_a^2$, $G_{bb} = \frac{1}{2}\partial^2 G/\partial g_b^2$, and $G_{ab} = \frac{1}{2}\partial^2 G/\partial g_a \partial g_b$ at $g_a = g_a^*$ and $g_b = g_b^*$. The second derivatives describe the shape of the saddle point. While this expansion is more valid near the saddle point, the functional form is expected to be also correct in the outer region. Moreover, it will be shown later a more detailed expression for $G$ does not significantly change the result obtained. The above equation valid in the outer region is not easily solved except for the case in which no cross term appears in $G$. We thus have to diagonalize the matrix

$$\begin{pmatrix} G_{aa} & G_{ab} \\ G_{ba} & G_{bb} \end{pmatrix},$$

which can be accomplished by introducing an ordinary rotational transformation. This transformation can be introduced more clearly in solving for the inner solution given below.

#### 2. Inner solutions

Introducing the inner variables $X = (m-1)/\epsilon_a$, $Y = (n-1)/\epsilon_b$, and $Z = z$, we have the following equation valid in the inner region from Eqs. (1) and (2),

$$\frac{\partial Z}{\partial t} = \left(1 + \frac{X\sqrt{R_a^*} + \mu Y\sqrt{R_b^*}}{g^*}\right)^{2/3} \times\left(\frac{\partial^2 Z}{\partial X^2} + \frac{\partial^2 Z}{\partial Y^2} + \frac{\partial \ln f_0}{\partial X}\frac{\partial Z}{\partial X} + \frac{\partial \ln f_0}{\partial Y}\frac{\partial Z}{\partial Y} + \frac{2}{3}\epsilon_a\frac{g_a}{g^*}\frac{\partial Z}{\partial X} + \frac{2}{3}\epsilon_b\frac{g_b}{g^*}\frac{\partial Z}{\partial Y}\right), \quad (5)$$

where $\mu$ is the ratio of $a$- and $b$-monomer volumes and $g^* = g_a^* + \mu g_b^*$. By neglecting terms containing $\epsilon_a$ and smaller in Eq. (5) we have

$$\frac{\partial Z}{\partial t} = \frac{\partial^2 Z}{\partial X^2} + \frac{\partial^2 Z}{\partial Y^2} - \frac{\partial \beta G}{\partial X}\frac{\partial Z}{\partial X} - \frac{\partial \beta G}{\partial Y}\frac{\partial Z}{\partial Y}, \quad (6)$$

and now

$$\beta G = \beta G_* + D_{aa}X^2 + D_{bb}Y^2 + 2D_{ab}XY$$

with

$$D_{aa} = \beta G_{aa} R_a^*,$$

$$D_{bb} = \beta G_{bb} R_b^*,$$

and

$$D_{ab} = \beta G_{ab}\sqrt{R_a^* R_b^*}.$$

By diagonalization we have

$$\beta G - \beta G^* = -ux^2 + vy^2, \quad u, v > 0. \quad (7)$$

The minus and plus signs in Eq. (7) show that the variables $x$ and $y$ are, respectively, unstable and stable. Here

$$u = -\frac{1}{2}\left[D_{aa} + D_{bb} - \sqrt{(D_{aa} - D_{bb})^2 + 4D_{ab}^2}\right] \quad (8)$$

and

$$v = \frac{1}{2}\left[D_{aa} + D_{bb} + \sqrt{(D_{aa} - D_{bb})^2 + 4D_{ab}^2}\right], \quad (9)$$

which are the two eigenvalues of the matrix

$$D = \begin{pmatrix} D_{aa} & D_{ab} \\ D_{ba} & D_{bb} \end{pmatrix}.$$

The rotational transformation introduced to diagonalize the bilinear form of $G$ to a quadratic form allowing us to determine the stable and unstable variables is

$$x = X\cos\alpha + Y\sin\alpha,$$
$$y = -X\sin\alpha + Y\cos\alpha, \quad (10)$$
$$\tan\alpha = \frac{1}{2D_{ab}}\left[D_{bb} - D_{aa} + \sqrt{(D_{aa} - D_{bb})^2 + 4D_{ab}^2}\right].$$

In Eq. (7) that the squares of the variables have different signs means that the energy barrier has a saddle character ($G_{aa}G_{bb} - G_{ab}^2 < 0$). The determination of the stable and the unstable variables enables us to obtain the outer and inner solutions by solving Eqs. (3) and (6). First we address the inner solution. By using the variables $x$ and $y$ to describe the cluster, Eq. (6) becomes

$$\frac{\partial z}{\partial t} = \frac{\partial^2 z}{\partial x^2} + \frac{\partial^2 z}{\partial y^2} + 2ux\frac{\partial z}{\partial x} - 2vy\frac{\partial z}{\partial y}, \quad (11)$$

which is solved at steady state to give

$$w(x) = A\int_0^x \exp(-uk^2)dk + B \quad (12)$$

with

$$w(x) = \int_{-\infty}^{\infty} z(x,y)\exp(-vy^2)dy.$$

The constants $A$ and $B$ are to be determined by matching the outer and inner solutions. It is noted that Eq. (11) is similar in the form to the inner equation for homomolecular nucleation.[9]

The direction of the nucleation path at the saddle point is given by $\alpha$ which is an angle with respect to the $g_a$ axis. The value of the angle reduces to the classical result of Reiss[1] for isotropic reaction rates, $R_a = R_b$. Our result for $\alpha$, Eq. (10), is the same as that obtained by Stauffer.[2] In particular, in the limit of $R_b^* \ll R_a^*$, $\tan\alpha \to 0$, $\alpha = 0$, thus the nucleation proceeds along the $g_a$-axis direction. At the opposite limit, $\alpha = \pi/2$, the nucleation proceeds in the $g_b$-axis direction. Thus the directions of the nucleation path at those limits are kinetically consistent with physically based expectations. A continuous transition between the angle of the binary nucleation and that of the uniary nucleation of the more abundant component (if its concentration is large enough to be supersaturated) is ensured, i.e., the nucleation path changes from passing over the saddle point on the two-dimensional energy surface to a path going over a point on the mountain ridge in the one-dimensional energy curve. The problem now is why previous theories of binary nucleation do not reduce to that of uniary nucleation in a kinetically consistent way even though the direction of the nucleation path exhibits a proper transition? This is one of the questions we will address in the remainder of the paper.

### 3. Matching inner and outer solutions

Using the coordinate rotation introduced above to obtain the inner solution we can obtain the left steady state outer solution from Eq. (3),

$$z_{\text{left}} = 1 \quad (13)$$

This left outer solution satisfies one of the boundary conditions (B.C.) to Eq. (1), i.e.,

$$z \to 1 \quad \text{as} \quad g_a + g_b \to 1.$$

Satisfying the remaining B.C.,

$$z \to 0 \quad \text{as} \quad g_a + g_b \to \infty,$$

the right outer solution is given by

$$z_{\text{right}} = 0. \quad (14)$$

Matching the inner solution with the left outer solution,

$$\lim_{x\to-\infty}\lim_{\epsilon\to 0}\lim_{X\to 1} z = \lim_{x\to-\infty}\lim_{\epsilon\to 0}\lim_{X\to 1} z_{\text{left}} \quad (15)$$

and the right outer solution

$$\lim_{x\to\infty}\lim_{\epsilon\to 0}\lim_{X\to 1} z = \lim_{x\to\infty}\lim_{\epsilon\to 0}\lim_{X\to 1} z_{\text{right}} \quad (16)$$

gives

$$A = \frac{u}{\sqrt{R_a^* R_b^* |\det G|}},$$

and

$$B = \frac{1}{2}\sqrt{\pi/v}$$

with $\det G = G_{ab}^2 - G_{aa}G_{bb}$.

### 4. Steady-state rate of binary saddle-point nucleation

The total cluster flux in the size space in the case of binary nucleation is difficult to define.[1,2,6,7] From Eqs. (11) and (12), we have

$$\frac{\partial w}{\partial t} = \frac{\partial^2 w}{\partial x^2} + 2u\frac{\partial w}{\partial x} = -\frac{1}{f_0}\frac{\partial}{\partial x}\left(-f_0\frac{\partial w}{\partial x}\right)$$

or

$$\frac{\partial}{\partial t}\int_{-\infty}^{\infty} f(x,y)dy = -\frac{1}{f_0}e^{ux}\frac{\partial}{\partial x}\left(-f_0\frac{\partial w}{\partial x}\right). \quad (17)$$

The Jacobian of the transformation going from variables $g_a, g_b$ to $x, y$ in $f$ is $\sqrt{R_a^* R_b^*}$. Changing the variables $x, y$ into $g_a, g_b$ in $f$ on the left-hand side of Eq. (17), we have

$$\frac{\partial}{\partial t}\int_{-\infty}^{\infty} f[x(g_a,g_b),y(g_a,g_b)]dy(g_a,g_b)$$
$$= -\frac{\partial}{\partial x}\left(-\sqrt{R_a^* R_b^*}f_0 e^{ux}\frac{\partial w}{\partial x}\right) \equiv -\frac{\partial}{\partial x}J. \quad (18)$$

where $J$ is the one-dimensional cluster flux along the unstable variable $x$, averaged over the stability variable $y$

$$J = -\sqrt{R_a^* R_b^*} f_0 e^{\gamma t} \frac{\partial w}{\partial x} = -\sqrt{R_a^* R_b^*} \int_{y} f_0 \frac{\partial z}{\partial x} dy. \tag{19}$$

The left-hand side of Eq. (18) is the rate change of the cluster number concentration which is now equivalent to the left-hand side of Eq. (1); thus $J$ defined by Eq. (18) is also the total flux of clusters in the composition space. The rate of nucleation is given by the total cluster flux at the critical size, and we finally get for the steady-state rate of binary nucleation

$$J_{ss}^* = -\sqrt{R_a^* R_b^*} f_0 e^{\gamma t} \frac{\partial w}{\partial x} = \frac{u}{\beta \sqrt{\det G}} n_0 e^{-\beta G^*}. \tag{20}$$

The above expression for the rate of binary nucleation is similar in form to that of uniary nucleation (which is given by $ZR^* f_0^*$, where $Z$ is the Zeldovich factor, $R^*$ is the reaction rate of a critical-sized cluster, and $f_0^*$ is the cluster number concentration at the critical size). An important difference lies in the fact that the reaction rate in the expression for uniary nucleation is replaced by a complicated factor $u$ that is determined by the reaction rates as well as by the shape of the free energy surface at the saddle opint [Eq. (8)]. Our result for the steady-state rate of binary nucleation with the cluster flux lines passing over the saddle point is exactly the same as that obtained by Trinkaus[7] who employed a different coordinate transformation. Our result is also the same as that obtained by Stauffer.[2]

### 5. Limiting behavior of saddle point binary nucleation

The limiting behavior of binary nucleation taking a saddle trajectory for significantly different reaction rates is sought to examine the kinetic consistency of the theory.

Considering $R_b \ll R_a$ (we can also of course consider the analogous limit, $R_a \ll R_b$) we have from Eq. (8),

*a.* $G_{aa} < 0$. Negative $G_{aa}$ at the saddle point implies that a barrier exists along the axis $g_a$ on $G$ for a given small concentration of $g_b$. In this case, from Eq. (8),

$$u \simeq \beta R_a^* |G_{aa}|. \tag{21}$$

Thus, the kinetic factor in the rate of binary nucleation [Eq. (20)] is controlled by the fast (or more abundant) component $a$ (i.e., $R_a \gg R_b$), which seems on the surface to be contradictory to physical intuition and the direction of the nucleation path. This inconsistency has been attributed to the assumption that the trajectory of the cluster flux line even in the limit of $R_a \gg R_b$ crosses the saddle point.[7,11,12] However, we will show later that the steady-state prediction by Eq. (20) with $u$ given by Eq. (21) is kinetically unattainable because an infinite time lag is required as $R_a^*/R_b^* \to 0$ for $G_{aa} < 0$. Thus in this case the total rate of nucleation is zero because neither component is supersaturated. Therefore, the kinetic consistency of binary nucleation theory is ensured for the case of $R_a^* \gg R_b^*$ and $G_{aa} < 0$ which will be further discussed below. When the $a$ component is supersaturated with respect to its pure state, the total rate of nucleation in the system equals the rate of nucleation of the $a$ component at a given small concentration of the $b$ component with a path along a ridge of the one-dimensional free energy curve. A kinetically consistent theory of nucleation has to be developed by considering multiple nucleation pathways as will be done in the next section.

*b.* $G_{aa} > 0$. Positive $G_{aa}$ means the saddle point is a minimum along the $g_a$-axis in $G$ for a given negligible concentration of $g_b$. Under this condition,

$$u \simeq \beta R_b^* \det G / G_{aa}. \tag{22}$$

Thus, the slow (or the less abundant) component controls the kinetic factor in the nucleation rate. In the limit of $R_b^* \to 0$, the rate of binary nucleation thus goes to zero as expected physically. In this case as also shown below the steady-state rate predicted here [Eqs. (20) and (22)] might be realized without constraints due to the long time lag as for the case of $R_{aa} < 0$.

*c.* $G_{aa} = 0$. $G_{aa} = 0$ implies that the saddle point is not a critical point along the $g_a$ axis for a given small concentration of $g_b$. In this case, from Eq. (8),

$$u \simeq \frac{1}{2} \beta G_{ab} \sqrt{R_a^* R_b^*} \tag{23}$$

and the kinetic factor in the nucleation rate is determined by both the slow and fast components. In the limit of $R_b^* \to 0$, the rate of binary nucleation thus goes to zero as expected physically. As shown in a section below this is the most ideal case of a saddle point nucleation whether or not $a$ is supersaturated with respect to its pure state.

In the above three cases when $R_b \ll R_a$, the cluster flux line first traces along the equilibrium line $\partial G / \partial g_a = 0$, unless it either reaches the coordinate $g_b^*$ of a saddle point with $G_{aa} < 0$, or it reaches, after having passed over a saddle point with $G_{aa} > 0$, a point $G_{aa} = 0$ of unstable growth with respect to component $a$, or it just reaches the saddle point for the case of $G_{aa} = 0$. At those points it bends over into the fast reacting direction $a$ [Eq. (10)]. It should be noted that similar discussions are given for the first two cases by Trinkaus.[7]

In the following we will explore the relative contributions of different nucleation pathways to the total rate of nucleation (binary and uniary) in the system.

## III. MULTIPLE NUCLEATION PATHWAYS: CLUSTER FLUX LINE BYPASSES THE SADDLE POINT

As discussed above when one reaction rate is significantly different from the other the flux line can turn into the direction of the fast-reacting component before the saddle point coordinate of the slowly reacting component is reached. If the fast-reacting component is supersaturated with respect to its pure state, the cluster line can pass over the ridge in the direction of $a$ before $g_b^*$ is reached. This ridge pathway can always coexist with the saddle-point pathway since for very large values of $g_a$ and fixed $g_b$, the formation free energy approaches $-\infty$ for the pure bulk liquid of $a$

component. The valley pathway and the ridge pathway are two solutions to $\partial G/\partial g_u = 0$ for a given small $g_h$ when the activity of $a$ is greater than 1.[3]

The possibilities of multiple nucleation pathways were discussed by Stauffer and Kiang[3] but no results were derived. A recent attempt[7] to deal with this problem quantitatively was not successful. The problem lies in using an incorrect governing equation and an incorrect definition for the rate of nucleation as discussed below.

It is known physically that in the case of significantly different reaction modes, the fast mode adjusts itself to the slow one, the slow-reacting one thus determines the overall kinetics of the process.[13] For a binary nucleation system with significantly different reaction rates, the rate of overall nucleation is governed by the slow component. This means that we can exclude the rapidly relaxing variable, reducing the governing equation to an effective one-dimensional equation. This can be done by using the method of *elimination of the fast variable.*[13]

The resulting one-dimensional effective equation, obtained by integrating Eq. (1) with respect to $g_u$, is

$$\frac{\partial J(g_h)}{\partial g_h} + j_u = -\frac{\partial \int f dg_u}{\partial t}, \tag{24}$$

where the total cluster flux is

$$J = \int j_h \, dg_u. \tag{25}$$

$j_u$ is the cluster flux bending from the equilibrium line (or so-called valley defined by $\partial G/\partial g_u = 0$), passing over the ridge,

$$j_u(g_h) = \left[\frac{\beta |G^r_{uu}|}{2\pi}\right]^{1/2} R^r_u n_0 \exp(-\beta G^r), \tag{26}$$

where $r$ indicates values on the *ridge* defined by $\partial G/\partial g_u = 0$, $\partial^2 G/\partial g_u^2 < 0$. Thus by averaging over the fast variable in the anisotropic limit, the two-dimensional barrier crossing problem is reduced to a one-dimensional barrier crossing problem. The governing equation [Eqs. (24) to (26)] is new. Eq. (24) describes the cluster number conservation (continuity).

It is noted that $j_u$ given by Eq. (26) is different from the expression for the same flux given in previous work.[7] They used $f$ for $n_0$ in Eq. (26) resulting in an incorrect governing equation which is similar in the form to the diffusion equation with a sink term.[14,15] The governing equation obtained is also similar to the governing equation for homomolecular nucleation in the presence of cluster depletion.[8-10]

At steady state, by using Eq. (26), Eq. (24) can be integrated to give

$$J^r_{ss} = \left[\frac{\beta |G^r_{uu}|}{2\pi}\right]^{1/2} R^r_u n_0 \exp(-\beta G^{\text{eff}}), \tag{27}$$

where

$$\exp(-\beta G^{\text{eff}}) = \int_{\gamma} \exp(-\beta G^r) dg_u.$$

We see that the binary nucleation is reduced to a uniary nucleation with an effective free energy $G^{\text{eff}}(g_h)$. $G^{\text{eff}}(g_h)$ is essentially equal to $G^{\text{eff}}[g_u(g_h), g_h]$, where $g_u(g_h)$ is the value of $g_u$ in the valley defined by $\partial G/\partial g_u = 0$. This valley defines the minimum energy path leading from the outer region through the saddle point to a stable-growth region. In general, we can obtain the rate of nucleation passing over the ridge of the one-dimensional curve $G^{\text{eff}}$ from Eq. (27) which is one of the important results obtained. However, depending on the relative magnitudes of $g^r_h$ and $g^*_h$, we can determine the relative contributions of different nucleation pathways to the total rate of nucleation (binary and uniary) from Eq. (27). (Here $g^r_h$ and $g^*_h$ are the $b$-monomer numbers in the two critical sizes existing in a binary system with the activity of component $a$ greater than 1. One is the usual saddle point; the other, the activation size, is the one at which point the barrier to addition of molecules of the supersaturated component vanishes.)

### A. $g^r_h \approx g^*_h$

In the saddle point region the expansion for $G$ given by Eq. (4) can be used. From Eq. (27), the steady-state rate of nucleation at $g_h = g^r_h \approx g^*_h$ and $g_u = g^r_u \approx g^*_u$ is given by

$$J^r_{ss} = \left[\frac{-G^r_{uu}}{G_{hh}}\right]^{1/2} R^r_u n_0 \exp(-\beta G^*). \tag{28}$$

The ratio between $J^r_{ss}$ and the rate of the saddle-point nucleation in the limit of $R_u \gg R_h$ with $G^r_{uu} < 0$ is given by

$$\frac{J^*_{ss}}{J^r_{ss}} = \frac{1}{\sqrt{|1 - (G^2_{uh}/|G_{uu}G_{hh}|)|}}. \tag{29}$$

Thus, the relative contributions of the saddle point path and the mountain ridge path depend on the anisotropy in the free energy surface at the saddle point. When

$$1 > G^2_{uh} > |G_{uu}G_{hh}|$$

or

$$1 > |G_{uu}G_{hh}| > G^2_{uh},$$

then $J^*_{ss} > J^r_{ss}$, i.e., the contribution to the rate of nucleation from the saddle point is more important than that from the ridge path. For a symmetrical potential surface, $G^2_{uh} = |G_{uu}G_{hh}|$, $J^*_{ss}/J^r_{ss} \to \infty$. Also, $J^r_{ss} = 0$ for $G_{uu} = 0$. In those cases, the cluster flux lines can only pass over the saddle point regardless if either of the single species is supersaturated with respect to its pure state because of the dominant importance of the free energy surface. In other words under those conditions only saddle-point nucleation can occur. Of course in the limit of $R^*_h \to 0$, the rate of saddle point nucleation also tends to zero as given by Eqs. (20) and (23).

When the free energy surface at the saddle point becomes very anisotropic such that the ratios between $G^2_{uh}$ and the product $G_{uu}G_{hh}$ become larger than 1, then the cluster flux line can bypass the saddle point completely and the mountain ridge nucleation path becomes dominant in contributing to the total rate of nucleation. This is typically the case for a flatter potential surface.

Equation (29) is also valid for isotropic reaction rates,

i.e., $R_a = R_b$. Thus we have shown that aniostropic reaction rates are not the only cause for cluster flux lines to avoid passing over the saddle point. This saddle point avoidance caused by anisotropy in the potential surface near the saddle point even for isotropic reaction rates might also be a general phenomena in multidimensional activated rate process.[16–18]

### B. $g_b' \gg g_b^*$

Two pathways can be followed by the cluster flux line. The first one is the single barrier path. It is the usual path along which the cluster flux line will first go across the saddle point remain in the valley. Clusters may grow without thermodynamic constraints by accretion of both $a$ and $b$ monomers. This saddle point trajectory is the minimum resistance pathway. Another possible pathway is a double barrier pathway. After passing over the saddle point, clusters may avoid the valley and jump the mountain ridge at $g'$ to grow by adding mostly $a$ monomers.

Since the rate of this double barrier nucleation is smaller than that of the single barrier saddle-point nucleation by a factor of $\exp(-G')$ one expects

$$\frac{J'}{J^*} \approx 0,$$

and the contribution from the saddle point path is the decisive one in determining the total nucleation rate in a binary system when $g_b' \gg g_b^*$.

### C. $g_b' \ll g_b^*$

In this case we can expand $G'$ about $g_b' = 0$,

$$G' = G'_{g_b'=0} + G'_b g_b + G'_a (g_a - g_a'), \tag{30}$$

where $G_b = \partial G/\partial g_b$, $G_a = \partial G/\partial g_a$ at $g_b = g_b' = 0$, and $g_a = g_a'$. Thus, at $g_a = g_a'$ and $g_b = 0$,

$$\begin{aligned} J_{ss}' &= -\int j_a \, dg_b \\ &= \left(\frac{\beta |G_{aa}'|}{2\pi}\right)^{1/2} R_a' n_0 \frac{\exp(-\beta G_{g_b'=0})}{\beta G_b'} \\ &= \left(\frac{\beta |G_{aa}'|}{2\pi}\right)^{1/2} R_a' n_0 \exp(-\beta G^*), \end{aligned} \tag{31}$$

where

$$G^* = G'_{g_b'=0} - \frac{1}{\beta}\ln(\beta G_b').$$

Since

$$\frac{1}{\beta}\ln(\beta G_b')$$

is negligibly small in comparison with $G'_{g_b'=0}$ we have

$$G^* \approx G'_{g_b'=0}.$$

Equation (31) thus gives the exact expression for the rate of a uniary nucleation of component $a$.

We have therefore demonstrated for the first time a continuous transition between binary nucleation and uniary nucleation and the conditions under which this transition occurs.

The contribution to the total nucleation rate from nucleation across the saddle point is given by Eq. (20), with the eigenvalue given by Eq. (21). The ratio of the rate of saddle nucleation and to that of the ridge nucleation is

$$\begin{aligned} J_{ss}^*/J_{ss}' = \frac{R_a^*}{R_a'} \frac{|G_{aa}|}{\sqrt{|\det G|}} \left(\frac{2\pi}{\beta |G_{aa}'|}\right)^{1/2} \\ \times \exp[-\beta(G^* - G')], \end{aligned}$$

which is smaller than 1 if $G^* \gg G'$ but it is larger than 1 if det $G$ goes to zero. This is in contrast with our expectation that $J_{ss}' \gg J_{ss}^*$. Also it is surprising to find that the ratio does not depend on the ratio of $R_a/R_b$. That the ratio of the steady-state rate of nucleation taking the saddle point path over that taking the ridge path does not depend on the ratio of the reaction rates is also in contrast with previous propositions[3] and conclusions.[7]

It will be shown in the next section that the steady-state assumption of different paths might not be realized. The time lag associated with the different paths controls the relative importance in contributing to the total rate of nucleation in a binary system, and it is indeed the ratio of the reaction rates that determines the time lag. Thus a consistent theory for nucleation in a binary system must include the effect of this initial nonstationarity.

Before going on, it is worthwhile pointing out that in previous studies,[7] the governing equation used was incorrect as mentioned above, and the cluster flux at $g_b = 0$ was used as the rate of nucleation, which is only correct for $g_b' \ll g_b^*$.

## IV. TRANSIENT KINETICS OF BINARY NUCLEATION

### A. Effective time lag in binary nucleation

The pathways of nucleation that have been discussed up to now are stationary ones. We have shown that binary nucleation reduces to uniary nucleation of the fast-reacting component $a$ when $R_a \gg R_b$ and $G_{aa} < 0$. But what if no single species is saturated with respect to its pure state when $R_a \gg R_b$? Physically neither binary nucleation nor uniary nucleation should exist. The prediction given by Eqs. (20) and (21) is in contrast with this physically based expectation. In the following we will show the steady-state rate of binary nucleation as predicted by Eqs. (20) and (21) is kinetically unattainable because of the associated infinitely long time lag.

An explicit expression for the time lag for binary nucleation in the case of the trajectory of the cluster flux line passing over the saddle point will be obtained by solving the time-dependent governing equation (1) using the singular perturbation approach.

#### 1. Outer solution

Equation (1) can be simplified as follows:

$$\frac{\partial z}{\partial t} = -R_a \frac{\partial z}{\partial g_a} \frac{\partial \beta G}{\partial g_a} - R_b \frac{\partial z}{\partial g_b} \frac{\partial \beta G}{\partial g_b} \tag{32}$$

in the outer region as shown in Sec. II.

Using the coordinate rotation adopted above, we have

$$\frac{\partial z}{\partial t} = -2ux(1+cx)^{2/3}\frac{\partial z}{\partial x} - 2vy(1+cx)^{2/3}\frac{\partial z}{\partial y}, \quad (33)$$

where

$$c = \frac{\sqrt{R_u^*}\cos\alpha + \mu\sqrt{R_n^*}\sin\alpha}{g^*}. \quad (34)$$

Solving Eq. (33) by introducing $z(x,y,s) = \int_0^\infty \exp(-st)z(x,y,t)dt$, we obtain the Laplace transformation of the outer solution as

$$z_{\text{left}} = \frac{1}{s}\left(\frac{1-\xi}{1-\xi_0}\right)^{\nu/2u}\left(\frac{1+\xi+\xi^2}{1+\xi_0+\xi_0^2}\right)^{-\nu/4u} \times\exp\left\{-\sqrt{3}\frac{s}{2u}\left[\tan^{-1}\left(\frac{2\xi+1}{\sqrt{3}}\right) - \tan^{-1}\left(\frac{2\xi_0+1}{\sqrt{3}}\right)\right]\right\}, \quad (35)$$

where

$$\xi = (1+cx)^{1/3} \quad (36)$$

and $\xi_0$ is the value of $\xi$ at $g_u = 1, g_n = 1$.

For the diffusion-limited nucleation in a condensed phase system, we have

$$z_{\text{left}} = \frac{1}{s}\left(\frac{1-\xi}{1-\xi_0}\right)^{\nu/2u}\left(\frac{1+\xi+\xi^2}{1+\xi_0+\xi_0^2}\right)^{-\nu/4u} \times\exp\left\{\sqrt{3}\frac{s}{2u}\left[\tan^{-1}\left(\frac{2\zeta+1}{\sqrt{3}}\right) - \tan^{-1}\left(\frac{2\xi_0+1}{\sqrt{3}}\right)\right]\right\} \quad (37)$$

and the right outer solution still is $z_{\text{right}} = 0$ for both cases.

In obtaining the above outer solutions we have assumed that the solutions depend only on the unstable variable ($x$). The reason that cluster nucleation can be generally described in terms of a single nucleation path in the outer region is that for relative large $g^*$ the system is essentially in equilibrium everywhere outside the saddle point region. In the inner (saddle point) region the solution has to be obtained by solving the complete equation in terms of unstable and stable variables as will be done below. The accuracy of our solution will be confirmed by reducing it to the known asymptotic result. Our solution is an improvement over that of Wilemski[19] who assumed that the solution depends solely on the unstable variable over the whole region, which is physically incorrect as he pointed out. Another improvement is that we have adopted a more proper coordinate transformation scheme. Wilemski assumed that $\tan\alpha = g_n^*/g_u^*$ which is also incorrect physically in view of the present result [Eq. (10)]. Finally our result is analytically expressed in terms of the properties of the free energy surface and the reaction rates of the two species present. A stochastic approach[11] and a variational method[12] have been developed to study the transient kinetics of binary nucleation, but no explicit analytical expression for the time lag was obtained.

### 2. Inner solution

Solving the time-dependent equation (11) by using Laplace transformation, we obtain the inner solution in terms of two repeated error functions,

$$w = Ai^{\nu/2u}\,\text{erfc}(x\sqrt{u}) + Bi^{\nu/2u}\,\text{erfc}(-x\sqrt{u}), \quad (38)$$

which is the same for both gas-phase and diffusion-limited condensed phase nucleation.

### 3. Matching outer and inner solutions

By matching the outer and inner solutions we get

$$A = \frac{1}{2s}\Gamma\left(1+\frac{s}{2u}\right)\left\{\frac{c\sqrt{1+\xi_0+\xi_0^2}}{3\sqrt{3u}(1-\xi_0)} \times\exp\left[-\sqrt{3}\left(\frac{\pi}{3} - \tan^{-1}\frac{1+2\xi_0}{\sqrt{3}}\right)\right]\right\}^{\nu/2u}\sqrt{\frac{\pi}{v}} \quad (39)$$

for the case of the gas phase, and

$$A = \frac{1}{2s}\Gamma\left(1+\frac{s}{2u}\right)\left\{\frac{c\sqrt{1+\xi_0+\xi_0^2}}{3\sqrt{3u}(1-\xi_0)} \times\exp\left[\sqrt{3}\left(\frac{\pi}{3} - \tan^{-1}\frac{1+2\xi_0}{\sqrt{3}}\right)\right]\right\}^{\nu/2u}\sqrt{\frac{\pi}{v}} \quad (40)$$

for the case of diffusion-limited nucleation in the condensed phase, and $B = 0$ for both cases.

### 4. Time-dependent rate of binary nucleation

After an inversion, we have, from Eqs. (38)–(40),

$$w = \frac{1}{2}\sqrt{\frac{\pi}{v}}\,\text{erfc}\left[\sqrt{u}x + \exp\left(-\frac{t-\lambda\tau}{\tau}\right)\right] \quad (41)$$

for both of the diffusion-limited and gas-phase nucleation. Using Eq. (19) and the above obtained cluster size distribution,

$$J = J_s^* \exp\left[-\exp\left(-2\frac{t-\lambda\tau}{\tau}\right)\right], \quad (42)$$

where

$$\tau = (2u)^{-1} \quad (43)$$

is the characteristic time scale of binary nucleation determined by the collision frequency between monomers and a critical-sized mixed cluster, and

$$\lambda = \sqrt{3}\left(\frac{\pi}{3} - \tan^{-1}\frac{1+2\xi_0}{\sqrt{3}}\right) + \ln\left[\frac{3\sqrt{3u}(1-\xi_0)}{c\sqrt{1+\xi_0+\xi_0^2}}\right] \quad (44)$$

for gas-phase nucleation. For diffusion-limited condensed phase nucleation, we have,

$$\lambda = -\sqrt{3}\left(\frac{\pi}{3} - \tan^{-1}\frac{1+2\xi_0}{\sqrt{3}}\right) + \ln\left[\frac{3\sqrt{3u}(1-\xi_0)}{c\sqrt{1+\xi_0+\xi_0^2}}\right] \quad (45)$$

and $c$ is given by Eq. (34). The difference between the gas-phase and diffusion-limited cases is obviously due to the difference in the reaction rates.

Equation (42) is given at $g_a = g_a^*$ and $g_b = g_b^*$. Different time dependency can be observed at different cluster sizes. It is also noted that the time dependency of the rate of binary of nucleation is similar to that of uniary nucleation.[9] This double exponential dependency of the transient rate of nucleation differs functionally from all other previously obtained results (for a more detailed discussion see Ref. 9).

### 5. Effective time lag of binary nucleation

The number density of critical sized clusters formed in the system following the increase in activities of both components at $t = 0$ is the integrated flux $N(t) = \int_0^t J(t')dt'$. Using Eq. (42), the dimensionless total number is

$$\frac{N(t)}{J_{ss}\tau} = \frac{1}{2}\int_{e^{2(t/\tau-\lambda)}}^{e^{2\lambda}} \frac{dx}{xe^x}$$

$$= \frac{1}{2}[E_1(e^{2(t/\tau-\lambda)}) - E_1(e^{2\lambda})], \tag{46}$$

where $E_1$ is the exponential integral.

As $(t/\tau - \lambda) \to \infty$, we have $e^{2(t/\tau-\lambda)} \to 0$, and $E_1[e^{2(t/\tau-\lambda)}] = -\gamma - 2(\lambda - t/\tau) + O[e^{2(t/\tau-\lambda)}]$, thus

$$\frac{N(t)}{J_{ss}\tau} = -\frac{1}{2}[E_1(e^{2\lambda}) + \gamma + 2\lambda] + \frac{t}{\tau}, \tag{47}$$

where $\gamma = 0.5772$ is Euler's constant.

Eq. (47) thus indicates that at large times, $N(t)$ increases linearly with time $t$ as expected. The beginning of the steady state regime can be determined experimentally by the time at which the increase of $N(t)$ becomes linear with time. The time lag ($\tau_l$) defined in such a way is the effective time lag which is given by

$$\tau_l = \frac{1}{2}[E_1(e^{2\lambda}) + \gamma + 2\lambda]\tau \tag{48}$$

with $\lambda$ given by Eq. (44) for gas-phase nucleation and Eq. (45) for diffusion-limited nucleation in the condensed phase.

The effective time lag for binary nucleation is functionally the same as that for uniary nucleation.[9] In analogy to uniary nucleation, the term $c^{-1}\sqrt{u}$ is equivalent to the small parameter ($\epsilon$). Also the present expression for $\tau$ reduces to the same $\tau$ in the case of an uniary nucleation when $R_a$ or $R_b$ equals zero. Thus we can examine the accuracy of the quadratic expansion for $G$ in solving for the time lag for the binary nucleation by comparing the expressions for the time lag for uniary nucleation using the quadratic expansion for $G$ and using the complete conventional expression for $G$. In using the quadratic expression,

$$\lambda = \sqrt{3}\left[\frac{\pi}{3} - \tan^{-1}\frac{2(g^*)^{-1/3}+1}{\sqrt{3}}\right] + \frac{1}{2}\ln\left[\frac{3}{1+(g^*)^{-1/3}+(g^*)^{-2/3}}\right] + \ln\left\{\frac{3}{\epsilon}[1-(g^*)^{-1/3}]\right\}$$

while

$$\lambda = (g^*)^{-1/3} - 1 + \ln\left\{\frac{3}{\epsilon}[1-(g^*)^{-1/3}]\right\}$$

using the complete conventional expression for $G$.[9] For $g^* = 30$, the difference between the two expressions for $\lambda$ is $1.55\tau$. Using the quadratic approximation, we have overestimated the value of $\lambda$. Since the term $\ln(3/\epsilon)$ is the dominant one in the expression for the $\lambda$, the small difference ($1.55\tau$) in the above expressions for $\lambda$ implies that the quadratic expansion for $G$ used in the present work for deriving the expression for the time lag of binary nucleation is acceptable. However if $G$ is known the procedure presented can be followed to obtain a more accurate expression as done in the case of an uniary nucleation.[9]

### B. Transient kinetics and nucleation paths in a binary system

Let us first examine the time lag at the limit of $R_b \ll R_a$. In this limit, we have

$$c^{-1}\sqrt{u} \approx \frac{g^*}{\mu}\sqrt{\frac{\beta R_a^* |G_{aa}|}{R_b^*}}, \quad G_{aa} < 0, \tag{49}$$

$$c^{-1}\sqrt{u} \approx \frac{g^*}{\mu}\sqrt{\frac{\beta |\det G|}{G_{aa}}}, \quad G_{aa} > 0, \tag{50}$$

$$c^{-1}\sqrt{u} \approx \frac{g^*}{\mu}\sqrt{\frac{\beta G_{ab}}{2}\sqrt{\frac{R_a^*}{R_b^*}}}, \quad G_{aa} = 0. \tag{51}$$

Thus, we observe the following important behavior. First for $G_{aa} < 0$, the time lag for saddle point nucleation in the limit of $R_b \ll R_a$ can be relatively long (depending on the ratio of $R_a^*/R_b^*$) since $\tau_l$ is proportional to $\ln(3c^{-1}u)$. As $R_b/R_a$ goes to zero, the time lag $\tau_l$ approaches infinity. The physics of the problem is clear. If the concentration of one species becomes vanishingly small, heteromolecular nucleation becomes impossible when the remaining species is not supersaturated with respect to its pure state. An infinite time lag of nucleation corresponds to a zero rate of binary nucleation in this case. Thus, although Eqs. (20) and (21) predict that the steady-state rate of nucleation for $G_{aa} < 0$ depends on the fast reactive component $a$, the actual rate depends on the transient kinetics. If $a$ is supersaturated with respect to its pure state, then for $R_a \gg R_b$ and $G_{aa} < 0$, since the time lag of heteromolecular nucleation is longer than that for ridge nucleation, the degeneration of the saddle-point binary nucleation into uniary nucleation as discussed in Sec. III (case 3) will be realizable.

We have thus resolved the conflicit between the prediction by Eqs. (20) and (21) in the case of $R_a \gg R_b$ and $G_{aa} < 0$ and the physical expectation. The theory of nucleation in a binary system is therefore consistently developed.

The first case ($G_{aa} < 0$) shows how the anisotropy in the reaction rates affects the transient kinetics of nucleation. The second case ($G_{aa} > 0$) will show how the anisotropy in

the free energy surface affects the transient kinetics. From the above expression for $G_{uu} > 0$, as $|\det G|$ decreases, the time lag of nucleation increases. It should be noted that in this case the time lag is independent of the anisotropy in the reaction rates. Although the transient kinetics might not be the controlling factor in realizing the steady-state rate of nucleation, the rate is controlled by the slow-reacting component $b$ as predicted by Eqs. (20) and (23). If $a$ is also supersaturated with respect to its pure state, then the concept of nucleation becomes meaningless for $G_{uu}^{\text{eff}} > 0$ at the ridge ($G_{uu}^{\text{eff}} > 0$ because of $G_{uu} > 0$).

In the third case of $G_{uu} = 0$, the effective time lag also increases with increasing $R_u/R_v$. In this case the ridge crossing nucleation is impossible as discussed in Sec. III A. The prediction for the rate of saddle point nucleation given by Eqs. (20) and (23) will be realized after a relatively long time lag for a nonzero concentration of $b$.

## V. RELATIONSHIP TO OTHER ACTIVATED RATE PROCESSES

Kramers classical theory of activated barrier crossing deals only with the case of isotropic diffusion rates. Recently, the role of anisotropy in both potential surface and diffusion rates in affecting the rate of barrier crossing has been an active area of investigation.[16–18,20–22] Since nucleation is an activated barrier crossing rate process, our present results have some implications to the other activated barrier crossing processes. First our results show that saddle-point avoidance can occur even for isotropic diffusion rates when the shape of the potential surface in the saddle region is very asymmetric. In the context of chemical kinetics, this effect is still under study.[19,23]

The saddle point avoidance caused by the anisotropy in diffusion rates is related to the time lag required for system to reach its steady state. The importance of transient kinetics in determining the rate of multidimensional barrier crossing process has not been fully addressed.[21] It will be interesting to apply the present procedure to study the rate and the transient kinetics of a general multidimensional barrier crossing process.

## VI. CONCLUSIONS

Explicit analytical expressions are obtained for the rate of nucleation taking different stationary paths in a binary system. It is shown that not only the anisotropy in reaction rates but also the anisotropy in the free energy surface can cause nucleation to bypass the saddle point completely. Homomolecular nucleation is shown to be the natural limit of heteromolecular nucleation as the concentration of one component goes to zero. Explicit expressions are also obtained for the time lag of binary nucleation by using the singular perturbation approach. Knowledge of the steady state rate of nucleation taking different paths is not sufficient to determine the relative importance of different paths. The saddle point avoidance caused by the anisotropy in diffusion rates is shown to be related to the time lag required for system to reach its steady state.

## ACKNOWLEDGMENT

This work was supported by National Science Foundation Grant No. ATM-9003186.

[1] H. Reiss, J. Chem. Phys. **18**, 840 (1950).
[2] D. Stauffer, J. Aerosol Sci. **7**, 319 (1976).
[3] D. Stauffer and C. S. Kiang, Icarcus **21**, 129 (1974).
[4] P. Mirabel and J. L. Clavelin, J. Aerosol Sci. **9**, 219 (1978).
[5] P. Mirabel and J. L. Katz, J. Chem. Phys. **60**, 1138 (1973); **67**, 1138 (1977); J. L. Schmitt, J. Whitten, G. W. Adams and R. A. Zalabsky, J. Chem. Phys. **92**, 3693 (1990); P. Wagner and G. Vali, *Lecture Notes in Physics*, Vol. 309, Atmospheric Aerosols and Nucleation (Springer, Berlin, 1988), pp. 3 and 367; S. M. Kreidenweis, R. C. Flagan, J. H. Seinfeld and K. Okuyama, J. Aerosol Sci. **20**, 585 (1989).
[6] K. Binder and D. Stauffer, Adv. Phys. **25**, 343 (1976).
[7] H. Trinkaus, Phys. Rev. B **12**, 7372 (1983).
[8] G. Shi and J. H. Seinfeld, J. Colloid Interface Sci. **135**, 252 (1990).
[9] G. Shi, J. H. Seinfeld and K. Okuyama, Phys. Rev. A **41**, 2101 (1990).
[10] G. Shi and J. H. Seinfeld, J. Chem. Phys. **92**, 687 (1990).
[11] W. J. Shugard and H. Reiss, J. Chem. Phys. **65**, 2827 (1976).
[12] W. F. J. Schelling and H. Reiss, J. Chem. Phys. **74**, 3527 (1981).
[13] C. W. Garder, *Handbook of Stochastic Methods for Physics, Chemistry and Natural Sciences* (Springer, Berlin, 1985).
[14] N. Agmon and J. J. Hopfield, J. Chem. Phys. **78**, 6947 (1983).
[15] H. Sumi and R. A. Marcus, J. Chem. Phys. **84**, 4894 (1986).
[16] A. M. Berezhkovskii and V. Y. Zitserman, Chem. Phys. Lett. **158**, 369 (1989).
[17] A. M. Berezhkovskii, L. M. Berezhkovskii, and V. Y. Zitserman, Chem. Phys. **130**, 55 (1989).
[18] R. S. Larson and M. D. Kostin, J. Chem. Phys. **77**, 149 (1983).
[19] G. Wilemskii, J. Chem. Phys. **62**, 3772 (1975).
[20] R. S. Larson, Physica A **137**, 295 (1986).
[21] M. M. Klosek-Dygas, B. M. Hoffman, B. J. Matkowsky, A. Nitzan, M. A. Ratner, and Z. Schuss, J. Chem. Phys. **90**, 1141 (1989).
[22] M. Berkowitz, J. D. Morgan, J. A. McCammon, and S. H. Northrup, J. Chem. Phys. **79**, 5563 (1983).
[23] B. J. Matkowsky, A. Nitzan and Z. Schuss, J. Chem. Phys. **88**, 4765 (1988); **90**, 1292 (1989); and R. S. Larson, *ibid.* **90**, 1291 (1989).

# CHAPTER 8

# TRANSIENT KINETICS OF NUCLEATION AT THE NUCLEATED SIZE

# Transient kinetics of nucleation and crystallization: Part I. Nucleation

G. Shi and J.H. Seinfeld
*Department of Chemical Engineering, California Institute of Technology, Pasadena, California 91125*

(Received 22 April 1991; accepted 4 June 1991)

Analytical results obtained for the transient kinetics of nucleation enable one to interpret $N(g_d, t)$, the accumulated number concentration of clusters at the instrumentally detectable size, $g_d$. The new results enable one to extract kinetic and thermodynamic parameters of nucleation from experimentally measured cluster concentrations and to test nucleation theories experimentally. An approach to estimate the mean time to form the first nucleated cluster in a given sample is also presented.

## I. INTRODUCTION

When an amorphous material is heated to a certain temperature, atoms may rearrange themselves to form small crystalline clusters. The phase transformation from amorphous ($a$-) to crystalline ($c$-) phases is generally considered to be initiated by a nucleation process, and the Gibbs free energy change for this nucleation process is determined by the gain in volume free energy for atoms in the crystalline phase relative to the amorphous phase and by the cost of the free energy necessary to form an interface between the crystalline cluster and the amorphous matrix.[1,2]

Phase transformations from $a$- to $c$-phases or vice versa have various technological applications, one of which is processing of $a$–Si films or layers to obtain high quality SOI (Silicon on Insulator) structures. To obtain high quality SOI, lateral solid-phase epitaxial (LSPE) growth of $a$–Si films deposited on Si substrates with $SiO_2$ patterns has been extensively investigated as a promising technique.[3] Random nucleation in the $a$–Si, however, can compete with LSPE so that the growth of a single crystal over $SiO_2$ is currently limited to length scales smaller than about 10 $\mu$m.[3] A similar problem arises in enlarging grain sizes of a polycrystalline film from an $a$–Si film by thermal annealing.[4,5] The effective time lag for nucleation is often taken as the maximum length of a period of annealing during which random nucleation and thus random crystallization is supposed not to occur.[4]

The technological importance of transient nucleation has stimulated extensive experimental studies of nucleation and crystallization of $a$–Si.[4–6] The fundamental parameters characterizing nucleation and crystallization have to be extracted from experimental data based on theoretical formulations for the transient kinetics. The time required to form a specified crystallized volume fraction is the measure of the stability of an amorphous phase[7] and has to be evaluated based on theoretical expressions for the transient rate of nucleation and time-dependent crystallized volume fraction. In view of its importance, it is surprising to find that little theoretical analysis of transient kinetics of nucleation has been performed[8–14] in the past two decades.

The present work presents new theoretical results for the transient kinetics of nucleation and time-dependent crystallized volume fraction.

## II. TRANSIENT KINETICS OF NUCLEATION IN THE CRITICAL REGION

Results presented below and in Part II for the transient kinetics of nucleation and crystallization are independent of the specific nucleating system (e.g., vapor to liquid, liquid to solid, solid to solid) as long as the Gibbs free energy ($\Delta G$) of formation consists of a volume and a surface energy term, i.e.,

$$\Delta G = -g\Delta\mu + s_1\sigma g^{2/3}$$

and the rate of addition of atoms to a cluster, $\beta(g)$, is proportional to the surface area of the cluster, i.e.,

$$\beta(g) \propto \frac{kT}{h}\exp\left(-\frac{E_d}{kT}\right)s_1 g^{2/3} n_1$$

where $g$ is the number of atoms in a cluster, $\Delta\mu$ is the chemical potential difference of an atom in the nucleating phase and in the nucleated phase, $s_1 = (4\pi)^{1/3}(3v_1)^{2/3}$, $v_1$ is the atomic volume in the nucleating phase, $\sigma$ is the specific interfacial surface free energy, $n_1$ is the number of atoms per unit area near the surface of a cluster, $E_d$ is the activation energy of migration of interfacial atoms from the nucleating phase to the nucleated phase, k is Boltzmann's constant, $T$ is temperature, and h is Planck's constant. For nucleation and crystallization of $a$–Si, for example, the above form of the Gibbs formation energy was proposed by Turnbull[1] and discussed by Roorda and Sinke.[2] It should also be noted that results presented below may be extended to cases with different forms of the Gibbs free energy of

  

formation[2] and different forms of the addition rate, such as a diffusion limited rate. Binary or multicomponent nucleation may also be studied accordingly.[15]

The number of atoms in the critical cluster will be denoted as $g_*$. The critical cluster is that corresponding to the maximum of $\Delta G(g)$. The critical region is the region of clusters, $g_* - \delta < g < g_* + \delta$, which is defined as the region of $g$ satisfying $|\Delta G(g) - \Delta G(g_*)| \leqslant kT$, $\delta = 3g_*^{2/3}\theta^{-1/2}$, and $\theta = s_1\sigma/kT$. The critical region consists of a left region, $g_* - \delta < g < g_*$, and a right region, $g_* < g < g_* + \delta$. To the left of the critical region is the left outer region where $1 \leqslant g < g_* - \delta$; the right outer region is $g > g_* + \delta$. The steepest variation in cluster concentration with size occurs over the critical region, which can be treated as a transition layer.[12] The approach of singular perturbation developed for transition layers[16] can be employed to obtain an inner solution in the critical region and a right outer solution in the right region, and a left outer solution in the left outer region. Two unknowns in the inner solution can be determined by matching the inner solution with the two outer solutions. It should be noted that the singular perturbation approach developed for conventional boundary layers cannot be used for solving nucleation problems since the left outer boundary condition cannot be directly applied to the inner solution.

The transient cluster flux $J(g,t)$ valid strictly in the entire critical region, $g_* - \delta < g < g_* + \delta$, was the key result obtained by a singular perturbation analysis outlined above, as[12]

$$J(g,t) = J_s(g)\exp\left\{-\left[\frac{g-g_*}{\delta} + \exp\left(-\frac{t-\lambda\tau}{\tau}\right)\right]^2\right\} \quad (1)$$

where

$$J_s(g) = \beta(g)n(g)Z$$

and $n(g)$ is the equilibrium cluster number concentration, $Z$ is the Zeldovich factor, $g_* = (2s_1\theta/3\Delta\mu)^3$, $2\delta$ is the width of the entire critical region, and $\tau$ is the characteristic time for a cluster to diffuse over the free energy barrier of the characteristic scale $\delta$,

$$\tau = \frac{\delta^2}{2\beta_*} = \frac{9g_*^{4/3}\theta^{-1}}{2\beta_*} \quad (2)$$

where $\beta_* = \beta(g_*)$. Also $\lambda$ is given by

$$\lambda = g_*^{-1/3} - 1 + \ln\left[\left(g_*^{1/3} - 1\right)\theta^{1/2}\right] \quad (3)$$

It should be pointed out that the solutions obtained by the approach of singular perturbation are accurate for $\Delta G \gg kT$.

By substituting $g = g_*$ in Eq. (1), the transient cluster flux at the critical size is,[12]

$$J(g_*,t) = J_s(g_*)\exp\left\{-\left[\exp\left(-2\frac{t-\lambda\tau}{\tau}\right)\right]\right\} \quad (4)$$

from which one can obtain an expression for the total number concentration of critical clusters formed from 0 to $t$,

$$N(g_*,t) \equiv \int_0^t J(g_*,t)\,dt = \frac{1}{2}J_s(g_*)\tau\left[E_1\left(ae^{-bt}\right) - E_1(a)\right] \quad (5)$$

where $b = 2/\tau$, $a = e^{2\lambda}$, and $E_1$ is the integral exponential function. Equation (5) reduces to a particularly simple form,

$$N(g_*,t) = -\frac{1}{2}J_s(g_*)\tau[E_1(a) + \gamma + 2\lambda] \equiv J_s(g_*)[t - \tau_e(g_*)] \quad (6)$$

when

$$t \gg \left(\frac{1}{2} + \lambda\right)\tau = \tau_e(g_*) + \frac{1}{2}\tau[1 - \lambda - E_1(a)] \quad (7)$$

where $\gamma = 0.5772$ is Euler's constant. Equation (6) thus allows one to identify $\tau_e(g_*)$ as the effective nucleation time lag associated with $N(g_*,t)$,

$$\tau_e(g_*) = \frac{1}{2}\tau[2\lambda + \gamma + E_1(a)] \quad (8)$$

## III. TRANSIENT BEHAVIOR OF THE CLUSTERS AT A DETECTABLE SIZE $g_d$

Ordinarily clusters of the critical size $g_*$ are too small to be detected experimentally. Rather there is a larger size, $g_d$, which will be termed the detectable size. To evaluate observations of the time-dependent behavior of clusters at $g_d$, as evidenced by the accumulated number concentration of $N(g_d,t)$, it is necessary to relate $N(g_d,t)$ theoretically to the parameters of nucleation theory. The derivation of such a relation is the subject of this section.

### A. The nucleated cluster

Since critical clusters of size $g_*$ have an equal average probability to grow and decay, not every cluster that reaches size $g_*$ will subsequently grow to $g_d$, i.e.,

$$N(g_d,t) \neq N[g_*, t - t_d(g_*,g_d)]$$

where $t_d(g_*,g_d)$ would be the time required for a cluster to grow from $g_*$ to $g_d$. In order to interpret $N(g_d,t)$ from nucleation theory and thus to obtain fundamental information about nucleation from the observed $N(g_d,t)$, it

is necessary to know at which size, $g_0$, $g_0 > g_*$, one has the conservation of total clusters,

$$N(g_d, t) = N[g_0, t - t_d(g_0, g_d)] \tag{9}$$

that is, every cluster that reaches size $g_0$ will grow to $g_d$, with a finite time lag $t_d(g_0, g_d)$. Evidently, $g_0 > g_*$ and $g_0$ will be chosen as a size at which the probability to grow exceeds that to decay. Figure 1 illustrates the relationship among $g_*$, the critical region, $g_0$, and $g_d$.

The time to grow from any size $g$ to size $g_d$, $t_d(g, g_d)$ is given by the integrated inverse of the growth rate $\dot{g}$,

$$t_d(g, g_d) = \int_g^{g_d} \frac{dg}{\dot{g}}$$

which is a stochastic variable for $g$ near $g_*$. The deterministic part of the growth rate ($\dot{g}_m$),[10]

$$\dot{g}_m = -\frac{\beta(g)}{kT}\frac{\partial \Delta G}{\partial g}, \qquad \frac{\partial \Delta G}{\partial g} < kT \tag{10}$$

is dominant for a size $g \gg g_* + \delta$; i.e., outside the right critical region, a cluster has a much larger probability to grow than to decay. It is therefore appropriate to take $g_0 \gg g_* + \delta$, for which the growth rate is

$$\dot{g} = \dot{g}_m, \qquad g \gg g_* + \delta \tag{11}$$

from which $t_d(g_0, g_d)$ can be obtained directly.

### B. Transient kinetics at $g_0$ and $g_d$

To obtain $N(g_0, t)$, one has first to obtain $J(g_0, t)$. Equation (1) is strictly valid in the critical region $g_* - \delta > g > g_* + \delta$. According to the principle of singular perturbation,[16] Eq. (1) is also asymptotically correct for $z < 1/\epsilon$, i.e., $g < 2g_*$, where $\epsilon = \delta/g_*$ is the small perturbation parameter.[12] An approximate $J(g_0, t)$ can be obtained from Eq. (1) for $t \gg (\lambda - \ln 2z_0)\tau$ with $z_0 = (g_0 - g_*)/\delta \gg 1$ as,

$$J(g_0, t) = J_s(g_0)e^{z_0^{-2}} \exp\left[-\exp\left(-\frac{t - \tau_0}{\tau}\right)\right] \tag{12}$$

where

$$\tau_0 = [\lambda + \ln 2z_0]\tau \tag{13}$$

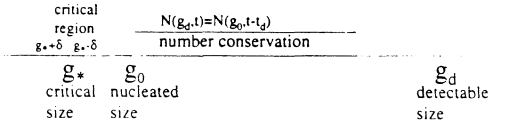


FIG. 1. Relationship between the critical size, nucleated size, and the detectable size. Not every cluster that reaches size $g_*$ can reach $g_d$, but every cluster reaching size $g_0$ can grow to $g_d$. Since Eq. (1) is valid in the critical region[12] as well as asymptotically valid for $g < 2g_*$, one can obtain $N(g_0, t)$ from Eq. (1), as shown below. One then can use the fact that the total accumulated number concentration of nucleated clusters is conserved to obtain $N(g_d, t)$.

Since $\dot{g} \approx \dot{g}_m$ for $g \approx g_* + \delta$ and Eq. (1) is valid for $g < 2g_*$, we thus can take the average of the above upper and lower limits for $g$ as $g_0 = \frac{1}{2}(2g_* + g_* + \delta) = \frac{1}{2}(3g_* + \delta)$.

$J_s(g_0)e^{z_0^{-2}}$ should be exactly equal to $J_s(g_*)$ since the steady-state cluster flux is the same at all sizes.[10] It should be noted that the difference (about 10%) between $J_s(g_0)e^{z_0^{-2}}$ and $J_s(g_*)$ is due to the fact that Eq. (1) is strictly valid only in the critical region and only approximately correct at $g_0$. The error is not due to the singular perturbation approach itself; that is, including higher-order contributions does not improve the accuracy of the result. Since the steady-state rate of nucleation is the same at all sizes, and $J_s(g_0)e^{z_0^{-2}}$ is the steady-state rate of nucleation at $g_0$, the small error can be corrected by simply taking $J_s(g_0)e^{z_0^{-2}} = J_s(g_*)$ in the expression for $J(g_0, t)$. Equation (12) is in a similar form to that obtained by Shneidman[14] who, however, obtained a different expression for $\tau_0$.

Subsequently, from Eq. (12), one can obtain

$$N(g_0, t) = J_s(g_*)\tau[E_1(e^{-[(t-\tau_0)/\tau]}) - E_1(e^{\tau_0/\tau})] \tag{14}$$

For sufficiently large times, i.e., $t \gg \tau_0 + \tau$, Eq. (14) reduces to

$$N(g_0, t) = J_s(g_*)[t - \tau_e(g_0)] \tag{15}$$

The effective time lag associated with $N(g_0, t)$ is then given by

$$\tau_e \equiv \tau_e(g_0) = \tau[\gamma + \tau_0/\tau + E_1(e^{\tau_0/\tau})] \tag{16}$$

which can usually be approximated as

$$\frac{\tau_e}{\tau} = \gamma + \tau_0/\tau \tag{17}$$

since $E_1(e^{\tau_0/\tau}) \approx 0$. Using the fact that the total number concentration of *nucleated* clusters is conserved, the experimentally determined $N(g_d, t)$ is equal to the total accumulated number at $g_0$,

$$N(g_d, t) \equiv N(g_0, t - t_d) \tag{18}$$

which, for sufficiently large times, $t > \tau_0 + \tau + t_d$, reduces to

$$N(g_d, t) = J_s(g_*)(t - t_d - \tau_e) \tag{19}$$

where $t_d$ is given by,

$$t_d \equiv t_d(g_0, g_d) = \int_{g_0}^{g_d} \frac{dg}{\dot{g}_m}$$

$$= \tau\left\{\left(\frac{g_d}{g_*}\right)^{1/3} - \left(\frac{g_0}{g_*}\right)^{1/3} + \ln\left[\frac{\left(\frac{g_d}{g_*}\right)^{1/3} - 1}{\left(\frac{g_0}{g_*}\right)^{1/3} - 1}\right]\right\} \tag{20}$$

The total time lag associated with $N(g_d,t)$ defined by Eqs. (19) and (20) can be regrouped as

$$\frac{t_d+\tau_e}{\tau} = \gamma - 1 + \ln\frac{2}{3} + E_1\left(e^{\tau_0/\tau}\right) + g_*^{-1/3} + \ln\left[g_*^{1/3}\theta\left(1-g_*^{1/3}\right)\right] + \left(\frac{g_d}{g_*}\right)^{-1/3} + \ln\left[\left(\frac{g_d}{g_*}\right)^{-1/3} - 1\right] - \left(\frac{g_0}{g_*}\right)^{1/3} + \ln\left[\left(\frac{g_0}{g_*}\right)^{2/3} + \left(\frac{g_0}{g_*}\right)^{1/3} + 1\right] \quad (21)$$

Since $E_1(e^{\tau_0/\tau}) \approx 0$ and the value of $-(g_0/g_*)^{1/3} + \ln[(g_0/g_*)^{2/3} + g_0/g_* + 1]$ varies from 0.1 to 0.01 as $g_0/g_*$ varies from 1.5 to 2, the choice of $g_0$ does not affect the final result for the total time lag $\tau_e + t_d$ associated with $N(g_d,t)$.

Equations (14) to (21) enable one to extract the thermodynamic and kinetic parameters from measured $N(g_d,t)$ and thus also enable one to test nucleation theories. Figure 2 shows the schematic relationship between $N(g_d,t)$ and $N(g_0,t)$ according to Eqs. (14) to (19). The time for a cluster to grow from $g_0$ to $g_d$, $t_d(g_0,g_d)/\tau$ increases with the detectable size $r_d/r_*$, as shown in Fig. 3, where $r_d$ and $r_*$ are the radius of a cluster at the detectable size and critical size, respectively.

The expressions for the transient rate of nucleation and the accumulated number concentration of nucleated clusters are functionally different from those obtained previously by Kashchiev[11] for the reasons explained in Ref. 12.

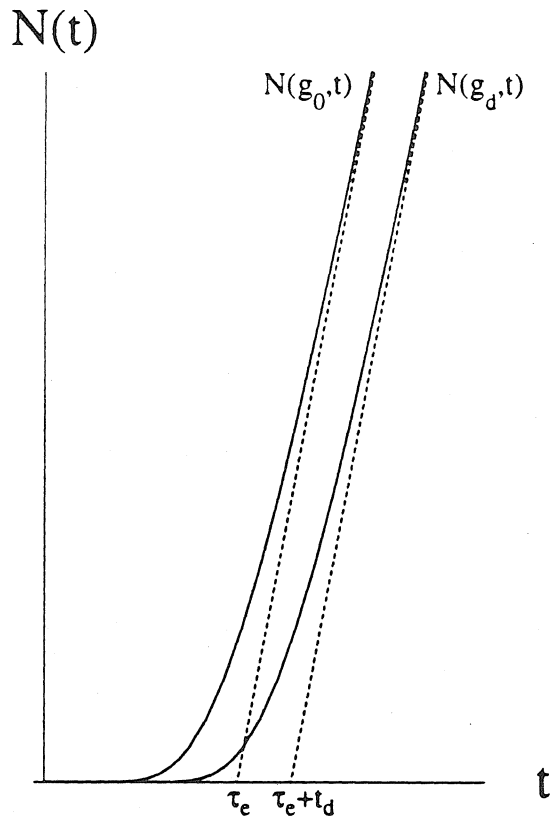


FIG. 2. The relationship between total number concentration of nucleated clusters, $N(g_0,t)$ given by Eq. (14), and at the instrumentally detectable size $g_d$, $N(g_d,t)$, given by Eq. (18). The dashed lines are the large time limits of $N(g_0,t)$ and $N(g_d,t)$, which are given by Eqs. (15) and (19), respectively.

### C. Effective time lag for nucleation

The effective time lag associated with $N(g_0,t)$ obtained above, Eq. (16), can be written as

$$\frac{\tau_e(g_0)}{\tau} = \gamma - 1 - \ln 6 + E_1\left(e^{\tau_0/\tau}\right) + g_*^{-1/3} + \ln\left[\theta^{1/2}\left(g_*^{1/3}-1\right)\left(3+g_*^{1/3}\theta^{1/2}\right)\right] \quad (22)$$

where $\gamma - 1 - \ln 6 \approx -2.2146$ and $E_1\left(e^{\tau_0/\tau}\right) \approx 0$. Similarly, the time lag associated with $N(g_*,t)$ given by Eq. (8) can be written as

$$\frac{\tau_e(g_*)}{\tau} = \gamma/2 - 1 + E_1\left(e^{2\lambda}\right) + g_*^{-1/3} + \ln\left[\theta^{1/2}\left(g_*^{1/3}-1\right)\right] \quad (23)$$

The ratio of $\tau_e(g_0)/\tau$ and $\tau_e(g_*)/\tau$ thus depends on both $g_* = (2\theta kT/3\Delta\mu)^3$ and $\theta = s_1\sigma/kT$. In contrast, the effective time lag associated with $N(g_*,t)$ obtained previously by Kashchiev,[11] whose solution has been regarded as the most accurate,[8] is a constant, $\pi^2/6\tau_k$ where $\tau_k = 8\tau/\pi^2$. In our notation, Kashchiev's result for the effective time lag associated with $N(g_*,t)$ is $4\tau/3$.

Figures 4 and 5 show the ratios of $\tau_e(g_0)/\tau$ and $\tau_e(g_*)/\tau$ as a function of $g_*$ for various values of the dimensionless surface free energy[17] according to Eqs. (22) and (23). The dashed lines in Figs. 4 and 5 are $\tau_e(g_0)/\tau$ and $\tau_e(g_*)/\tau = 4/3$. It is seen from Figs. 4 and 5 that the ratios of $\tau_e(g_0)/\tau$ and $\tau_e(g_*)/\tau$ are different from 4/3, even though no large variation is observed for $\theta$ in the range of 2 to 10.[17]

Physically, the problem underlying previous results for the effective time lag $\tau_e(g_*)$ associated with $N(g_*,t)$, as has been discussed,[12,9,10] is that the time to form the subcritical cluster distribution is not taken into account properly. Obviously $\tau_e(g_0) \neq \tau_e(g_*)$ since the time taken in the formation of the supercritical cluster distribution

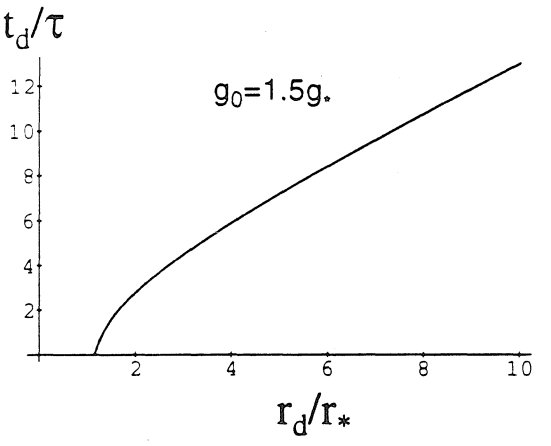


FIG. 3. The time, $t_d$, given by Eq. (20), for a cluster to grow from $g_0$ to the detectable size $g_d$ as a function of $r_d/r_*$. Here $r_d$ and $r_*$ are the radius of a cluster at the detectable size and the critical size, respectively.

from $g_*$ to $g_0$ is not included in $\tau_e(g_*)$. The time for the formation of the subcritical and supercritical cluster distribution depends on the height of the Gibbs energy barrier, and is reflected in the coefficient of $\tau_e(g_0)/\tau$.

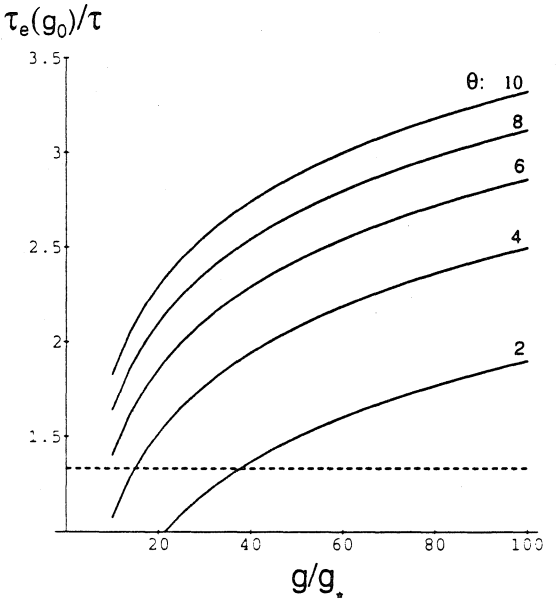


FIG. 4. The ratio between the effective time lag $\tau_e$ associated with $N(g_0, t)$ and the characteristic time scale $\tau$ for cluster diffusion over the energy barrier, $\tau_e/\tau$, as a function of the critical size $g_*$ for different values of dimensionless specific surface energy $\theta$,[17] as given by Eq. (22). The dashed line gives $\tau_e/\tau = 4/3$ obtained previously.[10]

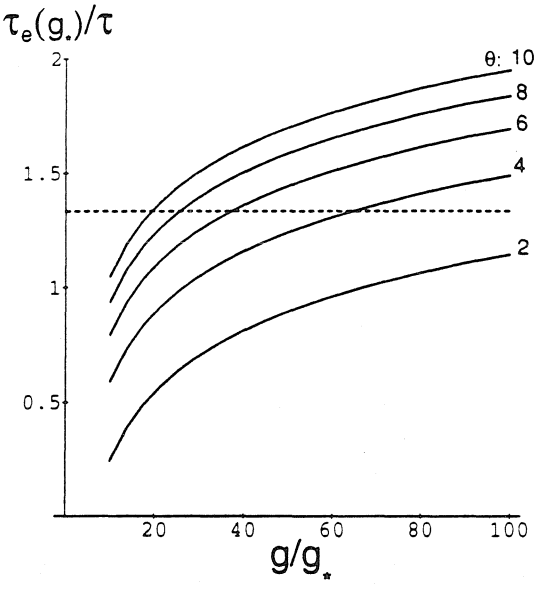


FIG. 5. The ratio between the effective time lag $\tau_e(g_*)$ associated with $N(g_*, t)$ and $\tau$, $\tau_e/\tau$, as a function of $g_*$ for different values of dimensionless specific surface energy $\theta$,[17] as given by Eq. (23). The dashed line is $\tau_e(g_*)/\tau = 4/3$.

## IV. TIME TO FORM THE FIRST NUCLEATED CLUSTER IN A GIVEN VOLUME

By setting $N(g_0, t) = 1$, Eq. (15) presents a general formulation for estimating the average time to observe the first nucleated cluster in a *unit* volume, $t_1$.

The conventional expression for $t_1$ has the form[18–21]

$$t_1 = \frac{1}{J_s(g_*)} + \tau_e(g_*)$$

Replacing $\tau_e(g_*)$ by $\tau_e(g_0)$, one has

$$t_1 = \frac{1}{J_s(g_*)} + \tau_e(g_0) \tag{24}$$

which can be easily obtained from Eq. (15) but is not a universally valid expression to estimate $t_1$ because of the assumptions inherent in Eq. (15).

Equation (24) indicates that the time to observe the first nucleated cluster in a unit volume, $t_1$, is equal to the sum of the effective time lag associated with $N(g_0, t)$ and the inverse of the steady-state nucleation rate. This is probably the root of the erroneous concept that the rate of nucleation is negligible during the period of the effective time lag for nucleation and consequently that the stability of amorphous phases is measured by the length of the effective time lag for nucleation.

Since Eq. (15) is valid only for $t \gg \tau_0 + \tau$, Eq. (24) can be used to estimate the time to form the first nucleated cluster only for

$$J_s(g_*)\,\tau \ll \frac{1}{1-\gamma} = 2.365 \qquad (25)$$

Using experimental data[4,5] obtained for crystallization of $a$–Si at about 900 K, the order of $\tau$ is about $10^3$ s and $J_s$ is of order $10^8$ $s^{-1}$ $cm^{-2}$. Thus the condition for using the conventional formula, Eq. (24), is not satisfied in this case. Instead, Eq. (14) should be used in general. An estimation based on Eq. (14) gives the time to form the first nucleated cluster per $cm^3$ in the above cited system to be the order of about $10^{-6}$ $\tau_e$. For other systems, the above condition can be easily checked if the order of magnitude of $\tau$ and $J_s$ can be estimated.

The time to form the first nucleated cluster in a given volume as a measure of the stability of an amorphous phase has also been used to construct models for the existence of a critical thickness in solid state amorphization (SSA).[18,19] For modeling the critical thickness in SSA of NiZr, Meng *et al.*[18] used $1/J_s(g_*)$, and Highmore *et al.*[19] used $\tau_e(g_*)$ given by Kashchiev as the time to form the first *critical* cluster (in a unit volume). Unfortunately, those applications of $t_1$ are invalid for two reasons. First, the approximation for $t_1$ used by both is inapplicable for nucleation with a long time lag in NiZr at low temperatures (360 °C),[19] as discussed above. Second, neither realized that $t_1$ is the time to form the first nucleated cluster in a *unit sample* (unit volume or surface), which cannot be used unless one has specified the critical volume or surface. Also, in all previous applications no distinction was made between a *critical* cluster and a *nucleated* cluster.

## V. CONCLUSION

New results are presented that enable one to extract fundamental kinetic and thermodynamic information for nucleation from $N(g_d, t)$, the accumulated number concentration of clusters at the instrumentally detectable size, $g_d$, and to test nucleation theories experimentally. Relationships between the effective time lag for nucleation and the time to form the first nucleated cluster in a given volume have been developed.

## REFERENCES

1. D. Turnbull, J. Chem. Phys. **18**, 198 (1950); Comtemp. Phys. **10**, 473 (1969); G. L. Olson and J. A. Roth, Mater. Sci. Rep. **3**, 1 (1988) and references therein.
2. S. Roorda and W. C. Sinke, Appl. Surf. Sci. **36**, 588 (1989).
3. Y. Kuni, M. Tabe, and K. Kajiyama, J. Appl. Phys. **54**, L23 (1980); M. Tamura, H. Tamura, and T. Tokuyama, Jpn. J. Appl. Phys. **19**, 2847 (1983); H. Ishiwara, A. Tamba, and S. Turukawa, Appl. Phys. Lett. **48**, 733 (1986); H. Ishiwara, H. Yamamoto, and S. Turukawa, Appl. Phys. Lett. **43**, 1028 (1983); T. Dan, H. Ishiwara, and S. Furukawa, Appl. Phys. Lett. **53**, 2626 (1988); M. Miyao, M. Moniwa, K. Kusukawa, and W. Sinke, J. Appl. Phys. **64**, 3018 (1983).
4. D. B. Korin, R. Reif, and B. Mikic, Thin Solid Films **167**, 101 (1988); R. B. Inverson and R. Reif, J. Appl. Phys. **62**, 1675 (1987); R. B. Inverson and R. Reif, Appl. Phys. Lett. **52**, 645 (1988).
5. S. Roorda, P. Kammann, W. C. Sinke, G. F. A. Walle, and A. A. van Gorkum, Mater. Lett. **9**, 259 (1990).
6. M. Suzuki, M. Hiramoto, M. Oyuura, W. Kamisaka, and S. Hasegawa, Jpn. J. Appl. Phys. **27**, L1380 (1988); S. Kambayash, S. Onga, I. Mizushima, K. Higachi, and H. Kuwano, Extended Abs. of the 21st Conf. on Solid State Devices and Mater., Tokyo, 1989, p. 169; K. Zallama, P. Germain, S. Squeland, J. C. Bourjoin, and P. A. Thomas, Appl. Phys. **50**, 6995 (1979); U. Köster, Phys. Status Solidi **48**, 313 (1978); C. C. Pai, S. S. Lau, and I. Suni, Thin Solid Films **109**, 263 (1983); R. Bisaro, J. Magarino, Y. Pastol, P. Germain, and K. Zellama, Phys. Rev. B **40**, 7655 (1989); J. S. Im and H. A. Atwater, Appl. Phys. Lett. **57**, 1766 (1990); I. W. Wu, A. Chiang, M. Fuse, L. Ovecoglu, and T. Y. Huang, J. Appl. Phys. **65**, 4036 (1989); E. E. Marinero, Appl. Surf. Sci. **43**, 117 (1989).
7. D. R. Uhlmann, J. Non-Cryst. Solids **25**, 73 (1977); J. Non-Cryst. Solids **7**, 73 (1972).
8. K. F. Kelton, A. L. Greer, and C. V. Thompson, J. Chem. Phys. **79**, 6261 (1983); K. G. Harstad, JPL Tech. Mem., 33-666, Jet Propulsion Laboratory, Pasadena, CA, January 1974.
9. V. Voltera and A. R. Cooper, J. Non-Cryst. Solids **74**, 85 (1985).
10. J. Feder, K. C. Russell, J. Lothe, and G. M. Pound, Adv. Phys. **5**, 111 (1966).
11. D. Kashchiev, Surf. Sci. **14**, 209 (1969).
12. G. Shi, J. H. Seinfeld, and K. Okuyama, Phys. Rev. A **41**, 2101 (1990).
13. H. Trankaus and M. H. Yoo, Philos. Mag. A **55**, 269 (1987).
14. V. A. Shneidman, Sov. Phys. Tech. Phys. **33**, 1338 (1988).
15. G. Shi and J. H. Seinfeld, J. Chem. Phys. **92** (12), 9033 (1990).
16. C. M. Bender and S. A. Orszag, *Advanced Mathematical Methods for Scientists and Engineers* (McGraw-Hill Co., New York, 1978).
17. The value of $\theta$ for $a$–Si is generally unknown since the $a$–Si/$c$–Si interfacial specific energy $\sigma$ is not accurately known. For example, model-building studies of planar interfaces separating bulklike $c$–Si and $a$–Si yield 0.12 eV/atom (about 112 erg/$cm^2$) and experimental studies give a 0.04 eV/atom as cited by J. Y. Tsao and P. S. Peercy, Phys. Rev. Lett. **58**, 2782 (1987); values of 430 erg/$cm^2$ for $\sigma$ were used in Ref. 2; 219 to 275 erg/$cm^2$ for $\sigma$ was used by R. F. Wood, D. H. Lowndes, and J. Marayan, Appl. Phys. Lett. **44**, 770 (1984); 125 erg/$cm^2$ for $\sigma$ was used by D. Stock, H. D. Geiler, and K. Hehl, Phys. Status Solidi (a) **89**, 2782 (1987). For $\sigma$ in the range of 40 to 400 erg/$cm^2$, $\theta = 25\sigma/T$ varies from 1 to 10 for $T$ = 1000 K.
18. W. J. Meng, C. W. Nieh, E. Ma, B. Fultz, and W. L. Johnson, Mater. Sci. Eng. **97**, 871 (1988).
19. R. J. Highmore, A. L. Greer, J. A. Leake, and J. E. Evetts, Mater. Lett. **6**, 401 (1988); R. J. Highmore, Philos. Mag. B **62**, 455 (1990).
20. See reviews in J. W. Christian, *The Theory of Phase Transformations in Metals and Alloys*, 2nd ed. (Pergamon, Oxford, 1975).
21. I. Gutzow, Contemp. Phys. **21**, 121 (1980).

# CHAPTER 9

# EFFECTS OF TRANSIENT NUCLEATION IN THE AVRAMI MODEL FOR CRYSTALLIZATION

# Transient kinetics of nucleation and crystallization: Part II. Crystallization

G. Shi and J. H. Seinfeld
*Department of Chemical Engineering, California Institute of Technology, Pasadena, California 91125*

(Received 22 April 1991; accepted 4 June 1991)

Analytical expressions for the time-dependent crystallized volume fraction are derived from new results for the transient rate of nucleation reported in Part I. Conventional formulations that have been used in interpreting crystallization experimental data and for assessing the stability of amorphous phases are shown to be large time limits of the newly derived expressions. An approach for assessing the stability of an amorphous phase is proposed.

## I. INTRODUCTION

Theoretical expressions for the time-dependent crystallized volume fraction allow one to extract kinetic and thermodynamic parameters of crystallization from experimentally measured crystallized volume fraction. This enables one to test nucleation and crystallization theories and to address technological issues such as determining the stability of an amorphous phase at a given temperature, critical in processing of $a$–Si films or layers to obtain high quality SOI (Silicon on Insulator) structures,[1] and designing processing procedures to enlarge grain sizes of a polycrystalline film by thermal annealing.[2,3] Assessing the stability of an amorphous phase is critical in evaluating materials suitable for erasable phase-change optical recording.[4]

The time-dependent crystallized volume fraction, $\alpha$, is generally described by the Avrami model,[6–8]

$$\alpha(t) = 1 - \exp\left[-k_d V^d \int_0^t J(t')\,(t-t')^d\,dt'\right] \equiv 1 - \exp(-y_d) \tag{1}$$

where $d = 1, 2, 3$ corresponds to one-, two-, and three-dimensional growth of a cluster, $k_d$ is a geometrical factor (e.g., $k_3 = 4\pi/3$, $k_2 = \pi$, and $k_1 = 2$ for a spherical crystalline cluster). $V(t-t')$ is the linear dimension of a cluster at time $t$ that is nucleated at $t'$, $V$ is the growth rate of a crystalline cluster that can be taken as a constant for an isothermal annealing process, and $y_d$ is the extended-volume.[6] $J(t)$ is the transient rate of nucleation, which is generally taken as $J(g_*, t)$. Based on the difference between $J(g_*, t)$ and $J(g_0, t)$ and the definition of *nucleated* clusters as described in Part I, it is clear that $J(g_0, t)$ is a more appropriate choice for $J(t)$ in the Avrami equation.

The expression for the transient rate of nucleation at the nucleated cluster size $g_0$, $J(g_0, t)$ derived in Part I,[9] will be used to obtain analytical expressions for the time-dependent crystallized volume fraction based on Eq. (1). The conventional Avrami-like expressions that have been used in interpreting crystallization experimental data and in assessing the stability of amorphous phases are shown to be the large time limits of the present results. Throughout the paper, the crystallization of $a$–Si will be discussed as an example of application of the results, although the results can be applied to other crystallizing systems.

## II. BULK CRYSTALLIZATION: HOMOGENEOUS NUCLEATION AND 3-D GROWTH

In this section, we will derive an expression for $\alpha(t)$ for the case of nucleation occurring in the bulk and with subsequent three-dimensional growth of nucleated clusters.

By substituting the expression for $J(g_0, t)$ obtained from Part I[9] into Eq. (1), one obtains

$$\alpha(t) = 1 - e^{-y_3}$$
$$y_3 = \left(\frac{t}{\tau_3}\right)^4 \left\{1 - 4\frac{\tau_e}{t} + 24\left(\frac{\tau}{t}\right)^4 \sum_{n=1}^{\infty} \frac{(-q)^n}{n^4 n!} \cdot \left[e^{-nt/\tau} - 1 + \frac{nt}{\tau} - \frac{1}{2}\left(\frac{nt}{\tau}\right)^2\right]\right\} \tag{2}$$

where $q = e^{\tau_0/\tau}$ and

$$\tau_3 = \left[\frac{3}{\pi J_s(g_*) V^3}\right]^{1/4} \tag{3}$$

which, together with $\tau_e$ and $\tau$, characterizes the speed of crystallization. Using expressions for $J_s(g_*)$ and $V$ from Part I,[9] Eq. (3) can be rewritten as

$$\frac{\tau_3}{\tau} = \left[\frac{2}{\sqrt{\pi} r_1^3 n_1}\right]^{1/4} g_*^{-5/12} \theta^{1/8} \exp\left[\frac{1}{12}\theta g_*^{2/3}\right] \tag{4}$$

where $r_1^3 n_1 \approx 1$.

As shown in Fig. 1, $\tau_3/\tau$ depends strongly on $\theta$ and $g_*$ because of the strong dependence of the rate

  

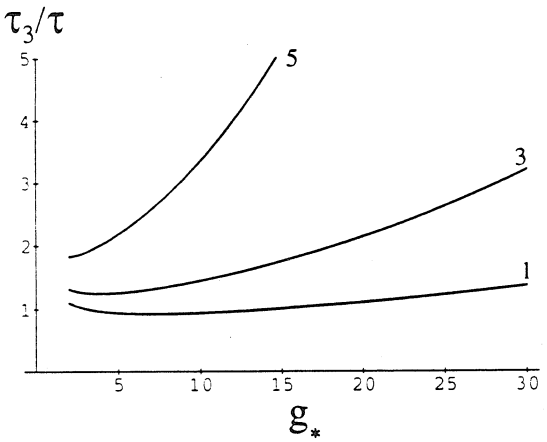


FIG. 1. Characteristic time scale for crystallization $\tau_3/\tau$ as a function of $g_*$ for various values of $\theta$, as given by Eq. (4).

of nucleation on $\theta$ and $g_*$, which are determined by temperature and the type of material.

### A. Comparison with previous results

Equation (2) indicates that the change of the crystallized volume fraction with time depends on $\tau_3/\tau_e(g_0)$, $\tau_e(g_0)/\tau$ and $t/\tau$, while $\alpha(t)$ was found to be a function only of $t/\tau$ and $\tau_3/\tau$ by Gutzow *et al.*,[8] which is the only previous systematic study of the role of the nucleation time lag in crystallization. Their previous result, in terms of the present notations, is

$$y_3^{\mathrm{GKA}} = \left(\frac{t}{\tau_3}\right)^4 \left[1 - \frac{16}{3}\frac{\tau}{t} + \frac{224}{15}\left(\frac{\tau}{t}\right)^2 - \frac{7936}{315}\left(\frac{\tau}{t}\right)^3 + \frac{32512}{1575}\left(\frac{\tau}{t}\right)^4 + \frac{196608}{\pi^8}\left(\frac{\tau}{t}\right)^4 \cdot \sum_{n=1}^{\infty} \frac{(-1)^n}{n^8} e^{-(n^2\pi^2/8)(t/\tau)}\right] \quad (5)$$

Figure 2 compares the predictions of $\alpha(t)$ by Eqs. (2) and (5) for $\tau_e/\tau = 1, 2, 3$ at $\tau_3/\tau = 1, 3$. The dashed lines in Fig. 2 are given by Eq. (5), which predicts that $\alpha(t)$ is independent of $\tau_e/\tau$. Since $\alpha(t)$ clearly depends on $\tau_e(g_0)/\tau$, Eq. (5) is not capable of predicting $\alpha(t)$ even qualitatively.

It should be emphasized that although numerical values of $\tau_e$ resulting from newly derived and previous expressions for the transient rate of nucleation are not similar, as shown in Part I, the functional difference between those expressions results in significant differences when used to evaluate $\alpha(t)$. Another reason for such differences is that the nucleated cluster is properly defined at $g_0$ instead of $g_*$ as in all previous work. The role of the nucleation time lag in the overall kinetics

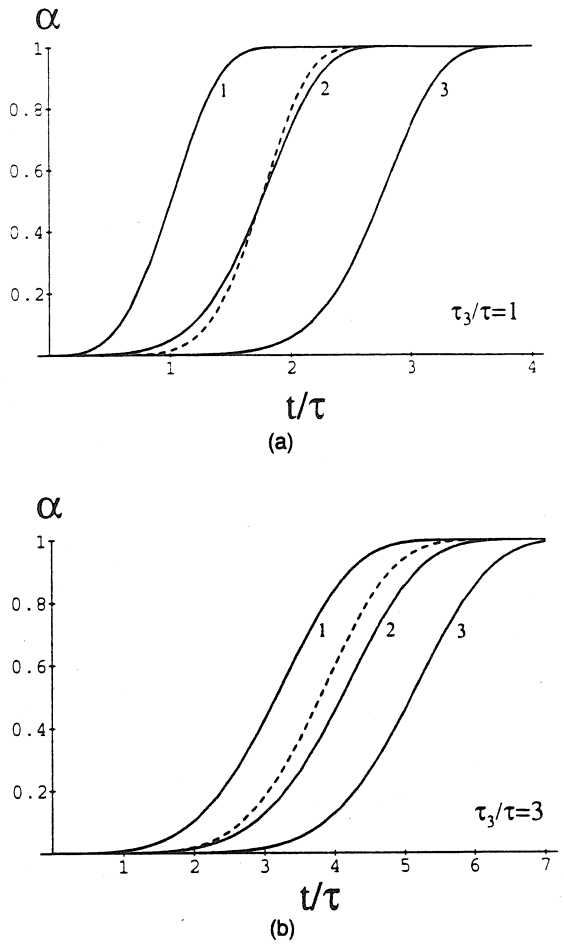


FIG. 2. (a) Crystallized volume fraction $\alpha(t)$ as a function of time as predicted by Eqs. (2) and (5) for $\tau_e/\tau = 1, 2, 3$ at $\tau_3/\tau = 1$; (b) and at $\tau_3/\tau = 3$. The dashed curves give the prediction[8] by Eq. (5).

of crystallization is overestimated or underestimated by Eq. (5), which cannot be used either as an expression to fit data of $\alpha(t)$ nor as a predictive tool.

### B. Large time limit

The conventional expression for fitting observed $\alpha(t)$ in the case of homogeneous nucleation and three-dimensional growth has the form,[7,8]

$$\alpha(t) = 1 - \exp\left[-\left(\frac{t - \tau_e}{\tau_3}\right)^4\right] \quad (6)$$

which, as shown below, is a large time limit of Eq. (2).

Under the condition of $t \gg \sqrt{6}\tau_e$, Eq. (2) can be approximated as,

$$y_3 \approx \left(\frac{t}{\tau_3}\right)^4 \left(1 - 4\frac{\tau_e}{t}\right)$$
$$\approx \frac{\pi}{3} J_s(g_*) V^3 t^4 \left(1 - \frac{\tau_e}{t}\right)^4 = \left(\frac{t - \tau_e}{\tau_3}\right)^4 \quad (7)$$

Equation (6) is obtained by substituting Eq. (7) into Eq. (1). Thus Eq. (6) is valid only for $t \gg \sqrt{6}\tau_e$.

In Fig. 3, we compare the predictions given by Eq. (2) and its large time limit given by Eq. (6). Indicated on the curves are the values of $\tau_e/\tau$. The solid curves are predictions according to Eq. (2). The dashed lines correspond to large time limits given by Eq. (6).

Figures 3(a) and 3(b) show that at given conditions the crystallization is completed within $\sqrt{6}\tau_e$, thus Eq. (6) is obviously not suitable to predict $\alpha(t)$. Strictly speaking, Eq. (6) may not be used to fit experimental data on $\alpha(t)$, either, since the shape of the solid curve and its corresponding dashed curve for a given $\tau_e/\tau$ are not equivalent. This observation also invalidates the previous assessment that the role of the nucleation time lag is simply to displace the origin of the curve of $\alpha(t)$ by $\tau_e$ or a fraction of $\tau_e$.[8]

As shown in Fig. 3(c), the differences between the predictions by Eqs. (6) and (2) become negligible as $\tau_3$ increases, i.e., for a small rate of nucleation and/or growth rate. There are no data available for $\tau_3/\tau$ for bulk crystallization of $a$–Si or other materials to allow us to draw further comparisons.

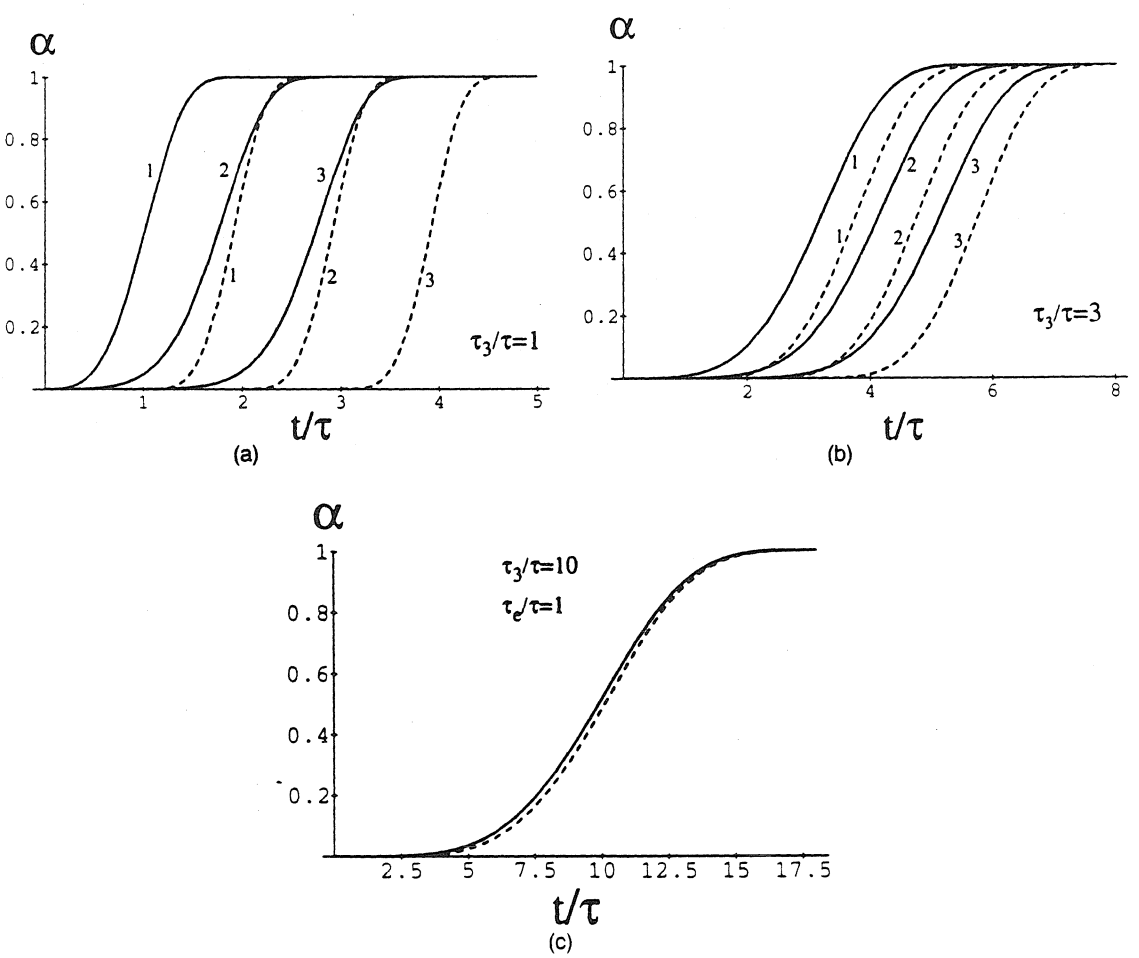


FIG. 3. Crystallized volume fraction $\alpha(t)$ as a function of time as predicted by Eqs. (2) and (6) for $\tau_e/\tau = 1, 2, 3$ (a) at $\tau_3/\tau = 1$; (b) at $\tau_3/\tau = 3$, (c) at $\tau_e/\tau = 1$ and $\tau_3/\tau = 1$. The dashed curves are given by the conventional expression Eq. (6).

### C. Time to form a specified crystallized volume fraction: stability of amorphous phases

The time, $t_c$, taken to form a given crystallized volume fraction $\alpha_c$ in an amorphous phase can be taken as a measure of its stability. This concept originated in assessing glass formation in a melt at given conditions.[5] $\alpha_c$ is frequently taken as $10^{-6}$, which is usually instrumentally undetectable. Theoretical prediction thus is the only possible way to assess the stability of an amorphous phase in this case. Equation (2) can be used to extract values of $\tau_e$, $\tau_3$, and $\tau$ from observed $N(g_d, t)$ and $\alpha(t)$ and to predict experimentally inassessible quantities such as the critical time to form a volume fraction of $10^{-6}$ of an amorphous phase.[10] The previously obtained expression,[8] Eq. (5), and the conventionally used expression, Eq. (6), cannot be used in such applications.

From Eq. (6), one obtains the time taken to form a given critical fraction $\alpha_c \ll 1$,

$$t_c = \tau_e + \left[-\frac{3\ln(1-\alpha_c)}{\pi J_s(g_*)V^3}\right]^{1/4} = \tau_e + \left(\frac{3\alpha_c}{\pi J_s(g_*)V^3}\right)^{1/4} \equiv \tau_e + \tau_3\alpha_c^{1/4} \tag{8}$$

However, because Eq. (8) is valid only when

$$\tau_3 \gg \alpha_c^{-1/4}\left(\sqrt{6}-1\right)\tau_e \tag{9}$$

(for $\alpha_c = 10^{-6}$, $\alpha_c^{-1/4}(\sqrt{6}-1) \approx 46$) and generally $\tau_3$ is not much larger than $46\tau_e$, Eq. (8) is not a valid expression to calculate $t_c$. Since Eq. (8) indicates that $t_c > \tau_e$, one often assumes that almost no crystallization can occur within the period of the effective time lag for nucleation, and this conclusion is not true. We will return to this issue in the next section on two-dimensional growth.

For $\alpha_c \ll 1$, Eq. (2) can be rewritten as

$$y^4 = \alpha_c\left\{x^4 - 4\frac{\tau_e}{\tau}x^3 + 24\sum_{n=1}^{\infty}\frac{(-q)^n}{n^4 n!}\cdot\left[e^{-nx} - 1 + nx - \frac{1}{2}(nx)^2\right]\right\} \tag{10}$$

where $y = \tau_3/\tau$ and $x = t_c/\tau$. Equation (10) thus gives $t_c$ as a function of $\tau_3$, $\tau_e$, and $\tau$ and should be used to obtain $t_c$.

Figure 4 gives the critical time, $t_c$, to form a given small volume fraction ($\alpha_c = 10^{-6}$) as a function of $\tau_3$. The solid lines give the prediction from Eq. (10) and dashed lines are according to Eq. (8). The numbers on the curves are the values of $\tau_e/\tau$. Obviously, for a wide range of $\tau_3$, the large time limits given by Eq. (8) cannot be used in predicting the stability of amorphous phases.

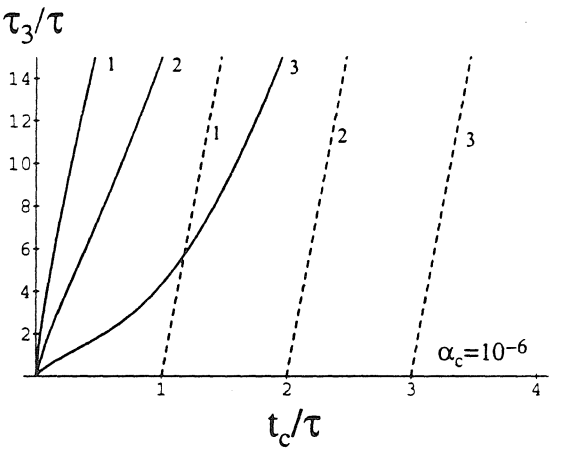


FIG. 4. The critical time $t_c$ taken to reach a given crystallized volume fraction $\alpha_c = 10^{-6}$ as a function of characteristic time for crystallization ($\tau_3$), as predicted by Eqs. (10) (solid) and (8) (dashed).

The values of $t_c$ predicted by Eq. (10), shown in Fig. 4, are all only a fraction of $\tau_e$.

## III. BULK CRYSTALLIZATION: HOMOGENEOUS NUCLEATION AND TWO-DIMENSIONAL GROWTH

For homogeneous nucleation in a thin film of thickness $l$ with the nucleated crystalline clusters growing two-dimensionally, one can obtain an equation analogous to Eq. (1),

$$\alpha(t) = 1 - \exp\left[-k_2V^2l\int_0^t J(t')l(t-t')^2\,dt'\right] \equiv 1 - \exp(-y_2) \tag{11}$$

By substituting $J(g_0, t)$ obtained in Part I for $J(t)$ in Eq. (11), one obtains,

$$\alpha(t) = 1 - e^{-y_2}$$
$$y_2 = \left(\frac{t}{\tau_2}\right)^3\left[1 - 3\frac{\tau_e}{t} - 6\left(\frac{\tau}{t}\right)^3\sum_{n=1}^{\infty}\cdot\frac{(-q)^n}{n^3 n!}\left(e^{-n(t/\tau)} - 1 + n\frac{t}{\tau}\right)\right] \tag{12}$$

where

$$\tau_2 = \left(\frac{3}{\pi V^2 J_s(g_*)l}\right)^{1/3} \tag{13}$$

Equation (13) can be rewritten as

$$\frac{\tau_2}{\tau} = \left(\frac{2}{\sqrt{\pi}\tau_1^2 n_1 l}\right)^{1/3} g_*^{-4/9}\theta^{1/6}\exp\left(+\frac{1}{9}\theta g_*^{2/3}\right) \tag{14}$$

From experimentally obtained[2,3,11] curves of $\alpha(t)$ and the accumulated grain number concentration $N(t)$, one finds that $\tau_2/\tau$ is about 0.5 to 2 for crystallization of $a$–Si at about 900 K. Thus $\tau_2/\tau$ is about 0.5 to 6, since $\tau_e/\tau$ is usually in the range of 1 to 3, as shown in Part I.

In the case of homogeneous nucleation and two-dimensional growth, the conventionally used expression to fit the measured $\alpha(t)$ is in the form,[2,3,11,12]

$$\alpha(t) = 1 - \exp\left[-\left(\frac{t-\tau_e}{\tau_2}\right)^3\right] \tag{15}$$

which can be shown to be the limit of Eq. (12) for $t \gg \sqrt{3}\,\tau_e$. Figure 5 shows $\alpha(t)$ given by Eq. (12) (solid curves) and by Eq. (15) (dashed curves), where the values of $\tau_e/\tau$ are indicated. As in the 3-D case, the conventional expression, Eq. (15), cannot be used as a predictive tool.

The critical time taken to reach a given fraction $\alpha_c (\ll 1)$, from Eq. (15), is,

$$t_c = \tau_e + \left(\frac{3\alpha_c}{\pi V^2 J_s(g_*) l}\right)^{1/3} \equiv \tau_e + \tau_2 \alpha_c^{1/3} \tag{16}$$

which is valid only for $t \gg \sqrt{3}\tau_e$, i.e., for

$$\tau_2 \gg \alpha_c^{-1/3}\left(\sqrt{3}-1\right)\tau_e = 73\tau_e \tag{17}$$

Since experimental data[2,3,11] show that $\tau_2$ is much smaller than $73\tau_e$, Eq. (16) cannot be used to predict $t_c$. Thus the concept that the effective time lag can be regarded as the time period during which no nucleation and crystallization can occur is usually incorrect. Instead, $t_c$ should be estimated from the following equation obtained from Eq. (12),

$$y^3 = \alpha_c\left[x^3 - 3\frac{\tau_e}{\tau}x^2 - 6\sum_{n=1}^{\infty}\frac{(-q)^n}{n^3 n!} \cdot \left(e^{-nx} - 1 + nx\right)\right] \tag{18}$$

where $y = \tau_2/\tau$ and $x = t_c/\tau$.

Figure 6 shows the critical time $t_c$ to reach a crystallized volume fraction $\alpha_c = 10^{-6}$ predicted by Eqs. (18) and (16). It is evident that the conventional expression, Eq. (16), can overestimate greatly the time taken to reach $\alpha_c$. Figure 6 also clearly shows that the critical time to reach $\alpha_c$ is usually only a fraction of $\tau_e$ even for $\tau_2/\tau$ as large as 25.

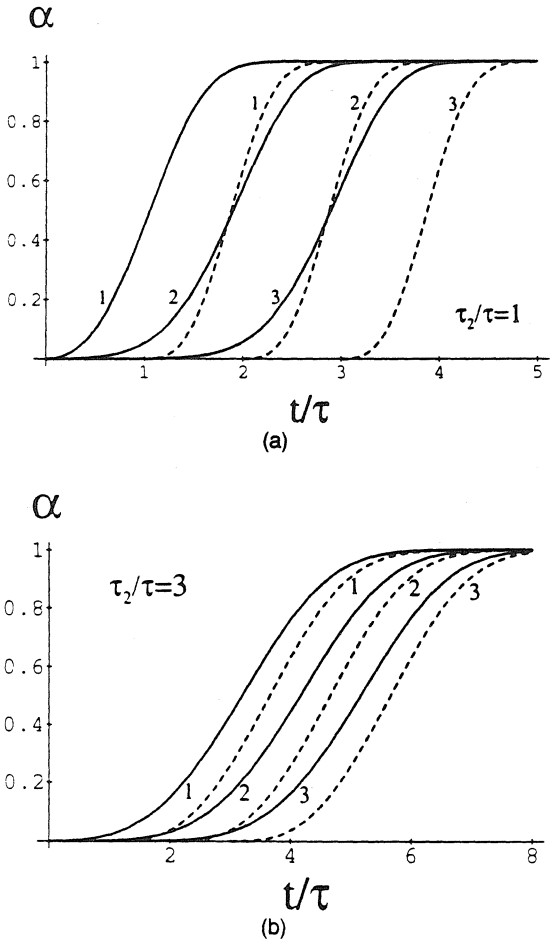


FIG. 5. (a) Crystallized volume fraction $\alpha(t)$ as a function of time as predicted by Eqs. (12) and (15) for $\tau_e/\tau = 1, 2, 3$ at $\tau_2/\tau = 1$; (b) and at $\tau_2/\tau = 3$. The dashed curves correspond to Eq. (15).

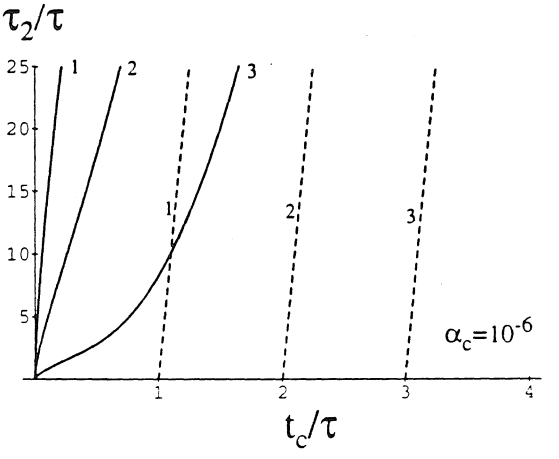


FIG. 6. The critical time $t_c$ taken to reach a given crystallized volume fraction $\alpha_c = 10^{-6}$ as a function of characteristic time for crystallization ($\tau_2$), as predicted by Eqs. (18) (solid) and (16) (dashed).

The above results for volume nucleation with 3-D or 2-D growth can also be extended to the cases of surface-induced crystallization with surface nucleation and 1-D or 2-D growth of nucleated clusters.

## IV. CONCLUSION

Theoretical expressions for the time-dependent crystallized volume fraction are presented using the new expression for the rate of nucleation. Conventional formulations in interpreting crystallization experimental data and for assessing the stability of amorphous phases are shown to be the large time limits of the present results and not generally applicable. Our results enable one to interpret experimentally obtained $\alpha(t)$ and thus to extract crystallization information from the data. Newly derived formulations for $\alpha(t)$ also enable one to assess the stability of an amorphous phase at given conditions.

## REFERENCES

1. For example, Y. Kuni, M. Tabe, and K. Kajiyama, J. Appl. Phys. **54**, L23 (1980); M. Tamura, H. Tamura, and T. Tokuyama, Jpn. J. Appl. Phys. **19**, 2847 (1983); H. Ishiwara, A. Tamba, and S. Furukawa, Appl. Phys. Lett. **48**, 733 (1986); H. Ishiwara, H. Yamamoto, and S. Furukawa, Appl. Phys. Lett. **43**, 1028 (1983); T. Dan, H. Ishiwara, and S. Furukawa, Appl. Phys. Lett. **53**, 2626 (1988); M. Miyao, M. Moniwa, K. Kusukawa, and W. Sinke, J. Appl. Phys. **64**, 3018 (1983).
2. D. B. Korin, R. Reif, and B. Mikic, Thin Solid Films **167**, 101 (1988); R. B. Inverson and R. Reif, J. Appl. Phys. **62**, 1675 (1987) and references therein.
3. S. Roorda, P. Kammann, W. C. Sinke, G. F. A. Walle, and A. A. van Gorkum, Mater. Lett. **9**, 259 (1990).
4. D. J. Gravesteijn, Appl. Opt. **27**, 726 (1988); E. E. Marinero, Appl. Surf. Sci. **43**, 117 (1989) and references therein.
5. D. R. Uhlmann, J. Non-Cryst. Solids **25**, 73 (1977).
6. M. Avrami, J. Chem. Phys. **9**, 177 (1941).
7. I. Gutzow, Contemp. Phys. **21**, 121 (1980).
8. I. Gutzow, D. Kashchiev, and I. Avramov, J. Non-Cryst. Solids **73**, 473 (1985).
9. G. Shi and J. H. Seinfeld, J. Mater. Res. **6**, 2091 (1991).
10. The value of $\tau_e$ can be obtained from the measured $N(g_d, t)$, as shown in Part I. $\tau$ can be estimated from the value of $\tau_e$ based on estimations of $\theta$ and $g_*$ since $\tau_e/\tau$ is a function of only $\theta$ and $g_*$ and is not very sensitive to $\theta$ and $g_*$, as shown in Part I. $\tau_3$ can be obtained from measured $\alpha(t)$ since $\alpha(t)$ is a function only of $\tau$, $\tau_e$, and $\tau_3$.
11. R. B. Inverson and R. Reif, Appl. Phys. Lett. **52**, 645 (1988).
12. See reviews in J. W. Christian, *The Theory of Phase Transformations in Metals and Alloys*, 2nd ed. (Pergamon, Oxford, 1975).

# CHAPTER 10

# TRANSIENT KINETICS OF NUCLEATION BEYOND THE BARRIER REGION

(Shi and Seinfeld, submitted for publication)

# Kinetics of Nucleation Beyond the Critical Region: Basis for Interpretation of Measurements

Frank G. Shi and John H. Seinfeld
Department of Chemical Engineering, 210-41
California Institute of Technology
Pasadena, California 91125

**Abstract**

Closed-form analytical expressions are obtained for the transient cluster size distribution function, the cluster flux and the number density of grains above the critical size of nucleation. These new results provide the basis for interpreting kinetic nucleation measurements at the instrumentally detectable size and enable one to extract the fundamental information on nucleation processes in amorphous materials. It is also shown that previous results used in interpreting transient nucleation measurements are generally invalid.

# 1 Introduction

The time dependence of the number density of grains, $N(g_d, t)$, and the time dependence of the grain size distribution, $f(g, t)$, $g \geq g_d$, are significant measurements in nucleation experiments. Here $g$ is the number of atoms or molecules in a cluster, and $g_d$ is the instrumentally detectable size. Such kinetic measurements provide insight into the fundamental mechanisms involved in nucleation and growth and provide an opportunity to obtain important fundamental information on the nature of the nucleation and growth processes. Various instrumental techniques have been available to make reliable kinetic measurements such as X-ray diffraction and Raman scattering.[1] The high resolution modern electron microscopy is more suitable for the single cluster studies.

However, the data evaluation and the verification of nucleation models[2] against such measurements turn out to be difficult and have limited the usefulness of data from the the various techniques.

One obvious difficulty is that previous theoretical studies have been able only to predict the behavior at the critical cluster size for nucleation, $g_*$ and $g_*$ is usually much smaller than that which can be detected, $g_d$. There is no physically consistent expression for $N(g_d, t)$, which can be compared directly with the measurements.

The relation

$$N(g_d, t) = N[g_*, t - t_d(g_*, g_d)] \tag{1}$$

and its variants have often been proposed to obtain $N(g_d, t)$, where $t_d(g_*, g_d)$ would be the time needed for a cluster at $g_*$ to grow to $g_d$. The underlying assumption in Eq. [1] is that the number density of grains measured at $g_*$,

$N(g_*, t)$, is conserved over the time to grow from $g_*$ to $g_d$ and is equal to the number density measured at $g_d$, $N(g_d, t)$. However, Eq. [1] is physically invalid. Since critical clusters of size $g_*$ have an equal average probability to grow and decay (for a symmetrical barrier), not every cluster that reaches size $g_*$ will subsequently grow to $g_d$.

In previous work, we have introduced the concept of a nucleated cluster, which is defined as the smallest cluster for which the probability to grow is much larger than to decay.[3] We have shown that the nucleated cluster size $g_0$ should satisfy

$$g_0 > g_* + \delta, \tag{2}$$

where $\delta$ is the half-width of the critical region defined by the difference in free energy about the critical size,

$$[W(g) - W(g_*)] \leq kT \tag{3}$$

and thus

$$\delta = [-\frac{1}{2kT}\frac{\partial^2 W}{\partial g^2}]^{-1/2} \mid_{g=g_*} . \tag{4}$$

However, the exact size of $g_0$ remains to be determined. Our stochastic simulations of nucleation indicate that $g_0$ can be taken $g_* + 1.1\delta$. We proposed $g_0 = 1.5g_*$ previously.[3]

The critical region is also the region where thermal fluctuations play the dominant role in causing clusters to cross the nucleation barrier. $\delta$ is related to the Zeldovich factor $Z$ by[6]

$$\delta = \frac{1}{\sqrt{\pi} Z} = 3g_*^{2/3}\theta^{-1/2} \tag{5}$$

for a free energy expressed in the general form[4]

$$W(g) = -g\Delta\mu + s_1\sigma g^{2/3}, \tag{6}$$

where $g_* = (2s_1\theta/3\Delta\mu)^3$, $\theta = s_1\sigma/kT$, $\Delta\mu$ is the chemical potential difference of an atom or molecule in the amorphous phase and in the crystalline phase, $\sigma$ is the specific interfacial surface free energy between the two phases, $s_1 = (4\pi)^{1/3}(3v_1)^{2/3}$ for a spherical cluster, $v_1$ is the crystalline atomic volume, $k$ is Boltzmann's constant and $T$ is temperature.

According to the definition of $g_0$, almost all clusters at $g_0$ will grow. Thus,[3] one might suggest

$$N(g_d, t) = N[g_0, t - t_d(g_0, g_d)], \tag{7}$$

where $t_d(g_*, g_d)$ is the time needed for a cluster at $g_0$ to grow to $g_d$ and $N(g_0, t)$ is obtained in Ref. 3. As will be shown, Eq. [7] is invalid in general and is strictly only correct for steady-state nucleation . Even though the cluster of size $g_0$ can grow to $g_d$, the time $t_d(g_0, g_d)$ is a stochastic variable because thermal fluctuations still play a non-negligible role in determining the growth of the cluster.

A problem common to all previous work that has the aim of obtaining $N(g_d, t)$ is that $N(g_d, t)$ is obtained in a manner similar to Eq. [1] or Eq. [7]. No result for the grain cluster size distribution function and the flux $J(g_d, t)$ have been reported. The purpose of this work is to provide such closed-form expressions and represent a continuation of our recent effort to systematically study the data interpretation problems in transient nucleation and crystallization kinetic experiments.[3,5] For example, nucleation in amorphous materials may exhibit a considerable transient period, from several seconds to hours, depending on temperature and materials, and an understanding of the transient kinetics of nucleation is necessary to be able to perform data extraction and model verification. The procedure we will present is extendable to other forms of $W(g)$ and $\beta(g)$ than the

models considered in this work. Our results presented will facilitate testing nucleation models and experiments by comparing $f(g_d, t)$ and $N(g_d, t)$ directly with kinetic measurements at the instrumentally detectable size. For a given nucleation model, one can obtain unknown material properties such as the specific interfacial free energy by fitting the presently obtained $f(g_d, t)$ and/or $N(g_d, t)$ with the relevant kinetic data. Thus our work will lay the basis for one to eventually control or use the initial stage of nucleation in processing devices and for new materials developments.

# 2 New Approach for Concurrent Nucleation and Growth

## 2.1 Kinetic Equation for Nucleation and Growth

The kinetic equation valid for the nucleation and growth processes can be written as,[6]

$$\frac{\partial f(g,t)}{\partial t} = -\frac{\partial J(g,t)}{\partial g} = \frac{\partial}{\partial g}[\beta(g)\frac{\partial f}{\partial g} + \frac{\beta f}{kT}\frac{\partial W}{\partial g}]. \tag{8}$$

The term $\frac{\partial}{\partial g}[\beta(g)\frac{\partial f}{\partial g}]$ represents the contribution of the random thermal fluctuations to the evolution of $f(g,t)$ and plays a critical role in nucleation of clusters. It is important to note that validation of the models for $W(g)$ and $\beta(g)$ is one of the important tasks for obtaining $f(g,t)$, $g \geq g_d$ and $N(g_d, t)$. The approach employed subsequently can be applied to obtain the transient nucleation kinetics for other models for $W(g)$ and $\beta(g)$, even though we will limit ourselves to considering $W(g)$ consisting of a surface energy term and a volume term, that is, Eq. [6] and $\beta(g) \propto g^{2/3}$. We will also limit ourselves to the case of isothermal annealing.

## 2.2 Our Previous Approach and Results for $g \leq g_0$

By identifying $\epsilon = \delta/g_*$ as the small parameter of the problem, we obtained[7] a reduced equation (first-order) valid in the the left outer region, $g < g_* - \delta$, and right outer region, $g > g_* + \delta$, and a simplified equation (2nd-order) in the critical region, $g_* - \delta < g < g_* + \delta$. By treating the critical region as a transitional boundary layer and using the appropriate singular perturbation approach, two unknowns associated with the inner solution were determined by matching the expression for the inner solution with the two known outer solutions. In doing so, we have obtained the transient cluster size distribution function, cluster flux and the accumulated cluster concentration in the *critical region.*[7]

The singular perturbation approach used in large part is a natural extension of the earlier analysis of the nucleation problem by Zeldovich and others.[6] In particular, Feder et. al.'s graphical steady-state solution is just a qualitative version of the more systematic approach.[8] Our approach is sufficiently general to solve many complex nucleation problems such as nucleation in the presence of clusters sinks,[9] high-dimension barrier-crossing[10], nucleation in spatially inhomogeneous systems[11] and time-dependent problems.[7]

In summary, no results for the cluster size distribution, the cluster flux and the accumulated number concentration have been obtained previously for $g > g_0$ by *directly* solving Eq. [8], without imposing the conservation of number density of grains, expressed by Eq. [7] and its variants.

## 2.3 New Approach: Direct Solution for $g > g_0 > g_*$

Nucleation and growth can be described by a single equation, Eq. [8], subject to proper boundary conditions. Eq. [8] has not been solved previously in a

case where nucleation and growth proceed simultaneously.

By introducing the same small parameter $\epsilon$, the order of Eq. [8] valid for $g >> g_*$ can be reduced by one and our previously obtained $f(g,t)$ at $g_0$ can be taken as the only boundary condition needed to solve the reduced equation. In doing so, we can solve for the cluster size distribution function and the cluster flux valid to any larger size as long as the evolution of the cluster size distribution results from the mechanism of growth alone. Of course, we finally can obtain $N(g_d,t)$ from $J(g,t)$.

This approach on the surface appears inconsistent with that employed to obtain the solution in the critical region[7] as briefly outlined above, since the solutions valid in the critical region are obtained on the basis of the fact that the right outer solution for $f(g,t)/n(g)$ asymptotically approaches zero at large sizes. In fact our previous approach for obtaining the solution in the critical region is physically reasonable; $f(g,t)$ in the critical region is not affected directly by the cluster growth at far larger sizes and the present approach proposed above relies on the fact that the evolution of the cluster size distribution starts from that at the nucleated size.

Introducing $x = g/g_*$, Eq. [8] can be written as,

$$\tau x^{-2/3}\frac{\partial f(x,t)}{\partial t} = \frac{\epsilon^2}{2}\frac{\partial^2 f(x,t)}{\partial x^2}+\frac{\partial f(x,t)}{\partial x}[\frac{1}{3x}\epsilon^2-3(1-x^{-1/3})]-[x^{-4/3}+\frac{2}{x}(1-x^{-1/3})]f. \tag{9}$$

Since $3kT/W(g_*) = \epsilon^2 << 1$, and the derivatives of $f$ with respect to $g$ for $g > g_0$ are finite, the terms containing $\epsilon^2$ in Eq. [9] can be neglected. Thus the reduced kinetic equation valid for $g > g_0$ is

$$\tau x^{-2/3}\frac{\partial f(x,t)}{\partial t} = -3(1-x^{-1/3})\frac{\partial f}{\partial x} - [x^{-4/3}+\frac{2}{x}(1-x^{-1/3})]f. \tag{10}$$

Our previously obtained $f(g,t)$ at $g_0$ is the boundary condition,[7]

$$f(g,t) = \frac{1}{2}n(g)\mathrm{erfc}[\frac{g-g_*}{\delta} + \exp(-\frac{t-\lambda\tau}{\tau})], \qquad \text{for} \quad g \to g_0, \qquad (11)$$

where $\tau = \delta^2/2\beta(g_*)$ and $\lambda = g_*^{-1/3} - 1 + \ln[\theta^{1/2}(g_*^{1/3}-1)]$, and $n(g) = n_1 \exp(-W(g)/kT)$ and $n_1$ is the number density of atoms in the nucleating phase.

# 3 Nucleation and Growth in Amorphous Materials in the Case of Isothermal Annealing: Analytical Results for for $g >> g_*$

## 3.1 Cluster Size Distribution Function

Eqs. [10] and [11] can be Laplace transformed to

$$x^{-2/3}s\tau f(x,s) = -3(1-x^{-1/3})\frac{\partial f(x,s)}{\partial x} - [x^{-4/3} + \frac{2}{x}(1-x^{-1/3})]f, \quad (12)$$

and

$$f(x_0,s) = \frac{1}{2s}n(x_0)\mathrm{e}^{-\lambda s\tau}(s\tau)!\ \mathrm{i}^{s\tau}\mathrm{erfc}[\frac{x_0-1}{\epsilon}] \qquad (13)$$

using $f(x,s) = \int_0^\infty f(x,t)e^{-st}dt$.

Eqs. [12] and [13] admit the following solution for $f(x,s)$,

$$f(x,s) = f(x_0,s)\exp[s\tau(x_0^{1/3} - x^{1/3})](\frac{x_0^{1/3}-1}{x^{1/3}-1})^{s\tau}(\frac{x}{x_0})^{-1/3}\frac{x_0^{1/3}-1}{x^{1/3}-1}, \quad (14)$$

which gives the grain size distribution valid for $g > g_0 > g_*$,

$$f(x,t) = \frac{1}{2}n(g_0)(\frac{x}{x_0})^{-1/3}(\frac{x_0^{1/3}-1}{x^{1/3}-1})\mathrm{erfc}[\frac{x_0-1}{\epsilon} + \exp(-\frac{t-t_f}{\tau})], \qquad (15)$$

where

$$t_f = \lambda\tau + \tau[x^{1/3} - x_0^{1/3} + \ln\frac{x^{1/3}-1}{x_0^{1/3}-1}] \qquad (16)$$

$f(x,t)$ given by Eq. [15] reduces to the known result at $x = x_0$, $f(x_0,t)$.

Eq. [15] represents the first result reported for the grain size distribution valid at $g > g_0$, for phase transformations governed by nucleation and growth.

### Relaxation of Grain Size Distribution Function

The time $t_f(g)$ is that needed for $f(g,t)$ for $g > g_0$ to relax to its steady state value. We see from Eq. [16] that this time is the sum of the characteristic time to form the cluster size distribution in the critical region, $\lambda\tau$, and the time for a cluster to grow from $g_0$ to $g$, $t_d(g_0,g)$, determined by the deterministic growth rate,[7]

$$\dot{g}_m = -\frac{\beta(g)}{kT}\frac{\partial W(g)}{\partial g}. \tag{17}$$

For $t >> t_f$,

$$f(g,t) \rightarrow f_s(g) = \frac{n(g_0)}{2}\left(\frac{x}{x_0}\right)^{-1/3}\left(\frac{1-x_0^{1/3}}{1-x^{1/3}}\right)\mathrm{erfc}\left(\frac{x_0-1}{\epsilon}\right). \tag{18}$$

Eqs. [15] and [18] for $g > g_0$ indicate that the evolution of the cluster distribution over time is not conservative, that is that $f(g,t) \neq f[g_0, t - t_d(g_0,g)]$.

The cluster size distribution function, Eq. [15] normalized by its steady-state limit, Eq. [18], is shown in Fig. 1 for $t_f/\tau = 2, 5, 8$.

### Asymptotic Power-Law Cluster Size Distribution Function

Eq. [15] predicts a universal grain size distribution function in phase transformations governed by nucleation and growth. For $g > g_0$ and $t >> t_f$, Eq.

[15] can be written as,

$$f(g) = const.\ x^{-1/3}(x^{1/3} - x_0^{1/3})^{-1} \propto g^{-2/3} = r^{-2}, \tag{19}$$

where $r$ is the radius of a cluster. It is shown that in the region $r > r_0$ there is a universal power-law asymptotic limit $f \propto r^{\nu}$, whose exponent depends only on the mechanism of atom migration in forming a cluster, i.e., $\beta(r)$. We present the universal size distribution function in Fig. 2.

### 3.2 Transient Rate of Nucleation

The cluster flux valid at any large size, $g > g_0$, can be obtained from $J(g,t) = \beta(g)\frac{\partial f}{\partial g} + \frac{\beta f}{kT}\frac{\partial W}{\partial g}$. From Eq. [15], we obtain

$$\begin{aligned} \frac{J(g,t)}{J_s(g_*)} &= \frac{n(g_0)\sqrt{\pi}}{n(g_*)}[\frac{3}{\epsilon}x_0^{1/3}(x_0^{1/3}-1) \\ &+ \frac{\epsilon x_0^{1/3}(1-x_0^{1/3})(2x^{1/3}-1)}{6x^{4/3}(x^{1/3}-1)^2}]\mathrm{erfc}[\frac{x_0-1}{\epsilon} + \exp(-\frac{t-t_f}{\tau})] \\ &+ \exp[-\exp(-2\frac{t-t_f}{\tau}) - \exp(-\frac{t-t_j}{\tau}) - \frac{t-t_1}{\tau}], \end{aligned} \tag{20}$$

where

$$t_j = t_f + \tau \ln 2z_0 > t_f,\ \ z_0 = (g_0 - g_*)/\delta \tag{21}$$

and

$$t_1 = t_f - \tau \ln[\frac{3(x^{1/3}-1)^2}{\epsilon x_0^{1/3}(x_0^{1/3}-1)}] < t_f. \tag{22}$$

To a good approximation, $n(g_0)/n(g_*) \approx \exp(z_0^2)$, and $\mathrm{erfc}(z) \approx \exp(-z^2)/(\sqrt{\pi}z)$, Eq. [20] can be accurately rewritten as

$$\begin{aligned} \frac{J(g,t)}{J_s(g_*)} &= \exp[-\exp(-2\frac{t-t_f}{\tau}) - \exp(-\frac{t-t_j}{\tau}) - \frac{t-t_1}{\tau}] \\ &+ \frac{x_0-1}{x_0-1+\epsilon\exp(-\frac{t-t_f}{\tau})}\exp[-\exp(-2\frac{t-t_f}{\tau}) - \exp(-\frac{t-t_j}{\tau})]. \end{aligned} \tag{23}$$

The second term in the first bracket on the RHS of Eq. [20] can be neglected as it is much smaller than the two other terms.

### Relaxation of Cluster Flux

For $t >> t_f$, Eq. [23] reduces to

$$J(g,t) = J_s(g_*)\exp[-\exp(-\frac{t-t_j}{\tau})][1+\exp(-\frac{t-t_1}{\tau})] \qquad (24)$$

and since $t_f > t_1$, Eq. [23] can be approximated as,

$$J(g,t) = J_s(g_*)\exp[-\exp(-\frac{t-t_j}{\tau})] \qquad (25)$$

Eq. [25] also can be obtained by using

$$J(g,t) = J[g_0, t - t_d(g_0,g)], \quad g > g_0. \qquad (26)$$

It is clear that Eq. [25] is only the large time limit of the more complete result Eq. [23]. The preservation of the cluster flux over time, i.e., Eq. [26], is established only after the cluster size distribution has attained its steady state, since the condition for reducing Eq. [23] to Eq. [25], is $t >> t_j$ while $t_j > t_f$.

Eq. [23] is compared with Eq. [25] in Fig. 3 for $t_f = 5\tau$ and $g_0 = g_* + 1.1\delta$. The cluster flux obtained by using Eq. [25] can significantly deviate from its true value predicted by Eq. [23].

## 3.3 Time Dependence of Number Density Measured at Resolution Limits of Instruments

We can obtain the accumulated number concentration at the instrumentally detectable size $g_d$ from Eq. [23],

$$\begin{aligned} N(g_d,t) &= J_s(g_*)\int_0^t \{\exp[-\exp(-2\frac{t-t_f}{\tau}) - \exp(-\frac{t-t_j}{\tau}) - \frac{t-t_1}{\tau}] \qquad (27) \\ &+ \frac{x_0-1}{x_0-1+\epsilon\exp(-\frac{t-t_f}{\tau})}\exp[-\exp(-2\frac{t-t_f}{\tau}) - \exp(-\frac{t-t_j}{\tau})]\}dt \end{aligned}$$

which shows that in general $N(g_d,t) \neq N[g_0, t - t_d(g_0, g_d)]$. Thus the assumption underlying all previous work in obtaining $N(g_d,t)$ using Eq. [1] and Eq. [7] is not valid.

### Asymptotic Results

For $t >> t_f$, Eq. [25] can be used to obtain $N(g_d,t)$,

$$\frac{N(g_d,t)}{J_s(g_*)\tau} = \mathrm{E}_1(\mathrm{e}^{-\frac{t-t_j}{\tau}}) - \mathrm{E}_1(\mathrm{e}^{t_j/\tau}), \tag{28}$$

which also can be obtained[3] by using the conservation of number concentration at $g_0$ and $g_d$. Thus the number conservation of clusters between $g_d$ and $g_0$ is only correct after the cluster concentration at $g_0$ has reached a steady state.

For a still larger time limit of $t >> t_j$, we obtain from Eq. [28],

$$N(g_d,t) = J_s(g_*)[t - \tau_e(g_d)] \tag{29}$$

which is a well-known relation. The slope of $N(g_d,t)$ vs. $t$ at large time limit is the steady-state rate of nucleation and the intercept of $N(g_d,t)$ vs. $t$ with the axis of $t$ gives the effective time lag associated with $N(g_d,t)$,

$$\tau_e(g_d) = \gamma\tau + t_j + \tau\mathrm{E}_1(\mathrm{e}^{t_j/\tau}), \tag{30}$$

where $\gamma = 0.5772$ is Euler's constant. Our derivation of the relation Eq. [29] removes the uncertainty associated with using Eq. [29] in practice by giving explicitly the condition $t >> t_j$ under which Eq. [29] is obtained. That is the linear relationship between $N(g_d,t)$ and time $t$ is established only after the cluster flux has attained its steady state. Fig. [4] presents the comparison between Eq. [27] and the asymptotic results Eqs. [28] and [29].

Eq. [28] deviates obviously from the true time dependent behavior given by Eq. [27]. Eq. [29] asymptotically approaches Eq. [28] but not Eq. [27], since Eq. [29] is derived as a direct large time limit of Eq. [28] while Eq. [28] is not the direct large time limit of Eq. [27]. Instead, Eq. [28] is derived by using Eq. [25], the large time limit of Eq. [23]. This also explains why the deviation between Eq. [28] and Eq. [27] seems to be constant with time.

The slope of $N(g_d, t)$ is taken as the steady-state rate of nucleation, from which nucleation models are often tested and the energy barrier for nucleation and its temperature dependency are obtained. The arbitrary assignment of the slope of $N(g_d, t)$ can lead to error. With the proper expression for $N(g_d, t)$, the desired approach is to fit the whole time course of $N(g_d, t)$ to obtain the unknowns.

# 4 Summary and Conclusion

By solving directly the governing nucleation and growth equation for a nucleation energy barrier $W(g)$ consisting of surface and volume energy terms, and an addition rate of atoms to a cluster, $\beta(g) \propto g^{2/3}$, we have obtained the following new results:

1. the cluster size distribution function, $f(g, t)$, valid at $g > g_0$
2. the cluster flux, $J(g, t)$, valid at $g > g_0$
3. the time dependence of grain number density measured at the instrumentally detectable size, $N(g_d, t)$.

New results provide the basis for nucleation kinetic measurements and enable one to extract unknown material properties and thus fundamental information for nucleation processes from the data. New results also suggest a simpler and a more reliable strategy in conducting nucleation experiments.

Our approach can be used to obtain the relevant expressions corresponding to different models for $W(g)$ and $\beta(g)$. Since the time dependencies of $f(g,t)$, $J(g,t)$ and $N(g_d,t)$ are sensitive to both $W(g)$ and $\beta(g)$, results obtained provide an excellent test of the nucleation model.

The new results show that the form for the cluster flux and cluster number concentration measured at $g_0$ are preserved over time only after the establishment of the steady-state cluster size distribution at $g_0$. Previous results for $N(g_d,t)$ obtained from $N(g,t), g = g_*, g_0$ are not correct.

## References

[1]D. B. Korin, R. Reif and B. Mikic, Thin Solid Films **167**, 101(1988); R. B. Inverson and R. Reif, Appl. Phys. Lett. **52**, 645(1988); S. Roorda, P. Kammann, W. C. Sinke, G. F. A. Walle and A. A. van Gorkum, Mater. Lett. **9**, 259(1990); M. Suzuki, M. Hiramoto, M. Oyuura, W. Kamisaka and S. Hasegawa, Jpn. J. Appl. Phys. **27**, L1380(1988); S. Kambayash, S. Onga, I. Mizushima, K. Hignchi and H. Kuwano, Extended Abs. of the 21st. Conf. on Solid State Devices and Mater., Tokyo, 1989, p.169; K. Zellama, P. Germain, S. Squeland, J. C. Bourjoin and P. A. Thomas, Appl. Phys. **50**, 6995(1979); U. Koster, Phys. Status Solidi **48**, 313(1978); C. C. Pai, S. S. Lau and I. Suni, Thin Solid Films **109**, 263(1983); J. S. Im and H. A. Atwater, Appl. Phys. Lett. **57**, 1766(1990); E. E. Marinero, Appl. Surf. Sci. **43**, 117(1989); H. J. Fecht, J. H. Perepezko, M. C. Lee and W. L. Johnson, J. Appl. Phys. **68**, 4494(1990); R. Bisaro, J. Magarino, Y. Pastol,P. Germain and K. Zellama, Phys. Rev. **B 40**, 7655(1989)

[2] A decisive test of a nucleation model cannot be accomplished without comparing $N(g_d, t)$ and/or $f(g, t)$, $g >> g_*$ derived from the model with the kinetic data obtained under different conditions.

[3]G. Shi and J. H. Seinfeld, J. Material Res. **6**, 2091(1991)

[4]D. Turnbull, J. Chem. Phys. **18**, 198(1950); Comtemp. Phys. **10**, 473, 1969

[5]G. Shi and J. H. Seinfeld, J. Material Res. **6**, 2097(1991)

[6]See reviews in F. F. Abraham, *Homogeneous Nucleation Theory* (Academic, New York, 1974); K. Binder, Rep. Prog. Phys, **50**, 783, 1987;

A. C. Zettlemoyer (ed), *Nucleation* (R. Decker, New York 1969); S. Kotake and I. I Glass, Prog. Aerospace Sic., **19**, 129(1981); K. C. Russell, Adv. in Colloid and interface Sci., **13**, 205(1980)

[7]G. Shi, J. H. Seinfeld and K. Okuyama, Phys. Rev. A **41**, 2101(1990); a reply to a comment by Shneidman to appear in Phys. Rev. A.

[8]J. Feder, K. C. Russell, J. Lothe and G. M. Pound, Adv. Phys. **5**, 111, 1966

[9]G. Shi and J. H. Seinfeld, J.Chem. Phys., 92(1), 687, 1990; G. Shi and J. H. Seinfeld, J. Colloid and Interface Science, 135 (1), 252, 1990

[10]G. Shi and J. H. Seinfeld, J. Chem. Phys. 93(12), 9033, 1990

[11]G. Shi and J. H. Seinfeld and K. Okuyama, J. Appl. Phys., 68(9), 4550, 1990

[12]K. N. Tu, Appl. Phys. A, 53(1), 32, 1991 and references therein

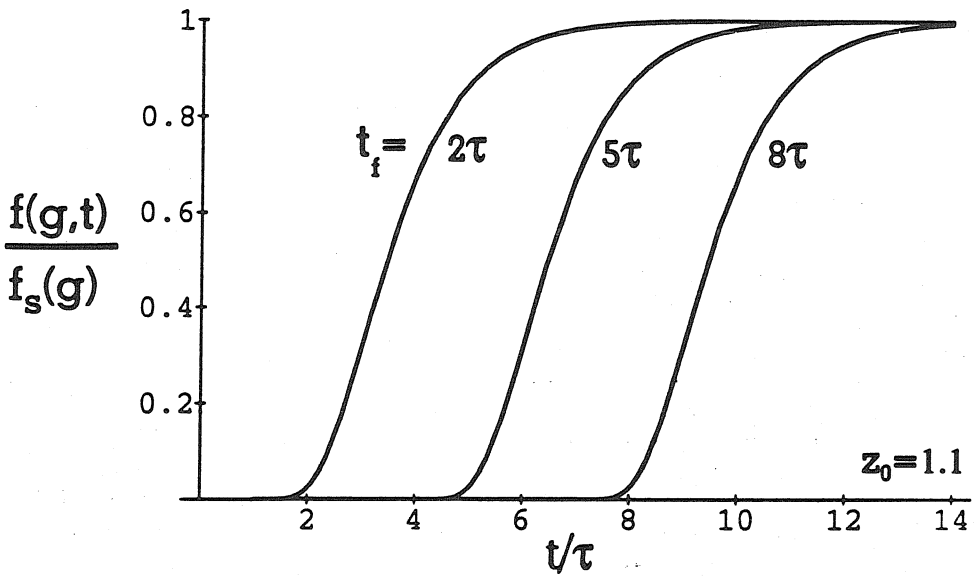


Figure 1. Cluster Size Distribution function given by Eq. [15] normalized by its steady-state limit given by Eq. [18]

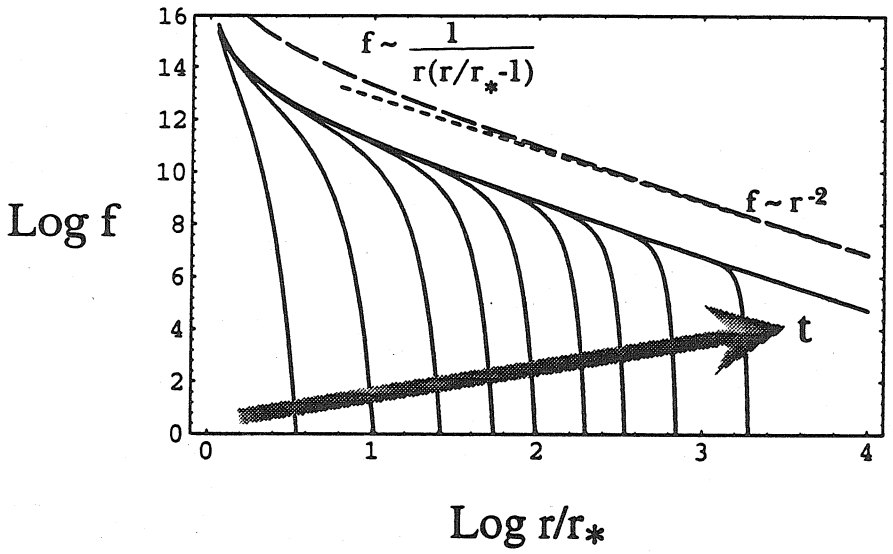


Figure 2. Temporal evolution of the cluster size distribution and its asymptotic behavior.

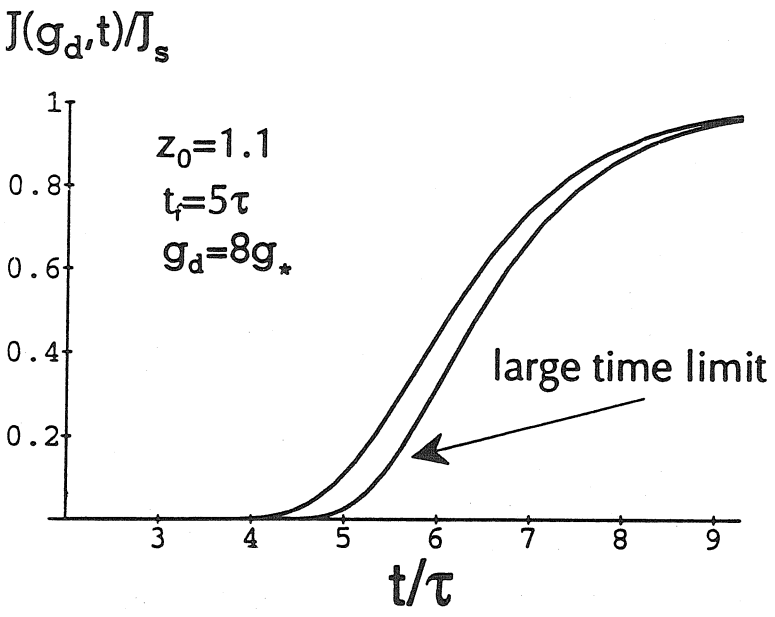


Figure 3. Time dependence of cluster flux given by Eq. [23] and its large time limit give by Eq. [25]

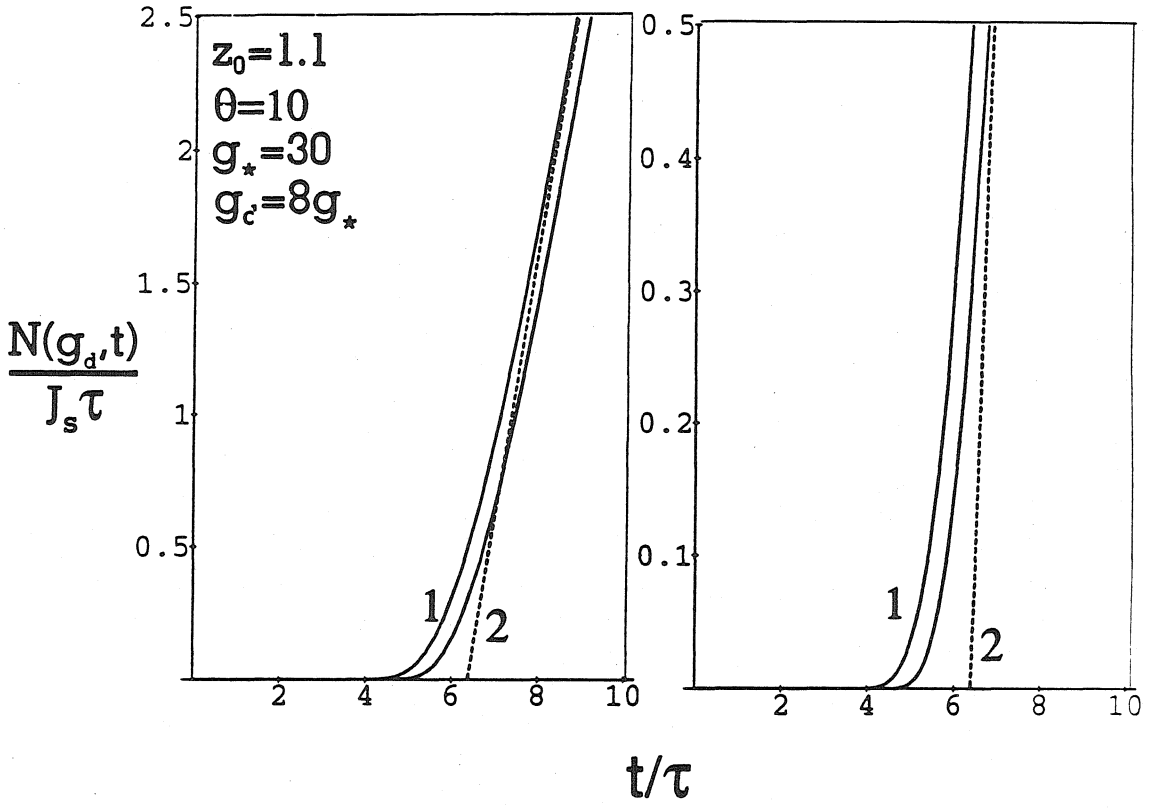


Figure 4. Time dependence of number density of grains, $N(g_d,t)$ given by Eq. [24] and its large time limits given by Eq. [25] and Eq. [26].

# CHAPTER 11

# UNIVERSAL CLUSTER SIZE DISTRIBUTION IN NUCLEATION

(Shi and Seinfeld, submitted for publication)

# Universal Cluster Size Distribution in Nucleation

Frank G. Shi and John H. Seinfeld
Department of Chemical Engineering
California Institute of Technology
Pasadena, California 91125

**Abstract**

We show that transient cluster size distributions in phase transformations governed by nucleation and growth processes, with a nucleation energy barrier consisting of surface and volume energy terms, obey a scaling relation. The cluster size distribution beyond the nucleation barrier region exhibits a universal asymptotic power law distribution, the exponent of which depends only on the mechanism of atom addition to the nucleating and growing clusters.

PACS numbers: 05.40.+j, 05.70.-a, 64.60.Qb, 82.20.Mj

Nucleation can be viewed as a nonequilibrium reversible aggregation process different from the irreversible aggregation processes studied using scaling theories.[1] Understanding the temporal evolution of the cluster size distribution (CSD) in phase transformations governed by nucleation and growth is important for the development of controlled crystallization methods for the microstructural design of materials.[2,3] The time evolution of the CSD for the case of surface reaction site-limited nucleation has been obtained for uniary[4] and for binary nucleation[5] in the nucleation barrier region. More importantly, the CSD has also been obtained far beyond the nucleation barrier region which enables a direct comparison between observations and theories.[6] It has been shown that there is a universal power-law asymptotic limit for the CSD beyond the nucleation barrier region, the exponent of which depends only on the mechanism of atom addition to clusters. The time taken for the CSD to relax to its steady state is a function of the cluster size and depends on the height of the nucleation energy barrier as well as on the the atom migration mechanism.[6]

In this letter, we will present the first result for transient evolution of the CSD governed by nucleation and growth of compact and fractal clusters of arbitrary dimension for different possible mechanisms of atom incorporation into the nucleating and growing clusters for a nucleation energy barrier consisting of surface and volume energy terms.

Defining the cluster flux as arising by addition or dissociation only of individual monomers, the kinetic equation for the nucleation and growth processes in terms of the continuous CSD $f(g,t)$ is,

$$\frac{\partial f(g,t)}{\partial t} = \frac{\partial}{\partial g}[\beta(g)\frac{\partial f(g,t)}{\partial g} + \frac{\beta(g)f(g,t)}{kT}\frac{\partial W(g)}{\partial g}], \qquad (1)$$

where cluster size $g$ indicates the number of atoms in the cluster and $\beta(g)$

is the rate of addition of atoms to a cluster of size $g$.[7-9]

In phenomenological nucleation theories,[7] the formation energy of a nucleus, $W(g)$, is generally considered to consist of surface and volume energy terms,

$$W(g) = -g\Delta\mu + s\sigma g^{\frac{d-1}{d}}, \tag{2}$$

where $\Delta\mu$ is the chemical potential difference between the nucleated and nucleating phases, $\theta = s_1\sigma/kT$, $\sigma$ is the specific free energy between the two phases, $s$ is a geometrical constant, $k$ is Boltzmann's constant, $T$ is temperature and $d$ is the effective dimensionality of the cluster. For a compact cluster in D-dimensional physical space $d$ =D; usually $d$ <D for fractal clusters. Other forms of $W(g)$ can also be considered.

By introducing an index $\nu$, most mechanisms for the addition of single atoms to clusters are included within the functional form,

$$\beta(g) \propto g^{\frac{d-\nu}{d}}. \tag{3}$$

For example, $\beta(g) \propto g^{2/3}$ for $d = 3$ and $\nu = 1$ for reaction site-limited nucleation of compact clusters, i.e., the cluster formation is controlled by the formation of a chemical bond between the atom and the cluster. If every atom within a cluster is a potential site for atom addition, one has $\nu = 0$, and $\beta(g) \propto g$. For diffusion-limited nucleation of compact clusters, i.e., in the case that the cluster formation process is controlled by the arrival of single atoms to the cluster, $\beta(g) \propto g^{1/3}$ for $d = 3$ and $\nu = 2$.

We will study the temporal evolution of the CSD after an initially homogeneous phase undergoes an abrupt change in supersaturation. The corresponding initial condition is,[7] for $g > 1$

$$f(g, 0) = 0 \tag{4}$$

and the only known boundary condition is,[7]

$$f(g,t)/n_1 \rightarrow 1 \tag{5}$$

for $g \rightarrow 1$. Here $n_1$ is the number density of atoms in the nucleating phase. Eq. [5] holds for nucleation in solid phases and for quasi-steady state situations.

A strategy for solving Eq. [1] together with Eqs. [4] and [5] for $f(g,t)$ valid for all $g$ has been developed.[6] The basic idea is to employ the approach of singular perturbation to solve first for $f(g,t)$ valid in the nucleation barrier region,[4,6] and then obtain $f(g,t)$ for the region beyond the barrier region, $g >> g_*$.

The nucleation barrier region, or the critical region, $g_* - \delta < g < g_* + \delta$, is that in which random fluctuations play the dominant role in causing clusters to overcome the nucleation barrier.[10] Here, the critical cluster size $g_*$ is that corresponding to the maximum of $W(g)$, and the barrier region half width $\delta$ is given by

$$\delta = (\frac{d-1}{2d^2})^{-1/2} g_*^{-\frac{d+1}{2d}} \theta^{-1/2}. \tag{6}$$

The two other regions to the right and left of the nucleation barrier region are defined by $g >> g_* + \delta$ and $g << g_* + \delta$ respectively.[10,4]

By using the fact $W(g) >> kT$, Eq. [1] can be reduced to a first-order equation in the right and left regions, while Eq. [1] can be simplified in the barrier region but remains a second-order equation.[4]

Two unknown constants in the inner solution valid for the barrier region can be determined by matching the inner solution with the two outer solutions. The left outer solution can be obtained with the left outer boundary condition given by Eq. [5].[4,6] However, we do not know the right outer

solution beforehand, and in fact, it is our goal to obtain $f(g,t)$ valid in that region. In the right region, since $n(g) = n_1 \exp[-W(g)/kT]$ becomes exponentially large for $g >> g_* + \delta$, while $f(g,t)$ is finite, one has

$$f(g,t)/n(g) \to 0. \tag{7}$$

Therefore by considering the normalized variable $f(g,t)/n(g)$ in Eq. [1], we can determine the right outer solution needed to obtain the inner solution in the barrier region.[4–6] Eq. [7] is different physically from the conventional boundary condition,[7] which is one of the most important keys in our perturbation approach.

The right outer solution obtained is $f(g,t)/n(g) = 0$ which does not imply $f(g,t) = 0$,[4,11–13] but states the fact that $f(g,t)$ is exponentially smaller than $n(g)$ for $g >> g_* + \delta$, i.e., $f(g,t) = 0(\mathrm{e}^{-1/\epsilon^2})n(g)$. Here the small parameter is $\epsilon = \delta/g_*$. Both the right and left outer solutions in terms of $f(g,t)/n(g)$ are used to obtain $f(g,t)$ in the barrier region. The actual CSD in the right region is obtained by solving the corresponding equation for $f(g,t)$ and taking the solution obtained for the barrier region as the boundary condition.

Following the approach outlined above, one can obtain the CSD in the barrier region as

$$f(g,t) = \frac{1}{2} n(g) \mathrm{erfc}[\frac{g - g_*}{\delta} + \exp(-\frac{t - \lambda\tau}{\tau})], \tag{8}$$

which indicates, as expected, a steep variation in $f/n$ in the barrier region. Here

$$\lambda = -\int_{g_*^{-1/d}}^{1} \frac{z^\nu - 1}{z - 1} dz + \ln[1 - g_*^{-1/d}] + \frac{1}{2} \ln \frac{d(d-1)W(g_*)}{2kT} \tag{9}$$

and $\tau = \delta^2/2\beta(g_*)$. Eq. [8] reduces to that for $d = 3$ and $\nu = 1$.[4]

Eq. [8] indicates that in the barrier region, the CSD has a universal form for arbitrary values of $d$ and $\nu$. This form of the time evolution of CSD also holds for binary nucleation[5] or nucleation in external fields,[14], and is expected to hold for heterogeneous nucleation. Nucleation mode differences are reflected by different values of $g_*$, $\delta$, $\lambda$ and $\tau$. For $t >> \lambda\tau$, the CSD given by Eq. [8] relaxes to its steady-state form which is a known result.[4,7] A particular $W(g)$ different from Eq. [2] does not change the form of Eq. [8]. However, the time taken for $f(g,t)$ to relax to its steady-state will be changed.

Observations of CSD are usually available at cluster sizes well beyond those in the barrier region. It is therefore necessary to predict the nucleation behavior for $g >> g_*$.

Introducing $x = g/g_*$ and neglecting the terms containing $\epsilon^2(<< 1)$, Eq. [1] for $g >> g_*$ reduces to,

$$\tau x^{-\frac{d-\nu}{d}} \frac{\partial f(x,t)}{\partial t} = -d(1-x^{-1/d})\frac{\partial f}{\partial x} - [x^{-\frac{1+d}{d}} + \frac{d-\nu}{x}(1-x^{-1/d})]f. \quad (10)$$

Defining $g_0$ as the smallest cluster for which the probability of growth is much larger than that for decay,[4] Eq. [8] for $f(g,t)$ in the barrier region can be taken as the boundary condition for solving Eq. [10] for $f(g,t)$ in the region of $g >> g_*$,[6]

$$f(x,t) = \frac{1}{2}n(g)\mathrm{erfc}[\frac{x-1}{\epsilon} + \exp(-\frac{t-\lambda\tau}{\tau})], \qquad \text{for} \quad x \to x_0 \qquad (11)$$

where $x_0 = g_0/g_*$ and $\lambda$ is given by Eq. [9]. Stochastic simulations of nucleation indicate that $g_0$ can be taken as about $g_* + 1.1\delta$.

Eqs. [10] and [11] admit the following solution for the Laplace-transformed

CSD, $f(x,s)$,

$$f(x,s) = f(x_0,s)\exp[\frac{s\tau}{d}\int_{x_0}^{x}\frac{x^{-(d-\nu)/d}}{x^{-1/d}-1}dx](\frac{x}{x_0})^{-1/d}\frac{x_0^{1/d}-1}{x^{1/d}-1}, \qquad (12)$$

where $f(x_0,s)$ is the Laplace transformation of Eq. [11],

$$f(x_0,s) = \frac{1}{2s}n(g_0)\mathrm{e}^{-\lambda s\tau}(s\tau)!\ \mathrm{i}^{s\tau}\mathrm{erfc}[\frac{x_0-1}{\epsilon}]$$

. Eq. [12] yields the CSD valid for $g > g_0 > g_*$,

$$f(x,t) = \frac{1}{2}n(g_0)(\frac{x}{x_0})^{-1/\nu}(\frac{x_0^{1/d}-1}{x^{1/d}-1})\mathrm{erfc}[\frac{x_0-1}{\epsilon}+\exp(-\frac{t-t_f}{\tau})] \qquad (13)$$

where

$$t_f(g) = \tau[\lambda + \ln\frac{x^{1/d}-1}{x_0^{1/d}-1} + \int_{x_0^{1/d}}^{x^{1/d}}\frac{z^\nu-1}{z-1}dz] \qquad (14)$$

which reduces to the known result at $x = x_0$, $f(x_0,t)$, and the known result for $d = 3$ and $\nu = 1$.[6] $\lambda\tau$ is the time to reach a steady-state CSD in the barrier region and the remainder of the terms on the right hand side of Eq. [14] represent the time needed for a cluster at $g_0$ to reach $g$, and thus $t_f(g)$ is the total time required for a cluster of size $g$ to reach a steady-state concentration.

Eq. [13] can be rewritten as

$$f(r,t) = \frac{z_0}{2d}n(g_*)\mathrm{e}^{z_0^2}\frac{r_*^{d-\nu}\epsilon}{r^{d-\nu}(1-r/r_*)}\mathrm{erfc}[z_0+\exp(-\frac{t-t_f}{\tau})] = \eta(r)\phi(t), \qquad (15)$$

where $r \propto g^{1/d}$ is the radius of a $g$-sized cluster of $d$-dimension, $r_*$ is the critical radius, and $z_0 = (x_0-1)/\epsilon \approx 1.1$.

Eq. [13] represents the desired result for the transient CSD valid at $g > g_0 > g_*$, for phase transformations governed by nucleation and growth of clusters with a monomer addition rate $\beta(g) \propto g^{\frac{d-\nu}{d}}$ and a nucleation energy barrier consisting of surface and volume energy terms. As found

previously,[6] the time evolution of the CSD can be used to test models for $\beta(g)$.

Eq. [15] predicts a scaling relation for the CSD at any time $t$,

$$f(r,t)/\phi(t) = \eta(r) \propto \frac{(r/r_*)^{-(d-\nu-1)}}{r/r_* - 1} \propto r^{-(d-\nu)}, \tag{16}$$

For $t >> t_f(g)$,

$$\phi(t) \rightarrow constant. \tag{17}$$

Then, for $t >> t_f(g)$, one also has

$$f(r) \propto \frac{(r/r_*)^{-(d-\nu-1)}}{r/r_* - 1} \propto r^{-(d-\nu)}. \tag{18}$$

We note that in the region $r > r_*$ and $t > t_f(r)$, there is a universal power-law asymptotic limit, $f \propto r^{-(d-\nu)}$, the exponent of which depends only on the mechanism of single atom addition to clusters, i.e., $\beta(r) \propto r^{d-\nu}$. For compact clusters of 3-D , $f \propto r^{-2}$ for $d = 3$, $\nu = 1$. It is predicted that $f \propto r^{-1}$ for $\nu = 2$ and $d = 3$, that is for diffusion-limited nucleation of compact 3-D clusters or a reaction-limited nucleation of 2-D compact clusters, $\nu = 1$ and $d = 2$. The maximum possible value of the exponent for compact clusters is 3, i.e., $f \propto r^{-3}$ in the case of $\beta(g) \propto g$. For example, when the atom constituting the cluster is produced by chemical reaction,[15] one has $\beta(g) \propto g$. For fractal clusters of $d$ dimension, it is predicted that the exponent associated with the power law of $f$ is always smaller than the corresponding compact case, since $d < D$.

Fig. 1 shows the time evolution of the CSD for $d = 3$ and $\nu = 1$ according to Eq. [15] for $g > g_0$. As time increases, the cluster concentrations at larger and larger sizes $r$ reach steady-state. The steady-state CSD is a power-law (Eq. [18]) with exponent of -2, although the CSD is given by Eq. [15] which

deviates from a simple power law for $r$ close to $r_*$. Since $t_f(r)$ increases with $r$, at a given time $t = t_f(r_a)$, the CSD for $r \leq r_a$ has reached steady-state and thus the power-law is applicable for $r \leq r_a$, while the same law is not applicable for the CSD for $r > r_a$.

The boundary condition, Eq. [5] is appropriate for solid-state nucleation where the untransformed amorphous phase is essentially not altered in composition,[2] and more generally for quasi-stationary nucleation where the depletion of the monomer occurs on a time scale longer than that for nucleation. Comparison of the measured temporal evolution of the CSD beyond the barrier region (within the instrumental resolution limits) in solid phase nucleation with the present results could offer a test of models for $W(g)$ and $\beta(g)$ in nucleation theories.

This work was supported by National Science Foundation grant, ATM-9003186. The authors are grateful for useful discussions with Dr. R. C. Flagan, Dr. W.C. Johnson and B. Zhao.

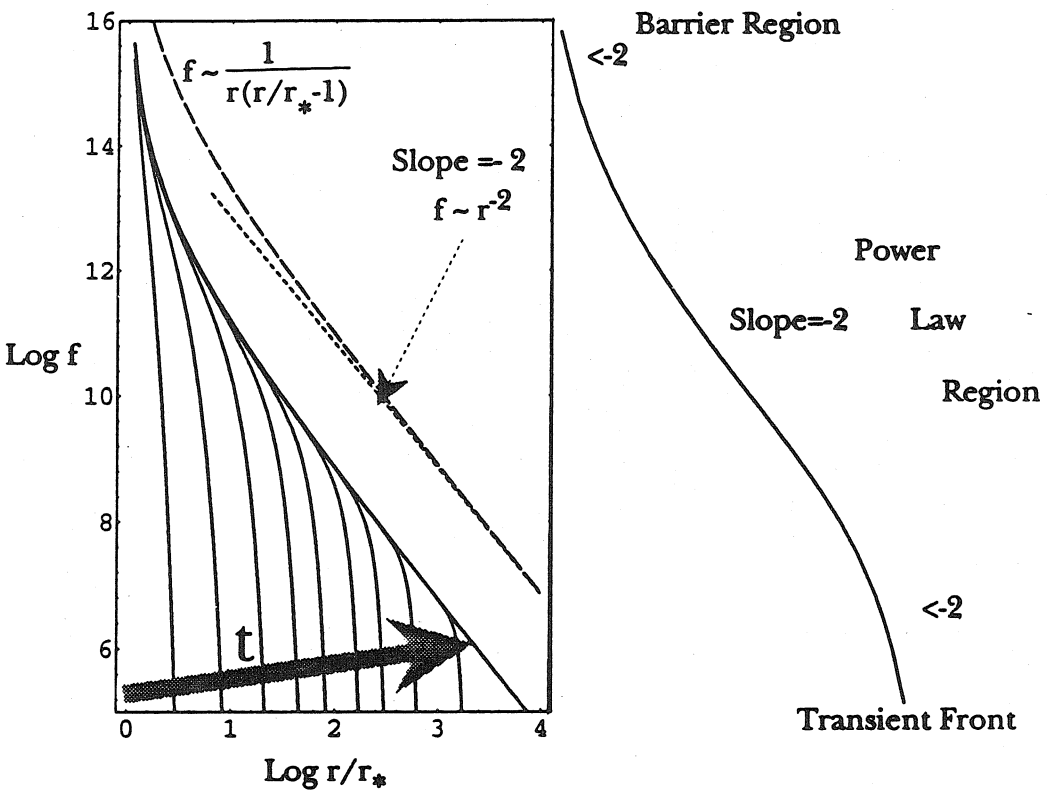


Figure 1. Temporal evolution of the cluster size distribution and its asymptotic behavior for d=3, $\nu$=1 according to Eq. [13].

[1]see reviews by R. M. Ziff, *Kinetic of Aggregation and Gelation*, ed F. Family and D. P. Landau (Amsterdam: Elsevier, 1984)

[2]M. Blank-Bewersdorff and U. Koster, Mater. Sci. Eng., **97**, 313(1988); M. A. Gibson and G. W. Delamore, Acta. Metall. Mater., **38**, 2621(1990)

[3]W. L. Johnson, in Glassy Metals I, ed H. S. Güntherodt and H. Beck (Springer-Verlay, Berlin, 1981)

[4]G. Shi, J. H. Seinfeld and K. Okuyama, Phys. Rev. A **41**, 2101(1990)

[5]G. Shi and J. H. Seinfeld, J. Chem. Phys. 93(12), 9033(1990)

[6]F. G. Shi and J. H. Seinfeld, submitted to J. Non-Cryst. Solids

[7]See reviews in F. F. Abraham, *Homogeneous Nucleation Theory* (Academic, New York, 1974); K. Binder, Rep. Prog. Phys, **50**, 783, 1987; S. Kotake and I. I. Glass, Prog. Aerospace Sic., **19**, 129(1981); K. C. Russell, Adv. in Coll. and Interf. Sci., **13**, 205(1980); D. Turnbull, Contemp. Phys. **10**, 473, 1969

[8]Z. G. Zhang, J. Colloid. Interf. Sci. **124**, 262, 1988; A. G. Bashkirov, J. Chem. Phys. **96**, 3488(1992)

[9]C. Y. Mou and R. Lovett, J. Chem. Phys. **70**, 3488, 1977

[10]J. Feder, K. C. Russell, J. Lothe and G. M. Pound, Adv. Phys. **5**, 111, 1966

[11]G. Shi, J. H. Seinfeld and K. Okuyama, Phys. Rev. A **44**, 8443(1991).

[12]G. Shi and J. H. Seinfeld, J. Material Res. **6**, 2097(1991);**6**, 2091(1991)

[13]V. A. Shneidman, Phys. Rev. A **44**, 8441(1991).

[14]G. Shi and J. H. Seinfeld and K. Okuyama, J. Appl. Phys., 68(9), 4550, 1990; G. Shi and J. H. Seinfeld, J. Chem. Phys., 92(1), 687, 1990 and J. Coll. and Inter. Sci., 135(1), 252, 1990

[15]J. L. Katz and M. D. Donohue, J. Coll. and Interf. Sci. 85, 267(1982)

# CHAPTER 12

# DIRECT MEASUREMENT OF NUCLEATION ENERGY BARRIER

# DIRECT MEASUREMENT OF THE NUCLEATION ENERGY BARRIER

**Abstract**

By providing a theoretical basis for measuring directly the nucleation energy barrier and its temperature dependency and an approach for determing the interfacial atomic transfer mechanism in the enucleation process, it is shown that nucleation models can be tested experimentally.

## 1 INTRODUCTION

Nucleation as the first stage of the first-order phase transformation plays an essential role in many natural processes[1] and increasingly plays an important part in developing new techniques for electronic and photonic devices processing and materials developments.[2] Current nucleation theories only predict the behavior of cluster formation at the so-called critical size while one is only able to observe the cluster formation behavior at the sizes far larger than the critical one.[1] As a result, nucleation models usually cannot be tested and kinetic nucleation data cannot be interpreted in terms of nucleation models. Such a situation is typified by the fact that the nucleation energy barrier has never been measured experimentally and directly and the value of the atom addition rate is often found to vary by serveral orders of magnitude. Consequently the progress in controlling nucleation in applications has been very slow.

A recent systematic effort has been attempted to understand the kinetic behavior of nucleation at the instrumental detectable sizes (Chapters 6 to 11).[3–6] We have indentified that the cluster size distribution (CSD) is the most single important measurement in understanding the nucleation process. We have obtained the temporal evolution of CSD in the nucleation barrier region (which is the region about the critical size) for both single energy barrier and higher-dimensional barrier[3] and the region beyond the barrier region (i.e., the only region which is accessible to most instruments for a good kinetic measurement).[5,6]

The obtained temporal evolution of CSD at instrumental resolution limits enables one to verify one's nucleation models and to interpret one's kinetic nucleation data.[5,6] It will be shown that the temporal evolution of CSD is extremely sensitive to the value of one of two most important keys in nucleation models, i.e., the additional rate of single atoms to clusters, $\beta(g)$. Based on our obtained results for CSD at large sizes,[5,6] an approach for measuring directly the nucleation energy barrier and its temperature dependency will also be developed in this chapter. This approach is the only known method for measuring of the nucleation energy barrier directly. Our results therefore provide an excellent test of the nucleation models.

## 2 TRANSIENT EVOLUTION AND MODEL FOR MONOMER ADDITION RATE

Results for $N(g_d, t)$ given by Eq. [27], $f(g, t), g > g_0$ given by Eq. [15] and $J(g, t), g > g_0$ given by Eq. [23] in Chapter 10 provide the basis for data extraction from kinetic measurements in isothermal nucleation experiments.

A nucleation model is usually characterized by $\Delta\mu$, $\sigma$, $T$ and $E_d$, the dif-

fusion activation energy in the amorphous phase. $g_*$, $g_0$, $\tau$, $t_f$, $t_j$, $t_1$, $t_d$, $\delta$, $\epsilon$, $\lambda$, etc. appearing in the expressions for $f(g,t)$, $J(g,t)$ $(g > g_0)$ and $N(g_d,t)$ all can be expressed explicitly in terms of the above four parameters. Since $\Delta\mu$ usually can be measured independently,[7] using expressions for $f(g,t)$ and/or $J(g,t)$ and $N(g_d,t)$ to fit the relevant data obtained at different temperatures, one can obtain the usually unknown material properties $E_d$, $\sigma$ and $W(g)$ and their temperature dependencies.

## 2.1 Transient Evolution and Model for $\beta$

For a nucleation model with known material properties, the results presented above certainly provide a decisive test of the nucleation model. Because the time dependencies of $f(g,t)$, $J(g,t)$ and $N(g_d,t)$ are very sensitive to not only $W(g)$ but also $\beta(g)$ as shown in Figs. 1 to 3. Our results provide an excellent test of the models for $\beta(g)$ and $W(g)$. In Figs. 1 to 3, we show the cluster size distribution, the cluster flux and the accumulated cluster number density for three different values of $\beta(g_*)/\beta_* = 0.5, 1, 2$. For a relatively small variance of $\beta(g_*)$, substantial differences in the time dependence of $f(g,t)$, $J(g,t)$ and $N(g,t)$ are observed. Such a sensitive test of $\beta(g)$ has not been achieved previously, as the steady-state rate of nucleation is insensitive to the value of $\beta(g_*)$. This finding is important in view of the large uncertainties (orders of magnitude) regarding the value of $\beta(g)$.[8]

## 2.2 New Experimental Strategy

The observed time dependences of $f(g,t)$ and $N(g_d,t)$ may result from the combination of transient effects and other possible time-variations of the system parameters such as the temperature change due to heat release in the phase transformation process. At the very early stage of phase transfor-

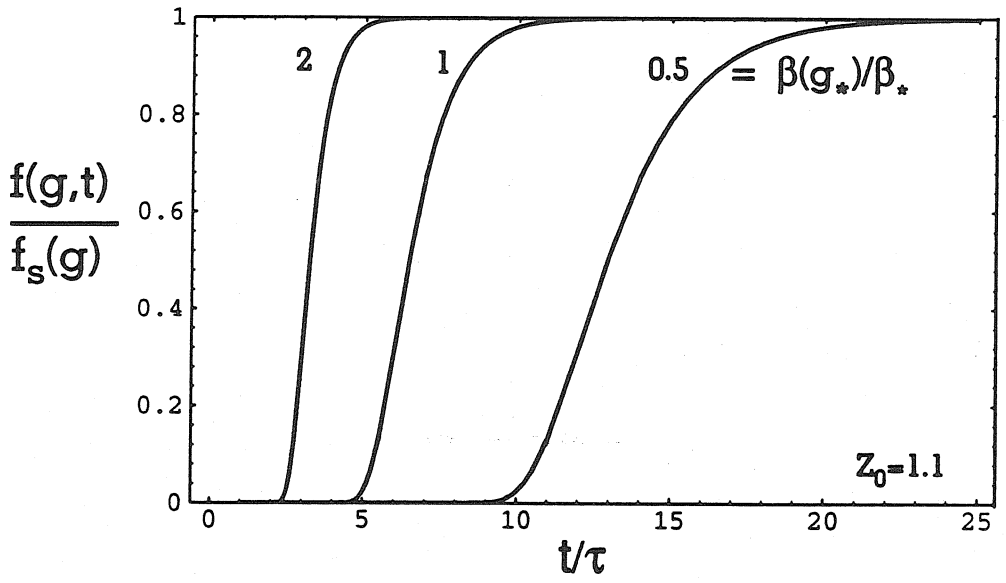


Figure 1. The sensitivity of the cluster size distribution to the additional rate of atoms to a cluster, $\beta(g_*)$ for $g_*=30$, $\theta=10$ and $g_d/g_*=8$. The time t is normalized by $\tau$ for $\beta(g_*)/\beta_* = 1$.

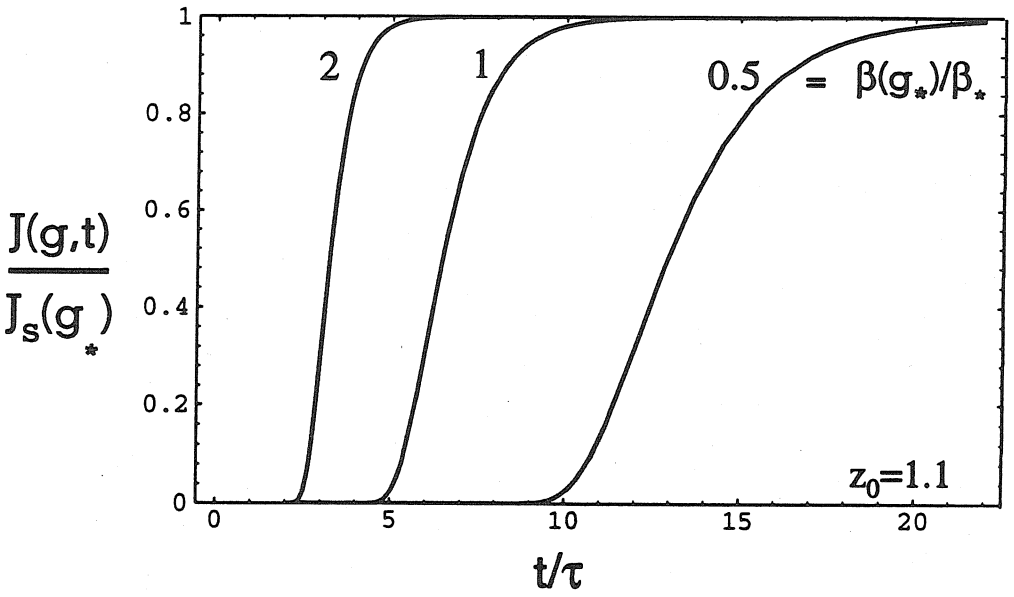


Figure 2. The sensitivity of cluster flux to the additional rate of atoms to a cluster, $\beta(g_*)$.

The time t is normalized by $\tau$ for $\beta(g_*)/\beta_* = 1$.

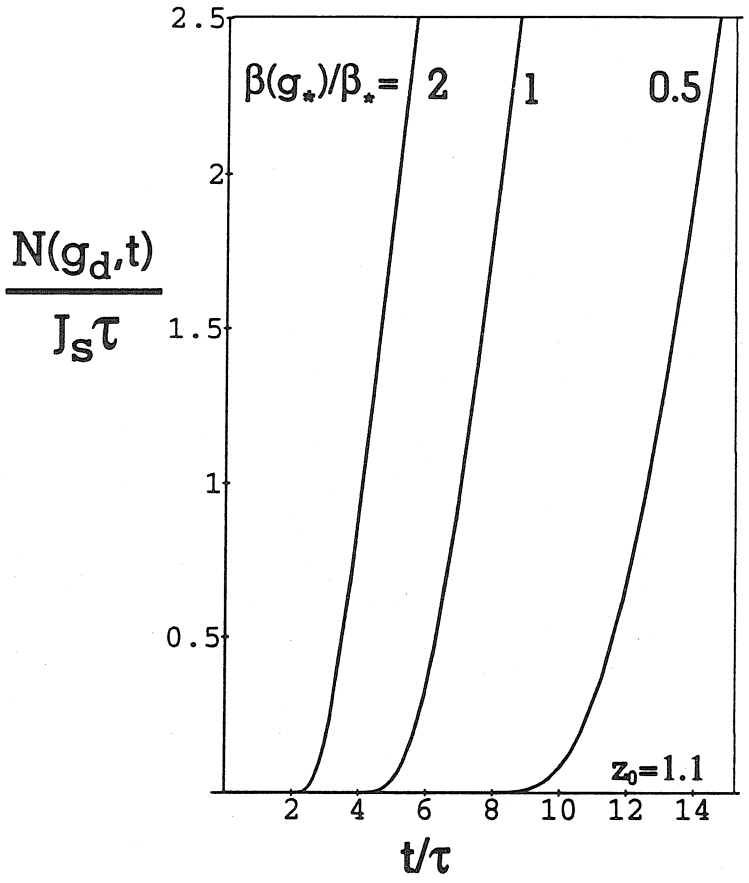


Figure 3. The sensitivity of the observed accumulated grain number density to the additional rate of atoms to a cluster, $\beta(g_*)$ for $g_*=30$, $\theta=10$ and $g_d/g_* =8$. The time t is normalized by $\tau$ for $\beta(g_*)/\beta_* = 1$.

mation, the time dependences of $f(g,t)$ and $N(g_d,t)$ mainly result from the transient effect and the results reported above enable one to extract the desired parameters from observations at the earliest stage of nucleation. The same considerations lead one to design a new strategy to conduct nucleation experiments, i.e., it is only necessary to conduct relatively few observations at the earliest stage of nucleation. For example, by measuring the time to observe the first grain (or first $N$ grains) in a given volume, one is able to extract the desired parameters from Eq. [27] in Chapter 10. In the same vein, one can test nucleation models.

# 3 DIRECT MEASUREMNT OF NUCLEATION ENERGY BARRIER

For simplicity, we will take $d = 3$ and $\nu = 1$ as an illustration. In the present case, Eq. [15] in Chapter 11 can be rewritten as

$$f(r,t) = \frac{1}{6} n(g_*) e^{z_0^2} \frac{r_*^2(x_0-1)}{r^2(1-r_*/r)} \text{erfc}[z_0 + \exp(-\frac{t-t_f}{\tau})], \tag{1}$$

where $z_0 = (x_0 - 1)/\epsilon = 1.1$.

For $t >> t_f(r)$,

$$f(r) = C \ \frac{r^{-2}}{1-r_*/r}, \tag{2}$$

which reduces to, for $r >> r_*$,

$$f(r) \approx C \ r^{-2}, \tag{3}$$

where

$$C = C_1 \exp(-\frac{W_*}{kT}) \qquad C_1 = \frac{n_1 \theta^{1/2} r_1^2 kT}{3\sqrt{\pi}\Delta\mu}. \tag{4}$$

Eq. [3] can be rewritten as,

$$\ln f = -2\ln r + \ln C_1 - \frac{W_*}{kT}, \tag{5}$$

which gives the value of $\ln C$ at a given value of $r$. For example, at $\ln r = 0$, one has

$$\ln C = \ln C_1 - \frac{W_*}{kT} \tag{6}$$

as shown in Fig. 4. In calculating for Fig. 4, we have employed $r_1 = 0.003\mu$m, $\theta = 10$ and $\Delta\mu/kT = 2$. Of course, the value of $\ln C$ can be obtained at any given value of $\ln r$ as given by Eq. [5] and as shown in Fig. 4.

$\Delta\mu/kT$ can be measured separately for a given temperature $T$.[8] The only unknown in $C_1$ and $W_*/kT$ is the interfacial energy $\sigma$. One thus can obtain $\sigma$ and thus $W(g_*)$ directly from $\ln C$ based on Eq. [6].

By plotting $\ln C$ v.s. $1/T$, one can obtain the slope of the curve $\ln C$. The slope is the value of $W(g_*)$. This is an accurate approach since $\Delta\mu/kT$ and $\theta$ only vary with temperature slightly compared with the linear variation of temperature $1/T$.

# 4 CONCLUSION

Two most important results reported above are the relationship between the nucleation energy barrier and the cluster size distribution given by Eq. [5] and the finding that the transient evolution of $f(g,t)$ and others are strongly sensetive to the value of $\beta(g_*)$. For the form of $W(g)$ different from that given by Eq. [2] in Chapter 11, the similar relationship as Eq. [5] is expected. The only difference for different forms of $W(g)$ is to be found in $C_1$. $C_1$, is determined by material properties and temperature, and is a

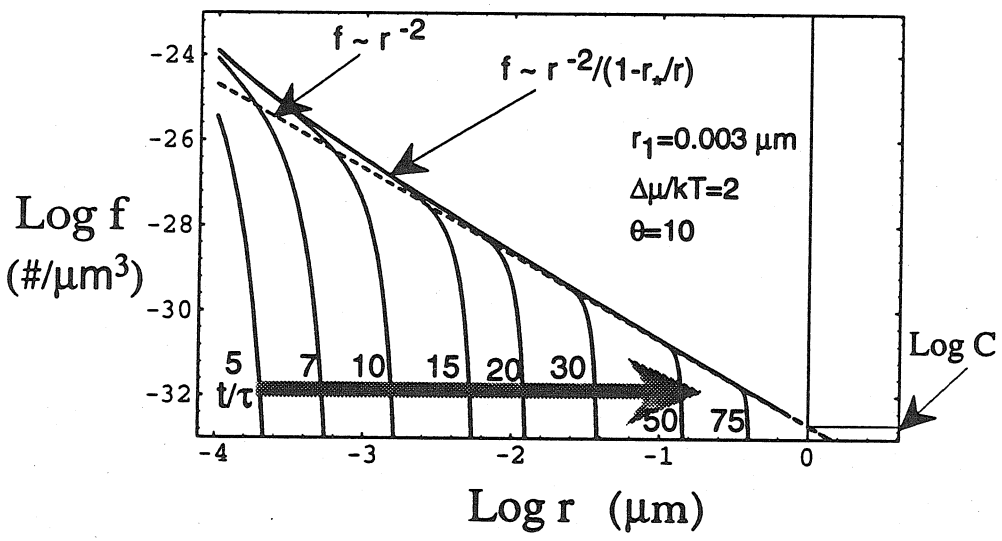


Figure 4. The temporal evolution of cluster size distribution for the surface reaction site-limited (ν=1) nucleation of clusters with the effective dimensionality d=3. Cluster size distribution approaches steady-state behavior of a power-law distribution. The intersection of the power-law with the axis of ln f at ln r=0 gives the value of ln C which gives the value of the nucleation energy barrier and from which the temperature dependency of the nucleation energy barrier can be obtained.

quite constant value. Also the similar relationship as Eq. [5] for different dimension of clusters and different mechanism of monomer addition can be obtained from the results presented in Chapter 11.

It is therefore shown that one can obtain the nucleation energy barrier and its temperature dependency directly from the cluster size distribution measurements. The strong sensitivity of transient evolution of $f(g,t)$ and others provides a sensitive test of the model for the monomer addition rate.

# References

[1]See reviews in F. F. Abraham, *Homogeneous Nucleation Theory* (Academic, New York, 1974); K. Binder, Rep. Prog. Phys. **50**, 783, 1987; A. C. Zettlemoyer (ed), *Nucleation* (R. Decker, New York 1969); D. Turnbull, J. Chem. Phys. **18**, 198(1950); Comtemp. Phys. **10**, 473, 1969

[2]M. Blank-Bewersdorff and U. Köster, Mater. Sci. Eng., **97**, 313(1988); M. A. Gibson and G. W. Delamore, Acta. Metall. Mater., **38**, 2621(1990);W. L. Johnson, in Glassy Metals I, ed. H. S. Güntherodt and H. Beck (Springer-Verlay, Berlin, 1981)

[3]G. Shi, J. H. Seinfeld and K. Okuyama, Phys. Rev. A **41**, 2101(1990); G. Shi and J. H. Seinfeld, J. Chem. Phys. 93(12), 9033, 1990

[4]G. Shi and J. H. Seinfeld, J. Material Res. **6**, 2097(1991); G. Shi and J. H. Seinfeld, J. Material Res. **6**, 2091(1991)

[5]F. G. Shi and J. H. Seinfeld, submitted

[6]F. G. Shi and J. H. Seinfeld, submitted

[7]K. N. Tu, Appl. Phys. A, 53(1), 32, 1991 and references therein

[8]M. G. Scott, in *Amorphous Metallic Alloys*, F. M. Luborsky (ed), (Butterworths, London, 1983)

# CHAPTER 13

# BOUNDARY-LAYER THEORY FOR NUCLEATION PROBLEMS

# BOUNDARY-LAYER THEORY FOR NUCLEATION PROBLEMS

**Abstract**

The existence of a boundary layer structure is established in the nucleation kinetic equation. This boundary layer is shown to be a transition or internal boundary layer, whose location and the thickness is found to be coincident with that of the nucleation barrier region. An approach is developed based on the boundary-layer theory to study for the cluster size distribution in the nucleation barrier region. Moreover, another approach for obtaining the cluster size distribution, which underlies prediction of all the transient kinetics of nucleation, far beyond the nucleation barrier region is developed.

## 1 INTRODUCTION

There has been considerable interest in transient nucleation kinetics over the years as reviewed in Chapter 1. However, the basic question of the subject still remains, that is, to understand the transient evolution of the CSD, $f(g,t)$, which underlies prediction of all the transient features of nucleation. In particular, understanding the temporal evolution of the CSD at sizes beyond the critical one is the most essential, since expressions for the transient kinetics of nucleation at instrumentally detectable sizes offer a connection between nucleation models and experimental observations.

A systematic effort has been recently undertaken to understand the kinetics of nucleation (Shi et al., 1990a; Shi and Seinfeld, 1990a; 1991ab;

1992ab). Using an approach that was developed on the basis of boundary-layer theory, we have obtained the temporal evolution of the CSD in the nucleation barrier region , the region about the critical size, for both a single energy barrier (Shi et al., 1990a) and a higher-dimensional barrier (Shi and Seinfeld,1990a) as well as that in the region beyond the barrier region, generally the only region that is instrumentally accessible (Shi and Seinfeld, 1990a; 1991ab; 1992ab).

Our approach was developed during the process of studying the kinetics of some complex nucleation problems, in particular, the transient kinetics of nucleation. The development of the approach and the results obtained have been scattered over several previous chapters. Here, an overview of the approach developed for nucleation problems will be given. In particular, the major concepts of the approach will be outlined, details will be referred to in other chapters.

## 2 STATEMENT OF THE PROBLEM

Defining the cluster flux as arising by addition or dissociation only of individual monomers, the kinetic equation for the homomolecular nucleation and growth process is,

$$\frac{\partial f(g,t)}{\partial t} = -\frac{\partial J(g,t)}{\partial g} = \frac{\partial}{\partial g}[\beta(g)\frac{\partial f(g,t)}{\partial g} + \frac{\beta(g)f(g,t)}{kT}\frac{\partial W(g)}{\partial g}], \quad (1)$$

where $J(g,t)$ is the cluster flux defined as $J(g,t) = -\beta(g,t)n(g,t)\frac{\partial}{\partial g}\frac{f(g,t)}{n(g,t)}$, cluster size $g$ indicates the number of atoms in the cluster and $\beta(g)$ is the rate of addition of atoms to a cluster of size $g$ (Abraham, 1974; Zhang, 1988; Bashkirov, 1992). $n(g)$ is the equilibrium cluster population of $g$-mers. The presence of $n(g)$ in Eq. [1] implies only that an equilibrium

cluster population of $g$-mers may be defined as $n(g) \propto \exp(-W/kT)$; no particular energetic model for $W(g)$ is assumed or implied (Russell, 1980), although in phenomenological nucleation theories (Abraham, 1974; Russell, 1980), the formation energy of a nucleus, $W(g)$, is generally considered to consist of surface and volume energy terms,

$$W(g) = -g\Delta\mu + s\sigma g^{\frac{d-1}{d}}, \tag{2}$$

where $\Delta\mu$ is the chemical potential difference between the nucleated and nucleating phases under given conditions, $\theta = s\sigma/kT$, $\sigma$ is the specific free energy between the two phases, $s$ is a geometrical constant, $k$ is Boltzmann's constant, $T$ is temperature, and $d$ is the effective dimensionality of the cluster. For a compact cluster in D-dimensional physical space $d$ =D; usually $d$ <D for fractal clusters. Other forms of $W(g)$ can also be considered.

No particular form for the monomer addition rate to a $g$-mer is assumed in Eq. [1]. By introducing an index $\nu$, most physically known mechanisms for the addition of single atoms to clusters are included within the functional form,

$$\beta(g) \propto g^{\frac{d-\nu}{d}}. \tag{3}$$

For example, $\beta(g) \propto g^{2/3}$ for $d = 3$ and $\nu = 1$ for reaction site-limited nucleation of compact clusters, i.e., the cluster formation is controlled by the formation of a chemical bond between the atom and the cluster. If every atom within a cluster is a potential site for atom addition, one has $\nu = 0$, and $\beta(g) \propto g$. For diffusion-limited nucleation of compact clusters, i.e., in the case that the cluster formation process is controlled by the arrival of single atoms to the cluster, $\beta(g) \propto g^{1/3}$ for $d = 3$ and $\nu = 2$.

We will study the temporal evolution of the CSD after an initially ho-

mogeneous phase undergoes an abrupt change in supersaturation. The corresponding initial condition is, for $g > 1$

$$f(g, 0) = 0 \tag{4}$$

and the only known boundary condition is,

$$f(g, t)/n_1 \rightarrow 1 \tag{5}$$

for $g \rightarrow 1$. Here $n_1$ is the number density of atoms in the nucleating phase. Eq. [5] holds for nucleation in solid phases and for quasi-steady state situations.

# 3 OVERALL APPROACH

An approach for solving Eq. [1] together with Eqs. [4] and [5] for $f(g, t)$ valid for all $g$ has been developed (Shi et al., 1990a; Shi and Seinfeld, 1990a; 1991ab; 1992ab). The basic idea is to employ boundary-layer theory to solve first for $f(g, t)$ valid in the nucleation barrier region, at the size of the nucleated cluster, and then obtain $f(g, t)$ for the region beyond the barrier region using the regular perturbation method.

The procedure we will present is extendable to forms of $W(g)$ and $\beta(g)$ other than the models considered in this work. Also, the approach that was developed can be used to investigate other complex nucleation problems (Shi and Seinfeld, 1990bc; 1992c; Shi et al., 1990b), to study nucleation kinetics of higher-dimensional barriers (Shi and Seinfeld, 1990a) or other barrier-crossing problems.

# 4 SOLUTIONS IN THE BARRIER REGION

## 4.1 BOUNDARY-LAYER THEORY (Bender and Orszag, 1978)

### 4.1.1 Basic Ideas

Boundary-layer theory is a collection of perturbation methods for obtaining an asymptotic approximation to the solution $y(x)$ of a differential equation whose highest derivative is multiplied by a small parameter $\epsilon$. Solutions to such equations usually develop regions of rapid variation as $\epsilon \to 0$. If the thickness of these regions approaches 0 as $\epsilon \to 0$, they are called boundary layers, and boundary-layer theory may be used to approximate $y(x)$. For linear equations boundary-layer theory is a special case of WKB theory which applies to the boundary layer thicknesses remaining finite as $\epsilon \to 0$. Boundary-layer theory also applies directly to nonlinear equations, while WKB theory does not.

The basic ideas of boundary-layer theory can be understood as the following. In the outer region (away from boundary-layer) $y(x)$ is slowly varying, so it is valid to neglect any derivatives of $y(x)$ which are multiplied by $\epsilon$. Inside a boundary-layer the derivatives of $y(x)$ are large, but the boundary-layer is so narrow that we may approximate the coefficient functions of differential equations by constants. Thus, we can replace a single differential equation by a sequence of much simpler approximate equations in each of several inner and outer regions. In every region the solution of the approximate equation will contain one or more unknown constants of integration. Those constants are then determined from the boundary or initial conditions using the conventional techniques of asymptotic matching.

Boundary-Layer theory is indeed a singular, and not a regular, perturbation theory. The singular nature of boundary-layer theory is intrinsic to both the inner and outer expansions. The outer expansion is singular because there is an abrupt change in the order of differential equations when $\epsilon = 0$. By contrast, the inner expansion is a regular perturbation expansion for finite value of the inner variable, $X$. However, singular asymptotic matching takes places in the limit of $X \rightarrow \infty$, the inner expansion is also singular. In this narrow sense, we thus have refered boundary-layer theory as a singular perturbation theory (Shi et al. 1990a).

### 4.1.2 Core of Boundary-Layer Theory

The core of boundary-layer theory is not perturbation and asymptotic matching techniques which are readily available, but the necessary boundary-layer analysis of the problem, that is, to answer the following questions,

1. How can one know *a priori* whether the solution to a differential equation has boundary-layer structure?

2. How can one predict the locations of the boundary-layers.?

3. How does one estimate the thickness of the boundary layer?

4. How can we be sure that there is an overlap region between the inner and outer regions on which to perform asymptotic matching?

5. Is it useful to decompose a solution into its inner and outer parts if one is seeking a higher-order approximation to the exact answer?

Mathematical analysis has been performed to establish the boundary-layer structure of Eq. [1]. We have established that the boundary-layer structure of Eq. [1] is not a conventional one , but an internal or transition boundary-layer. The location of this transition boundary layer is coincident

with that of the nucleation barrier or critical region. The thickness of this transition layer is also the same as that of the barrier region, which is in the order of $\epsilon$. The overlap region between inner and outer regions is shown to exist. Also, it is shown that the leading-order solution is accurate enough. In the following, we will highlight the main points of the approach especially those that can easily be confused.

## 4.2 Nucleation Barrier Region

The nucleation barrier region, or the critical region, is that in which random fluctuations play the dominant role in causing clusters to overcome the nucleation barrier, and is defined as the region in which (Feder et al., 1966)

$$| W(g) - W(g_*) | \leq kT. \tag{6}$$

The half width of which is given by (Shi et al., 1990a)

$$\delta = [-\frac{1}{2kT}\frac{\partial^2 W}{\partial g^2}]^{-1/2} |_{g=g_*} \tag{7}$$

which is related to the Zeldovich factor $Z$ by

$$\delta = \frac{1}{\sqrt{\pi} Z}. \tag{8}$$

The critical cluster size $g_*$ is that corresponding to the maximum of $W(g)$, and the barrier region half width $\delta$ is given by

$$\delta = (\frac{d-1}{2d^2})^{-1/2} g_*^{-\frac{d+1}{2d}} \theta^{-1/2}. \tag{9}$$

Based on the concept of the barrier region, one is able to obtain the steady-state rate of nucleation without solving Eq. [1] itself as done by Feder et al. (1966). In calculating the steady-state rate of nucleation, one

only needs to know the value for $\frac{\partial}{\partial g}\frac{f(g)}{n(g)}$ at $g_*$. Since $f/n$ approaches one for $g < g_* - \delta$ and $f/n$ tend to zero on the right outside of the barrier region, $f/n$ at $g_*$ approximates to $1/2\delta$. Therefore, $J_s \approx \frac{1}{2}\beta(g_*)n(g_*)/\delta$ which differs from the true rate by a small numerical difference $2/\sqrt{\pi}$.

## 4.3 Transition Boundary Layer

The two regions to the right and left of the nucleation barrier region, $g_* - \delta < g < g_* + \delta$, are defined by $g >> g_* + \delta$ and $g << g_* + \delta$, respectively.

As long as $W(g_*) >> kT$, Eq. [1] can be simplified in the different regions (Shi et al., 1990a). Eq. [1] can be reduced to a first-order equation in the right and left regions, while Eq. [1] can be simplified in the barrier region but remains a second-order equation. In line with this finding, it is also clear that the steepest variation in $f(g,t)/n(g)$ is found about $g_*$, while $f(g,t)/n(g)$ either approaches 1 in the left region or 0 in the right region (Feder et al., 1966). Thus a transition boundary layer structure is found about the critical sized cluster $g_*$(Shi and Seinfeld, 1990bc; Shi et al., 1990a).

The existence of the transition boundary layer about $g_*$ that was developed on the basis of physical reasoning can be verified by using mathematical arguments (Shi and Seinfeld, 1990bc, Shi et al., 1990a). First, the proper small parameter is mathematically determined to be $\epsilon = \delta/g_*$, which multiplies the term containing the highest derivative in Eq. [1]. Since the dominant term of Eq. [1] changes sign at $g/g_* = 1$ in the interval $[1/g_*, \infty]$, a transition boundary layer at $g_*$ is expected. Thus a singular perturbation approach (Bender and Orszag, 1978) can be used to solve Eq. [1] to obtain $f(g,t)$ in the barrier region, which is the inner solution of the two unknowns

which have to be determined by matching it with two outer solutions.

## 4.4 Left Outer Solution

Eq. [1] can be reduced to a first order equation in the left region, the left outer solution can be obtained with the left outer boundary condition given by Eq. [5] (Shi et al., 1990a).

## 4.5 Right Outer Solution

We do not know the right outer solution a priori, and, in fact, it is our ultimate goal to obtain $f(g,t)$ in that region. Thus the singular perturbation approach for transition boundary layers (Bender and Orszag, 1978) cannot be applied straightforwardly to the present nucleation problem.

In the right region, since $n(g)$ becomes exponentially large for $g >> g_* + \delta$, while $f(g,t)$ is finite, one has

$$f(g,t)/n(g) \to 0. \tag{10}$$

Therefore by considering the normalized variable $f(g,t)/n(g)$ in Eq. [1] with Eq. [10] as the left boundary condition, we can determine the right outer solution needed to obtain the inner solution in the barrier region.

Eq. [10] is obtained in the sense of a perturbation solution. The right outer solution obtained is $f(g,t)/n(g) = 0$ which does not imply that $f(g,t) = 0$ (Shi et al., 1990a; 1992; Shneidman, 1992) but states the fact that $f(g,t)$ is exponentially smaller than $n(g)$ for $g >> g_* + \delta$, i.e., $f(g,t) = 0(\mathrm{e}^{-1/\epsilon^2})n(g)$. The above point is essential to understand our approach used to obtain the CSD in the region beyond the barrier region as presented in section 3.2.

### 4.6 Inner Solution

Since one only knows the right outer solution in terms of $f(g,t)/n(g)$, therefore the inner solution will be obtained by considering the normalized variable $f(g,t)/n(g)$ in Eq. [1]. Eq. [1] can be simplified in the barrier region but remains a second-order equation. The nucleation barrier region is thus not a conventional boundary layer, but a transition boundary layer, as noted above.

Two unknown constants in the inner solution valid for the barrier region can be determined by matching the inner solution with the two outer solutions. The right and left outer solutions obtained in terms of $f(g,t)/n(g)$ are solely used to obtain $f(g,t)$ in the barrier region. The actual CSD in the right region is obtained by solving the corresponding equation for $f(g,t)$ and taking the solution obtained for the barrier region as the boundary condition.

## 5 SOLUTIONS BEYOND THE BARRIER REGION

We have developed an approach for solving Eq. [1] for $g > g_*$ directly. By virtue of the fact that $W(g_*) >> kT$, we first reduce Eq. [1] to a first order equation in the region beyond the barrier region. Therefore, only one boundary condition is needed for solving the reduced Eq. [1] to obtain $f(g,t)$ for $g > g_o$. The critical part of the approach is therefore to establish the required boundary condition. It is established that the boundary condition required is $f(g_o,t)$. The magnitude of $g_o$ has been found to be about $g_*+1.1\delta$ by using stochastic simulations. The expression for $f(g_o,t)$ can be obtained from $f(g,t)$ in the barrier region of $g_* - \delta < g < g_* + \delta$, since $f(g,t)$

in the barrier region based on the boundary-layer theory is also correct asymptotically at $g_o$. With the given expression for $f(g_o, t)$ as the only boundary condition needed for solving the reduced Eq. [1], we have obtained $f(g, t)$ for $g > g_o > g_*$.

The approach reported above enables one to study for the first time the transient kinetics of nucleation beyond the nucleation barrier region. The procedure presented is extendable to forms of $W(g)$ and $\beta(g)$ other than the models considered. Although the approach is discussed above for a one-dimensional nucleation barrier, it is equivalently applicable to higher-dimensional nucleation barrier as has already been demonstrated by Shi and Seinfeld (1990a).

# 6 OTHER BARRIER-CROSSING PROBLEMS

The approach outlined above for solving the cluster size distribution in nucleation problems, is also applicable to other barrier-crossing problems. In particular, it is applicable to investigate the most difficult and interesting aspect of the problem: the temporal evolution of $f(g, t)$, which can be any probability or distribution of other barrier-crossing processes.

The mathematical approach that was developed on the basis of boundary-layer theory to solve nucleation kinetic equation and its likes offers a tool for investigating other transient barrier-crossing problems (Fultz, 1991ab) and those with higher-dimensional barriers, since such transient kinetics is indispensable in developing or discarding various theories based on experimental measurements. Since nucleation is an activated barrier crossing rate process, our present results for nucleation have implications to the other activated barrier crossing processes. Some implications for multi-dimensional

barrier-crossing processes have been already discussed (Shi and Seinfeld, 1990a). Here it is interesting to point out one common feature of barrier-crossing problems: the transient-induced non-exponential relaxation. This non-exponential relaxation due to the transient effects can be important for many barrier-crossing processes in condensed matters. The relaxation process in glasses is an example. Similar nonexponential relaxation (non-Debye relaxation, the stretched exponential relaxation) behavior can be found in rather different systems such as polymers, viscous fluids, disordered dielectrics and complex liquids, amorphous semiconductors and other glassy materials.

# 7 CONCLUSIONS

The existence of a boundary layer structure is found in the nucleation kinetic equation. This boundary layer is a transition or internal boundary layer. The location and the thickness of this boundary layer is found to be coincident with that of the nucleation barrier region. An approach is developed based on the boundary-layer theory to solve the nucleation kinetic equation and to obtain the cluster size distribution in the nucleation barrier region. An additional approach is also developed for solving the nucleation kinetic equation directly in the region beyond the barrier region. The essential of this approach is to establish the boundary condition required. By establishing a concept of a nucleated cluster and estimating its size, $g_o$, it is found that $f(g_o, t)$ is the required boundary condition. It is established that the result for $f(g, t)$ in the barrier region is also correct at $g_o$. As a result, we have obtained $f(g, t)$ for $g > g_o > g_*$.

The approaches reported above enable one to study for the first time

the transient kinetics of nucleation in the barrier region and beyond. The procedure presented is extendable to forms of $W(g)$ and $\beta(g)$ other than the models considered. The approach is also applicable to other barrier-crossing problems and those with higher-dimensional barriers.

# REFERENCES


Abraham, F. F., *Homogeneous Nucleation Theory*, (Academic, New York, 1974)

Bashkirov, A. G., *J. Chem. Phys.*, **96**, 1484(1992)

Bender, C. M. and S. A. Orszag,*Advanced Mathematical Methods for Scientists and Engineers*, (McGraw-Hill Co., New York, 1978)

Binder, K and D. Stauffer, *Adv. Phys.*, **25**, 343(1976)

Feder, J., K. C. Russell, J. Lothe and G. M. Pound, *Adv. Phys.*, **5**, 111(1966)

Fultz, B., *J. Less Met.*, **168**, 145(1991a)

Fultz, B., *Phy. Rev. B*, **44**, 9805(1991b)

Kelton, K. F., *Solid State Phys.*, **45**, 75(1992)

Kozisek, Z., In *Kinetic Phase Diagrams: Nonequilibrium Phase Transitions*, Z. Chvoj, J. Sestak and A. Triska (Eds.), (Elsevier, New York, 277-331, 1991)

Russell, K. C., *Adv. Coll. Interf. Sci.*, **13**, 205(1980)

Shi, G., J. H. Seinfeld and K. Okuyama, *Phys. Rev. A*,**41**, 2101(1990a)

Shi, G., J. H. Seinfeld and K. Okuyama, *Phys. Rev. A*,**44**, 8443(1991)

Shi, G., J. H. Seinfeld and K. Okuyama, *Phys. Rev. A*,**68**, 4550(1990b)

Shi, G., and J. H. Seinfeld, *J. Chem. Phys.*, **93**, 9033(1990a).

Shi, G., and J. H. Seinfeld, *J. Chem. Phys.*, **92**, 687(1990b)

Shi, G., and J. H. Seinfeld, *J. Coll. Inter. Sci.*, **135**, 252(1990c)

Shi, G., and J. H. Seinfeld, *J. Materials Res.*,**6**, 2091(1991a)

Shi, G., and J. H. Seinfeld, *J. Materials Res.*,**6**, 2097(1991b)

Shi, F. G., and J. H. Seinfeld, 1992a: Kinetics of Nucleation Beyond the Barrier Region: Basis for Interpretation of Measurements, sub.

Shi, F. G., and J. H. Seinfeld, 1992b: Universal Cluster Size Distribution in Nucleation, sub.

Shi, F. G., and J. H. Seinfeld, 1992c: Selective Nucleation of Silicon Clusters in CVD, to appear in *J. Materials Res.*

Shneidman, V. A., *Phys. Rev. A*,**44**, 8441(1991)

Zhang, C. G., *J. Coll. Interf. Sci.*, **124**, 262(1988)

# CHAPTER 14

# SUMMARY AND CONCLUDING REMARKS

A major issue studied in this thesis is the transient evolution of the cluster size distribution in nucleation, which underlies the prediction of all the transient nucleation kinetics. It is found that transient cluster size distributions in phase transitions governed by nucleation and growth processes, with a nucleation energy barrier consisting of surface and volume energy terms, obey a scaling relation in the barrier region and beyond. The cluster size distribution beyond the nucleation barrier region exhibits a universal asymptotic power law distribution, the exponent of which depends only on the mechanism of monomer addition to the nucleating and growing clusters.

By developing the concept of a nucleated cluster size, and obtaining the transient kinetics of nucleation at that size, the transient effect of nucleation in the Avrami model for crystallization is reconsidered. It is shown that several concepts involving nucleation time scales, in particular those used for controlling the initial stage of nucleation and crystallization in devices applications are generally incorrect.

Transient kinetics of nucleation at sizes beyond the critical one provide for the first time a theoretical basis for measuring the nucleation barrier directly. An approach for determining the interfacial atomic transfer mechanism in the nucleation process is also developed based on the same new results. It is shown that the transient evolution of the cluster size distribution provides a link between nucleation models and experimental kinetic

measurements.

The rate of nucleation over different paths in a binary vapor system is studied. It is shown that anisotropy in addition rates and anisotropy in the free energy surface can cause nucleation to occur bypassing the saddle point. Homomolecular nucleation is demonstrated to be the natural limit of binary nucleation as the concentration of one component goes to zero. Explicit expressions are also obtained for the time lag of binary nucleation by using the approach that was developed on the basis of boundary-layer theory. It is shown that the time lag associated with different paths of nucleation is essential in determining the relative importance of different nucleation pathways.

Mathematical approaches developed include one based on boundary-layer theory developed to solve the nucleation kinetic equation and its likes in the barrier region and an approach for solving the kinetic equation in the region far beyond the barrier one. The approaches developed enable us to study for the first time the transient kinetics of nucleation in the barrier region and beyond, for homomolecular and binary nucleation processes. The procedure developed is extendable to models other than these considered. The approach is also applicable to other transient barrier-crossing problems and those with higher-dimensional barriers.

A chemical-nucleation model is developed by treating the chemical etching of atoms as an additional loss process besides thermal dissociation that competes with the process of atom addition in forming a cluster. The model has been used to study the selectivity of Si growth on amorphous and crystalline substates using CVD of $Si_2H_2/H_2/HCl$.

Besides, the nucleation kinetics in some spatially inhomogeneous systems

where subcritical clusters can be lost are studied.

It is concluded that a link between nucleation models and experimental kinetic measurements has been developed as a result of the present studies of the transient kinetics of nucleation. The present results on the transient kinetics of nucleation and crystallization can be applied for (1) developing or disapproving nucleation and crystallization models experimentally; (2) interpreting nucleation and crystallization kinetic measurements in terms of a proven nucleation model; (3) transferring nucleation and crystallization kinetic measurements to the device applications involving the initial nucleation stage.

The mathematical approach based on boundary-layer theory to solve nucleation kinetic equation and its likes offers a tool for investigating other transient barrier-crossing problems and those with higher-dimensional barriers, since such transient kinetics is indispensable in developing or discarding various theories based on experimental measurements. My studies indicate that the relaxation in a system described by a Fokker-Planck equation or a modified Fokker-Planck equation with a one-dimensional or a high-dimensional barrier, is always non-exponential in agreement with what we have found for the nucleation process. We believe that the transient-induced nonexponential relaxation will account for some of the observed nonexponential decay of physical properties during the evolution of a system from a nonequilibrum state to an equilibrium one. The relaxation process in glasses is an example. Similar nonexponential relaxation (non-Debye relaxation, the stretched exponential relaxation) behavior can be found in rather different systems such as polymers, viscous fluids, disordered dielectrics and complex liquids, amorphous semiconductors and other glassy materials.